

SECRET

TECHNICAL

of the

1/19756

SPECIAL WEAPONS PROJECT

JAN 14 1975

AT-782

Copy No. 267 A

TEMPO

KTL 2224

No. of Copies, Series A

Operation

UPSHOT-KNOTHOLE

cc1

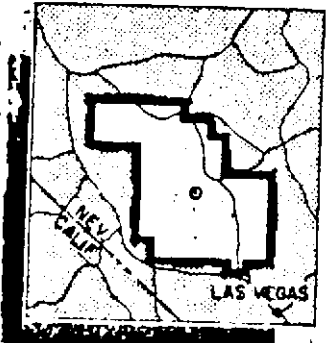
NEVADA PROVING GROUNDS

DEFENSE NUCLEAR
AGENCY
TECHNICAL LIBRARY
DIVISION

March - June 1953

Programs 1-9

SUMMARY REPORT OF THE
TECHNICAL DIRECTOR



[REDACTED]
[REDACTED]
[REDACTED]
[REDACTED]

DNA 14445
DDE

RESTRICTED

[REDACTED]
[REDACTED]
[REDACTED]

HEADQUARTERS FIELD COMMAND, ARMED FORCES SPECIAL WEAPONS PROJECT
SANDIA BASE, ALBUQUERQUE, NEW MEXICO

DECLASSIFIED WITH DELETIONS BY
DNA (ISTS) COORDINATED WITH DDE,
ARMY, NAVY, + AIR FORCE

DATE: 4/22/01

to be made available

SECRET

HRE-0434

DNAI 940906.084

~~SECRET~~

WT-782

This document consists of 232 pages
No. 2E7 of 275 copies, Series A

Report to the Test Director

SUMMARY REPORT OF THE TECHNICAL DIRECTOR

Programs 1-9 (U)

Headquarters, Field Command
Armed Forces Special Weapons Project
Sandia Base, Albuquerque, New Mexico,
March 1955

~~RESTRICTED DATA~~
~~...~~
The unauthorized disclosure of this information to an unauthorized person is prohibited.

~~SECRET~~

D.3537/1
2 K

ACKNOWLEDGMENTS

This report has been prepared from an evaluation of the military significance of the 79 individual project reports of the military effects tests portion of Operation UPSHOT-KNOTHOLE. An abstract of each report, with the exception of those in Program 7, is presented in Appendix B.

This report has been prepared by the program directors, representatives of Headquarters, Armed Forces Special Weapons Project (AFSWP), AFSWP consultants, and the Technical Director. No attempt is made to give credit for specific report sections, except to state that the following persons have made significant contributions to the material included herein:

Col H. K. Gilbert, USAF	E. A. Martell, Institute of Nuclear Studies,
CDR W. L. Carlson, USN	University of Chicago
Col E. Pinson, USAF	N. M. Newmark, University of Illinois
CDR K. H. Stefan, USN	Lt Col D. I. Prickett, USAF
Lt Col W. R. Hedrick, USAF	Lt Col H. S. Heaton, USAF
R. G. Preston, University of	LTJG R. J. Culp, USN
California Radiation Laboratory	Ben Sussholz, University of California
R. A. Burgin, FC, AFSWP	Radiation Laboratory
Jack Kelso, AFSWP	D. C. Sachs, Stanford Research Institute
F. H. Shelton, Sandia Corporation	Maj W. R. Greer, USA

CONTENTS

	Page
ACKNOWLEDGMENTS	3
ILLUSTRATIONS	10
TABLES	13
CHAPTER 1 INTRODUCTION	15
1.1 Background	15
1.2 Technical Program	16
1.3 Test of the 280-mm Gun	16
1.4 Organization	17
1.5 Shot Schedule	17
CHAPTER 2 BLAST MEASUREMENTS	20
2.1 Introduction	20
2.2 Scale Factors	20
2.3 Free Air Blast	21
2.3.1 Overpressure	21
2.3.2 Dynamic Pressure	22
2.3.3 Duration	22
2.3.4 TNT Efficiency	22
2.4 Air Blast Phenomena	22
2.4.1 Damage Parameters	23
2.4.2 Ideal Parameters	23
2.4.3 Surface and Thermal Effects	25
2.5 Air Overpressure	31
2.5.1 Ground Level	31
2.5.2 Aboveground	33
2.5.3 Positive Phase Duration and Impulse and Arrival Time	34
2.6 Dynamic Pressure	34
2.6.1 Instrumentation	34
2.6.2 Results	34
2.7 Precursor	35
2.7.1 General	35
2.7.2 Thermal Layer	36
2.7.3 Precursor Overpressure and Dynamic Pressure	36
2.7.4 Precursor Prediction Criteria	37
2.7.5 Smoke Experiment Precursor Effects	38
2.7.6 Thermal Shock	39

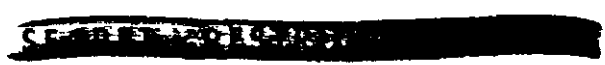
~~RESTRICTED DATA~~

D-3537

CONTENTS (Continued)

	Page
2.8 Triple Point (Mach Stem Considerations)	39
2.8.1 General	39
2.8.2 Use of the Height-of-burst Curves	41
2.8.3 Nuclear Vs TNT	40
2.9 Height-of-burst Curves	41
2.9.1 History	41
2.9.2 Philosophy	42
2.9.3 Air Overpressure	42
2.9.4 Dynamic Pressure	43
2.9.5 Summary	43
2.10 Damage Criteria	44
2.10.1 Basic Considerations	44
2.10.2 Use of the Height-of-burst Curves	44
2.11 Recommendations for Future Tests	45
CHAPTER 3 THERMAL-RADIATION MEASUREMENTS	98
3.1 Background	98
3.2 Instrumentation	98
3.2.1 Total Thermal Energy and Flux Vs Distance	98
3.2.2 Time-Intensity Relations	99
3.2.3 Spectral Characteristics	99
3.2.4 Special Studies	99
3.3 Results and Discussion	100
3.3.1 General	100
3.3.2 Total Energy Vs Ground Distance	100
3.3.3 Thermal Yields	100
3.3.4 Time Vs Intensity	102
3.3.5 Energy Vs Time	103
3.3.6 Energy Normal to the Ground	103
3.3.7 Thermal Layer	103
3.3.8 [REDACTED]	104
3.4 Conclusions	104
3.5 Recommendations	105
CHAPTER 4 NUCLEAR RADIATION MEASUREMENTS	112
4.1 Initial Gamma Exposure	112
4.2 Residual Gamma Spectrum	113
4.3 Neutron Flux	114
4.4 Radioactive Particles Inside Aircraft	115
4.5 Residual Gamma-radiation Depth Dose in Unity Density Material	115
CHAPTER 5 EFFECTS ON STRUCTURES	127
5.1 Introduction	127
5.2 Experiment Design	127
5.2.1 Loading Tests	127
5.2.2 Response Tests	128
5.3 Comments on Interpretation of Results	128
5.3.1 Drag, Diffraction, and Precursor Phenomena	128
5.3.2 Limiting Conditions	129

DATA
(1)
PAGE
112



CONTENTS (Continued)

	Page
5.4 Results	130
5.4.1 General Description of Leakage	130
5.4.2 Discussion	131
5.4.3 General Comments	132
CHAPTER 6 EFFECTS ON AIRCRAFT STRUCTURES	133
6.1 Introduction	133
6.1.1 Background	133
6.1.2 Scope	133
6.2 Thermal Effects	133
6.3 Blast Effects	134
6.4 Conclusions	135
CHAPTER 7 THERMAL EFFECTS.	136
7.1 General	136
7.2 Fire Effects	136
7.3 Thermal Burns Beneath Fabrics	136
7.3.1 Clothed Pigs	137
7.3.2 Fabric Damage and Mechanisms of Heat Transfer Through Fabrics	137
7.3.3 Skin Simulant	137
7.4 Protective Smoke	137
CHAPTER 8 BIOMEDICAL EFFECTS	139
8.1 Atomic Cloud Hazards	139
8.2 Beta Hazard	139
8.3 Neutron Effects	140
8.4 Primary Blast Injury	141
8.5 Flash Blindness	141
CHAPTER 9 TECHNICAL PHOTOGRAPHY	142
9.1 Background	142
9.2 Photography Plan	142
9.3 Stabilization	142
9.4 Results	143
CHAPTER 10 TESTS OF SERVICE EQUIPMENT AND TECHNIQUES	144
10.1 Radiac Equipment Tests	144
10.2 Tests and Development of Operational Techniques	145
CHAPTER 11 LONG-RANGE DETECTION	147
APPENDIX A SHOT PARTICIPATION	148
APPENDIX B PROJECT SUMMARIES	149
B.1 Program 1—Blast and Shock Measurements	149
B.1.1 Projects 1.1a and 1.2: Air Blast Measurements	149

CONTENTS (Continued)

	Page
B.1.2 Project 1.1a-1: Evaluation of Whancko and Vibrotron Gages and Development of New Circuitry for Atomic Blast Measurements	150
B.1.3 Project 1.1a-2: Development of Mechanical Pressure-Time and Peak Pressure Recorders for Atomic Blast Measurements	150
B.1.4 Project 1.1b: Basic Air Blast Measurements	151
B.1.5 Project 1.1c-1: Air Shock Pressure-Time Vs Distance for a Tower Shot	152
B.1.6 Project 1.1c-2: Air Shock Pressures As Affected by Hills and Dales	152
B.1.7 Project 1.1d: Basic Air Blast Supporting Measurements	153
B.1.8 Project 1.3: Free Air Blast Pressure Measurements	153
B.1.9 Project 1.4: Earth Measurements	154
B.1.10 Project 1.5: Test Procedures and Instrumentation for Projects 1.1c, 1.1d, 1.4a, and 1.4b.	154
B.2 Program 2 — Nuclear Measurements and Effects	155
B.2.1 Project 2.1: Studies of Airborne Particulate Material	155
B.2.2 Project 2.2a: Measurement of Gamma Radiation of Fission Products	155
B.2.3 Project 2.2b: Residual Gamma Depth Dose Measurements in Unit Density Material	156
B.2.4 Project 2.3: Neutron Flux and Spectrum Vs Range	156
B.3 Program 3 — Structures, Material, and Equipment	157
B.3.1 Project 3.1: Tests on the Loading of Building and Equipment Shapes	157
B.3.2 Project 3.1u: Shock Diffraction Study	159
B.3.3 Project 3.3: Tests on Horizontal Cylindrical Shapes	159
B.3.4 Project 3.4: Tests of Truss Systems Common to Open-Framed Structures.	160
B.3.5 Project 3.5: Tests of Wall and Roof Panels	161
B.3.6 Project 3.6: Tests of Railroad Equipment	163
B.3.7 Project 3.7: Effectiveness of Blast Baffles at Shelter Entrances, Air Intakes, and Outlets	164
B.3.8 Project 3.8: Effects of Air Blast on Buried Structures	165
B.3.9 Project 3.9: Design and Location of Field Fortifications	166
B.3.10 Project 3.11: Protective Measures for Existing Constructional Light Steel Frame Structures	167
B.3.11 Project 3.12: Protective Measures for Existing Construction; External Protective Measures	167
B.3.12 Project 3.13a and 3.13b: Precast Gable Shelters	168
B.3.13 Project 3.13c: Model of Blast-Resistant Panel	169
B.3.14 Project 3.14: Precast Warehouse	170
B.3.15 Project 3.15: Armco Steel Magazine	170
B.3.16 Project 3.16: Tests of Glazing and Window Construction	171
B.3.17 Project 3.18: Minefield Clearance.	172
B.3.18 Project 3.19: Effects of an Atomic Explosion on Trees in a Forest Stand	174
B.3.19 Project 3.20: Vulnerability of a Typical Tactical Communications System to Atomic Attack	175
B.3.20 Project 3.21: Statistical Determination of Damage Criteria for Critical Items of Military Equipment and Supplies	176



CONTENTS (Continued)

	Page
B.3.21 Project 3.22: Effects on Engineer Bridging Equipment	177
B.3.22 Project 3.24: Blast Effects on I/V's	179
B.3.23 Project 3.26.1: Test of the Effects on POL Installations	179
B.3.24 Project 3.26.2: Effects of Atomic Weapons on a POL Supply Point	181
B.3.25 Project 3.26.3: Effects of an Atomic Explosion upon an Amphibious Assault Fuel Handling System (Shore Phase)	182
B.3.26 Project 3.27: Effects of Atomic Weapons on Field Medical Installations	183
B.3.27 Project 3.28.1: Structures Instrumentation	184
B.3.28 Project 3.28.2: Structures Instrumentation	184
B.3.29 Project 3.28.3: Structures Instrumentation	185
B.3.30 Project 3.29: Tests of Four FCDA Curtain Wall and Partition Structures	185
B.3.31 Project 3.30: Air Blast Gage Studies	186
B.4 Program 4—Biomedical Effects	186
B.4.1 Project 4.1: Evaluation of the Hazard of Flying Through the Atomic Cloud	186
B.4.2 Project 4.2: Air Blast Injuries	187
B.4.3 Project 4.5: Flash Blindness	188
B.4.4 Project 4.7: Measurement of Beta Hazard in Bomb Contaminated Areas	189
B.4.5 Project 4.8: Biological Effects of Neutrons	190
B.5 Program 5—Aircraft Structures Tests	191
B.5.1 Project 5.1: Naval Aircraft Structures	191
B.5.2 Project 5.2: Blast, Thermal, and Gust Effects on Aircraft in Flight	192
B.5.3 Project 5.3: Blast and Gust Effects on B-36 in Flight	192
B.6 Program 6—Tests of Service Equipment and Operations	193
B.6.1 Project 6.2: Test of Radar Techniques for Accomplishing IBDA	193
B.6.2 Project 6.3: Field Test of IBDA	194
B.6.3 Project 6.4: Evaluation of the Chemical Dosimeter	194
B.6.4 Project 6.7: Electromagnetic Radiation over the Radio Spectrum	194
B.6.5 Project 6.8: Evaluation of Radiac Instrumentation, Equipment, and Operational Techniques	195
B.6.6 Project 6.8a: Gamma Exposure Vs Distance	196
B.6.7 Project 6.9: Evaluation of Airborne Radiac Equipment	196
B.6.8 Project 6.10: Rapid Aerial Radiological Survey	196
B.6.9 Project 6.11: Operational Training for TAC Crews	197
B.6.10 Project 6.12: Determination of Height of Burst and Ground Zero	197
B.6.11 Project 6.13: Effectiveness of Fast Scan Radar	197
B.7 Program 8—Thermal Measurements and Effects	198
B.7.1 Project 8.1a: Aircraft Structures Tests	198
B.7.2 Project 8.1b: Aircraft Structures Tests	198
B.7.3 Project 8.2: Measurements of Thermal Radiation by Means of Radiation Pressure Phenomenon	199
B.7.4 Project 8.4-1: Attenuation of Thermal Radiation by White Scattering Smoke	199

~~SECRET RESTRICTION DATA~~

CONTENTS (Continued)

	Page
B.7.5 Project 8.4-2: Effects of Black Absorbing Smoke on Thermal Radiation and Blast	200
B.7.6 Project 8.5: Degree and Extent of Burns Under Service Uniforms	200
B.7.7 Project 8.6: Thermal Effects on Clothing Materials	201
B.7.8 Project 8.9: Effects of Thermal Radiation on Materials	202
B.7.9 Project 8.10: Measurement of Basic Characteristics of Thermal Radiation	203
B.7.10 Project 8.11a: Initiation and Resistance of Primary Fires (Structures and Interior of Structures)	204
B.7.11 Project 8.11b: Initiation and Persistence of Primary Fires (Ignitable Litter)	205
B.7.12 Project 8.12a: Measurement of Velocity of Sound	205
B.7.13 Project 8.12b: Precursor Shock Study	206
B.7.14 Project 8.13: A Study of Fire Retardant Paints	207
B.8 Program 9—Technical Photography	207
B.8.1 Project 9.1: Technical Photography	207
B.8.2 Project 9.6: Stabilization (Production)	208
B.8.3 Project 9.7: Stabilization (Experimental)	208

ILLUSTRATIONS

CHAPTER 1 INTRODUCTION

1.1 Organization, Planning Phase	19
1.2 Organization, Operational Phase	19

CHAPTER 2 BLAST MEASUREMENTS

2.1 Composite UPSHOT-KNOTHOLE-TUMBLER-IVY Time-of-arrival Curve	47
2.2 Proposed Standard Free Air Peak Overpressure Curve	48
2.3 Free Air Peak Overpressure and Peak Dynamic Pressure for Various Altitudes	49
2.4 Free Air Overpressure Positive Phase Duration (A-Scaled)	50
2.5 TNT Efficiency Vs Free Air Peak Overpressure, Using Kirkwood-Brinkley Reference Curve for TNT	51
2.6 Free Air Peak Dynamic Pressure Vs Free Air Peak Overpressure for Various Altitudes	52
2.7 Schematic Drawing of Ideal Regular and Mach Reflection	53
2.8 Ideal Peak Overpressure Height-of-burst Curves	54
2.9 Ideal Peak Dynamic Pressure Height-of-burst Curves	54
2.10 Photograph of Preshock Popcorning, Operation TUMBER-SNAPPER	55
2.11 Schematic Diagrams of Precursor Formation	56
2.12 Ground-level Peak Overpressure, Shot 9, with Ideal Curve	57
2.13 Ground-level Peak Overpressure, Shot 10, with Ideal Curve	58
2.14 Sample Shot 10 Ground-level Overpressure Vs Time Records in Nonideal Region	59
2.15 Ground-level Peak Overpressure, Shots 1 and 11, with Ideal Curves	60
2.16 Sample Shot 1 and Shot 11 Ground-level Overpressure Vs Time Records in Nonideal Region	61
2.17 Shot 9 and TUMBLER Shot 1 Ground-level Peak Overpressure	62

ILLUSTRATIONS (Continued)

	Page
2.18 Shot 1 and GREENHOUSE Dog and Easy Peak Overpressure	63
2.19 Same as Shot 1 and GREENHOUSE Dog Overpressure Vs Time Records	64
2.20 Shot 9 Aboveground Peak Overpressure	65
2.21 Shot 10 Aboveground Peak Overpressure	66
2.22 Positive Phase Duration Vs Peak Overpressure, All Available Shots	67
2.23 Positive Phase Impulse Vs Peak Overpressure, All Available Shots	68
2.24 Positive Phase Duration and Arrival Time, Shot 9	69
2.25 Positive Phase Duration and Arrival Time, Shot 10	70
2.26 Measured Dynamic Pressure, Shot 9, Compared to Ideal and to Dynamic Pressure Computed from Measured Peak Overpressure	71
2.27 Sample Dynamic Pressure Vs Time Records, Shots 1, 10, and 11	72
2.28 Measured Dynamic Pressure, Shots 1, 10, and 11, Compared to Ideal and to Dynamic Pressure Computed from Measured Peak Overpressure	73
2.29 Precursor Development, Shot 11	74
2.30 Precursor Shock Contours, Shot 1	76
2.31 Precursor Shock Contours, Shot 10	77
2.32 Photograph of Dust Pedestal, Shot 11	78
2.33 Preshock Air Temperature, Shot 10	79
2.34 Preshock Air Temperature, Shot 11 and TUMBLER 4	80
2.35 A-scaled Overpressure Vs Time Records, Shots 10 and 11	81
2.36 A-scaled Overpressure Vs Time Records, Shots 11 and TUMBLER 4	82
2.37 Dynamic Pressure and Static Overpressure Vs Time, 2000 Ft, Shot 10	83
2.38 Comparison of Precursor Criteria	84
2.39 Overpressure Vs Time Records Along Main Blast Line and Smoke Line, Shot 10	85
2.40 Surface-level Peak Overpressure Vs Ground Range, Main Blast Line and Smoke Line, Shot 10	87
2.41 Arrival Time of Initial Disturbance Along Main Blast Line and Smoke Line, Shot 10	88
2.42 Photographs of Popcorning Phenomenon in the Laboratory	89
2.43 Preshock Pressure Vs Time Records, Shots 9 and 10	90
2.44 Mach Stem Height Vs Ground Range, Shot 9	91
2.45 A-scaled Mach Stem Height, Comparison of Shot 9 and TUMBLER 1	92
2.46 Mach Stem Height Vs Ground Range, Shots 1 and 10	93
2.47 Comparison of Scaled Nuclear and HE Data for Mach Stem Height	94
2.48 Ground-level Peak Overpressure Vs Ground Range, Shots 1, 3, 4, 9, 10, and 11 (A-scaled)	95
2.49 Comparison of Ideal Peak Overpressure Height-of-burst Curves with U-K Data	96
2.50 Comparison of Ideal Peak Dynamic Pressure Height-of-burst Curves with U-K Data	97
CHAPTER 3 THERMAL-RADIATION MEASUREMENTS	
3.1 Total Incident Thermal Energy Vs Ground Distance (NRDL Data)	106
3.2 Thermal Yield as a Function of Total Weapon Yield	107
3.3 Time of Minimum Vs Total Weapon Yield	107
3.4 Time of Second Maximum Vs Total Weapon Yield	108
3.5 Percentage of Total Thermal Energy Vs Time, Shots 4 and 9	109
3.6 Percentage of Total Thermal Energy Vs Time, Shots 10 and 11	110
3.7 Thermal Energy Normal to Ground Vs Ground Range, BUSTER- TUMBLER-KNOTHOLE Series	111

ILLUSTRATIONS (Continued)

Page

CHAPTER 4 NUCLEAR RADIATION MEASUREMENTS

4.1	Gamma Data, Shots 1, 2, 5, and 7 for Air Density = 1.0×10^{-3} g/cm ³	116
4.2	Gamma Data, Shots 3 and 6 for Air Density = 1.0×10^{-3} g/cm ³	117
4.3	Gamma Data, Shots 8 and 9 for Air Density = 1.0×10^{-3} g/cm ³	118
4.4	Gamma Data, Shot 10 for Air Density = 1.0×10^{-3} g/cm ³	119
4.5	Photon Spectral Distribution, Shot 11 (H + 3)	120
4.6	Dose Rate Vs Energy, Shot 11 (H + 3)	121
4.7	Shot 8 Gold and Tantalum Data	122
4.8	Shot 9 Gold and Tantalum Data	123
4.9	Shot 10 Gold and Tantalum Data	124
4.10	Sulfur Neutron Data for Shots 8, 9, and 10	125
4.11	Fission Threshold Detector Data	126

APPENDIX B PROJECT SUMMARIES

B.1	Instrumentation Chart, Shots 9 and 10	209
B.2	Instrumentation Chart, Shots 1, 3, 4, 7, and 11	211
B.3	Cubicles on Arc at 4900-ft Radius	212
B.4	A Typical Steel Cylinder (Project 3.3d)	212
B.5	Plate Girder Section (3.4f)	213
B.6	Postshot Failure of Truss Section, Structure 3.4a	213
B.7	Typical Roof Panels in Reinforced Concrete Cell Structure	214
B.8	Structure 3.5c Wall Panels in Place Prior to Shot 9	214
B.9	Structure 3.7 in the Process of Construction	215
B.10	Placing Beam Strips on Structure 3.8	215
B.11	View of some Typical Emplacements Prior to Shot 9	216
B.12	Foxhole Lined with Aluminum Sheeting Prior to Shot 9	216
B.13	Structure 3.11b After Shot 9	217
B.14	Structure 3.12 with Door Removed Prior to Shot 9	217
B.15	Structure 3.13b Prior to Shot 9	218
B.16	Structure 3.14 Frame Without Siding	218
B.17	Aerial View of Structure 3.14 After Shot 10	219
B.18	Corrugated Steel Shelter Before Placement of Earth Cover	219
B.19	Structure 3.16a After Shot 10	220
B.20	Tree Stand Prior to Shot 9	220
B.21	Tree Stand After Shot 9	221
B.22	Radial Pole Line with Aluminum Towers in the Distance	221
B.23	Bailey Bridge at 4100 Ft Prior to Shot 9	221
B.24	Bailey Bridge at 2100 Ft After Shot 10	222
B.25	LVT in Position Prior to Shot 10	222
B.26	LVT at 1030 Ft After Shot 10	222
B.27	Typical Quartermaster Corps POL Station Prior to Shot 9	223
B.28	Typical Marine Corps Assault Type POL System Prior to Shot 9	223
B.29	Medical Installation Before Shot 9	224
B.30	Medical Installation at 4163 Ft After Shot 9	224
B.31	Structure 3.29c Showing Solid Curtain Walls	225
B.32	Structure 3.29d Showing Curtain Walls with Window Openings	226
B.33	Nylon Thread and Carbon Paper Initiator on a Spring-wound Pressure-time Self-recording Gage	227



TABLES

	Page
CHAPTER 1 INTRODUCTION	
1.1 Summary Data for All Shots	18
CHAPTER 2 BLAST MEASUREMENTS	
2.1 UPSHOT-KNOTHOLE Shot Summary and Scaling Factors	21
2.2 Characteristics of Nuclear Detonations at Intermediate Height over Various Surfaces	31
2.3 Burst Heights, UPSHOT-KNOTHOLE Shot 1, GREENHOUSE Dog and Easy	33
2.4 Comparison of Measured and Calculated Dynamic Pressures in Precursor Region	37
CHAPTER 3 THERMAL-RADIATION MEASUREMENTS	
3.1 Total Thermal Energy and Air Transmissivity, All Shots	101
3.2 Times to First Minimum and Second Maximum, All Shots	102
CHAPTER 4 NUCLEAR RADIATION MEASUREMENTS	
4.1 Initial Gamma Data	113
4.2 Field Measurement Locations	113
4.3 Summary of Sulfur and Gold Neutron Data	115
APPENDIX B PROJECT SUMMARIES	
B.1 Summary of Test Data, Wall Panels	162
B.2 Summary of Test Data, Roof Panels	162

~~SECRET~~

CHAPTER 1

INTRODUCTION

1.1 BACKGROUND

Military weapons effects tests in the past have been conducted either in conjunction with the Atomic Energy Commission (AEC) development tests or for the purpose of studying certain basic phenomena. The AEC development tests are frequently unsuitable for effects studies because of the experimental nature of the devices being tested. There have been two effects phenomena tests, the surface and the underground detonations (Operation JANGLE) in the fall of 1951, and the air-burst detonations (Operation TUMBLER) in the spring of 1952. Operation JANGLE was not entirely suitable for general air blast effects studies because of the small size of the weapons and the peculiar nature of the detonations. Operation TUMBLER was conceived and executed in a period of less than six months in order to provide height-of-burst blast data which were urgently required for operational planning. This precluded the inclusion of weapons effects studies other than those directly related to the basic objective of the test.

In October 1951, the Chief, Armed Forces Special Weapons Project (AFSWP), recommended to the Chiefs of the services that a large-scale military weapons effects test be held in the spring of 1953 at the Nevada Proving Grounds (NPG). The objective of such a test was to provide the services with an opportunity to obtain general effects information. Although a considerable amount of effects data was obtained at Operation GREENHOUSE, it was felt that a large-scale test for the sole purpose of weapons effects studies was required in order to extend the GREENHOUSE results, which indicated serious gaps in the over-all knowledge of weapons effects. The logistical problems inherent in an overseas operation plus the proved feasibility of continental atomic tests resulted in the decision to recommend a test at the NPG. Specifically it was hoped that this test would permit the exposure of many critical items of military equipment as well as idealized structures and other targets of military significance. In recommending the test it was pointed out that the majority of the military requirements for effects information could probably be met by utilizing one nominal yield air-burst weapon, detonated at an operational height, but that additional weapons, not to exceed the total of three, might be required. In December 1951, the Joint Chiefs of Staff (JCS) approved the recommendations of the Chief, AFSWP, subject to a further recommendation at a later date as to the exact nature and number of the weapons to be fired. The code name KNOTHOLE was assigned to the operation.

On receipt of JCS approval, the AFSWP queried the services as to the specific test projects which they felt should be conducted, and in addition solicited recommendations as to the type of burst or bursts which they considered necessary. Replies for the most part indicated a desire for an air-burst weapon of approximately 30 KT at a height of approximately 2000 ft. The subject of another underground burst, utilizing a much larger weapon than was used in Operation JANGLE, was discussed. However, it was finally agreed that, due to the uncertainties concerning

~~SECRET~~

the significant effects parameters of an underground shot, no further consideration should be given to scheduling a second underground shot in the spring of 1953.

At the time that the military effects test was first recommended, no AEC development tests were scheduled for the spring of 1953. Therefore it was tentatively planned to conduct the operation in a suitable area of Yucca Flat where certain fixed facilities were available. The target date was to be 1 April 1953. In April 1952 a portion of TUMBLER was conducted on the dry lake in Frenchman Flat. An extensive instrument line consisting of gage towers and instrument shelters was constructed for this operation. In addition, timing lines and power were installed in the area. Therefore, when it was announced that there would be a series of development tests (UPSHOT) beginning approximately 1 March 1953 in the Yucca Flat area, an agreement was reached with the AEC to conduct the KNOTHOLE tests in the Frenchman Flat area where test construction could proceed without interruption during the period of the development shots in Yucca Flat. To avoid any possible interference and to meet construction and project participation schedules, the target date for KNOTHOLE was delayed to 1 May 1953.

1.2 TECHNICAL PROGRAM

Recommended test projects were received by the Chief, AFSWP, from the services during April 1952. These projects were carefully reviewed in an effort to eliminate duplications and to ensure that all proposals were technically sound and capable of accomplishment. After numerous conferences and discussions with the services, an integrated test program was formulated. This program was submitted to the Research and Development Board (RDB) in May 1952, where it was reviewed by an *ad hoc* panel. Extensive modifications to the program were recommended in order to reduce the total Research and Development (R&D) cost, and after further review by the AFSWP and the services, the program received final approval in September 1952. Because of the budgetary limitations which were imposed by the RDB, it was necessary for the Technical Director to review in detail each experimental project with a view toward reducing the costs to the absolute minimum consistent with the approved experimental objectives. This review was completed in November 1952, and all project agencies were informed of the funds which would be available for their projects. In the meantime, however, fund advances had been made by the Chief, AFSWP, to those agencies whose tasks required early procurement of critical items of equipment as well as the letting of contracts for preliminary design work. Fixed-cost contracts for construction of experimental structures in Frenchman Flat were let by the Santa Fe Operations Office, AEC, during early December 1952, and actual construction work commenced immediately thereafter.

In approving the conduct of a military effects test, the JCS had directed that an invitation be extended to the Federal Civil Defense Administration (FCDA) to participate in the test under conditions to be specified by the Department of Defense (DOD). These conditions precluded the completely "open" shot desired by the FCDA. However, it was possible to include in the technical program an extensive project designed by the FCDA to determine the reaction of various types of exterior wall panels to air blast.

1.3 TEST OF THE 280-MM GUN

In December 1952, the JCS directed the Chief, AFSWP, to include in the plans for Operation UPSHOT-KNOTHOLE a full-scale test firing of the 280-mm gun employing the Mk-9 projectile and to incorporate in this test those military effects experiments which could be adapted to this type of detonation. Because of the requirement for making accurate diagnostic measurements in connection with the firing of the Mk-9 weapon, it was necessary to fix the height of burst at 500 ft with Ground Zero the same as for the air-drop detonation. A careful review was made of all military effects experiments in order to ensure that test targets were located for maximum advantage on Shots 9 and 10. In addition, the scope of each of the basic measurement programs—blast, thermal, and nuclear—was extended to cover the Mk-9 shot.

1.4 ORGANIZATION

Effective 1 August 1952, the Chief, AFSWP, assigned to the Commanding General, Field Command, AFSWP, the responsibility for the detailed planning and implementation of approved military effects tests conducted in connection with continental atomic test operations. The Commanding General, Field Command, established within his headquarters the Directorate of Weapons Effects Tests (DWET) as the staff agency to carry out this responsibility, which included technical direction of the military effects experiments. Within the DWET, the Office of the Technical Director was responsible for implementing the directive of the Chief, AFSWP. The Technical Director was appointed in August 1952. His office functioned under the DWET until 1 March 1953. At that time operations commenced at the NPG, and a joint AEC-DOD organization became effective. Within this joint organization, the Office of the Technical Director became the Military Effects Group in the joint AEC-DOD organization. The Technical Director became the Director of the Military Effects Group, reporting directly to the Test Director. Figure 1.1 shows the organization during the planning phase, and Fig. 1.2 shows the organization at the NPG during the operational phase.

1.5 SHOT SCHEDULE

Original plans for UPSHOT-KNOTHOLE included a total of 10 shots, the first eight to be developmental and fired in Yucca Flat, and the last two for military effects, fired in Frenchman Flat. Toward the end of the operation another development shot was added to the test series. A complete listing of all shots in the UPSHOT-KNOTHOLE series is shown in Table 1.1

DNA
(6X3)

TABLE 1.1—Summary Data for All Shots

	SHOT 1	SHOT 2	SHOT 3	SHOT 4	SHOT 5	SHOT 6	SHOT 7	SHOT 8	SHOT 9	SHOT 10	SHOT 11
DATE	17 MAR	24 MAR	31 MAR	6 APR	18 APR	11 APR	25 APR	19 MAY	8 MAY	25 MAY	4 JUNE
TIME (GMT)	1310 00 128	1310 00 086	1259 59 995	1529 58 415	1234 59 958	1244 59 781	1229 59 763	1230	1529 55 562	1530	1115
LOCATION (AREA)	T-3	T-4	T-7-5-9	T-7-3	T-2	T-4-0	T-1	T-1-0	FF	FF	T-7-3
YIELD (KT)	16.2	24.5	0.20	11.0	23.0	0.22	43.4	27.0	26.0	14.9	60.8
RAD CHEM								HARRY	ENCORE	GRABLE	GLIMAX
GONE NAME	JANNIE	NANCY	RUTH	DIXIE	BADGER	RAY	SIMON				
WEAPON											
HEIGHT OF BURST (FT)	300 Tower	300 Tower	300 Tower	6027 Air	300 Tower	100 Tower	300 Tower	300 Tower	2423 Air	524 Air	1334 Air
HEIGHT OF BURST (FT) (SCALED TO 1 KT AT SEA LEVEL)	112.5	97.8	486.3	2377.5	99.6	157.2	60.8	94.8	764	203.6	316.6
GROUND ZERO - RELATIVE TO AIMING POINT (FT)				72 N 56.5 E					837 S 15 W	139 S 86 W	232 N 172 W
ATMOSPHERIC PRESSURE (mb)	876	870	873	861	862	869	870	874	900	901	887
GROUND ZERO	866	860	863	866	852	866	860	864	825	884	824
BURST HEIGHT	2.7	9.9	4.4	15.5	7.7	-0.3	11.7	14.3	16.7	14.8	13.3
AIR TEMPERATURES (DEGREE C)	7.9	13.3	8.2	-0.6	7.2	-0.1	15.3	18.3	18.0	13.1	12.2
GROUND ZERO											
BURST HEIGHT	4.3	3.9	4.8	2.5	4.0	4.3	2.6	3.5	1.9	3.2	3.0
RELATIVE HUMIDITY (%)	38	32	32	16	39	40	26	36	23	23	38
GROUND ZERO											
BURST HEIGHT											
SURFACE WIND - DIRECTION AND VELOCITY (KNOTS)	CALM	310 02	360 04	045 07	360 09	045 05	340 05	020 05	190 05	360 04	045 03
ATMOSPHERIC TRANSMISSION (% / mi)	9.4	9.4	9.5	9.2	9.7	9.5	9.57		92.5	91	93

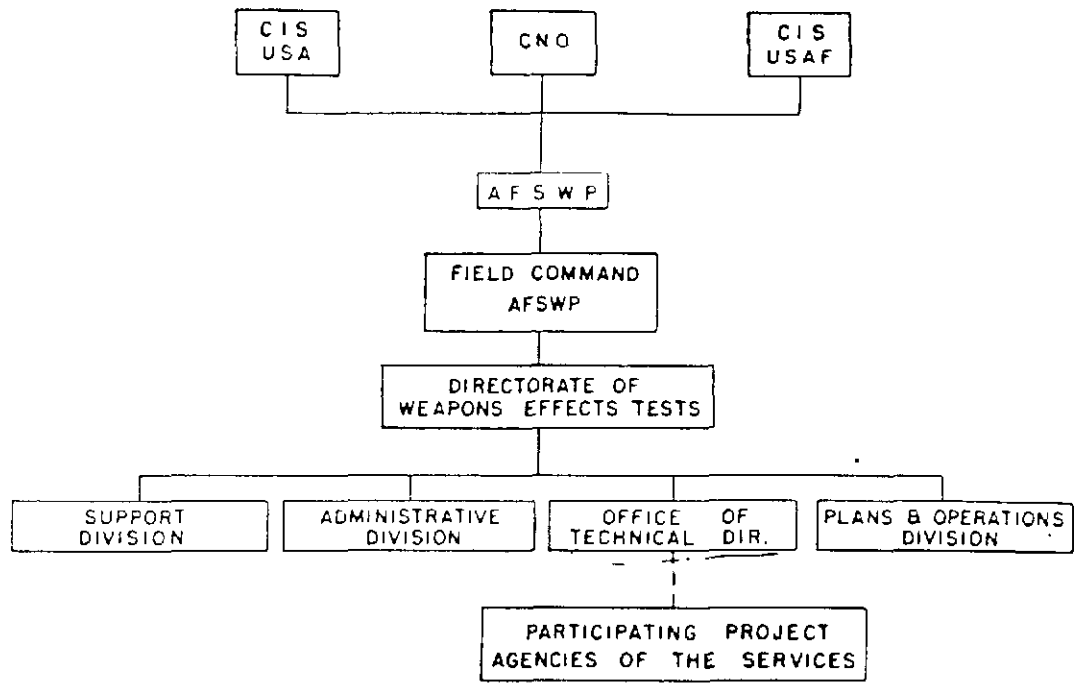


Fig 1 1 — Organization, Planning Phase.

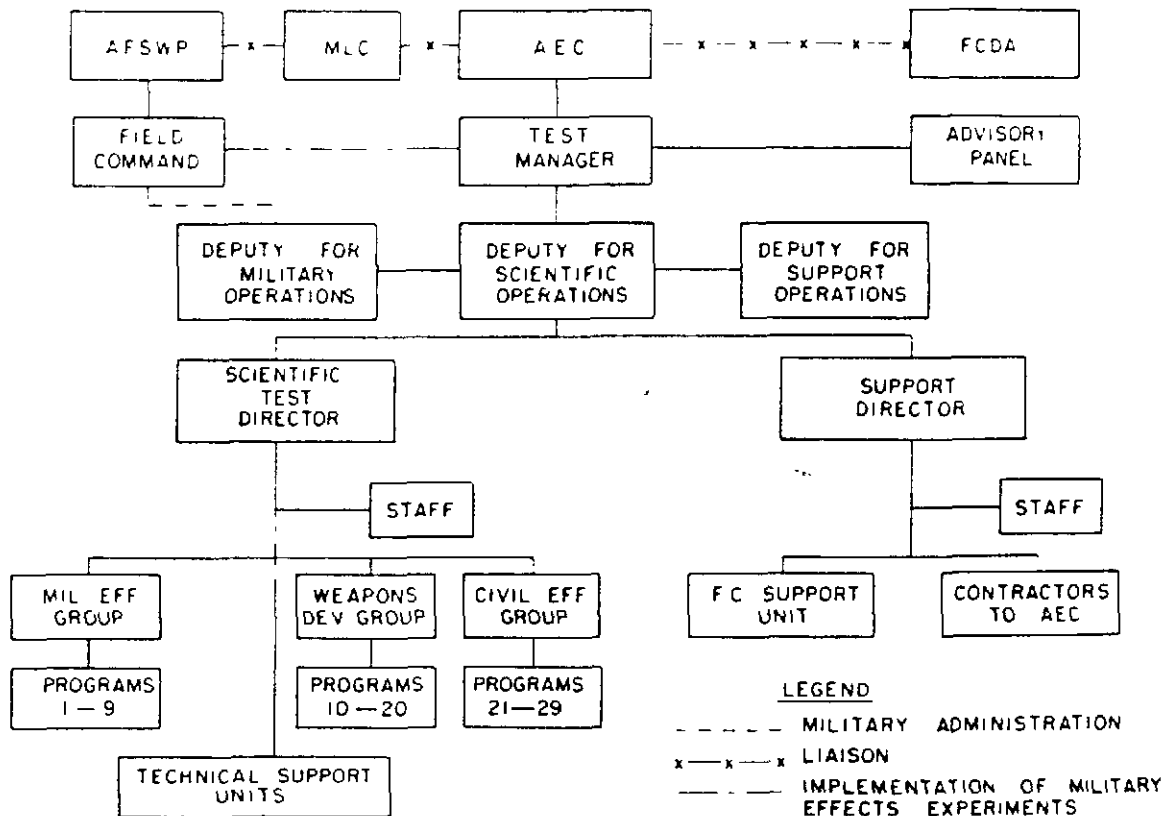


Fig 1 2 — Organization, Operational Phase.



CHAPTER 2

BLAST MEASUREMENTS

2.1 INTRODUCTION

Several agencies participated in the study of basic blast phenomena during UPSHOT-KNOTHOLE. The objectives were twofold, (1) to collect reference blast data in support of the major concurrent program studying the effects of blast on structures, and (2) to study further the fundamental characteristics of the blast phenomena of air-burst nuclear weapons.

Measurements were made on seven test shots of the series. For the first objective the program was highly successful. Many successful measurements were made for the second objective. However, the program served principally to define more clearly the areas of uncertainty in basic blast phenomena. In particular, much valuable information was obtained on the peculiar effects of thermal radiation on blast, but it was clear that major future tests would be required to obtain a satisfactory understanding of this most difficult and perplexing characteristic of air-burst nuclear weapons. The test results were invaluable as an aid in the design of future precise laboratory and full-scale experiments directed toward an adequate understanding of the complex thermal and surface effects of blast to meet military requirements.

In this summary report the pertinent results of the various projects are collected, correlated, and presented. Where appropriate and useful the results are compared to those of earlier nuclear tests. Individual project objectives and results are summarized in Appendix B. The interested reader is referred to the individual project reports for a full presentation of the results summarized here and for much additional information which is not presented here.

2.2 SCALE FACTORS

For many treatments it is desirable to compare the blast data obtained from different nuclear weapons at various burst altitudes. For such treatments the data are normalized to a common base. The term "A-scaled" is defined as "reduced to a standard atmosphere at sea level for 1 KT of radiochemical (RC)* yield." Conventional cube root yield scaling is used in conjunction with the Sachs' correction factors for burst-height atmospheric pressures and temperatures. The following A-scaling factors apply:

*In some cases other techniques, such as fireball analysis or the analytic solution, are used to determine the hydrodynamic yield of a nuclear detonation.

$$\text{Pressure } S_p = \frac{14.7}{P_c}$$

$$\text{Distance } S_d = \left[\frac{P_0}{14.7} \right]^{1/3} \left[\frac{1}{W} \right]^{1/3}$$

$$\text{Time } S_t = \left[\frac{T_0 + 273}{293} \right]^{1/2} \left[\frac{P_0}{14.7} \right]^{1/3} \left[\frac{1}{W} \right]^{1/3}$$

$$\text{Impulse } S_i = \left[\frac{T_0 + 273}{293} \right]^{1/2} \left[\frac{14.7}{P_c} \right]^{2/3} \left[\frac{1}{W} \right]^{1/3}$$

14.7 = 1013 mb

(2.1)

where P_0 and T_0 are the ambient pressure and temperature at the test burst height in pounds per square inch and degrees centigrade, and W is the finally determined radiochemical test yield. The Sachs' burst-height correction factors have been specified for use by all test groups to permit direct comparison of the test results with those from previous test series which have been normalized in this manner.

TABLE 2.1 — UPSHOT-KNOTHOLE Shot Summary and Scaling Factors

	Shot 1	Shot 4	Shot 9	Shot 10	Shot 11
Type of burst	Tower	Air	Air	Air	Air
KT (RC)	16.2	11.0	26.0	14.9	60.8
Height of burst (ft)	300	6022	2423	524	1334
Scaled height of burst	112.5	2377.5	764.0	203.6	316.6
S_p , Pressure factor	1.1704	1.4774	1.226	1.146	1.2301
S_d , Distance factor	0.3750	0.3948	0.3153	0.3885	0.2373
S_t , Time factor	0.3672	0.3807	0.3088	0.3839	0.2341
S_i , Impulse factor	0.4298	0.5624	0.3792	0.4399	0.2880

It has been suggested that the Sachs' conversion factors corresponding to gage height conditions or the more complex Fuchs' factors would afford better accuracy in conversion to sea level. It is probable that more realistic conversion is accomplished by one of these variations, but the errors introduced by the more simple conversion factor are generally unimportant for the test conditions encountered to date.

Table 2.1 presents the pertinent normalizing factors for the UPSHOT-KNOTHOLE shots of interest. A-scaled data reported herein have been obtained by applying these factors to the measured results.

2.3 FREE AIR BLAST

2.3.1 Overpressure

The primary free air peak overpressure measurements were made by the shock velocity method, using shock front photography against a vertical, rocket laid, smoke-trail background. Useful data for overpressures greater than 10 psi were obtained on Shots 4, 9, 10, and 11. The free air time-of-arrival data from these shots were normalized to standard 1 KT at sea level and combined with similar normalized data from TUMBLER Shots 1, 2, 3, and 4 and the IVY King shot to give the early portion of the resultant composite arrival time curve of Fig. 2.1. The balance of the composite time-of-arrival curve includes surface and airborne measurements. These data were then used to calculate a single peak overpressure vs distance curve applicable to the region where the peak overpressures were greater than 10 psi. Figure 2.2 presents this composite free air overpressure curve in this region.

Below 10 psi free air overpressure measurements were made by the use of Wiancko overpressure vs time gages mounted near the ground surface, but above the triple point, and by

UNCLASSIFIED DATA

parachute-borne gages at relatively high altitudes above the triple point. Measurements below 10 psi were obtained on Shots 4 and 9 of UPSHOT-KNOTHOLE and were combined with similar data from TUMBLER to obtain the composite curve shown in Fig. 2.2 for overpressures less than 10 psi.

Figure 2.2 presents a proposed standard free air peak overpressure curve for 1 KT at sea level, using all experimental data available to date. The yields used ranged from 1 to 500 KT, and it is believed that the curve is applicable up to yields of several megatons. For different yields and ambient pressures the proposed standard curve can be used by applying the appropriate scaling factors. To illustrate the effect of burst altitude (ambient pressure) using simple Sachs' scaling, the curves of Fig. 2.3 are included. These curves, which are useful in considering antiaircraft applications, are applicable only in the horizontal burst plane because of the nonuniform characteristic of the atmosphere. This restriction is significant for large yield weapons. However, it should be mentioned that experience on Shot 4 indicates that it may be reasonable to conclude that energy partition characteristics do not vary significantly for bursts up to an altitude of 10,000 ft MSL.

2.3.2 Dynamic Pressure

In some cases dynamic pressure, or q , is the free air blast parameter of principal importance. The peak free air dynamic pressure may be calculated directly from the peak overpressure. Figure 2.3 gives peak free air dynamic pressure for two widely different ambient pressures. It is worth noting that the dynamic pressure is nearly independent of the burst altitude. Once again, the nonuniform characteristic of the atmosphere limits direct application to the horizontal burst plane, but for dynamic pressure the restriction is not as severe as for overpressure. This parameter, free air dynamic pressure, is of importance in the gust loading on aircraft in flight and is frequently a useful damage parameter when considering nuclear weapons for antiaircraft purposes.

2.3.3 Duration

The free air overpressure positive phase durations for 1 KT at sea level are presented in Fig. 2.4. These data were obtained from IBM calculations,¹ and they have been checked by limited experimental measurements. Since the particle velocity does not fall to zero until after zero overpressure is reached, the positive phase durations for dynamic pressure are somewhat larger than shown in Fig. 2.4.

2.3.4 TNT Efficiency

The TNT efficiency of a nuclear explosion expressed in percentage of the radiochemical yield can be defined in terms of the amount of TNT required to produce an equal blast effect at the same distance using applicable scaling techniques. With peak free air overpressure chosen as the parameter for comparison, the TNT efficiency is a function of the overpressure level. Using the proposed nuclear free air overpressure curve of Fig. 2.2 and the Kirkwood-Brinkley data for TNT,² the TNT efficiency has been calculated as a function of peak free air overpressure as shown in Fig. 2.5. Over the wide pressure range of 1 to 350 psi, which covers the region of principal interest, the TNT efficiency ranges from 40 to 53 per cent. Over this pressure range an average TNT efficiency of 46.5 per cent results.

2.4 AIR BLAST PHENOMENA

Except where thermal and or surface effects were important, the blast measurements of UPSHOT-KNOTHOLE were consistent with predictions based on the results of previous full-scale tests and with analytical studies and laboratory and high-explosive tests. In fact, the UPSHOT-KNOTHOLE blast results are noteworthy principally because they clearly delineated

some of the unusual surface and/or thermal effects with a simultaneous demonstration of the damage effects of blast waves produced under such influences. On the basis of the UPSHOT-KNOTHOLE results, it is not possible to establish the behavior characteristics where thermal and or surface effects are important. The purpose of this section is to describe, in general terms, the blast phenomena investigated on UPSHOT-KNOTHOLE. The later sections, which summarize the blast results, will show the inconclusive nature of the results and will support a conclusion that extensive additional laboratory and full-scale experiments are required to permit a clear understanding of the military importance of thermal and/or surface effects on the air blast phenomena of air-burst nuclear weapons.

2.4.1 Damage Parameters

The damage effectiveness of a blast wave can be described by two parameters: static overpressure (p) and dynamic overpressure (q), both as functions of time. In most cases rise time, duration, and impulse are important in determining the effects of these two parameters, but some targets are predominately sensitive to the peak values of overpressure or dynamic pressure.

There have been a number of attempts to classify military blast targets as "pressure-sensitive" or "drag-sensitive," dependent upon whether they have principal sensitivity to overpressure or dynamic pressure, respectively. Except for extreme cases, such attempts are unsuccessful because most individual targets have appreciable sensitivity to both damage parameters. Target elements which have a rapid response to the relatively short duration reflected overpressures which are characteristic of a zero rise time ideal shock, such as window panes and stiff or brittle walls and roofs, are pressure-sensitive. Likewise, targets which are sensitive to a sustained crushing effect, likened to a sudden increase of the ambient pressure by the overpressure, without venting, are pressure-sensitive. Targets, such as poles and trees, which have a relatively slow response and which are insensitive to crushing effects, are nearly completely drag-sensitive. A large steel frame structure, which is well vented or which has been stripped of siding and or roof panels by initial overpressure action, is principally drag-sensitive. Many military targets, such as vehicles, tanks, artillery pieces, and troops, may suffer their principal damage by being hurled through the air or tumbled along the ground, with subsequent impacts with the ground or other obstacles. These targets are principally drag-sensitive. In general, where total translational forces are important and where the short durations of the reflected overpressures are substantially less than the response time of the target, the forces produced by dynamic pressure are of greatest importance. Most military target complexes are apt to contain a variety of individual target types, and any attempt to describe the whole as dynamic pressure-sensitive or as overpressure sensitive could be troublesome. In some cases the difference in the blast wave duration between kiloton and megaton weapons is important, and such targets can generally be described as dynamic-pressure-impulse sensitive.

In general, both overpressure and dynamic pressure are important with the relative importance being determined by the target type under consideration and by the relation between the two damage parameters. The overpressure characteristics of a nuclear explosion are fairly well known, whereas the dynamic pressure characteristics have been less clearly defined because of the lack of sufficient applicable experimental data. The results of UPSHOT-KNOTHOLE clearly demonstrated some of the damage effectiveness of dynamic pressure with few supporting basic measurements. Where possible, this report will treat both the overpressure and the dynamic pressure properties of air-burst nuclear explosions.

2.4.2 Ideal Parameters

An ideal blast wave may be defined as a shock wave where the classical Rankine-Hugoniot relations apply at the shock front. Such a shock wave is characterized by an instantaneous rise of pressure, density, temperature, and particle velocity. Assuming the ambient air to be at

rest with a pressure of P_c the relation between peak overpressure (p) and peak dynamic pressure (q) is:

$$q = \frac{1}{2} \rho u^2 = \left(\frac{5}{2}\right) \frac{p^2}{7 P_c + p} \quad (2.2)$$

where ρ = density of medium behind shock front and u = particle velocity of medium behind shock front. This relation is illustrated in Fig. 2.6 for different burst heights or ambient pressures.

If a nuclear weapon is burst in the air over an ideal surface,* the resultant blast wave may be described as ideal. This definition of the ideal case is valuable for comparison to practical nuclear burst cases, particularly where the thermal and/or surface effects cause marked departures from ideal behavior. The ideal case is characterized by two principal regions, the regular reflection region and the Mach region (see Fig. 2.7). The ground distance at which transition from regular reflection to Mach reflection takes place is not only dependent upon the height of burst but upon the height above the ground at which the observations are made. Thus the ground distance at which a surface target is completely in the Mach region is dependent upon the height of that target, becoming greater as the target height is increased.

For the Mach stem in the Mach region, it may be assumed that the expanding shock front is perpendicular to the surface with the flow or particle velocity parallel to the surface and with the shock front moving into uniform still air. In the Mach region the above ideal p - q relation applies, where q is defined to be horizontal or parallel to the surface, and the ideal peak dynamic pressures may be calculated directly from peak overpressure values.

In the region of regular reflection the situation is more complex. At the reflecting surface the ideal reflected shock completely cancels the vertical component of material velocity behind the incident shock and the flow is parallel to the surface. However, for a target near the surface the principal or effective q component is parallel to the surface but not perpendicular to the reflected shock since the reflected shock makes an acute angle with the surface. In addition, the reflected shock is moving into ambient air which is neither at rest nor at preshock ambient pressure because of the prior passage of the incident shock. Consequently it is clear that the dynamic pressure q (horizontal) cannot be calculated by the above ideal p - q relation. Directly under the burst (Ground Zero) there is no air flow parallel to the surface and the dynamic pressure ($\frac{1}{2}\rho u^2$) is zero. As the ground range is increased the dynamic pressure increases despite a decrease in overpressure. Dynamic pressure is not described by the above ideal p - q relation until the onset of Mach reflection. For near-surface targets in the ideal case, only the horizontal flow is considered important since any vertical flow is quickly canceled after the arrival of the reflected shock. In general, dynamic pressure may be considered a vector quantity with a direction parallel to the reflecting surface in the region of interest for near-surface targets behind the reflected shock in the regular reflection region or behind the Mach stem in the Mach region. Throughout this report, when dealing with near-surface blast phenomena, dynamic pressure (q) information will refer to the horizontal component only.

Using the composite A-scaled free air peak overpressure curve of Fig. 2.2, it is possible to calculate the A-scaled surface level peak overpressure height-of-burst chart of Fig. 2.8 for the ideal case. In the region of regular reflection and for zero burst height, conventional shock reflection theory was used assuming a perfect reflective surface. In the Mach region the form of the curves was derived from high-explosive experiments. The ideal A-scaled peak dynamic

*An ideal surface will be defined as one having perfect mechanical or shock reflection, no dust or other material which can be picked up by the blast wave, and properties (perfectly reflecting) such that the associated thermal radiation has no effect on the surface or on the air above the surface. Ice is perhaps the closest practical example. Except for the possibility of the blast wave picking up water droplets, water might be a reasonably close practical example.

pressure height-of-burst chart of Fig. 2.9 can be derived from Fig. 2.8.*

Throughout this report references to ideal blast behavior will be made. Such references refer to the values of peak overpressure and peak dynamic pressure calculated from Figs. 2.8 and 2.9 for the particular set of test conditions involved, assuming a perfect shock reflecting surface with no other surface, dust, or thermal effects. Substantial departures from ideal behavior have been attributed to surface, dust, and thermal effects on blast. Under such perturbations the rise time is generally slow and the time-wave form is substantially different from ideal. Surface, dust, and thermal effects on blast are most pronounced for relatively low bursts where the principal interest is in the Mach region. For such bursts careful studies are not warranted on the regular reflection region because the very intense blast conditions there are beyond the range of most military targets of interest.

Substantial departures from ideal behavior were obtained on the relatively low shots of UPSHOT-KNOTHOLE (1, 10, and 11), with only minor departures on the relatively high Shot 9. In all cases the blast wave behavior was essentially ideal except for the regions where the surface level measured peak overpressures were greater than about 6 psi (corresponding to about 7 psi at sea level, A-scaled). Where the measured peak overpressures were greater than 6 psi, the departure from ideal varied greatly, depending on yield, height of burst, overpressure level or ground range, and the blast parameter considered.

2.4.3 Surface and Thermal Effects

2.4.3.1 History

The most significant blast results of UPSHOT-KNOTHOLE were obtained where behavior departed from ideal. Such departures have been attributed to surface and/or thermal effects on blast. Since it has not been possible to study the blast characteristics of nuclear explosions without the effects of the companion thermal radiation on the surface,[†] there have been no means for experimentally separating the surface and thermal effects on blast. High-explosive tests, which have negligible companion thermal radiation, have shown rather minor blast effects due to differences in surface mechanical reflection properties and surface dust. Surface nuclear explosions, where the thermal radiation incident on the blast surface is minimized, give similar results. In any event, the extreme blast deviations from ideal which have been observed on several low burst nuclear detonations are far greater than the perturbations observed for scaled TNT tests or for surface nuclear tests over the same kinds of surfaces. It appears safe to assume that the thermal radiation is the principal cause of the blast departures from ideal. Of course, the surface properties, including dust, can have a profound influence upon the degree to which the thermal radiation affects blast.

Anomalous blast behavior was observed on most nuclear test series prior to UPSHOT-KNOTHOLE. The role of thermal effects on blast was first clearly delineated on TUMBLER-SNAPPER, where the precursor phenomenon was identified. Subsequent reexamination of BUSTER and GREENHOUSE blast measurements confirmed the precursor existence and showed similar thermal perturbations on blast. It remained for the UPSHOT-KNOTHOLE series to investigate the effects of such nonideal blast waves on targets and to study further the associated basic blast phenomena. The effects on targets are described elsewhere in this report. Thermal effects perturbations on blast were observed in some detail on Shots 1, 9, 10, and 11 of UPSHOT-KNOTHOLE, covering a variety of yields and burst heights. Much additional valuable informa-

*F. H. Shelton of the Sandia Corporation prepared these figures expressly for this report. Reference is made to Report LA-1665, where similar curves were developed by Porzel.

†Project 8.4-2, the black smoke experiment of UPSHOT-KNOTHOLE Shot 10, was a limited and somewhat inconclusive effort in this direction. Had Project 8.4-1, the white smoke experiment of UPSHOT-KNOTHOLE Shot 9, not been canceled because of unfavorable weather, additional useful information might have been obtained.

tion was obtained, but it remains for future tests of a more specialized nature to establish a quantitative understanding of the nonideal blast wave along with an understanding of the parameters responsible for the generation of such blast waves. This is particularly important to aid in the prediction of the blast behavior of nuclear weapons at low burst heights over surfaces other than those characteristic of desert areas.

2.4.3.2 Thermal Boundary

The blast perturbations observed on previous test series and on Shots 1, 9, 10, and 11 of UPSHOT-KNOTHOLE can be explained in part, qualitatively, by the hypothesis that the thermal radiation creates a warm layer of air adjacent to the ground surface prior to shock arrival at the location observed. Analytical considerations and some supporting shock-tube experiments indicate that a conventional shock wave is markedly influenced by passage into a region having a nonuniform temperature or, more particularly, a nonuniform sonic velocity. It appears almost certain that the principal factors of the nonideal blast behavior can be ascribed to the existence of such a thermal layer adjacent to the ground surface.

To date there has been no adequate description of the effective mechanism responsible for the generation of the assumed thermal layer. Experimental measurements on previous nuclear tests and additional measurements on UPSHOT-KNOTHOLE have investigated the properties of this thermal layer prior to shock arrival. Such measurements have been only moderately successful. Attempts have been made to measure the air temperature directly by the use of thermocouples and similar devices. Attempts have also been made to measure the velocity of sound over a relatively short length of air near the ground surface prior to shock arrival. These measurements have shown conclusively that a warm air layer was developed following the detonation but prior to shock arrival at the location used for measurement. General instrumentation problems plus turbulence and atmospheric instability effects inherent to the heated region being investigated have reduced the value of these measurements in a quantitative sense. However, such measurements on Shot 4 of TUMBLER and Shots 9 and 10 of UPSHOT-KNOTHOLE have conclusively proved the existence of a preshock thermal layer adjacent to the ground surface. Details concerning temperatures, temperature gradients, and height at shock arrival have been inconclusive. The limited UPSHOT-KNOTHOLE results are reported in a later section of this report.

The exact mechanism of heat transfer which permits the generation of the warm air layer has not been established. A number of explanations have been offered. A commonly accepted qualitative explanation presupposes the existence of "popcorning." Above a normal incident thermal radiation threshold of 10 to 30 cal cm², many surfaces have been shown to expel some particulate matter into the surrounding air. The desert surfaces used for the nuclear tests are particularly subject to this effect. Figure 2.10 illustrates the popcorning observed on a nuclear test prior to shock arrival. The popcorned particles reach a distance of several feet above the ground surface by their own momentum. It is possible that these suspended particles, which are in motion, can absorb thermal radiation directly and then transfer the heat to the surrounding air. The resultant convection and turbulence could lead to the establishment of a thermal layer several feet thick. Another explanation does not require the existence of popcorning or its equivalent. It may be supposed that the ground surface is heated to a relatively high temperature which, in turn, can heat the boundary air surface, setting up convection and turbulence to ultimately develop a thermal layer several feet high. Several variations and combinations of these hypotheses have been presented.

UPSHOT-KNOTHOLE added no significant experimental data to identify the mechanism of heat transfer into the boundary air layer. Until an adequate understanding of the characteristics of this phenomenon has been obtained, it is unlikely that quantitative estimates can be made of the characteristics of the thermal layer, which are undoubtedly required before a quantitative estimate can be made of the effects on the blast wave.

Limited experiments, both on UPSHOT-KNOTHOLE and in the laboratory, have shown that thermal radiation incident upon organic surfaces, such as leaves and other vegetation, produces a violent expulsion of hot gases from the surfaces. Here a heat-transfer mechanism can be

rather clearly established, and it is conceivable that a nuclear detonation over a large surface of such material could produce a warm boundary layer resultant from the mixing of the high-temperature expelled materials with the surrounding air. Chemically, the resultant gas would probably be somewhat different from air, with a different ratio of specific heats and a different velocity of sound for a given temperature. Such a boundary layer would have a substantial effect on a blast wave if generated prior to shock arrival.

On the basis of UPSHOT-KNOTHOLE results, it is not possible to make quantitative statements concerning the nature of the thermal boundary layer or the surface properties responsible for its generation. It can be clearly stated that such a boundary does exist and that the characteristics of the boundary layer are influenced by the properties of the surface when subjected to the intense thermal radiation characteristic of a nuclear detonation. Consequently, it can be expected that the blast effects of different surfaces will be a function of their behavior under intense thermal radiation. Surfaces with good thermal reflecting properties, such as water and ice, will probably produce little or no thermal layer, with little or no associated thermal blast effects. Desert surfaces are known to have pronounced thermal effects, and other practical surfaces will probably lie somewhere between.

2.4.3.3 Thermal Effects

In a qualitative sense the effects of the postulated warm boundary layer of air are illustrated in Fig. 2.11. It must be emphasized that this figure is for illustration purposes only and does not purport to detail the complex effects of the thermal layer on blast. Specifically, all reflected shocks, both from the thermal layer and from the ground surface, have been eliminated. A more precise and complex treatment will be discussed, to a limited extent, later in this report, and for a complete treatment the interested reader is referred to the pertinent individual project reports.³⁻⁶ Figure 2.11 is illustrative, in a general sense, of the combined conditions existing on UPSHOT-KNOTHOLE Shots 1, 10, and 11 and TUMBLER Shot 4. In Region A, close to Ground Zero, the small incident angle of the blast wave, the high shock strength with the resultant high shock velocity, and the relatively short time interval between detonation and shock arrival at the thermal layer, which limits the boundary layer temperature rise prior to shock arrival, give a horizontal component of shock velocity greater than sonic velocity in the boundary layer. This effect produces a minor perturbation on the shock wave, which somewhat modifies the wave form but does not markedly change the resultant blast wave from the ideal case. In Region B the increased incident angle, the lower shock strength, and the possibly higher boundary layer temperature, because of the greater time interval between detonation and shock arrival, lead to a condition where the sonic velocity in the boundary layer is greater than the horizontal component of the shock velocity in the undisturbed air above the boundary layer. To preserve continuity as the shock wave progresses out to greater distances, the shock wave disappears in the boundary layer, leading to the generation of a precursor pressure wave. The precursor wave develops when a significant amount of energy from the main blast wave is channeled into a thermal layer near the ground surface. In Region C the conditions are similar except that this is the region of Mach reflection, where the triple point has risen well above the boundary layer, and consequently the shock above the boundary layer has a horizontal component equal to the shock velocity into the undisturbed air. Here, again, the requirement of continuity of the blast wave as it progresses to greater distances leads to the generation of a precursor pressure wave, as illustrated. The precursor is not confined to the relatively thin thermal layer but can extend to considerable heights into the unheated air. Region D occurs at greater distances, where the temperatures of the thermal layer are lower, giving a sonic velocity less than the shock propagation velocity in the undisturbed air. In this region the thermal effect produces a minor perturbation on the shock wave, which modifies the wave form slightly without markedly changing the resultant blast wave from the ideal case. As the blast wave progresses to still greater distances, the effect of the thermal layer becomes negligible and the general blast wave characteristics approach the ideal case. In a practical sense the thermal layer cannot be described in simple terms. There is undoubtedly some vertical temperature gradient to provide transition into the undisturbed region. Furthermore, the preshock

thermal effects will induce some turbulence. The horizontal temperature gradient is by no means uniform, and consequently a full treatment of the problem is very complex indeed. Until the specific properties of the thermal layer are more clearly understood, it is not likely that a completely adequate analytical treatment can be made. Nevertheless, the general qualitative description above should permit an understanding of the general characteristics of the effects of the thermal layer on blast.

As the burst height is increased, the incident thermal radiation is decreased and a situation can exist where a thermal boundary layer is generated without a sufficient temperature rise to result in the generation of a precursor. UPSHOT-KNOTHOLE Shot 9 was representative of this case. The incident shock was refracted, as indicated in Region A of Fig. 2.11, changing its incident angle with the ground and leading to the early onset of Mach reflection at the ground surface. The resultant "thermal-Mach" phenomenon on Shot 9 produced an effective Mach reflection beginning at much shorter distances than would have been expected without the thermal effect. In the thermal-Mach region the Mach stem height was approximately the same as the estimated thermal boundary layer height. Beyond the minimum distance at which normal Mach reflection would have been expected on this shot, the general Mach behavior appeared to be normal.

It has been customary to use the term precursor as a description of the blast conditions representative of low bursts where the thermal effects on blast are of major significance. It must be noted that the thermal effects on blast can be significant without the actual generation of a precursor, or outside the range of the precursor. The precursor is perhaps the most startling phenomenon associated with this general behavior, and the term precursor is used frequently in a general sense to describe the whole region where the thermal effects on blast cause significant departures from the ideal case. In some circumstances the term nonideal is used to describe this behavior.

The blast measurements on UPSHOT-KNOTHOLE do not permit a detailed description of the characteristics in the nonideal region. In general, where the behavior is nonideal, the peak overpressures are substantially less than would be expected in the ideal case. This suppression of overpressure exists out to ground ranges corresponding to peak overpressures of about 6 psi (as measured, 7 psi when A-scaled to sea level). This general conclusion applies to Shots 1, 10, and 11, where the thermal effects were very pronounced but where the A-scaled burst heights covered the range 113 to 317 ft. The relative reduction in measured peak overpressure due to thermal effects was greatest in the region of 9 to 40 psi, although the effects were noticed up to the highest pressures reliably measured, about 150 psi. The suppressed overpressure effect appeared to be greatest at the ground surface, with an increase of peak overpressure as the gage height above the ground was increased. For pure pressure-sensitive targets (for instance a buried structure with a plane top ground surface), the thermal effects could greatly reduce the damaging effects of low-burst nuclear weapons. However, this conclusion is applicable only to pressures greater than 7 psi, with principal importance for pressures greater than about 11 psi. In general, pressure rise time was rather slow in the region 10 to 30 psi, and the effectiveness of reflected pressures in determining target loading would consequently be reduced. This again would reduce the effectiveness of nonideal low bursts against pure pressure-sensitive targets in this pressure region.

The results on dynamic pressure measurements were not very extensive. Dynamic pressure is defined in terms of particle velocity, or wind behind the blast wave, and the density of the moving material behind the blast wave. All dynamic pressures discussed in this report refer to the horizontal component parallel to the ground surface. The precursor pressure wave appears to be strongly turbulent, with an initial vertical component of flow which is probably followed by a flow pattern effective in the lifting of surface material. The desert surfaces used for the UPSHOT-KNOTHOLE tests were very dusty. It appears that the precursor pressure wave has the effect of scouring up a large quantity of surface dust which is then suspended in the moving air through which the main blast wave later travels. No specific measurements have been made, but it is likely that the net density of the moving mass of material behind the main blast wave could be substantially increased by the amount of suspended particulate matter

contained therein. Consequently, there exists an uncertainty in the definition of the dynamic pressure, or q , in such a blast wave because of the uncertainty of the associated density term. This uncertainty is increased still further because it is impossible that the moving air mass may have a different effect on a target than the moving dust particles. For a given target or target element the drag coefficients for clean air and moving dust particles can be different. It is believed that the dynamic pressure instruments used for the measurement of q on UPSHOT-KNOTHOLE included the effects of the associated moving dust, but the dust contribution to the measured q may be different than its contribution to the determination of drag forces on targets. The exact correlation of these q measurements with the effects on targets of interest was not established because of the limited nature of such q measurements. All q measurements obtained on UPSHOT-KNOTHOLE gave peak values at least equal to or greater than the expected peaks under ideal conditions. In other words, the measured values of q in the region of non-ideal blast behavior were equal to or greater than the expected values in the ideal case. This is in direct contrast to the much more reliable measured values of peak overpressure. No generalizations can be made at this time since few reliable q measurements were obtained in the precursor region and since there has been no adequate analytical treatment presented to support a conclusion that the q in the nonideal case should be about the same or greater than the q in the ideal case. There is a temptation to conclude that for the nonideal case the q of the air alone will be the same as for the ideal case and the effective q in the nonideal case will be substantially increased over that for the ideal case because of the much greater amount of dust contained in the blast wave due to the prior agitation by the precursor pressure wave. However, such a conclusion is not warranted from the blast measurements of UPSHOT-KNOTHOLE.

There is very little test information in the ideal or clean Mach region for nuclear weapon blast waves having intensities corresponding to those observed on UPSHOT-KNOTHOLE in the nonideal case. A surface burst or a low air burst over an ideal surface would probably provide such test information. Such direct target effects as were observed on isolated pieces of military equipment on the 1.2-KT surface burst of JANGLE, when compared to tests on similar equipment on UPSHOT-KNOTHOLE, indicate that the damage sustained by these predominantly drag-sensitive targets on the low burst Shot 10 of UPSHOT-KNOTHOLE was equal to or greater than would have been expected at the same distances from a yield comparable to Shot 10 detonated at the surface or over an ideal surface (snow or water). Furthermore, for targets of concern which are exposed to the relatively high intensity blast prevalent throughout the major portion of the nonideal region of the UPSHOT-KNOTHOLE low bursts, it is likely that the drag-sensitive characteristics are of major importance. With the established suppression of overpressure in this region, if the dynamic pressures are not correspondingly suppressed, the drag sensitivity of most targets of military interest will become more predominant in determining the damaging effectiveness of low bursts in the nonideal region, even for many targets sometimes classified as principally pressure-sensitive.

UPSHOT-KNOTHOLE clearly demonstrated the effectiveness of nonideal low bursts in producing damage on drag-sensitive military targets in the nonideal region. There is no conclusive evidence that the damage produced was greater than would have been obtained for similar bursts in the ideal case. There is a possibility that this conclusion is justified due to the uncertain effects of the greater amount of dust contained in the blast wave in the nonideal case. It is presumed that nonideal low bursts are less effective against pressure-sensitive targets than ideal low bursts. However, this was not conclusively demonstrated in UPSHOT-KNOTHOLE because such targets were not included in the nonideal region.

2.4.3.4 Surface Mechanical Reflection Effects

Surface mechanical reflection effects have been observed on high-explosive tests.⁷ The desert surfaces used for UPSHOT-KNOTHOLE undoubtedly have lower shock reflection coefficients than an ideal rigid surface. However, based on high-explosive tests, the effects of the mechanical reflection coefficient are relatively small compared to the major perturbations observed due to thermal effects. It is probably safe to assume that the UPSHOT-KNOTHOLE

blast measurements were not greatly influenced by the surface mechanical reflection characteristics and that the general surface effects noted can be ascribed completely to thermal effects.

2.4.3.5 Surface Dust Effects

High-explosive tests over dusty surfaces have demonstrated small blast perturbations due to the dust. However, these perturbations are much less than the gross blast perturbations observed in the nonideal region on UPSHOT-KNOTHOLE. Once again it seems safe to assume that the surface dust effects on UPSHOT-KNOTHOLE were primarily a result of the associated thermal effects. As discussed above, the accompanying dust may have a very pronounced influence on the effects of the blast wave in the nonideal region. However, it is believed that such dust effects first require the generation of the precursor pressure wave which is produced by thermal effects. An attempt to separate dust effects from thermal effects is probably academic for low bursts since any practical dusty surface will have thermal properties leading to pronounced thermal effects. For relatively high bursts, such as UPSHOT-KNOTHOLE Shot 9, over a dusty region the effects of dust loading in the air behind the blast wave appear to be negligible. In the case of a surface burst over a dusty region it is hypothesized that no precursor pressure wave will be formed. Likewise, the dust effects are expected to be much less pronounced than those from a low burst with associated precursor effects. It is believed that surface dust could possibly have a significant influence on the blast parameters of military importance, namely, affecting damage at a greater radial distance than the same yield burst over a dust-free (ideal) surface would produce. The surface detonation of JANGLE did not provide conclusive evidence in this regard. Consequently, one must await future tests to establish the relative effectiveness of a low air burst vs a surface burst over different reflecting surfaces.*

2.4.3.6 Ideal, Desert, and Organic Surfaces

For analysis purposes, three representative surface conditions have been postulated for air-burst nuclear weapons. These conditions are identified as ideal, desert, and organic. They may be roughly described as follows.

1. Ideal: See Sec. 2.4.2.
2. Desert: Represented by Frenchman Flat and Yucca Flat of the NPG, over which rather considerable blast information has been obtained.
3. Organic: This surface is postulated to be one which has a pronounced thermal effect to permit the generation of a warm boundary layer of air with the resultant precursor for certain burst conditions but without any loose dust or other particulate matter available at the surface. In other words, this surface would permit the generation of a dust-free precursor for a low-burst weapon.

In practice, it is unlikely that any one of these three idealized surfaces will be encountered in regions of military interest. However, surfaces which can be represented by one of these three idealizations might be encountered, or surfaces combining their characteristics might be of interest. The UPSHOT-KNOTHOLE test results were obtained exclusively over desert surfaces. However, some of the overseas test results have been obtained over water surfaces, which might be reasonably representative of the ideal case, with the possible exception of the water loading which could develop behind the blast wave. No tests have been conducted over organic surfaces, but such an idealization could be representative of many target areas of military interest which contain a substantial percentage of vegetation areas or of paved regions having adverse thermal properties without a surface layer of loose dust.

Table 2.2 has been prepared to describe the possible characteristics of nuclear detonations over each of the three idealized surfaces. For relatively high bursts, say A-scaled heights of

*This report was written prior to the TEAPOT test series at the NPG. The blast portion of the Military Effects Test program of TEAPOT was designed to attempt a resolution of some of the questions raised here and in the following section of this report

TABLE 2.2 — Characteristics of Nuclear Detonations at Intermediate Height over Various Surfaces

	Ideal	Desert	Organic
Precursor	No	Yes	Yes
Overpressure, p	p_0	$p < p_0, p > 7 \text{ psi}$ $p = p_0, p < 7 \text{ psi}$	$p < p_0, p > 7 \text{ psi}$ $p = p_0, p < 7 \text{ psi}$
Overpressure impulse, I_p	I_{p_0}	$I_p \geq I_{p_0}$	$I_p \geq I_{p_0}$
Dynamic pressure, q	q_0 $q_0 = F_{RH}(p_0)$	$q \geq q_0, q \geq 1.5 \text{ psi}$ $q = F_{RH}(p), q \geq 1.5 \text{ psi}$ $q = q_0, q \leq 1.5 \text{ psi}$ $q = F_{RH}(p), q \leq 1.5 \text{ psi}$	$q_0 \geq q \geq F_{RH}(p), q \geq 1.5 \text{ psi}$ $q = q_0 = F_{RH}(p), q \leq 1.5 \text{ psi}$
Dynamic pressure impulse, I_q	I_{q_0}	$I_q \geq I_{q_0}$	$I_q \geq I_{q_0}$

p = Surface level overpressure

F_{RH} = Classical Rankine-Hugoniot relation between p and q . See Sec. 2.4.2.

600 ft or more, it is likely that the blast conditions will not be greatly different over the three idealized surfaces. For very low or surface bursts, it is also likely that the blast characteristics will not be greatly different over the three idealized surfaces, with some uncertainty concerning the effects of dust loading and water loading. Considerable uncertainty exists for the interim region of A-scaled burst heights which, based upon Nevada experience, have been identified as "precursor forming low bursts." The statements concerning p , or overpressure, can be made with some confidence. The applicability is, however, rather uncertain since it is unlikely that very many targets of real military interest can be identified as only pressure-sensitive in the nonideal region, where different behavior occurs for the three surfaces. In this table q is used to describe the effects of dynamic pressure. This is determined in part by direct q measurements and in part by direct observation of damage effects on targets presumed to be principally drag-sensitive. In the region of greatest uncertainty, the precursor region, it is unlikely that there are many targets of military interest which do not have a rather substantial effective drag sensitivity. This is of course particularly true since in this region, for the nonideal case, the relative effect of q is considerably increased because of the clearly established overpressure suppression.

2.5 AIR OVERPRESSURE

2.5.1 Ground Level

2.5.1.1 General

Surface-level air overpressure vs time measurements were made on Shots 1, 3, 4, 9, 10, and 11 of UPSHOT-KNOTHOLE. Similar measurements have been made on a number of previous nuclear test series. Overpressure measurements at the ground surface have been more dependable than aboveground measurements for a number of reasons, including: gage mount stability; gage orientation errors; and effect of scaled gage height. Consequently, it has been the practice to describe nuclear weapon blast overpressure phenomena in terms of surface measurements. With few exceptions, no complete documentation of aboveground overpressures has been made on nuclear bursts. The results of TUMBLER-SNAPPER and UPSHOT-KNOTHOLE have indicated that sometimes there is a rather pronounced overpressure variation with height near the surface, particularly in the nonideal region when thermal effects exist. Because of the lack of sufficient aboveground overpressure data, surface measurements are still utilized extensively. In using such data it should be recognized that the thermal effects on peak overpressure are generally most pronounced at the surface.

2.5.1.2 UPSHOT-KNOTHOLE Results

Figures 2.12 and 2.13 present the ground-level peak overpressure vs ground range for Shots 9 and 10 along the main blast line. These data are of particular importance for use in connection with the large program on blast effects on structures, since most of the test structures were located reasonably close to the main blast line. In the case of Shot 9 the pressure vs time (p-t) records were nearly conventional in wave form. The small thermal effects had a minor influence on the rise times and wave forms for Shot 9. Some pressure measurements made along a secondary blast line 90° to the main line indicate slightly higher peak pressures than measured on the main blast line. The p-t records for Shot 10 were completely unconventional in the region of thermal effects, out to a ground range of about 3000 ft. Sample records are shown in Fig. 2.14,* and it may be seen that peak overpressure alone is hardly an adequate parameter. The precursor effect is clearly shown. On Fig. 2.13 the ideal curve for peak overpressures for Shot 10 is drawn. It can be seen that the precursor or thermal effects clearly suppressed the overpressures in the nonideal region for overpressures greater than 6 psi.

Figure 2.15 presents ground-level peak overpressures for Shots 1 and 11 in comparison to the ideal curves. Typical p-t records are shown in Fig. 2.16 for these two shots. Once again the pronounced precursor and thermal effects can be seen, with peak overpressure being a relatively poor descriptive parameter, particularly in the case of Shot 1.

2.5.1.3 UPSHOT-KNOTHOLE Shot 9 and TUMBLER Shot 1 Scaling

UPSHOT-KNOTHOLE Shot 9 and TUMBLER Shot 1 were fired at the same scaled height over the same ground surface with a yield ratio of approximately 25:1. The principal scaling comparison can be made on the basis of ground-level peak overpressure. In Fig. 2.17 the A-scaled UPSHOT-KNOTHOLE Shot 9 surface-level peak overpressures are shown as compared to the A-scaled surface-level peak overpressure vs distance curve reported for TUMBLER Shot 1. The scaling is very good, showing the onset of true Mach reflection at about 750 ft and good correspondence throughout. Near an A-scaled ground range of about 1300 ft, there is a slight indication of suppressed peak overpressures on Shot 9, perhaps due to the greater thermal effect to be expected because of the greater yield of this shot.

2.5.1.4 Tower Shot Scaling

Surface-level overpressure measurements on the UPSHOT-KNOTHOLE Shot 1 tower shot have been compared to measurements on the Dog and Easy tower shots of GREENHOUSE. Test conditions are given in Table 2.3.

The A-scaled overpressure vs distance curves are shown in Fig. 2.18. The two GREENHOUSE shots gave essentially identical curves. The thermal effects on UPSHOT-KNOTHOLE Shot 1 were much more pronounced than for the two GREENHOUSE shots for overpressure greater than about 10 psi. Several possible explanations have been offered. Although all three shots were at the same height, the lesser thermal efficiency, greater obliquity of incidence and slower delivery of thermal radiation may override the bonus anticipated from larger yield weapons. In short, the effective thermal radiation was more intense on UPSHOT-KNOTHOLE Shot 1. This fact, plus the lower "popcorn thresholds" reported for Nevada soils as compared to Eniwetok sand, leads to the expectation of greater thermal effects on blast for UPSHOT-KNOTHOLE Shot 1. Reference to Fig. 2.16 shows the difficulty of presenting UPSHOT-KNOTHOLE Shot 1 results in terms of a single peak for overpressure. In the nonideal region the peaks occur sometimes at different relative times, perhaps being the result of different phenomena. Figure 2.19 shows typical overpressure vs time records for the GREENHOUSE shots.

*In general, throughout this report only the early portion of p-t records is shown. This presentation is used to expand the detail in this more interesting region since the later portions of the records are conventional in wave form.

TABLE 2.3—Burst Heights, UPSHOT-KNOTHOLE Shot 1,
GREENHOUSE Dog and Easy

	Yield (KT)	Tower height (ft)	A-scaled height (ft)
UPSHOT-KNOTHOLE Shot 1	16.2	300	112.5
GREENHOUSE Dog	82.5	300	59
GREENHOUSE Easy	49.7	300	83

57EJ

It is clear that the simple comparison of Fig. 2.18 is rather inadequate for wave form of such complexity and differences. The thermal effects on overpressure were much more pronounced on UPSHOT-KNOTHOLE Shot 1 than for GREENHOUSE Dog and Easy, possibly as a result of yield effects, scaled burst-height effects, and the different properties of the two ground surfaces when subjected to thermal radiation. Because of the lack of GREENHOUSE data, no comparisons can be made for the more important dynamic pressure parameter.

2.5.2 Aboveground

Figure 2.20 presents the peak aboveground overpressures for Shot 9, with the ground level curve of Fig. 2.12 included for reference. The bombing error on this shot may have introduced measurement errors due to the relatively large incident angles on the aboveground gage baffles. However, these errors should have been nearly independent of gage height. If comparisons are confined to the Mach region, the overpressures at 10 ft were substantially higher than at ground level, with the ground level data agreeing with measurements made at higher elevations. Other considerations indicate the presence of a mild thermal layer on this relatively high shot, although no precursor was formed. Perhaps the anomalous 10-ft overpressure behavior can be ascribed to this thermal effect, with a depression of surface-level overpressure. The lower pressures at the greater heights might be explained by the gradual reduction of pressure with height observed on TUMBLER Shot 1, which was a low-yield shot at the same scaled height.

The Sandia Corporation overpressure measurements included in Fig. 2.20 were obtained from the static pressure side ports of the Pitot-static gages used for measuring dynamic pressure. It is to be noted that these data agree with the surface-level measurements and are consistently lower than the results of the circular gage baffles used in measurements by the Naval Ordnance Laboratory (NOL) and Stanford Research Institute (SRI). The yaw correction because of the bombing error on Shot 9 would have the effect of increasing the Sandia Corporation values. However, the application of a similar correction to the NOL and SRI baffles would still result in the 10-ft values being higher than those measured at greater elevations. It is probably not practicable to draw firm conclusions concerning the aboveground overpressure measurements on Shot 9 due, in part, to the unusually large bombing error, which was transverse to the principal blast line.

Figure 2.21 presents the peak aboveground overpressures for Shot 10, as compared to the ground-level curve of Fig. 2.13. Aboveground measurements in the high-intensity precursor region of low bursts are particularly difficult because of mechanical reasons. However, these measurements indicate that the aboveground overpressures were substantially greater than those at surface level in the precursor region from 8 to 20 psi. Even though the aboveground overpressures were still substantially below the ideal case, it appears evident that the thermal effects are most pronounced on the overpressures at the surface, or at least less than 10 ft above the surface. Caution should be used in using surface-level overpressure measurements to estimate damage to aboveground targets in the nonideal region of low bursts with significant thermal effects. It is noted from Fig. 2.21 that below 8 psi for Shot 10 the ground-level curve

gives higher pressures than the aboveground pressure curve, which indicates a decrease in pressure along the Mach stem similar to that observed for Shot 9 and TUMBLER 1.

2.5.3 Positive Phase Duration and Impulse and Arrival Time

Individual project reports present detailed positive phase duration results, with consideration of precursor effects. A generalized treatment is of some interest for general use, however. Figure 2.22 presents the composite A-scaled overpressure positive phase duration vs peak overpressure results from all nuclear air bursts to date. For A-scaled burst heights less than 1000 ft, an empirical relation

$$\Delta t_+ = 0.46 P_m^{-0.27} \text{ (sec) (A-scaled)} \quad (2.3)$$

P_m = peak overpressure (psi)

may be used. The ± 15 per cent limit lines include approximately 90 per cent of the data points. This relation is less reliable for peak overpressure greater than 30 psi.

Positive phase overpressure impulse has been treated similarly in Fig. 2.23. The resultant empirical relation for A-scaled burst heights less than 1000 ft is

$$I_+ = 0.18 P_m^{0.72} \text{ (psi-sec) (A-scaled)} \quad (2.4)$$

The ± 15 per cent limits show a somewhat greater scatter than for duration. Again, this relation is less applicable for overpressures greater than 30 psi.

Figure 2.24 presents the positive phase duration and first blast arrival time for Shot 9. The similar data for Shot 10 are shown in Fig. 2.25, where the precursor effect is evident. These figures are presented because of their general interest to the structures program.

2.6 DYNAMIC PRESSURE

2.6.1 Instrumentation

Dynamic pressure measurements as a function of time were made using the Pitot-static tube developed by the Sandia Corporation. This instrument gives a reliable measurement of dynamic pressure in clean air. However, the effect of air with a large amount of dust, such as occurs over desert surfaces in the precursor region, on the q measurements is somewhat uncertain. It has been established that the q -instrument responds to the dust loading. However, it has not been established that the structural drag coefficient to be used with this measured q value to determine loading force is the same as the drag coefficient in clean air. The only q measurements reported for UPSHOT-KNOTHOLE used these Pitot-static gages, which are known to respond to the airborne dust behind the blast wave. It is assumed at this time that the clean air drag coefficients for structures will apply to the measured values of q in the dusty air of the nonideal blast region, in lieu of definitive experimental data.

Dynamic pressure measurements must necessarily be made above the ground. In the intense blast region of nonideal behavior, it is most difficult to make dynamic pressure measurements because of mechanical vibration and stability problems. Most of the UPSHOT-KNOTHOLE q measurements in the nonideal or precursor region were erratic and incomplete. However, some useful results were obtained.

2.6.2 Results

Figure 2.26 presents the peak dynamic pressures as observed on Shot 9. On this shot, which had a relatively small thermal blast effect, it can be seen that the measured values of q agreed quite well with the values calculated from the measured overpressures and with the

ideal curve except for the uncertain region of transition from regular to Mach reflection.* In this case, where no precursor or other strong thermal effects were obtained, there is no apparent effect of dust loading, even though the measurements were made over a very dusty surface.

Figure 2.27 shows a typical dynamic pressure measurement in the precursor or thermal effects regions on Shots 1, 10, and 11. The erratic and limited nature of some of the q measurements is evident. Figure 2.28 shows the peak q measurements as compared to the ideal values for these three shots. Three data points are marked to show instrumentation saturation, with a strong likelihood that higher set ranges would show much greater peaks. The measured values of q in the strong precursor region are greater than ideal and much greater than would be calculated from the companion measured overpressures. At the outer limits of the precursor or thermal effects region, the measured values agree with ideal and are again substantially higher than would be calculated from the measured overpressures. In these latter cases it is likely that the effect of dust loading is small. However, the departure from the measured overpressure is also relatively small so no firm conclusion can be drawn. In the stronger precursor region, where the measured dynamic pressures are substantially greater than ideal, there is no means to estimate the quantitative effect of dust loading. It is not possible to conclude that the measured dynamic pressures would be ideal in the case of a precursor without dust ("organic"). Suffice it to say that it can be concluded that the Pitot-static tube dynamic pressures can be established as equal to or greater than ideal in the precursor region of low bursts over dusty desert surfaces. More full-scale test data are required to justify statements concerning the dynamic pressures of low bursts in the strong blast region over other surfaces.

2.7 PRECURSOR

2.7.1 General

Three of the instrumented UPSHOT-KNOTHOLE detonations, U-K Shots 1, 10, and 11, had pronounced precursors. The yields of the precursor shots ranged from about 15 to 60 KT, over a range of scaled heights of burst from 112 to 316 ft. This region of yields and burst heights is very favorable for precursor formation, and from a number of past operations it is known that the precursor region exists over a larger range of yields and burst heights than was represented by these three shots.

To obtain a general perspective of precursor formation and propagation, the high-speed photography yielded an excellent sequence of the various stages of the precursor shock waves, such an example being Fig. 2.29 taken on U-K Shot 11. The reflected shock wave is fully developed before there is any indication of a new pressure wave (precursor) propagating outward along the ground ahead of the reflected wave. The delayed appearance of the precursor is discussed in Sec. 2.4.3.3. Other excellent examples of the development and progress of precursor waves were prepared by NOL from shock photographs, such as Fig. 2.30 (U-K Shot 1) and Fig. 2.31 (U-K Shot 10). The precursor shock contours for U-K Shot 10 and U-K Shot 1 appear quite similar, although the pressure-time records are distinctively different (see Figs. 2.14 and 2.16). Thus similar precursor fronts can have quite different conditions prevailing on their interior. The vertical extent of the U-K Shot 1 precursor shock is rather impressive, being about 200 ft high at ground distances of about 1500 ft. The dust behind the precursor on U-K Shot 10 attains a height of 100 ft at 1300 ft ground distance. It is seen that a precursor would envelop com-

*The q values calculated from measured overpressure in the regular reflection region of Fig. 2.26 differ slightly from those given in Report WT-714⁶ (Fig. 1.12 and Table 1.10). The equation from which they were calculated, Eq. 1.3, should be corrected to read

$$q \frac{2.5 P_0}{\xi(\xi'+6)} \left[(1-\xi) \left(\frac{1+6\xi'}{1+6\xi} \right)^{1/2} \sin \alpha (\xi' - 1) \sin \alpha' \right]^2$$

pletely very sizable aboveground structures. The ultimate height and ground extent of the U-K Shot 11 dust pedestal is shown in Fig. 2.32 and is seen to be very sizable. It is certainly more than coincidence that the dust pedestal terminates at about the end of the precursor region (radius 3400 ft). The likelihood of dust contributing to the loading in the precursor region is obvious from such a figure.

2.7.2 Thermal Layer

A sizable fraction of the total energy released from a nuclear detonation is emitted in the form of thermal radiation. Large amounts of thermal radiation are incident upon the ground before shock arrival; thus the existence of a thermal layer near the surface is a sound assumption. Experimental results are only indicative of a general high temperature layer of air existing prior to shock arrival. The early formation of a Mach stem and the variation of peak pressure with elevation above the ground indicate some thermal effects even on relatively high-scaled heights of burst, such as U-K Shot 9. At lower heights of burst, such as U-K Shots 1, 10, and 11, the thermal effects are very pronounced and result in the unconventional precursor pressure wave.

Actual measurements of preshock sonic velocities were obtained by the Navy Electronics Laboratory (NEL) on two TUMBLER and two U-K shots. Although the results are only fragmentary, such measurements indicate substantial increases in preshock sonic velocities. In addition to actual measurements, it is possible with some assumptions to compute the preshock temperatures using (1) the SRI method of arrival time of the shock wave propagating through the thermal layer vs ground distance and (2) the NOL photographic data for the angle of the precursor front above the thermal layer. The arrival-time data are used to determine shock velocity in the thermal layer, which, by use of known shock relations, leads to temperature. The NOL method of obtaining preshock temperature is based on a relation between sonic velocity in the thermal layer and the angle of the precursor front in the ambient air above the thermal layer.

Figure 2.33 presents the results of these computations of preshock temperature vs ground range for U-K Shot 10. At ground ranges less than 1000 ft, there is a significant difference in the temperatures computed by the two methods, however, the individual points are probably subject to errors of as much as ± 25 per cent. It was possible to make similar shock velocity-preshock temperature computations for U-K Shot 11 (A-scaled height of burst, 316 ft); these results are plotted in Fig. 2.34 along with the experimental and computed results for TUMBLER 4 (A-scaled height of burst, 363 ft). The results from the two tests appear to compare favorably, indicating that average temperature values (at scaled ground ranges) may be comparable for shots detonated at about equal scaled burst heights; in addition, the TUMBLER 4 experimental curve [NEL and Naval Radiological Defense Laboratory (NRDL)] agrees well with the points computed by the shock velocity method (SRI).

2.7.3 Precursor Overpressure and Dynamic Pressure

Figure 2.35 compares U-K Shots 10 and 11 scaled pressure-time records at comparable scaled ground ranges. Although the peak pressures of the precursors and the second pressure peaks are not equal, there is a striking similarity in the general nature of the pressure-time records. Shot 10 was detonated at 202 ft (A-scaled) and Shot 11 at 316 ft (A-scaled). Further, comparison of U-K Shot 11 and TUMBLER 4, Fig. 2.36, which are shots not too different in scaled burst heights, results in almost identical pressure-time records both as to wave forms and as to values of peak pressure. To the extent that pressure-time records relate some of the general attributes of a precursor, U-K Shot 11 and TUMBLER 4 are nearly identical at the same scaled ground distances. It is to be noted that U-K Shot 11 and TUMBLER 4 were detonated over the same Yucca Flat terrain, whereas U-K Shot 10, which compares poorly with U-K Shot 11, was detonated over Frenchman Flat. One cannot conclusively say the differences in U-K Shot 10 and U-K Shot 11 peak overpressures at the same scaled distances are due to heights of burst, terrain, or combinations of both.

The pressure-time records for U-K Shot 1 (Fig. 2.16) are quite different from those obtained on U-K Shots 10 and 11 in that generally the U-K Shot 1 overpressure in the first peak is more nearly equal to that of the second peak overpressure. Further, U-K Shot 1 has a first peak pressure higher than the second peak when the pressure levels are less than about 15 psi. This is in marked contrast to the previous pressure-time records for U-K Shots 10 and 11 and TUMBLER 4. Because U-K Shot 1 was detonated over the same Yucca Flat terrain as U-K Shot 11 and TUMBLER 4, the only reasonable explanation is that the differences are due to the height of burst.

Dynamic pressure measurements in the precursor regions of U-K Shots 1, 10, and 11 are rather fragmentary but unquestionably show that measured peak values are not related to the Rankine-Hugoniot values of dynamic pressure obtained from measured peak overpressures. Comparisons are given in Table 2.4.

TABLE 2.4 — Comparison of Measured and Calculated Dynamic Pressures in Precursor Region

Shot	Gage	Ground range (ft)	ΔP used for calculation	q, calculated (psi)	q, measured (psi)	q, measured (calculated)	q, measured (ideal)
1	84F10	1250	15.0	5.4	115	21	2.50
	85F10	1450	13.0	4.1	40	9.8	1.18
	89F13	2600	4.4	0.52	0.55	1.06	
			9.7	2.38	2.20	0.925	0.76
10	82F13	1169	30.0	18.4	>57	>3.1	>1.24
	17F10	1422	26.4	15.1	>9.6	>0.64	>0.38
	17F40	1422	12.9	4.0	>11.6	>2.9	>0.46
	00F10	1920	11.0	2.95	10.9	3.7	1.28
	00F25	1920	12.1	3.55	11.6	3.3	1.37
	00F40	1920	6.1	1.65	12.4	7.5	1.46
11	4F5	3435	5.24	0.74	3.0	4.0	
			11.5	3.3	5.92	1.8	0.97

Figure 2.37 shows the dynamic pressure-time records in the dusty precursor region attaining nearly peak values at early times when the overpressures are slowly rising. It is thought that the rapid rise of dynamic pressure can be associated with the arrival of the dust at the station. Typical dynamic pressure-time records, Fig. 2.27, obtained in the precursor region show very rapid fluctuations in amplitude, an attribute not present at later times nor in the nonprecursor records. This suggests a high degree of turbulence in the precursor portion of the pressure wave. The contribution of turbulence to damage could be important.

It is well documented by photography that the precursor front has an upward component of flow. Indeed, dust originating near the surface ultimately attains heights of 100 ft or more. It is thus concluded that an upward component persists at aboveground stations for a finite time. No quantitative data exist as to the actual durations of the upward component. An upward component of motion imparted to movable drag targets enhances the damage considerably because of repeated impacts with the ground.

2.7.4 Precursor Prediction Criteria

Subsequent to TUMBLER, several reports appeared in which attempts were made to set down a number of idealized assumptions and from these to obtain predictions as to what yields and scaled burst heights would result in a precursor. Two sets of criteria that deserve attention are found in the TUMBLER Summary Report WT-514⁸ and a Sandia Corporation report

by Shelton.⁹ As will be seen later, these two prediction criteria differ as to precursor formation in several regions. The very strong precursors which occurred on U-K Shots 1, 10, and 11 would have been predicted by either of the above criteria. Operation UPSHOT-KNOTHOLE did not produce much relevant data from which more realistic prediction criteria could be developed. Actual temperature or sonic velocity measurements in the thermal layer are few, details of a thermal gradient with elevation are lacking, and, indeed, the exact mechanism for formation of the thermal layer is not defined.

The TUMBLER criteria, based upon empirical data, set limits on (1) scaled height of burst, (2) a yield-true height-of-burst relation ($W \cdot h^2$), and (3) the time required for shock wave to reach Ground Zero. Shelton's criteria are based partially upon empirical data and partially upon theoretical analysis. Two important assumptions are made that merit review: It is assumed that velocity of sound in the thermal layer (at a particular ground range) is a linear function of the preshock normal component of the incident thermal radiation; it is further assumed that this relation is invariant from one test to another (TUMBLER-4 data are used for all calculations). The first assumption above takes no account of the fact that portions of the thermal layer are expanding and cooling continuously. The second assumption is admittedly approximate, U-K Shots 10 and 11 data deviate from those of TUMBLER-4.

A summary of the two precursor formation analyses is presented in Fig. 2.38. In this figure the thick cross-hatched curve is due to Shelton and separates the "precursor" and "no precursor" regions. Also on the figure are found the limit curves from the TUMBLER analysis. In comparing these two criteria, the most interesting difference is revealed by the fact that the TUMBLER report predicts precursor formation for low-yield weapons (1 to 2 KT) at A-scaled heights of burst from 50 to 400 ft, whereas Shelton's curve indicates that no precursor is formed for these weapons at any burst height. The other significant deviation between the two criteria is found in the region of 500- to 600-ft burst heights and yields larger than about 30 KT; there are no available data for this region.

It is evident that future tests are required to define more clearly the criteria for precursor formation. In this regard some of the important deficiencies in this field include a knowledge of preshock temperatures as a function of ground range and height above the ground; the effects of various surface conditions upon the formation of the thermal layer; and the influence of blast geometry (yield and height of burst) upon the shock wave in the nonideal region. It is clear that such tests must be supported by a comprehensive analytical program to include such theoretical and laboratory investigation as may be necessary to apply full-scale results to real surfaces of military interest.

2.7.5 Smoke Experiment Precursor Effects

A smoke experiment was conducted on U-K Shot 10 to study the manner in which a thermally absorbing black smoke layer would modify the normally expected thermal effects on blast. Figure 2.39 shows the pressure-time records obtained by the surface level gages along the main blast line and the smoke line. The effect of the precursor is to distort the shock wave by increasing its duration, reducing the peak pressure, and usually degrading the rapid rise time of the shock front to a slow rate of rise. In the precursor regions the peak overpressures under the smoke were higher than on the main blast line, and the pressure rise times on the smoke line were much faster than at corresponding ground distances on the main blast line. At 1632 ft and beyond the shock wave under the black smoke shows no precursor, whereas on the main blast line the precursor effects were evident to about 2700 ft. Peak pressure data for the smoke line are plotted in Fig. 2.40 and compared to the curve established for the main blast line. The peak pressures on the smoke line are very close to those predicted over an ideal surface at a ground distance of about 1600 ft and beyond, whereas on the main blast line peak pressures are reduced below ideal out to ground distances of about 3000 ft. Comparison of the pressure-time records and values of peak overpressure at corresponding ground distances leaves no doubt that the thermally absorbing black smoke significantly reduced the thermal effects on the blast wave

The gage towers that failed or bent are examples of damage to drag-sensitive targets. Thus, to some extent, it is possible to compare damage under the black smoke and along the main blast line. The 10-ft gage towers were blown down along the main blast line out to 2166 ft and bent at 2660 ft and were undamaged beyond this distance. Along the smoke line similar 10-ft gage towers were blown down out to 1133 ft and bent at 1632 ft, beyond which the towers were undamaged. It would appear that gage towers were blown down or bent out to edges of the nonideal regions.

The time of arrival of the initial disturbance along the smoke line and blast line is presented in Fig. 2.41. It is seen that in the precursor region the pressure signal arrives earlier along the main blast line. This indicates that the air temperature near the ground along the main blast line is significantly higher than along the black smoke blast line.

Summarizing, as compared to a clear area, the black smoke area on U-K Shot 10, through the mechanism of thermal-radiation absorption, greatly reduced the air temperatures near the ground. This, in turn, greatly reduced the thermal effect on blast, maintained blast parameters much more nearly ideal out to about 1600 ft from Ground Zero, and eliminated the precursor on the smoke line entirely beyond this ground distance. Damage to drag-sensitive targets may be reduced under the black smoke as indicated by the gage towers. Finally, a thermally reflecting white smoke would probably reduce the precursor effects even more than the thermally absorbing black smoke.

2.7.6 Thermal Shock

It has been speculated that the precursor shock was perhaps generated by thermal radiation being absorbed at the ground surface and also in the popcorned dust near the surface. Air suddenly heated to temperatures of the order of 1000°C would be at pressures in excess of ambient pressure. Thus a thermal shock would propagate outward as the hot air mass expanded to ambient pressure. Because of the time dependence of thermal radiation, a thermal shock precursor should not form immediately but more nearly at times after the arrival of the main shock at Ground Zero.

In Fig. 2.42 photographs are shown of laboratory experiments on the response of three types of thermal materials to a high-intensity thermal pulse. Only one of the media, namely, the Frenchman Flat adobe surface, underwent a popcorning transition, whereas the other two did not. The particles ejected from the adobe surface extended out to distances to the order of 6 to 10 in. for this laboratory experiment. These studies were conducted by the Naval Material Laboratory (NML) in cooperation with the David Taylor Model Basin (DTMB). Full-scale tests by means of 10 ft x 10 ft panels were conducted by DTMB on U-K Shots 9 and 10. There seemed to be a very reasonable correlation between the surface conditions of the laboratory and field test members. Pressure gages with high time-resolution characteristics were located in the field panels which yielded records indicating, in general, that significant pressure values are not associated with popcorning. As indicated by the preshock pressure-time signals of Fig. 2.43 and also reviewing the above DTMB experimental results, one may conclude that to a reasonable approximation there are no significant preshock pressures associated with popcorning effects and subsequent thermal radiation. The further conclusion may be drawn that although thermal shock may occur close to Ground Zero, it is not significant as a mechanism for precursor generation, inasmuch as it is only expected to occur under those conditions where the precursor will form at slightly greater ranges according to the heated layer concept.

2.8 TRIPLE POINT (MACH STEM CONSIDERATIONS)

2.8.1 General

Detailed data on the path of the Mach triple point near the ground were obtained on Shot 9 of UPHOT-KNOTHOLE. In addition, the shock photography gave Mach stem data high above the ground surface (up to 500 ft) for Shots 1 and 10. No data on triple point path were obtained on Shot 11. Comparisons will be made between the Shot 9 data and similar measurements on

TUMBLER Shot 1, also, it will be valuable to show how these nuclear data compare with Mach stem data obtained from TNT detonations.

2.8.2 U-K Shot 9 and Thermal Mach

Theoretical considerations of shock-wave configuration show that the ground range at which a Mach reflection begins is a function of the shock strength and the burst height. The theory predicts Mach reflection starting at a ground range about equal to the burst height. In the absence of surface and/or thermal effects, this prediction has been substantiated by experiment.

For U-K Shot 9, the Mach stem was expected to originate at about 2400 ft ground range. The Mach stem development, as determined from the data shown in Fig. 2.44, indicates the existence of a Mach stem as close as 800 ft from Ground Zero. It is to be noted that a relatively similar early development of a Mach stem was reported for the nearest scale 1.0 KT shot of TUMBLER 1. It appears plausible to attribute this formation characteristic to the presence of a thermal layer similar to the results of shock-tube experiments performed at Princeton. The incident wave impinging upon a thermal layer above the normal ground layer will undergo reflections at both the thermal boundary and the ground. If this is the case, there will be a region wherein a Mach wave develops in the thermal layer from the interaction of the transmitted shock with the rigid earth boundary. This is termed a "thermal Mach shock," since it is produced as a result of the bending of the incident shock due to the thermal layer and occurs before the incident angle of the incident shock wave is large enough to form a Mach stem in the absence of a thermal layer.

It is to be noted that the data points of Fig. 2.44 are based upon a series of extrapolations from arrival-time data, assuming a standard Mach stem configuration exists, namely, an incident, reflected, and Mach wave meeting at a point. The sensitivity of this data reduction method to arrival-time errors is indicated in Fig. 2.44 where limit bars are drawn from each data point corresponding to 0.5 msec deviations in Δt_{IP} . The dashed lines in the figure indicate the gross limits within which the Mach triple point trajectory existed on U-K Shot 9.

The A-scaled comparison of the Mach stem height vs ground range data from TUMBLER 1^{10, 11} and U-K Shot 9 is presented in Fig. 2.45. Although the data from TUMBLER 1 are meager, the agreement is good and the figure indicates that Mach triple point trajectory does scale in the ideal wave form region.

Figure 2.46 presents the results of photographic data³ on Mach stem height vs ground range for U-K Shots 1 and 10. The U-K Shot 10 data indicate that a thermal Mach shock formed at close-in ground ranges before the extreme angle of regular Mach reflection was realized. For U-K Shot 1, the data do not extend to low enough ground ranges for any conclusions relative to the formation of the thermal Mach shock on this shot.

2.8.3 Nuclear Vs TNT

It is believed of value to present some summarizing analysis of Mach stem results to date with respect to nuclear tests. The basis for the summary will be comparisons of available nuclear data in the ideal shock region with the triple point curves (normalized to 1 KT) from Zirkind's recent report.¹² These curves, shown in Fig. 2.47, were obtained by taking the results of recent Ballistic Research Laboratories (BRL) Mach stem experiments with TNT charges assuming a TNT blast efficiency of 50 per cent for nuclear charges, and replottting the data for various A-scaled burst heights. Using the curves of Fig. 2.47 as the basis of comparison accomplishes the purpose of reviewing the relation between nuclear and TNT Mach reflection characteristics.

The agreement between the curves of Fig. 2.47 and the GREENHOUSE Easy, U-K Shot 1, and U-K Shot 10 Mach stem data is good. However, as the height of burst of the nuclear charge is increased, the agreement becomes progressively worse. The TUMBLER Shot 4 (A-scaled height of burst = 363 ft) data give a curve in the ideal shock wave region corresponding to an A-scaled height of burst of about 400 ft, for U-K Shot 9 and TUMBLER Shot 1 (A-scaled height of burst = 750 ft), the triple point data agree with a TNT equivalent height of burst in excess of

900 ft, for TUMBLER Shots 2 and 3 (A-scaled height of burst = 1000 ft), the agreement is poorer yet.

The general conclusion from the foregoing is that for low A-scaled burst heights (less than about 300 ft) the nuclear Mach stem data compare favorably with the curves from TNT. However, as the A-scaled burst heights are increased, the nuclear results correspond to triple point trajectories that would be predicted for TNT charges detonated at significantly higher heights of burst. The foregoing general conclusion is substantiated by the Air Force Cambridge Research Center (AFCRC) canister measurements, which determined some points on the triple point path at very high altitudes.

2.9 HEIGHT-OF-BURST CURVES

2.9.1 History

The original concept of the height-of-burst curves was to assist military planning groups in determining the most efficient utilization of atomic weapons for operational situations. An early requirement had been established for information relating the height of burst to blast effects at various ground ranges in order to select the proper yield and conditions of detonation for atomic weapons. Peak overpressure was selected as the most representative blast parameter in relation to damage criteria based largely on Japanese experience. The first set of height-of-burst curves were those prepared in 1949 by means of an analytical treatment of conventional shock-wave theory, small-scale HE and shock-tube experimental results, along with the nuclear air blast data for Bikini Able measured along the surface. These curves gave values of peak overpressure vs ground range as a function of height of burst for 1 KT (RC). The normal cube root scaling laws for blast phenomena were assumed valid in applying these curves to other weapon yields. In addition to operational planning, these curves were also used to provide criteria for weapon development.

It was noted in 1951 that air blast pressure measurements on both SANDSTONE and GREENHOUSE gave somewhat lower values than those predicted from the height-of-burst curves. These results did not appear to have serious operational significance since these tests involved only tower shots. However, plans were made to measure air blast pressures for the four air bursts of BUSTER.

The BUSTER results in the high-pressure region were very much lower than those predicted from TM 23-200 (1 October 51). Consequently, Supplement 1 to this publication was issued on 8 February 52 to provide the DOD with new height-of-burst curves on an interim basis. These curves, labeled good, fair, and poor, included pressure reductions based on theoretical consideration of both thermal and mechanical effects. Simultaneously, planning proceeded for TUMBLER during which it was proposed that comprehensive measurements of blast and thermal radiation be made following the detonation of different yield atomic weapons at various heights. In particular, data on peak overpressure gathered by different groups would be correlated to prepare new height-of-burst curves. The experimental program was also designed to provide enough scientific information on the nature of the blast wave to permit the application of the TUMBLER results to more realistic target areas.

The results of TUMBLER are presented in Report WT-514, Final Summary Report.⁸ An empirical set of height-of-burst curves was prepared, based primarily on ground-level pressure measurements for the TUMBLER shots. The blast data from the TRINITY, SANDSTONE, and GREENHOUSE tower shots, as well as the JANGLE surface shot, were used to obtain the zero height intercepts and the general nature of the contours for low burst heights. In the region above a scaled height of 1000 ft, where there were no full-scale experimental data at that time, a theoretical treatment of the TUMBLER free air pressure-distance relation was used to complete the curves.

A shaded area was presented in these curves to indicate the region of blast-wave distortion due to thermal effects, which were particularly evident on TUMBLER 4 where a precursor developed. For those weapon yields and heights of burst for which precursor effects are signifi-

cant, it was recommended that pressures in the shaded area be reduced by $\frac{1}{3}$ for certain unfavorable target conditions, such as extremely dusty areas. For those areas considered to represent favorable target conditions, such as water surfaces, pressures in the shaded area might be increased by as much as $\frac{1}{6}$. With these reservations, the TUMBLER height-of-burst curves were included in TM 23-200 (1 October 1952) for use in operational planning.

2.9.2 Philosophy

The philosophy of the TUMBLER height-of-burst curves was to use peak pressure as an arbitrary standard of reference since it was a physical effect easily measured and was considered to be the single phenomenon of importance in determining the effect of loading on a large class of important targets. At that time it was realized that several other parameters could just as easily be used for height-of-burst curves, such as dynamic pressure, particle velocity, density, or temperature, since these are interrelated properties of conventional pressure waves. Therefore it was generally understood that inherent in the designation of the pressure level was also the specification of the relative values of the other associated physical effects related by classical theoretical equations for ideal shock waves. Consequently, it was intended that the height-of-burst curves be used in conjunction with tabular data correlating type of structure, degree of damage, and corresponding peak pressure level in order to specify damage criteria for a variety of weapon sizes and heights.

During TUMBLER, a few dynamic pressure measurements were made. However, there appeared to be no significant departures in these measurements from what would be calculated from measured overpressures since values of q were obtained for high burst heights where thermal effects on the blast wave were minimized. As a result, the significance of dynamic pressures in the nonideal region for low bursts was not recognized. It was believed that the significant reduction in peak pressure and the badly distorted wave form might seriously reduce damage in the region near Ground Zero.

As noted previously, during UPSHOT-KNOTHOLE, several agencies participated in studying basic phenomena in order to supplement available full-scale data and permit a better understanding of the fundamental blast effects associated with air bursts of nuclear weapons. In order to investigate more fully the nonideal region, Program 1 included measurements of both overpressure and dynamic pressure for Shots 9 and 10, as well as preshock sound velocity over various surfaces. As a result of these measurements, it was clearly evident that the classical relation between p and q was no longer valid in the precursor region for low bursts. The measured values of q were considerably higher than would have been calculated from measured values of p by use of the Rankine-Hugoniot equations. It was subsequently found that the Pitot-static tube was susceptible to the effects of dust; thus the measured q values include the dust loading present in the shock wave. This fact must be considered in comparing measured q values to the ideal. The ideal height-of-burst curves for peak overpressure and dynamic pressure shown in Figs. 2.8 and 2.9 assume a perfect reflecting surface with no perturbations to the blast wave resulting from dust or thermal effects. The deviation of the UPSHOT-KNOTHOLE experimental data from the ideal as a function of height of burst will be discussed below. The surface-level pressure data (A-scaled) for Shots 1, 3, 4, 9, 10, and 11 are shown in Fig. 2.48.

2.9.3 Air Overpressure

Figure 2.49 presents the ideal peak air overpressure height-of-burst curves (Fig. 2.8) with the U-K data points included on the figure. A few pertinent general comments can be made with reference to this figure.

The experimental values of peak overpressures for Shot 9 appeared to agree well with the ideal curves for values of overpressure equal to 6 psi and below. However, even for this relatively high height-of-burst shot, there are significant deviations from the ideal at higher overpressures. For U-K Shot 1 (112 ft A-scaled burst height), Shot 10 (202 ft A-scaled burst height), and Shot 11 (314 ft A-scaled burst height), the data points for overpressures of 8 psi and lower seem to agree quite well with the ideal curves. However, in the stronger shock regions (10 to

50 psi) the deviations from ideal are marked. In particular, the points from Shot 1 corresponding to this stronger shock region indicate a serious reduction in overpressure for this low height of burst. If one is to retain the zero height-of-burst intercepts as obtained from the JANGLE surface experiment, then it is evident that the height-of-burst curves near 100 ft A-scaled height must exhibit a sharp inflection or "knee."

It would appear from the UPSHOT-KNOTHOLE results that there still remain uncertainties with relation to the nonideal region of the height-of-burst chart for peak overpressure.

2.9.4 Dynamic Pressure

The dynamic pressure height-of-burst curves for ideal conditions as presented in Fig. 2.9 were constructed using a peak air overpressure ideal height-of-burst chart and the classical shock-wave relations. It should be pointed out that there is a necessary ambiguity existing for dynamic pressure calculations near the region of transition between regular and Mach reflection. In this transition zone one may obtain a discontinuity in the dynamic pressure curves. For this reason it was necessary to fair in the curves of Fig. 2.9 near this transition region. In addition, by definition, the dynamic pressure approaches the value zero at Ground Zero; therefore it was necessary that these height-of-burst curves agree with this restriction.

The UPSHOT-KNOTHOLE experimental dynamic pressure results are indicated in Fig. 2.50 for Shot 9. The agreement with the ideal curves is quite good, the result which might be expected on the basis of small thermal effects experienced on this shot. It is evident that the peak dynamic pressures show significant scatter as compared to similar data taken for peak overpressure.

For the lower burst height, Shots 1 and 10, the comparisons with the ideal curves yield similar results. For dynamic pressures less than about 3 psi, the data, although meager, agree well with the ideal. However, for dynamic pressures of 10 psi and larger, the measurements indicate that the values are significantly higher than would correspond to ideal conditions. It should be noted that on Shot 10 three gages from which dynamic pressures were obtained indicated that they were overranged. In addition, the Pitot-static tube is sensitive to dust; therefore q measurements in the nonideal region for Shot 10 are necessarily limited in their significance. For Shot 11, a high-yield device at an A-scaled height of burst of about 300 ft, the single dynamic pressure measurement near 6 psi agrees well with ideal.

2.9.5 Summary

The over-all significance of UPSHOT-KNOTHOLE was to point out that thermal effects upon the blast wave could depress peak overpressures quite severely so that serious departures from the ideal could be expected for low burst heights depending on surface conditions. Furthermore, it was learned that height-of-burst curves for peak overpressures do not uniquely define all blast parameters in the nonideal region. It is considered that UPSHOT-KNOTHOLE substantiated the thermal layer concept for precursor generation. It should be noted, however, that nothing further was learned that would explain the results of BUSTER in so far as the extreme depressions of peak pressure from the ideal were observed for various burst heights on that operation.

It was also demonstrated in the nonideal region that dynamic pressures were not correspondingly depressed but could be larger than those calculated from ideal values of peak overpressures. It is considered that measured values of q as recorded during this operation included the effects of dust; however, the exact contribution of dust under such circumstances has not been completely determined. The dust pedestal actually extends to approximately one shock wave length beyond the range at which the precursor becomes extinct.

The usual characteristics of precursor formation and propagation were observed on Shots 1, 10, and 11, except that some deviations were noted on Shot 1. Shot 1 exhibited a steep rise in contrast to a more irregular wave form observed on Shots 10 and 11 and on TUMBLER 4. Shot 1 may be considered an anomaly in so far as more severe thermal effects were noted than on GREENHOUSE Dog and Easy, although the delivery of thermal radiation vs time was similar in

all three cases. It is considered that very little experimental data were obtained that would assist in developing criteria for predicting precursor formation and propagation.* However, UPSHOT-KNOTHOLE was successful in pointing out the need for further information on flow patterns behind the shock front in the nonideal region

2.10. DAMAGE CRITERIA

2.10.1 Basic Considerations

In determining damage criteria to targets of military interest, the geometry of the burst is a significant factor. The difference between high and low burst heights is pointed up by thermal considerations which affect blast-wave parameters for low bursts. Such effects are superimposed upon normal geometric considerations with regard to the extent of the regular reflection region and the triple point. Consequently, the effective blast parameters used to predict damage are implicitly related to burst position and weapon size. However, the extent to which thermal influences on the blast wave are significant in realistic situations has not yet been completely determined. A factor which most probably contributed to the extensive damage on U-K Shot 10 was the relatively high flat-top pressure wave form in the precursor region with constant blast pressure and corresponding dynamic pressure over an extensive portion of the positive phase. In the case of drag-sensitive targets, results of U-K Shot 10 indicated that relatively low burst heights may be most favorable for optimum damage because of strong wind loadings due to burst geometry. A question naturally arises as to the contribution of dust loading in the nonideal region and the significance of the flow pattern under such circumstances.

2.10.2 Use of the Height-of-burst Curves

The entire philosophy of the height-of-burst peak pressure curves has been revised as a result of the unexpectedly high dynamic pressure observed on Shots 10 and 11 in the nonideal region. The results have produced essentially a sharp deviation in the nature of damage criteria required for various types of structures. The original intent of the height-of-burst curves was not to present peak pressure values that would cause damage but rather to indicate distance from Ground Zero at which particular degrees of damage occur. The height-of-burst curves were to be used in conjunction with an auxiliary table presenting the types of structures and the so-called "pressure" level at which light, moderate, or severe damage may result. The combination of the table and set of height-of-burst curves was intended to correlate the type of structure and the distance from Ground Zero at which the specified damage is estimated to take place. The actual pressure values were not intended to be the sole criteria of damage. It is believed that the UPSHOT-KNOTHOLE results do not significantly alter the foregoing philosophy in the case of pressure-sensitive targets. One main conclusion resulting from the UPSHOT-KNOTHOLE program appears to be that there is a need for an equivalent set of height-of-burst curves presenting dynamic pressures rather than static overpressure to be applied in problems involving drag-sensitive targets. For example, in the case of mobile tanks and trucks, the vertical components of the precursor pressure wave may tend to lift the targets off the ground and thereby convert them essentially into missiles. As a result of severe impact forces experienced upon landing, these missiles can suffer very significant damage. Dynamic pressures in the precursor region appear to be the most significant contributing factor to phenomena of this type. Another area where drag effects are important is in the case of parked aircraft, which are more sensitive to gust loading than static overpressure.

* Following UPSHOT-KNOTHOLE, a series of tests (CASTLE) was held in the Pacific. It is considered that the results of these tests, for weapons ranging from 100 KT to 15 MT bursts at the surface over an essentially ideal reflecting plane, gave results consistent with predictions according to conventional scaling of blast-wave parameters. No significant thermal effects on the blast wave were observed during these tests, although nonideal wave forms were observed as well as possible water loading of the shock wave.

Since measured pressure varies with height above ground, the nature of the height-of-burst curves is governed by the choice of the data to be used. On the basis of the intended purpose of the height-of-burst curves, it appears satisfactory to use surface-level measurements, since the height-of-burst curves are used only as an arbitrary intermediate frame of reference to associate structures with areas of damage. One important factor that must be considered in the use of burst curves is the orientation of the structure with respect to the direction of blast loading. It is quite probable that a 10-psi pressure wave striking normally against the side of a structure will result in significantly different damage than a similar wave impinging on the roof of the same structure. This question can possibly be resolved by a study of the characteristics of response to blast loading for individual types of structures, and some modifying parameter can be used in problems where these structures are being considered. It is believed that the fundamental purpose of the height-of-burst curves is to give design engineers some reasonable estimates of the nature of the blast loads that will occur in various areas due to a nuclear blast.

2.11 RECOMMENDATIONS FOR FUTURE TESTS

As a result of UPSHOT-KNOTHOLE, it is now possible to define more clearly the areas of uncertainty in basic blast phenomena. It is considered that one of the primary deficiencies in the state of knowledge relates to the effects of thermal radiation on real surfaces and formation of the thermal layer. Indeed, the semiempirical criteria for precursor prediction apply largely to test surfaces such as desert, sand, and coral. Even for these surfaces, however, details of the preshock sound velocity or the mechanism of heat transfer necessary for a thermal gradient have not been established. Consequently, it is difficult to extrapolate full-scale test results to real surfaces of military interest, such as forest, vegetated areas, and cities, in order to determine their relative influence on the blast wave as a result of thermal irradiation. Since it is apparent that surface dust effects on UPSHOT-KNOTHOLE were significant in so far as measured values of dynamic pressure are concerned, an attempt should be made to investigate the precursor in the absence of dust to determine the various relations between the parameters. It is therefore recommended that a full-scale test be held at a low burst height for purposes of measuring the free field blast parameters over the representative surfaces discussed in Sec. 2.4.3.6, which were described as ideal, desert, and organic. In this way departures in blast behavior from the ideal could be observed for both a dust and nondusty precursor. These measurements should include overpressure and dynamic pressure vs time as a function of ground range and height above the ground on all three blast lines. In addition, an attempt should be made to measure such quantities as particle velocity, air and dust density, direction of particle motion, temperature, and preshock sound velocity at various stations to correlate with p and q measurements.

Another unresolved question relates to blast-wave characteristics and damage in the non-ideal region for a low precursor-forming burst, as compared to that which would be obtained in the same high-intensity blast region for an ideal burst. It is therefore recommended that a medium yield land surface burst be fired, preferably over a dusty region. This event would provide information as to the relative contribution of dust to the effects of blast in the strong shock region as well as to determine the significance of the additional dust loading as the result of the precursor. Such a test would also provide valuable data on cratering and ground shock as well as thermal and nuclear radiation.

As noted above there is very little test information in the ideal region for blast waves having an intensity corresponding to those observed on UPSHOT-KNOTHOLE in the nonideal case. It is considered that a low air burst over an ideal surface would provide such information. In order to avoid interaction of the fireball with the surface, a true air burst should be employed with an A-scaled height of burst equal to or greater than 1.5 fireball radius. It is therefore recommended that a high-yield air burst in the megaton range be fired to provide basic air blast data in the ideal case for low bursts as well as to confirm scaling under such blast conditions.

In order to resolve present differences in prediction criteria for precursor formation, it is recommended that blast measurements be made for a 1 to 2 KT burst fired at an A-scaled height between 50 and 450 ft. A development shot on a tower would be satisfactory for such purposes.*

REFERENCES

1. Cook and Broyles, *Curves of Atomic Weapons Effects for Various Burst Altitudes*, SC 3282, Mar. 9, 1954. SECRET RESTRICTED DATA
2. J. G. Kirkwood and S. R. Brinkley, *Theoretical Blast-wave Curves for Cast TNT*, Cornell University, Report OSRD-5481, Aug. 23, 1945. UNCLASSIFIED
3. Morris, Petes, Walthall, and Oliver, *Air Blast Measurements*, Naval Ordnance Laboratory, Operation UPSHOT-KNOTHOLE Projects 1.1a and 1.2, Report WT-710, August 1955. SECRET RESTRICTED DATA
4. L. M. Swift and D. C. Sachs, *Air Pressure and Ground Shock Measurements*, Stanford Research Institute, Operation UPSHOT-KNOTHOLE Project 1.1b, Report WT-711, January 1955. SECRET RESTRICTED DATA
5. J. D. Shreve, Jr., *Air Shock Pressure Time Vs Distance for a Tower Shot*, Operation UPSHOT-KNOTHOLE Project 1.1c-1, Report WT-712, April 1955. SECRET RESTRICTED DATA
6. C. D. Broyles, *Dynamic Pressure Vs Time and Supporting Air Blast Measurements*, Sandia Corporation, Operation UPSHOT-KNOTHOLE Project 1.1d, Report WT-714, February 1954. SECRET RESTRICTED DATA
7. J. D. Shreve, Jr., *Pressure-Distance-Height Study of 250-lb TNT Spheres*, Sandia Corporation, Operation TUMBLER-SNAPPER Project 1.10, Report WT-520, Mar. 13, 1953. SECRET RESTRICTED DATA
8. H. Scoville et al., *Final Summary Report*, Operation TUMBLER, Armed Forces Special Weapons Project, Report WT-514, May 1953. SECRET RESTRICTED DATA
9. F. H. Shelton, *The Precursor — Its Formation, Prediction, and Effects*, SC-2850 (TR), July 27, 1953. SECRET RESTRICTED DATA
10. V. Salmon, *Air Pressure Vs Time*, Stanford Research Institute, Operation TUMBLER-SNAPPER Project 1.2, Report WT-512, February 1953. SECRET RESTRICTED DATA
11. B. F. Murphey, *Air Shock Pressure-Time Vs Distance*, Sandia Corporation, Operation TUMBLER-SNAPPER Project 1.1a, Report WT-501, Aug. 1, 1952. SECRET RESTRICTED DATA
12. R. Zirkind, *Air Analysis of the Triple Point Curve*, DR 1517, April 1953. SECRET RESTRICTED DATA

*This report was written prior to the TEAPOT test series at the NPG.

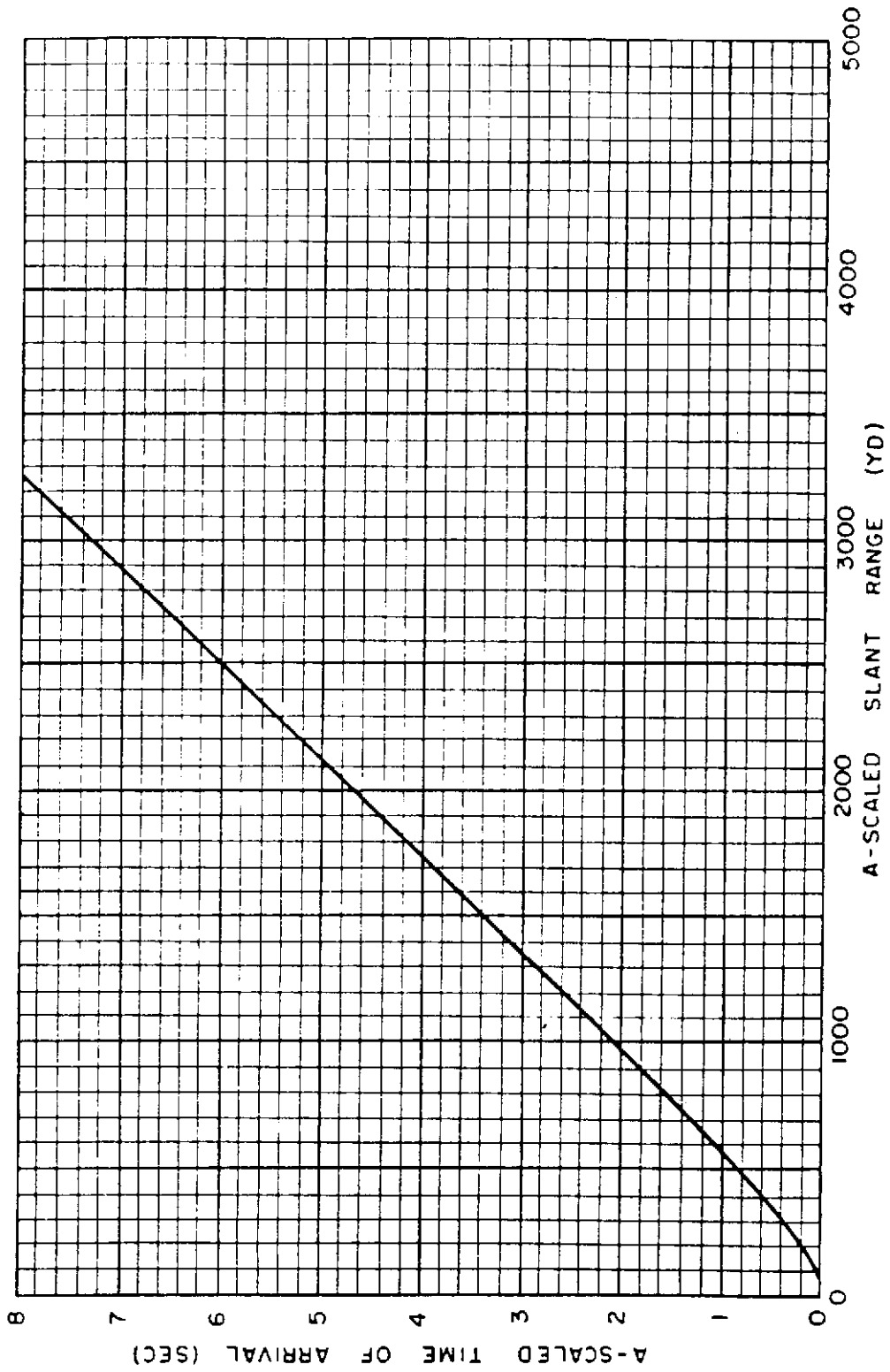


Fig. 2.1 — Composite UPSHOT-KNOTHOLE-TUMBLER-IVY Time-of-arrival Curve.



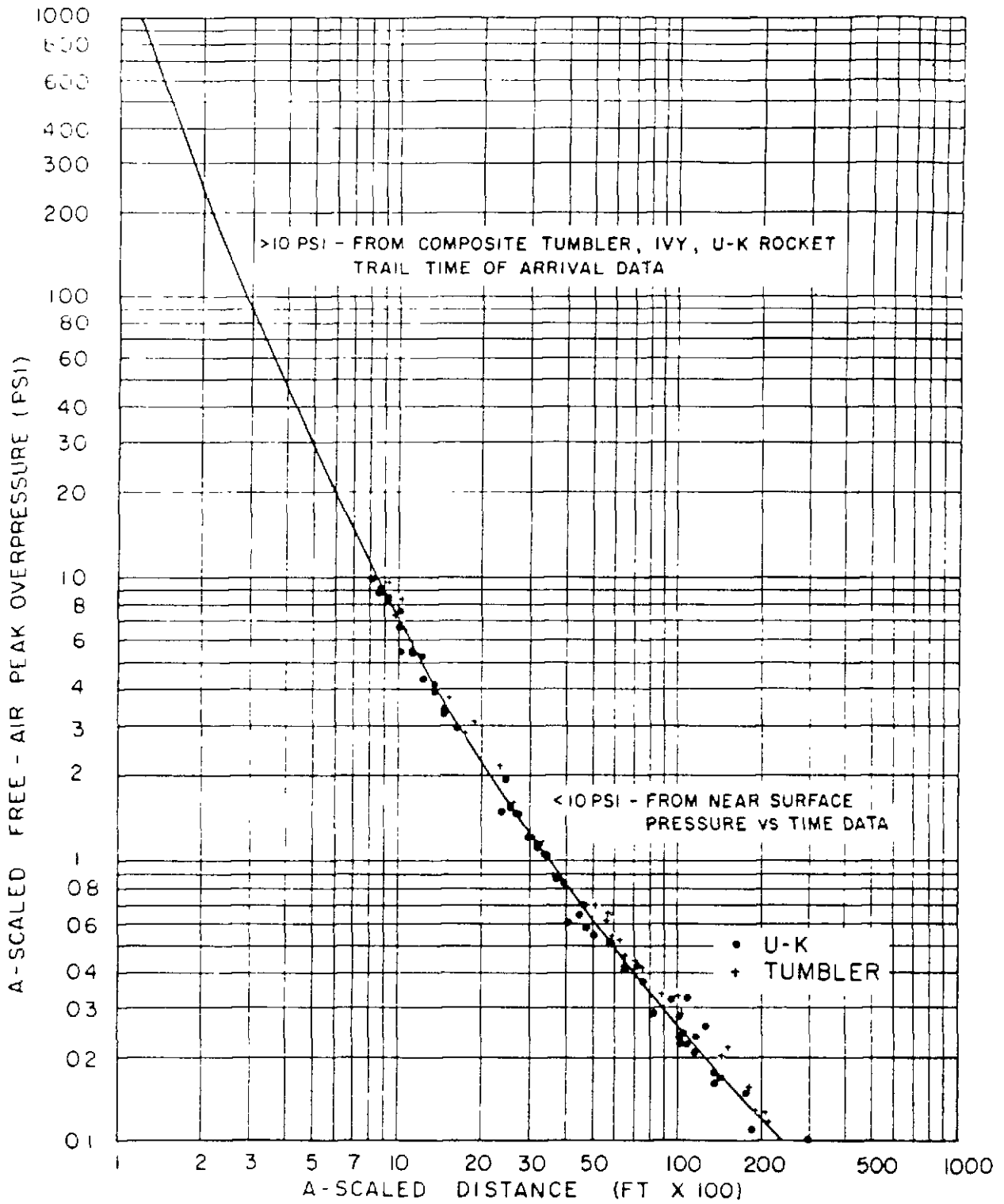


Fig. 2.2—Proposed Standard Free Air Peak Overpressure Curve.



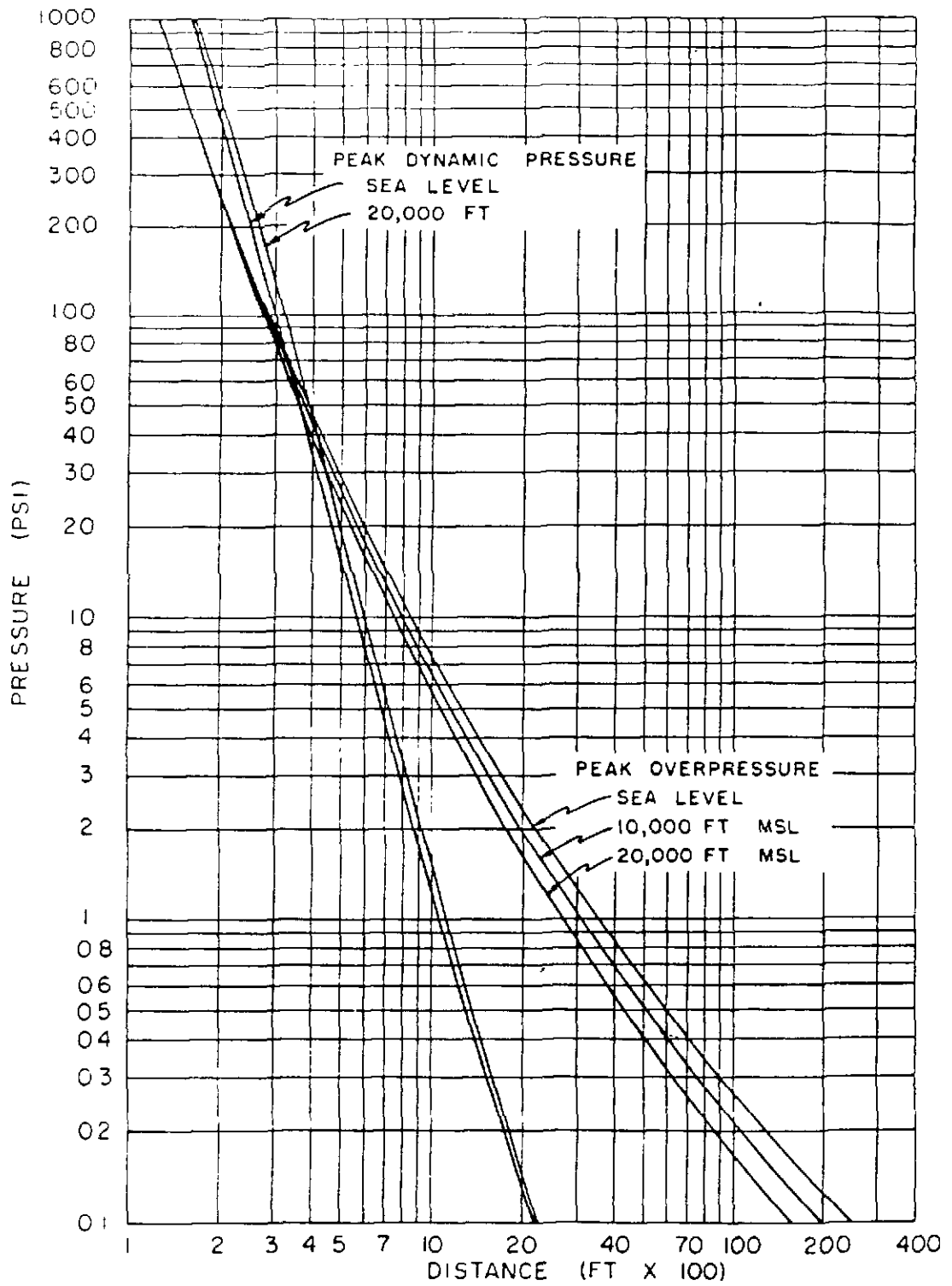


Fig. 2.3—Free Air Peak Overpressure and Peak Dynamic Pressure for Various Altitudes.

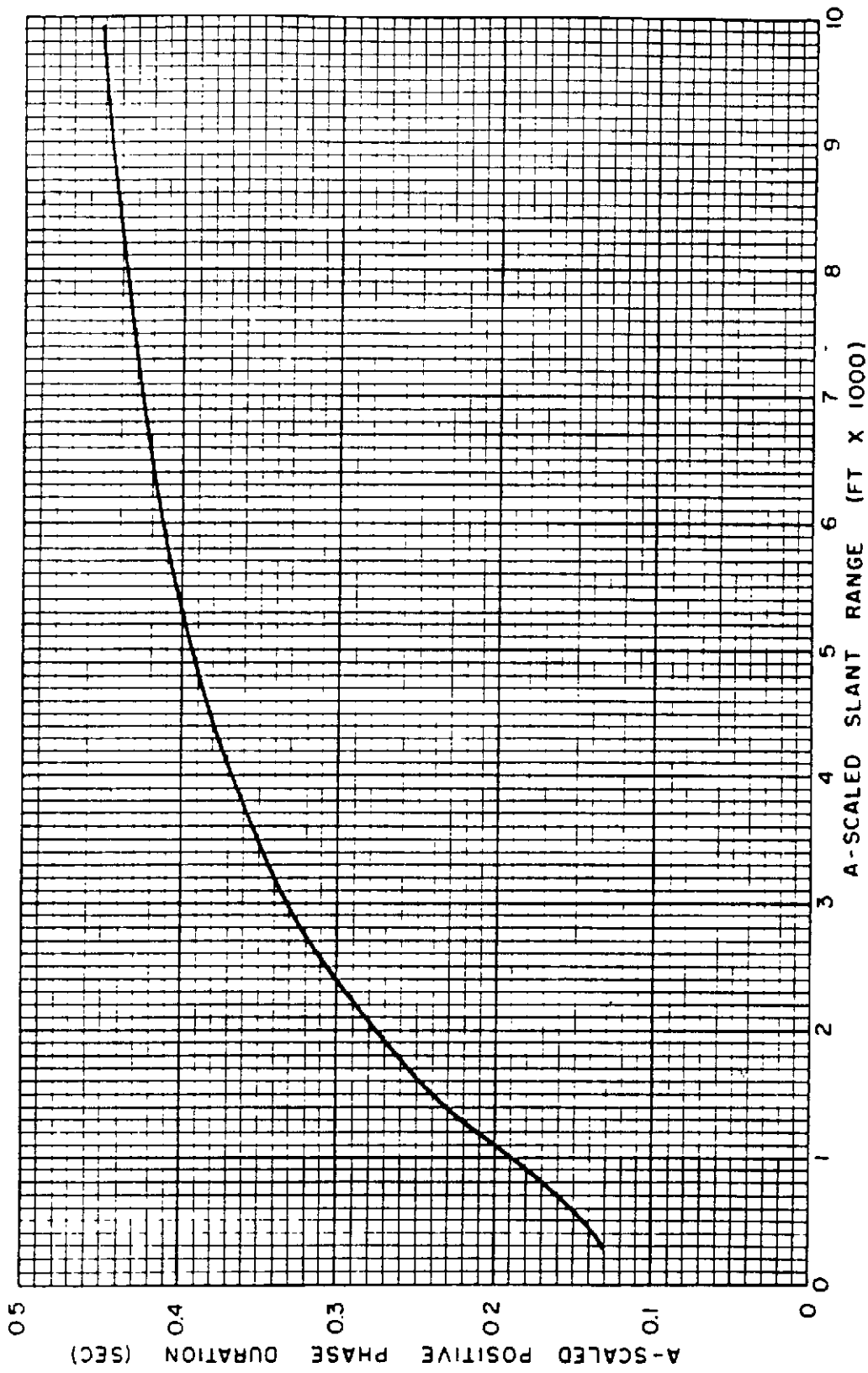


Fig. 2.4 — Free Air Overpressure Positive Phase Duration (A-Scaled).



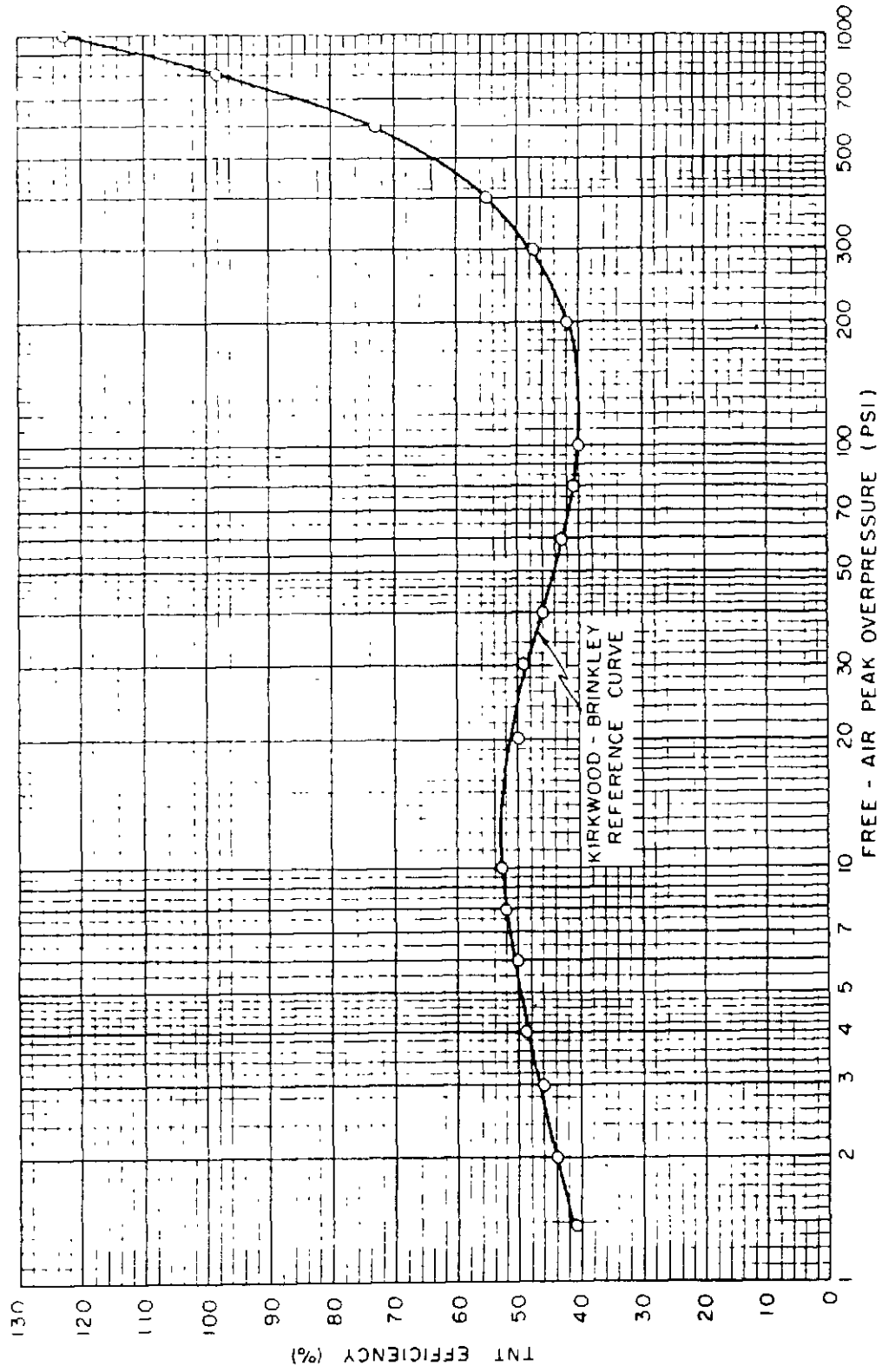


Fig. 2.5—TNT Efficiency Vs Free Air Peak Overpressure, Using Kirkwood-Brinkley Reference Curve for TNT.

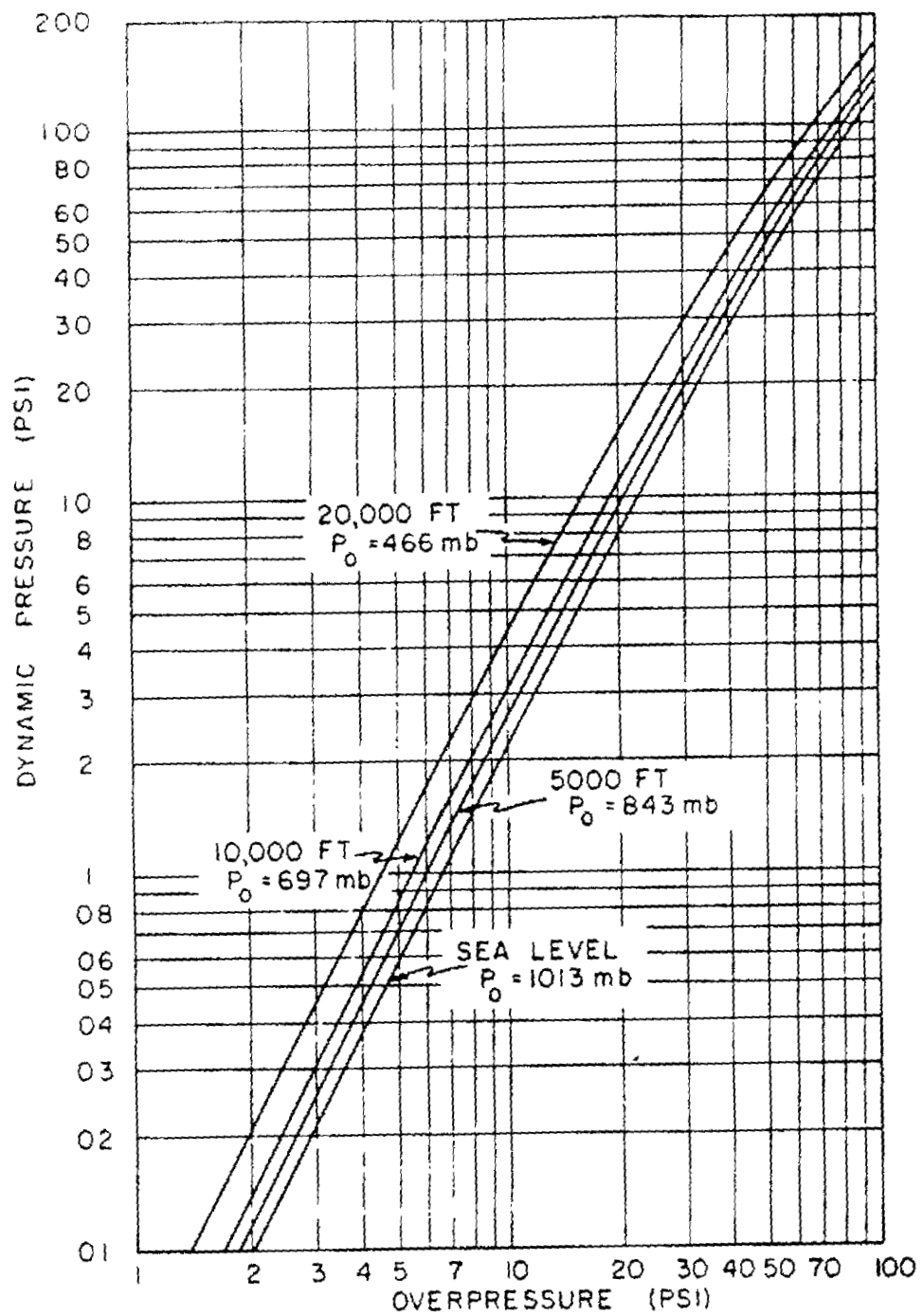


Fig. 2.6—Free Air Peak Dynamic Pressure Vs Free Air Peak Overpressure for Various Altitudes.

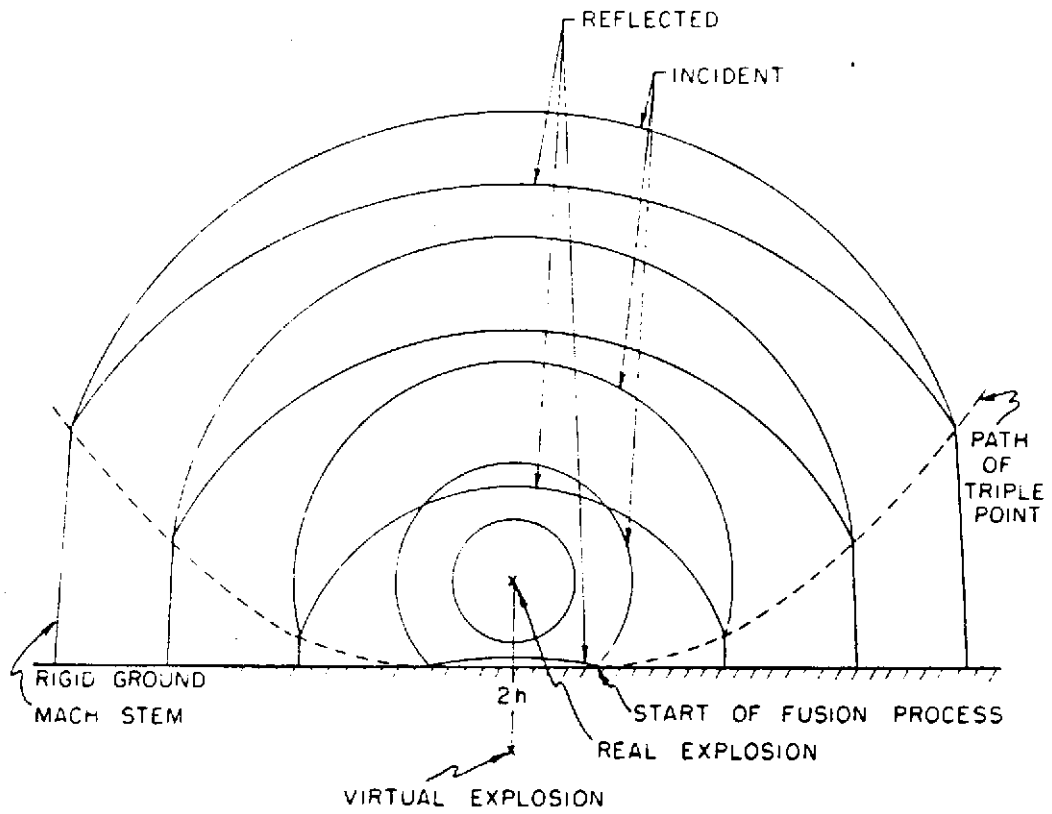


Fig. 2.7—Schematic Drawing of Ideal Regular and Mach Reflection.



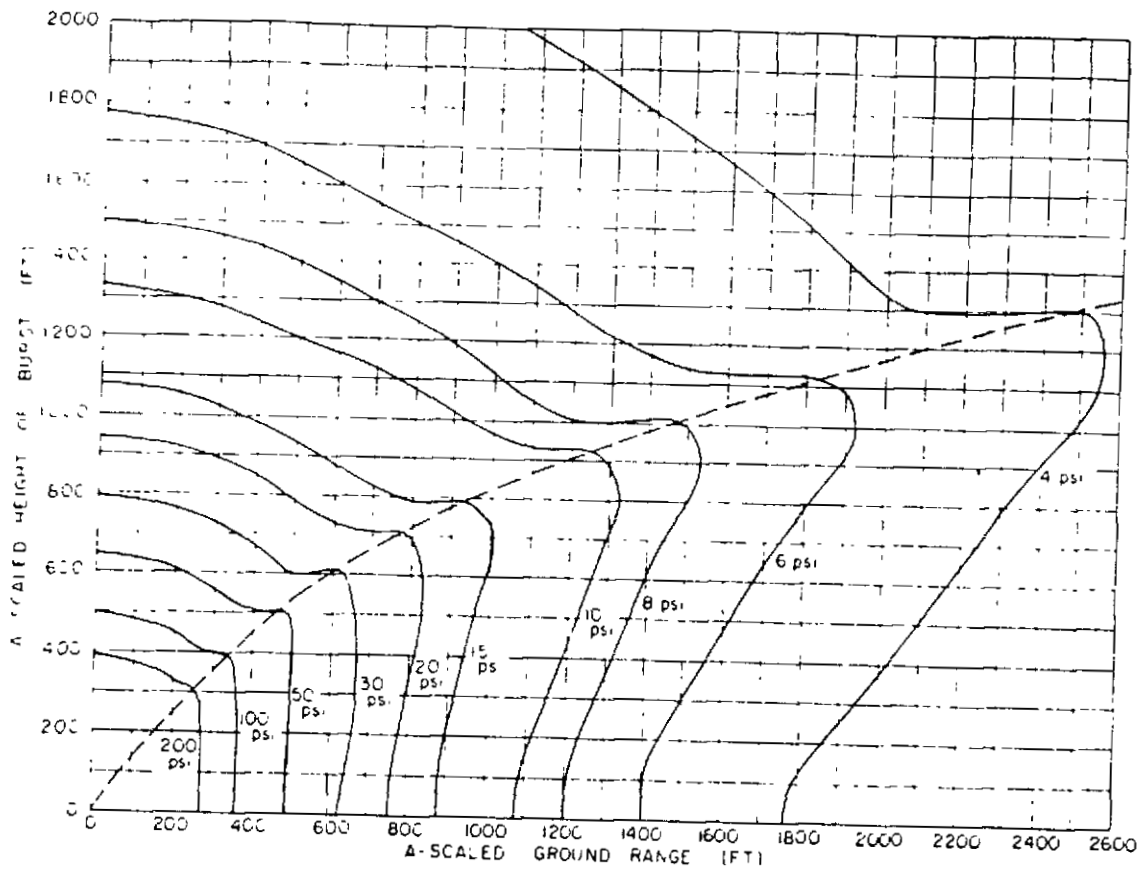


Fig. 2.8—Ideal Peak Overpressure Height-of-burst Curves.

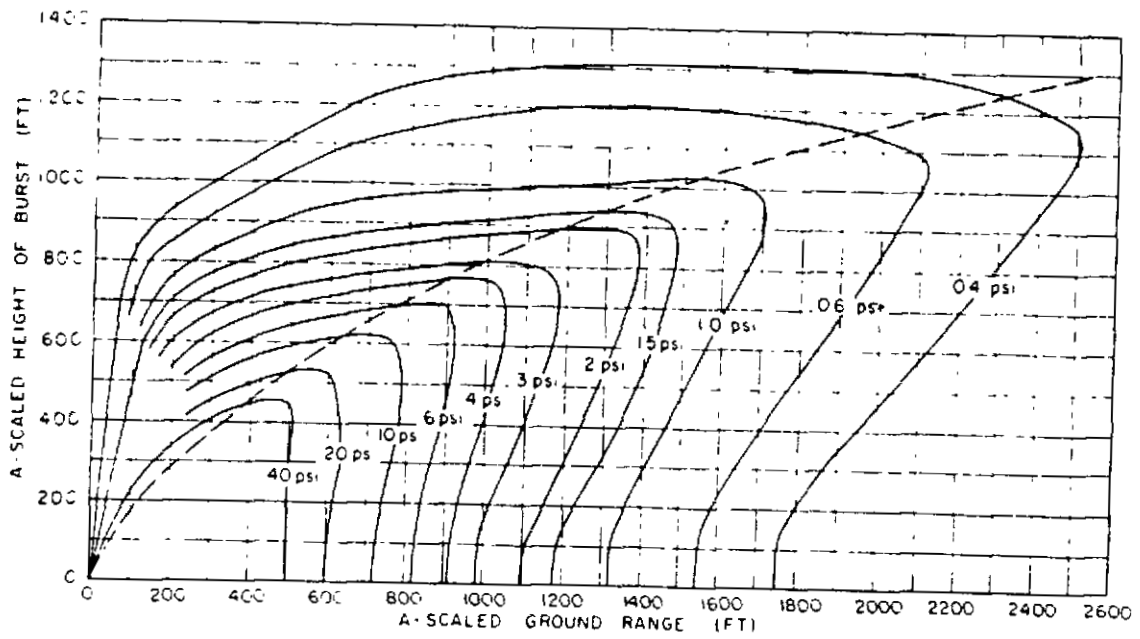
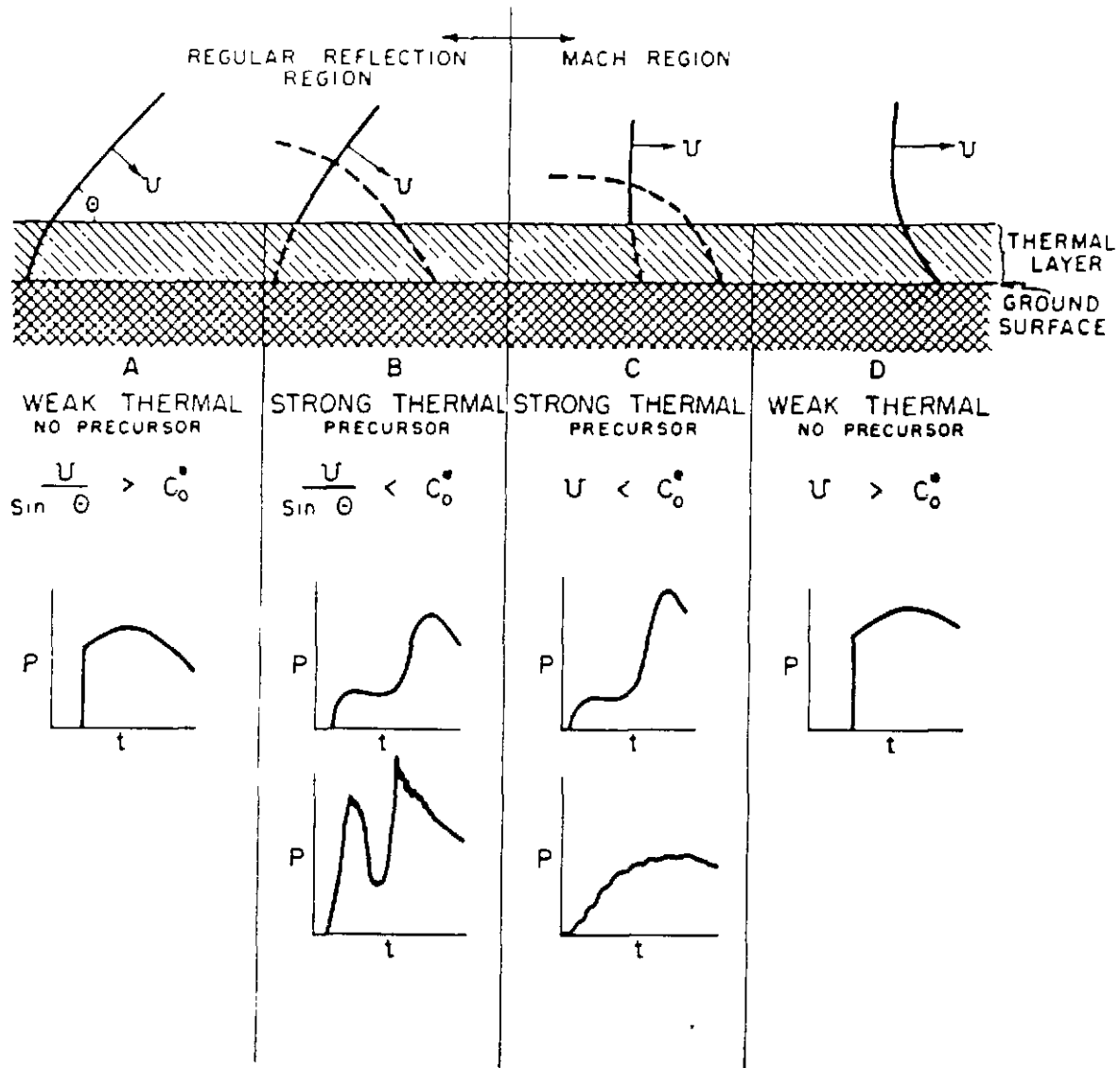


Fig. 2.9—Ideal Peak Dynamic Pressure Height-of-burst Curves.





Fig. 2.10 — Photograph of Freshock Popcorning. Operation TUMBLER-SNAPPER.



U - VELOCITY OF SHOCK TRANSMISSION IN UNHEATED AIR ABOVE THERMAL LAYER
 C_0^* - VELOCITY OF SOUND IN THERMAL LAYER - A FUNCTION OF HEIGHT, GROUND RANGE AND TIME
 (ALL REFLECTED SHOCKS OMITTED FOR SIMPLIFICATION)

Fig. 2.11 — Schematic Diagrams of Precursor Formation.

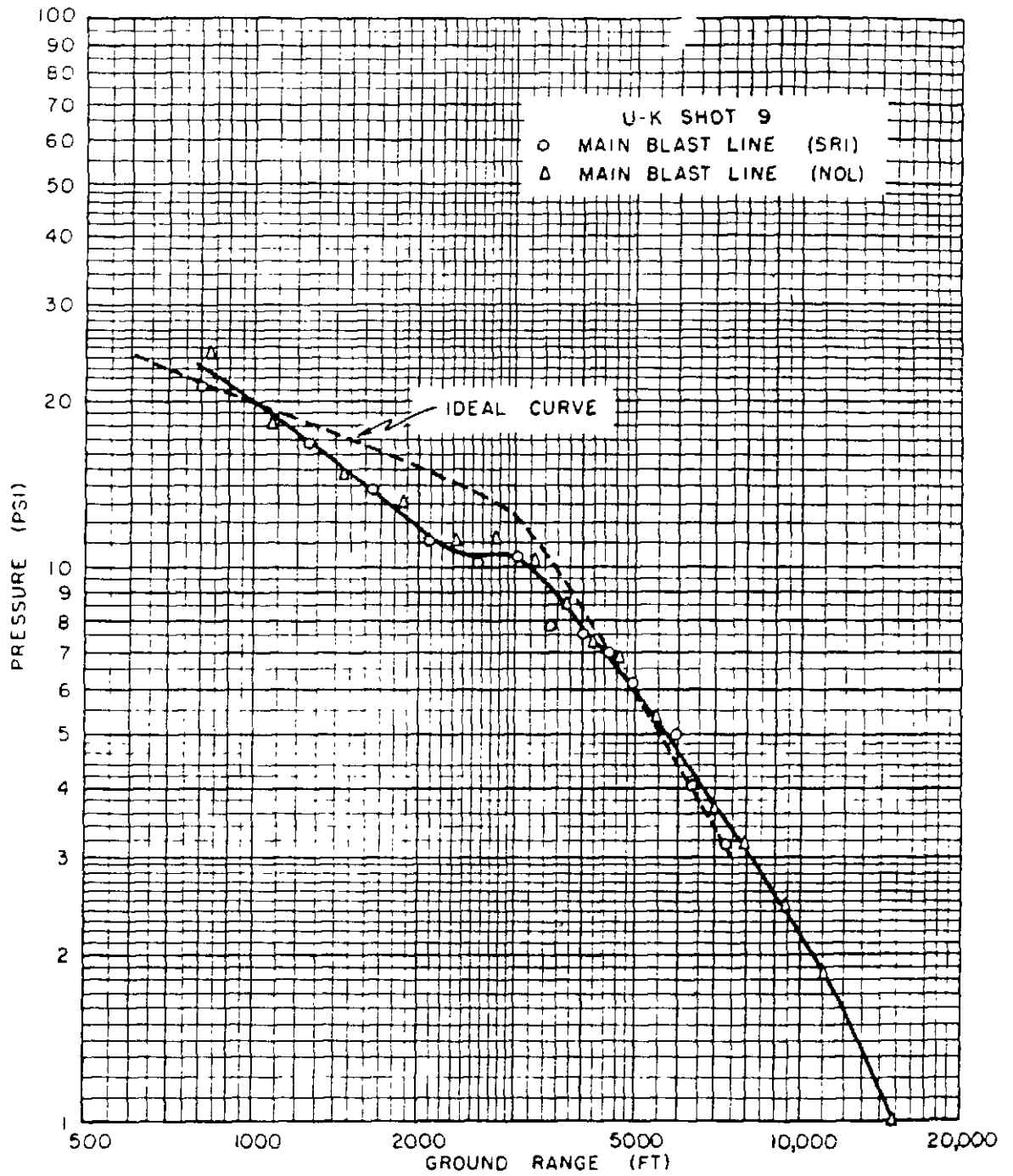


Fig. 2.12—Ground-level Peak Overpressure, Shot 9, with Ideal Curve.

CONFIDENTIAL DATA

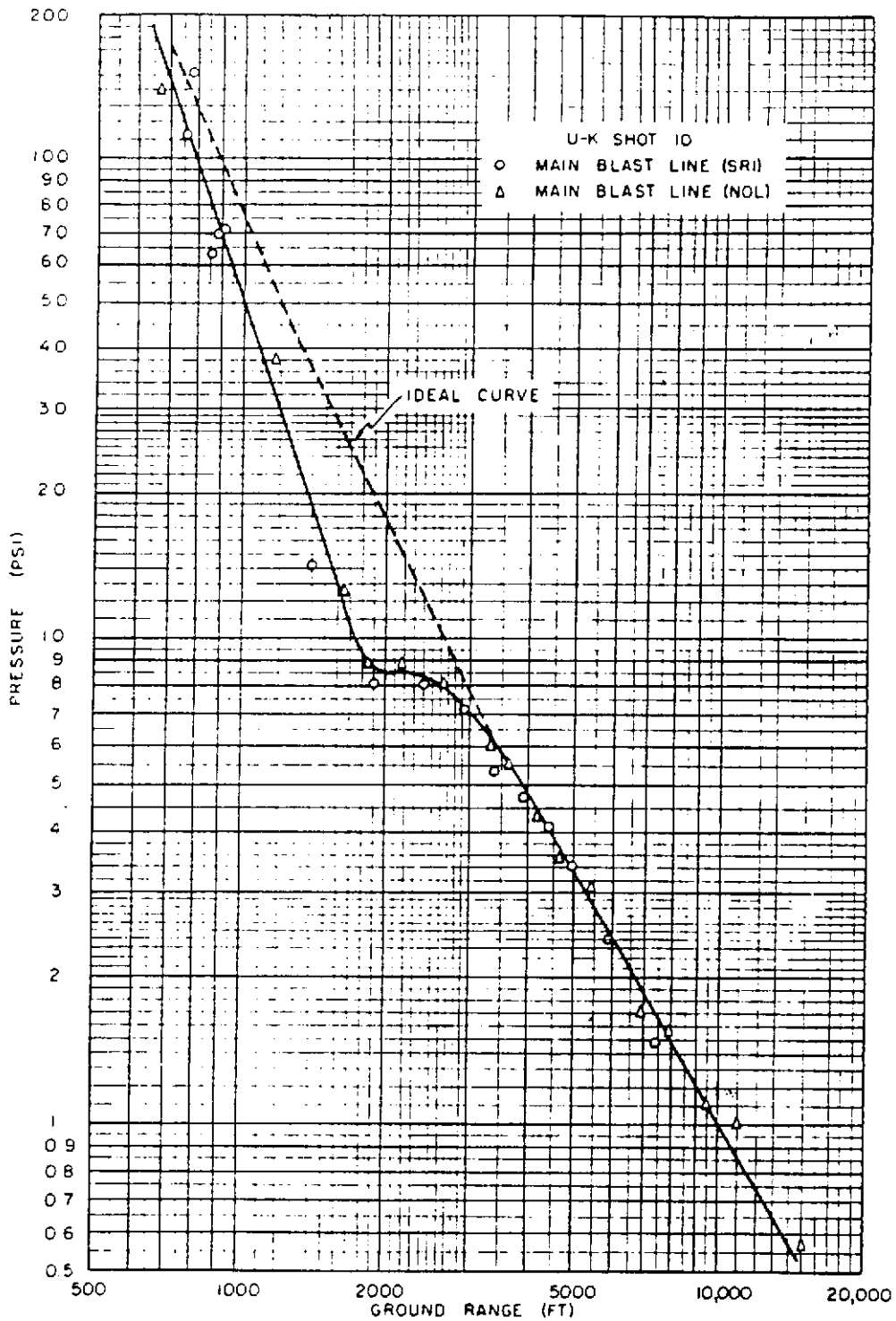


Fig. 2.13—Ground-level Peak Overpressure, Shot 10, with Ideal Curve.

GRAPH RESTRICTED DATA

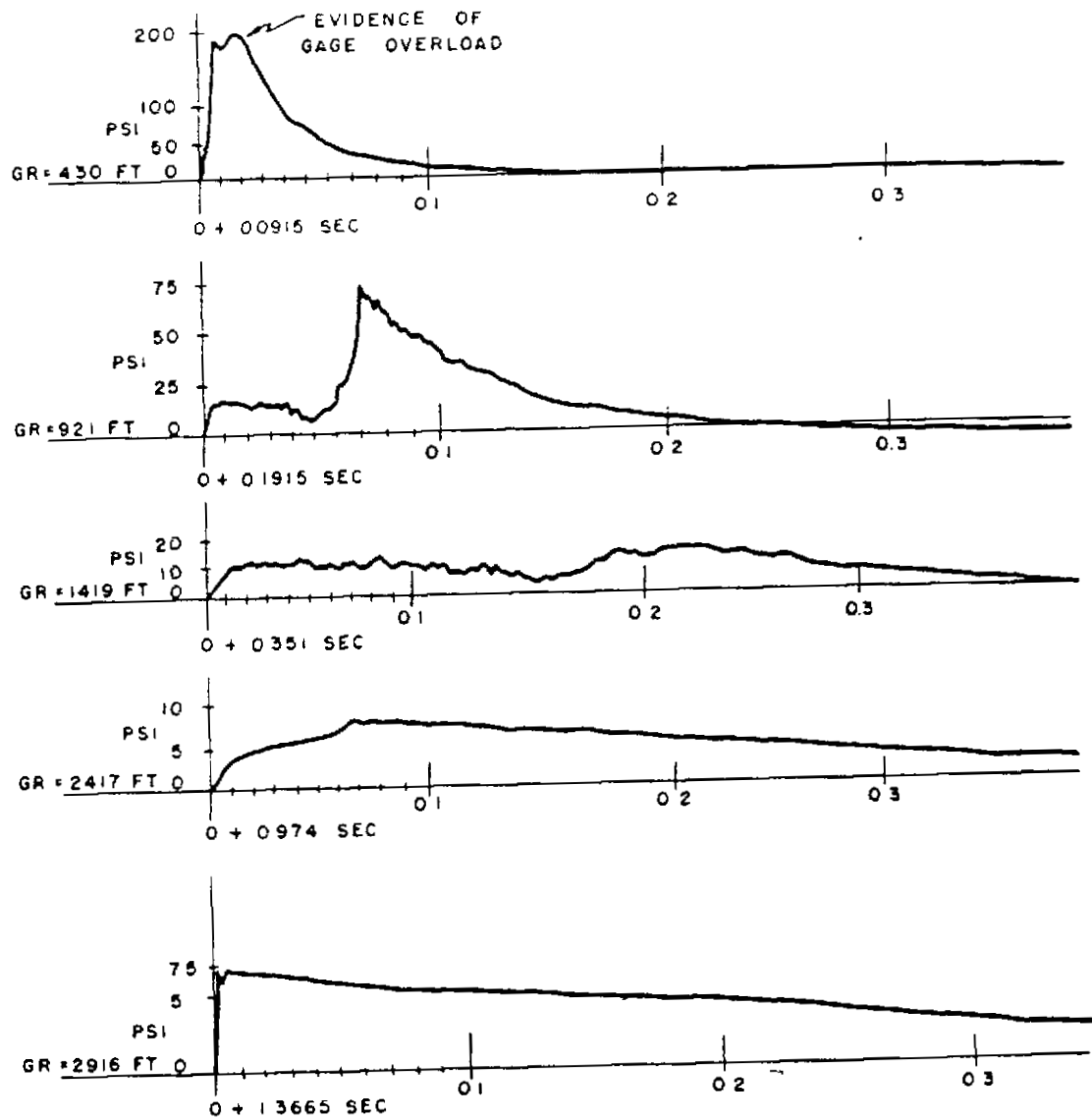


Fig. 2.14 Sample Shot 10 Ground-level Overpressure Vs Time Records in Nonideal Region.

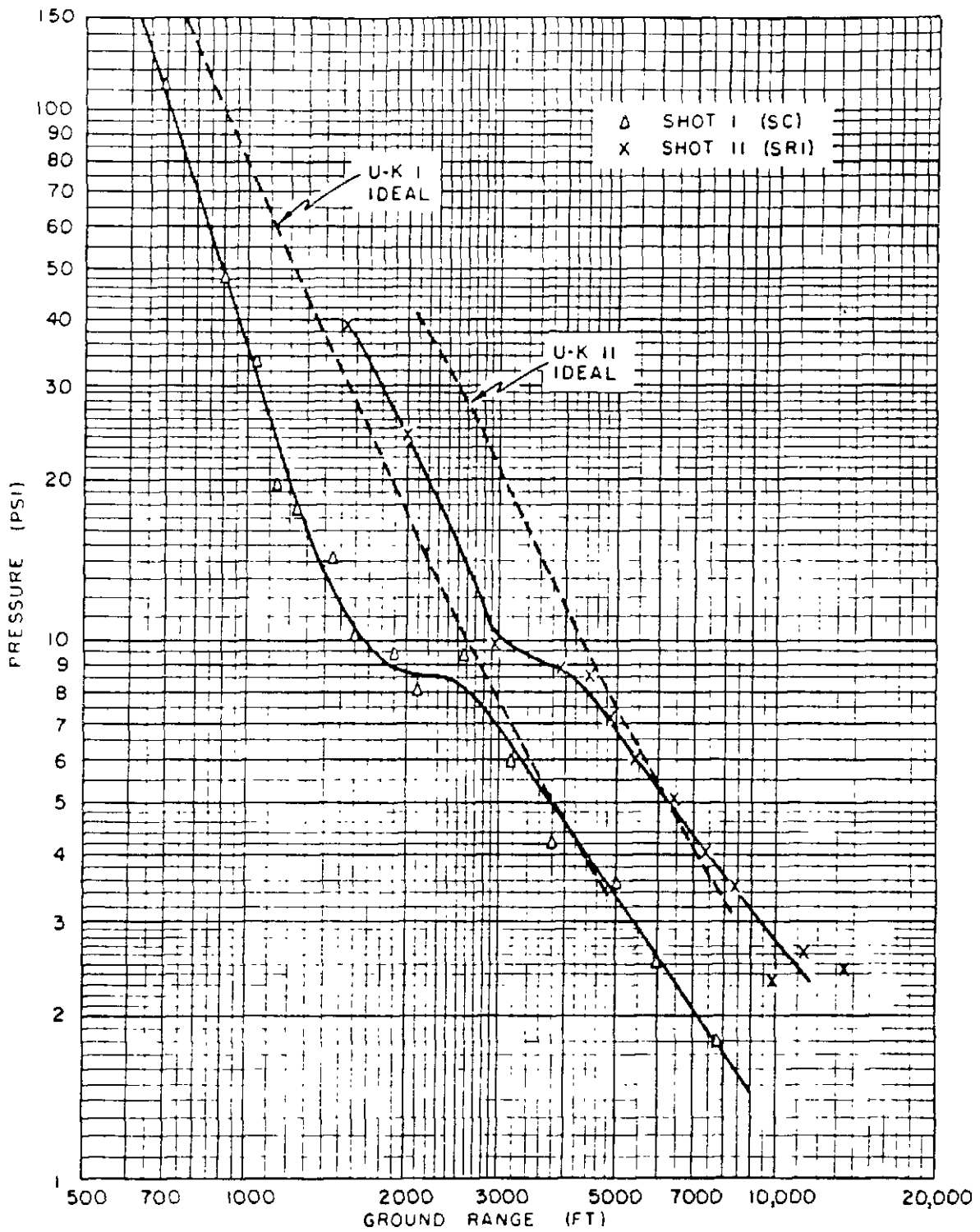


Fig. 2.15— Ground-level Peak Overpressure, Shots 1 and 11, with Ideal Curves.

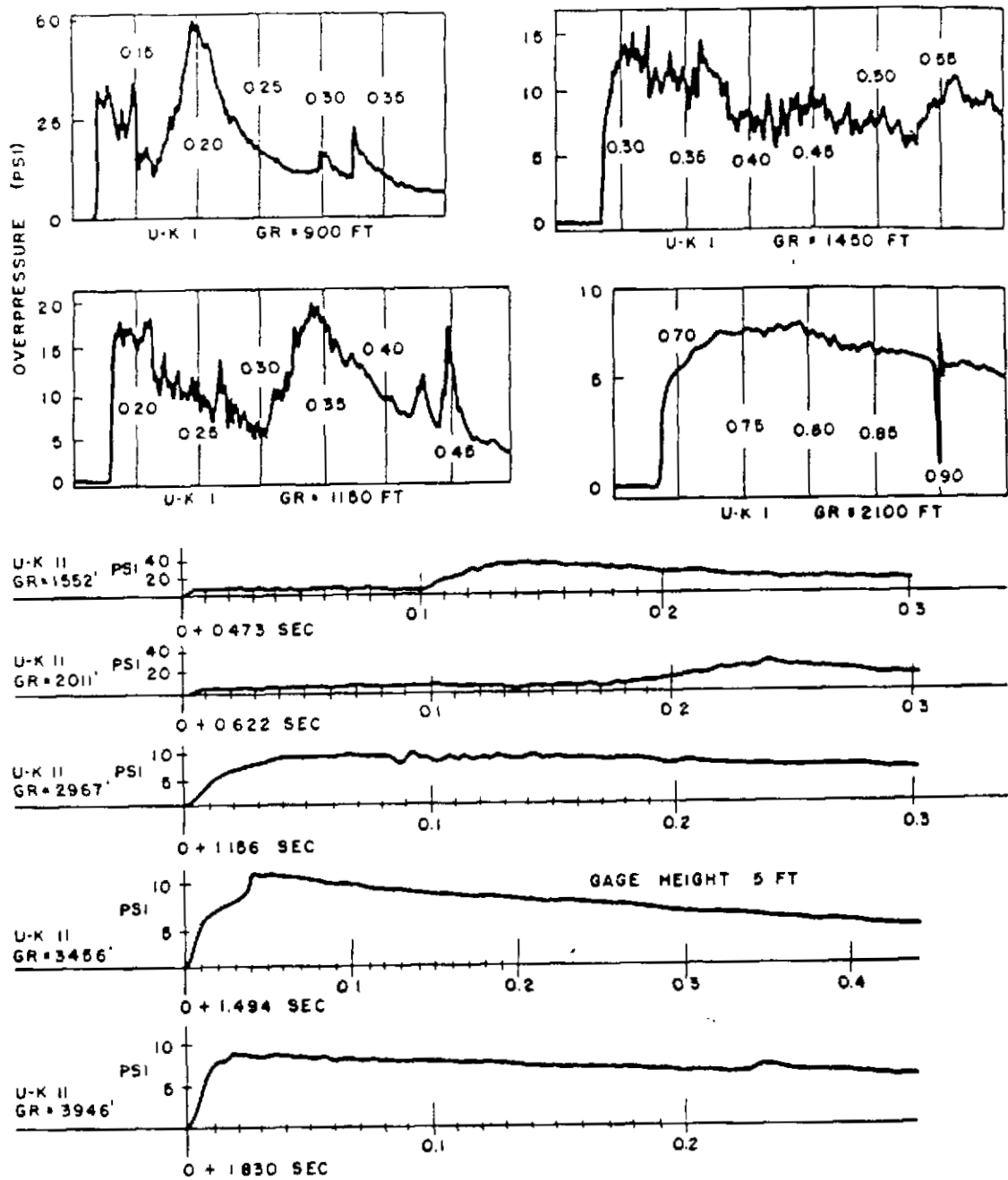


Fig. 2.16—Sample Shot 1 and Shot 11 Ground-level Overpressure Vs Time Records in Nonideal Region.

~~RESTRICTED DATA~~

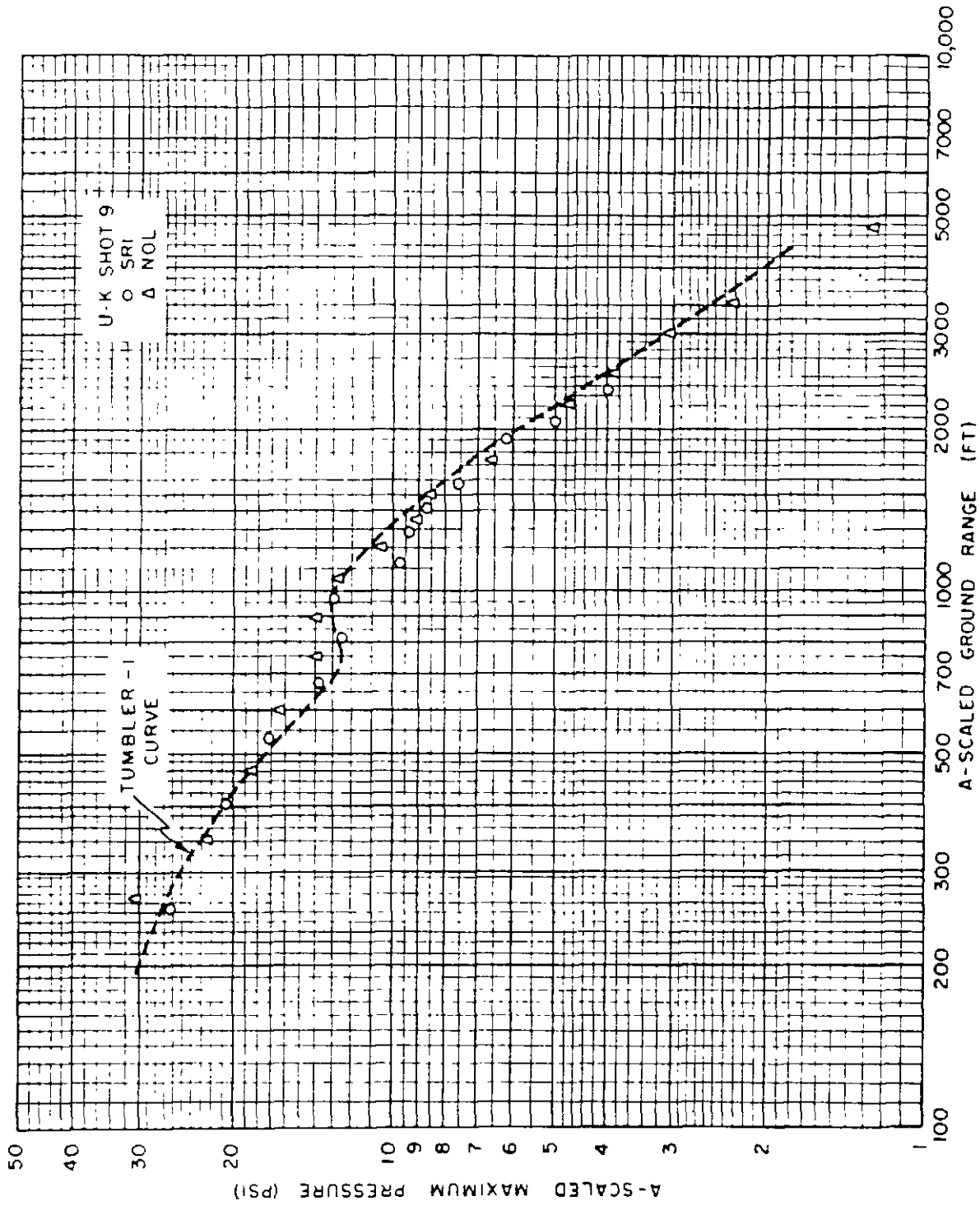


Fig. 2.17 — Shot 9 and TUMBLER Shot 1 Ground-level Peak Overpressure.

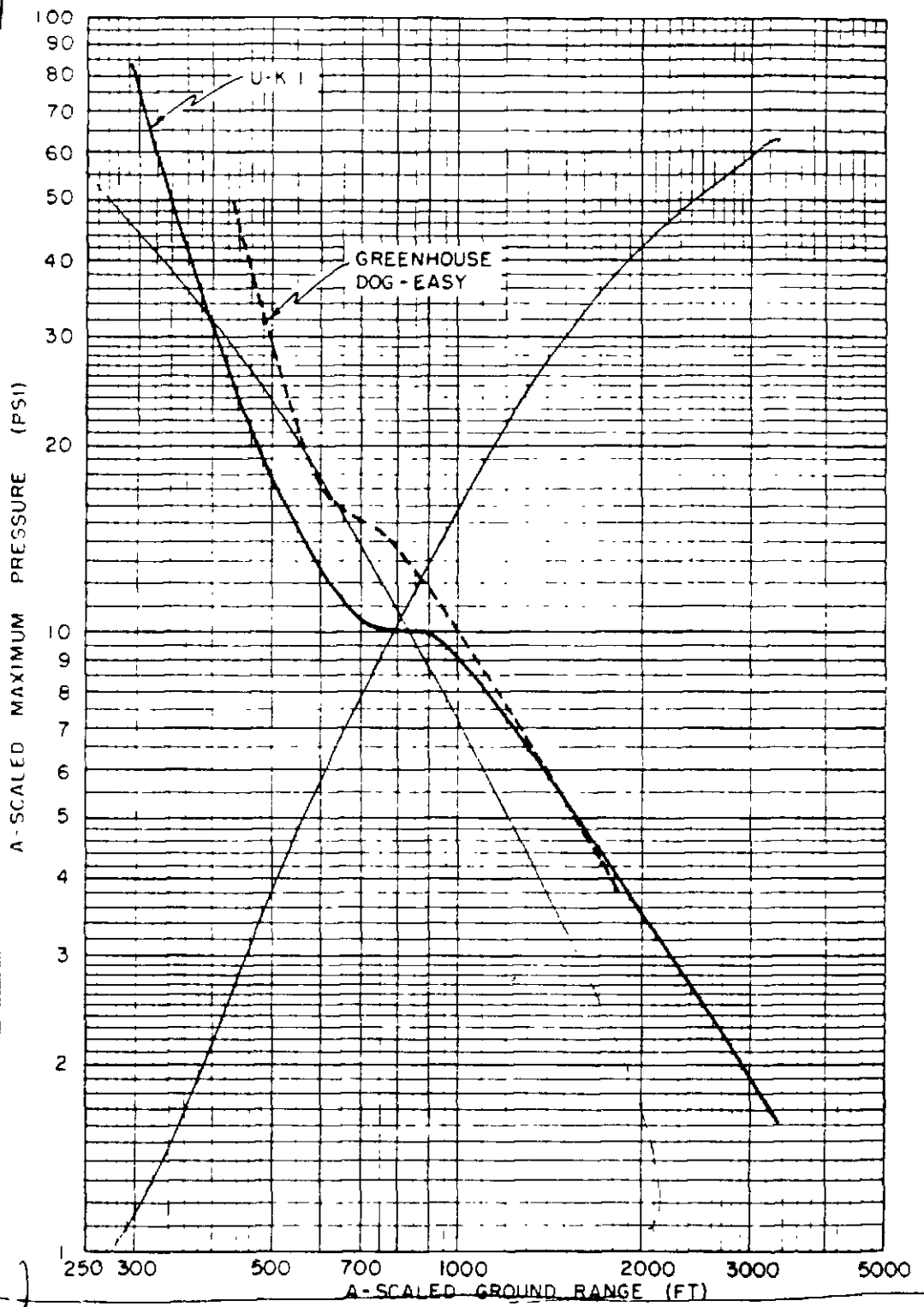


Fig 2 1a—Shot 1 and GREENHOUSE Dog and Easy Peak Overpressure.

55ET



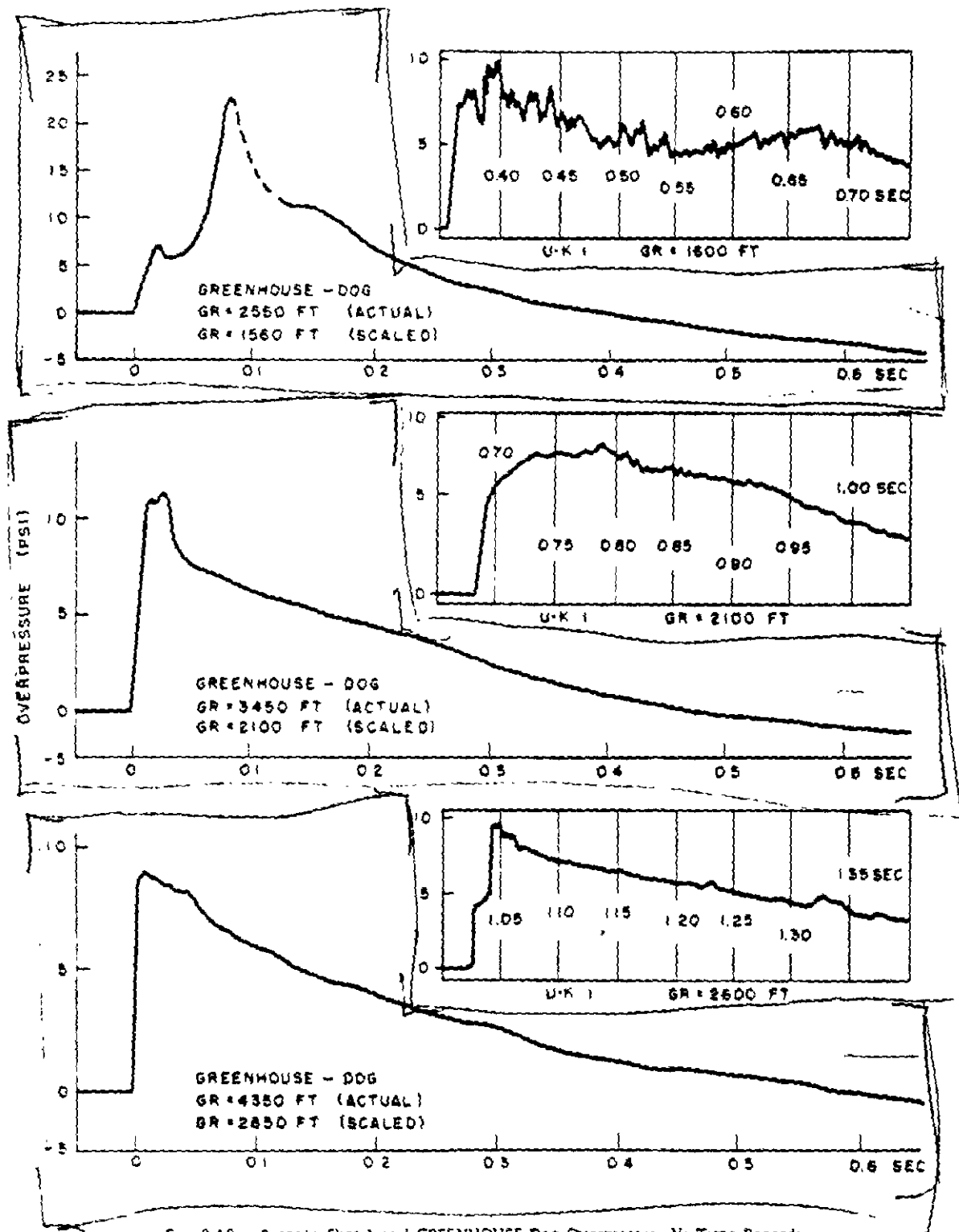


Fig. 2.19—Sample Shot 1 and GREENHOUSE Dog Overpressure Vs Time Records.

STET



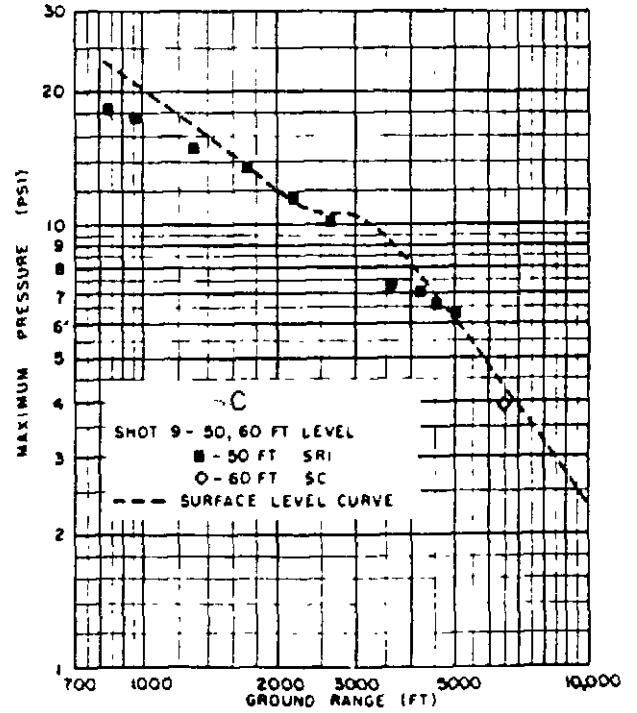
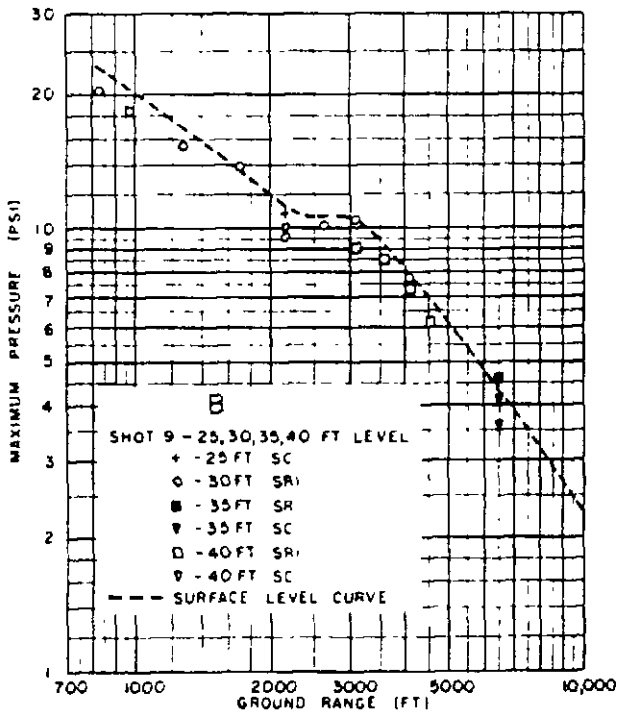
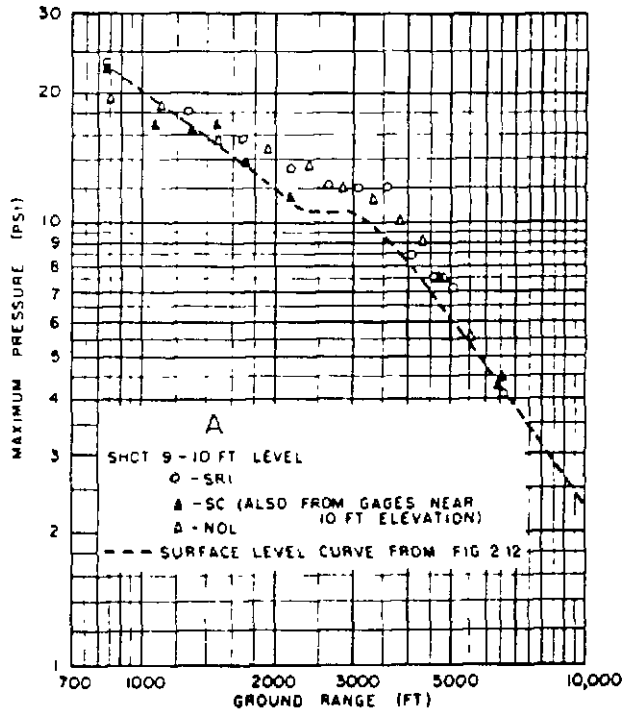


Fig. 2.20 — Shot 9 Aboveground Peak Overpressure.



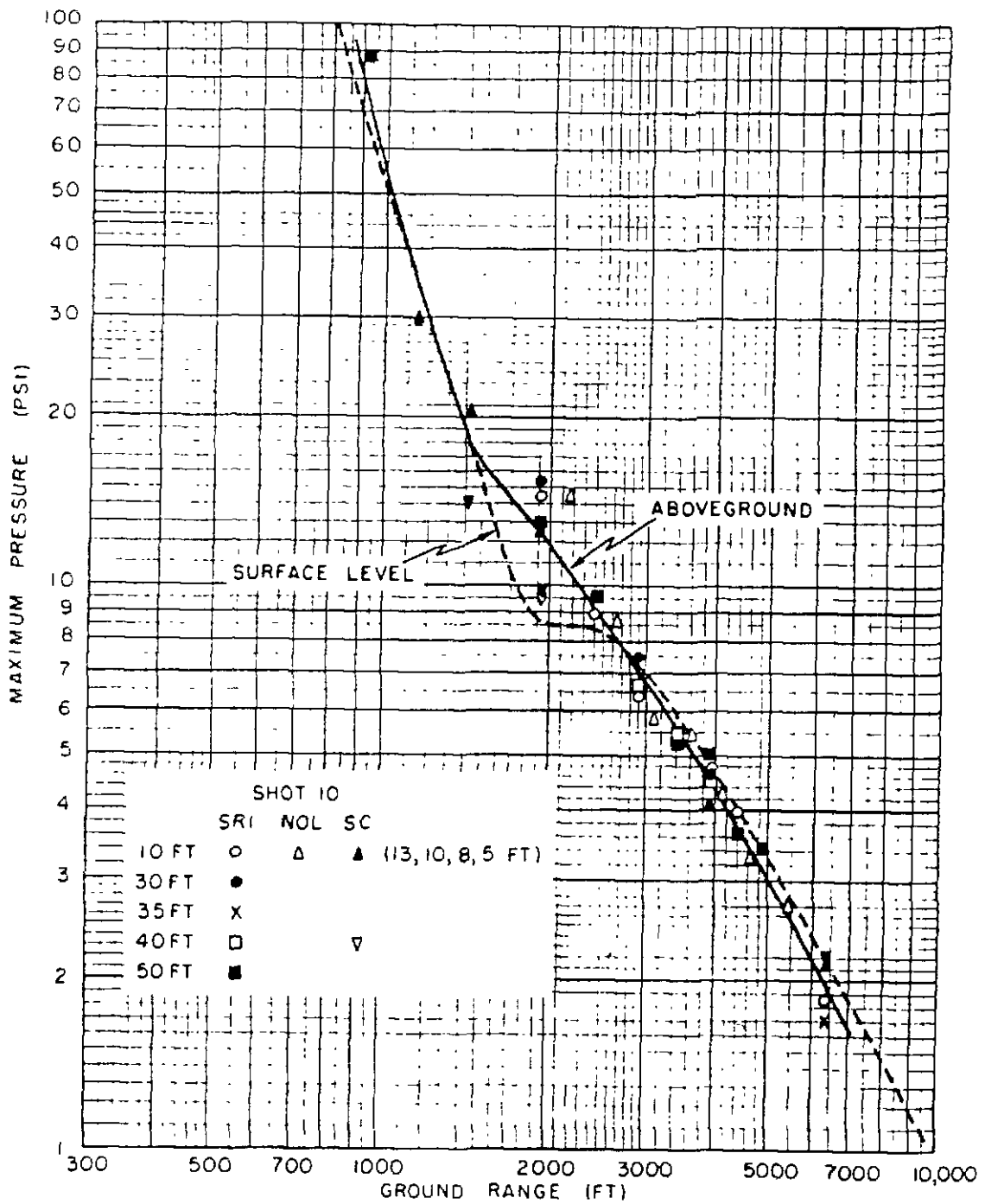


Fig. 2.21 — Shot 10: Aboveground Peak Overpressure.

CONFIDENTIAL

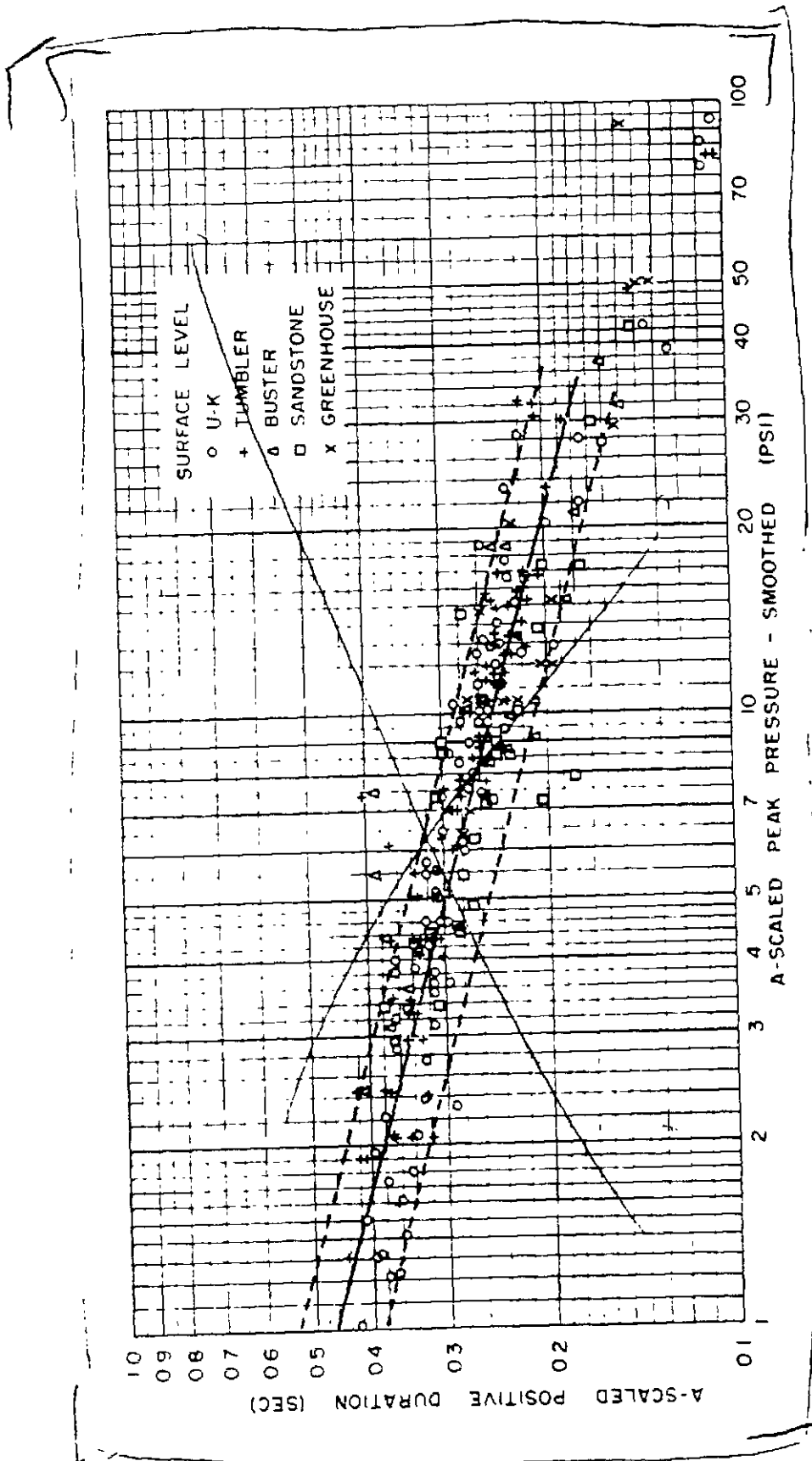


Fig. 2.22 -- Positive Phase Duration Vs Peak Overpressure, All Available Shots.

STEI

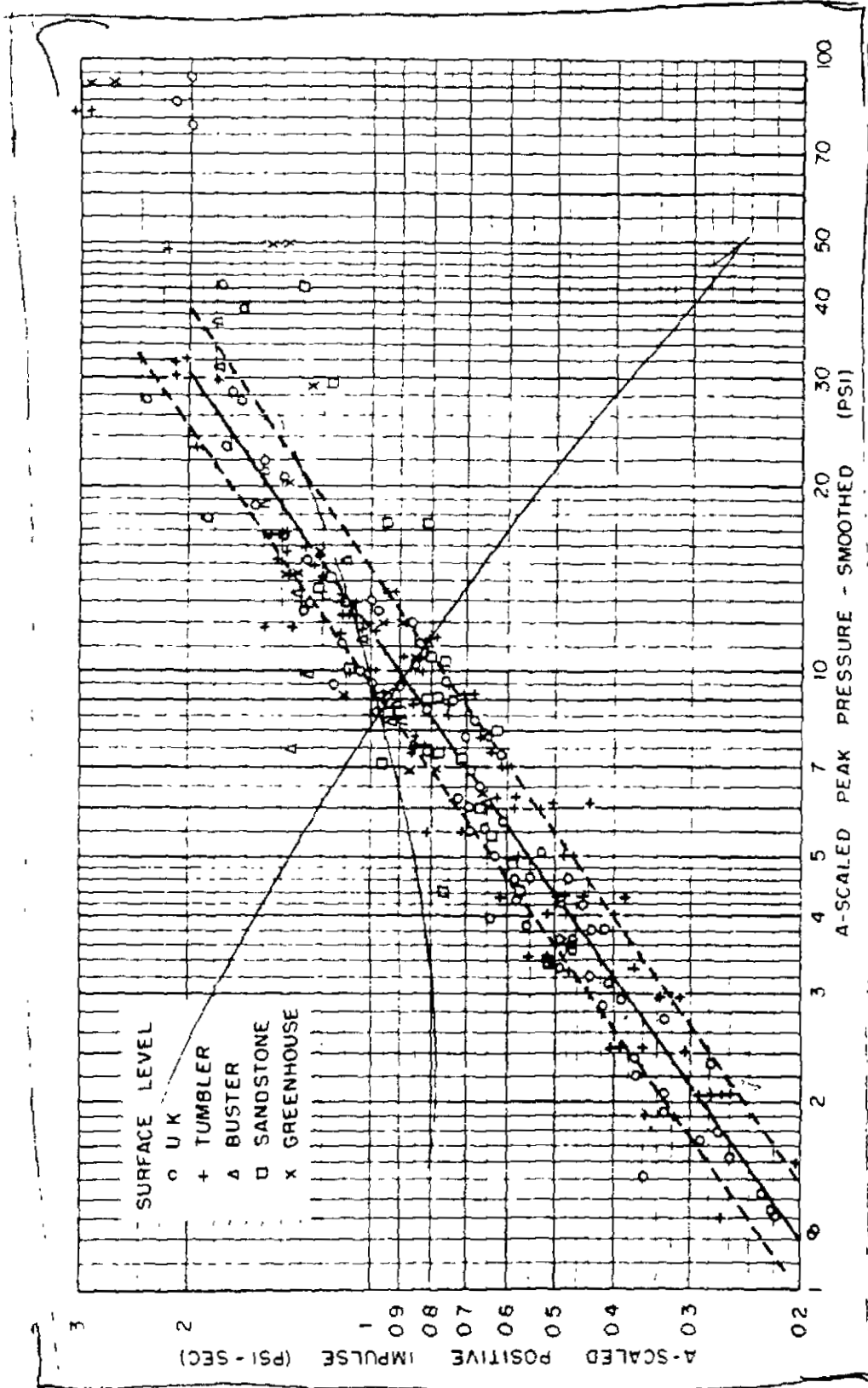


Fig. 2.23 — Positive Phase Impulse Vs Peak Overpressure, All Available Shots.

SIET

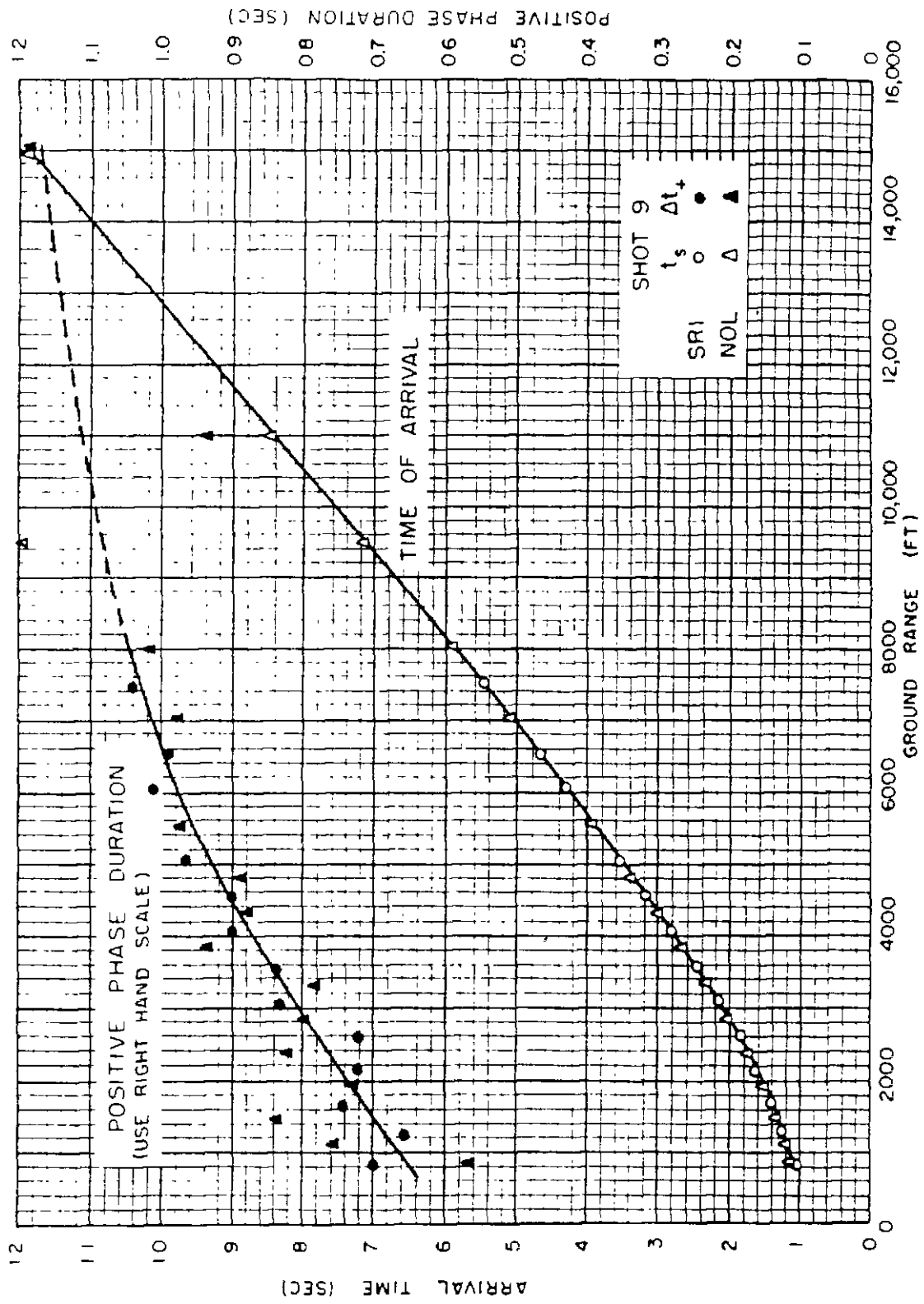


Fig. 2.24 — Positive Phase Duration and Arrival Time, Shot 9.

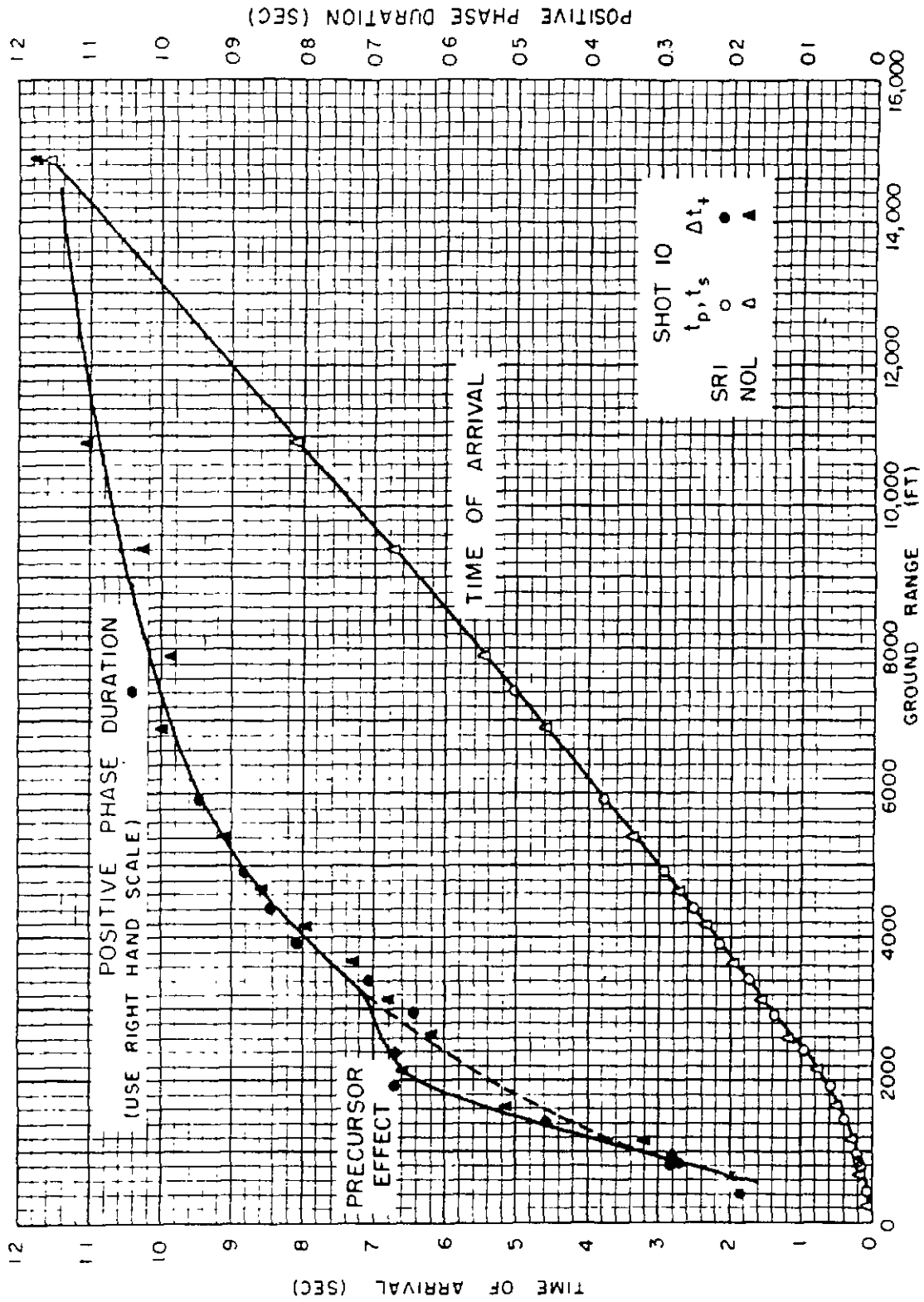


Fig. 2.25 Positive Phase Duration and Arrival Time, Shot 10.

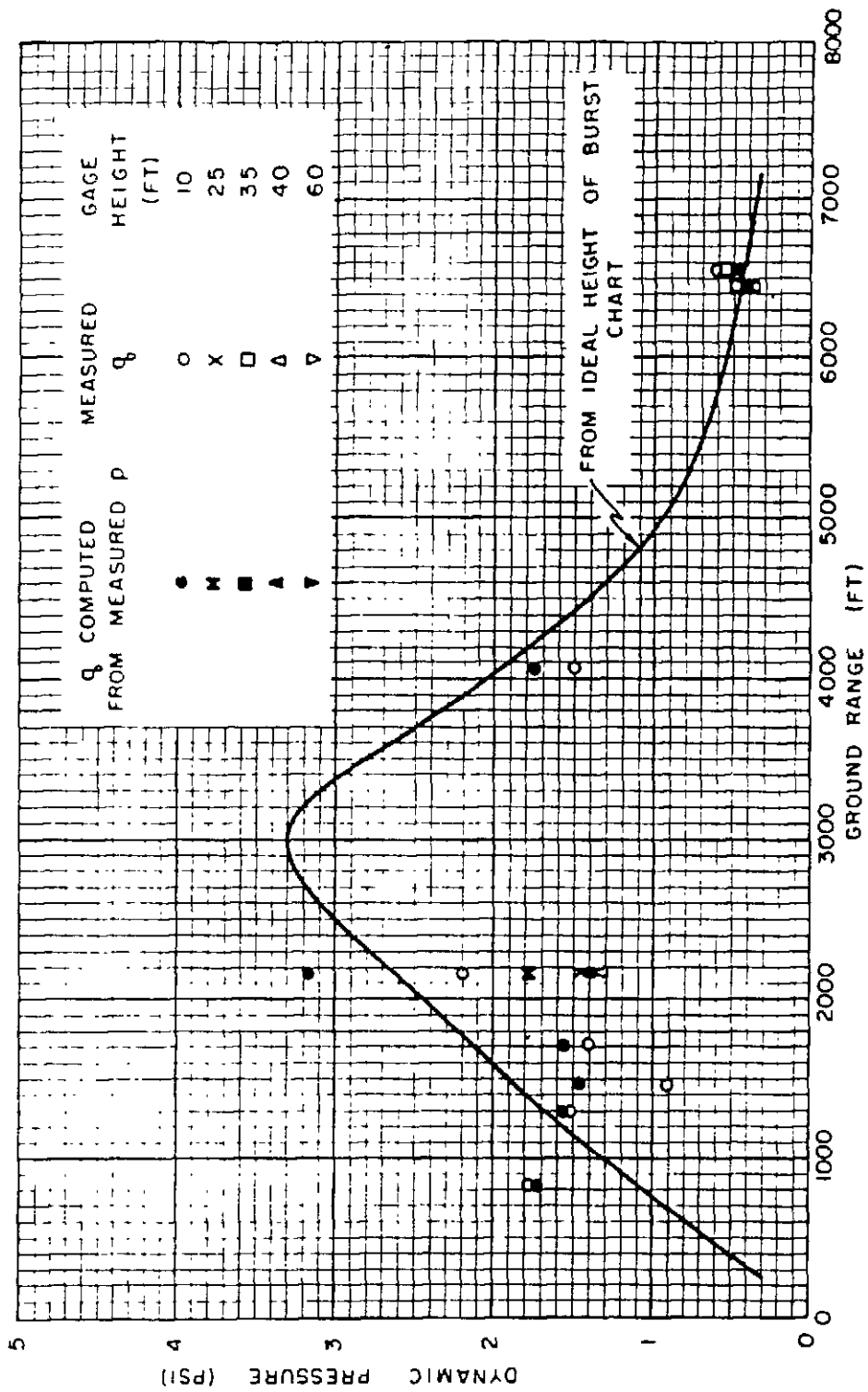


Fig. 2.26 — Measured Dynamic Pressure, Shot 8, Compared to Ideal and to Dynamic Pressure Computed from Measured Peak Overpressure.

59

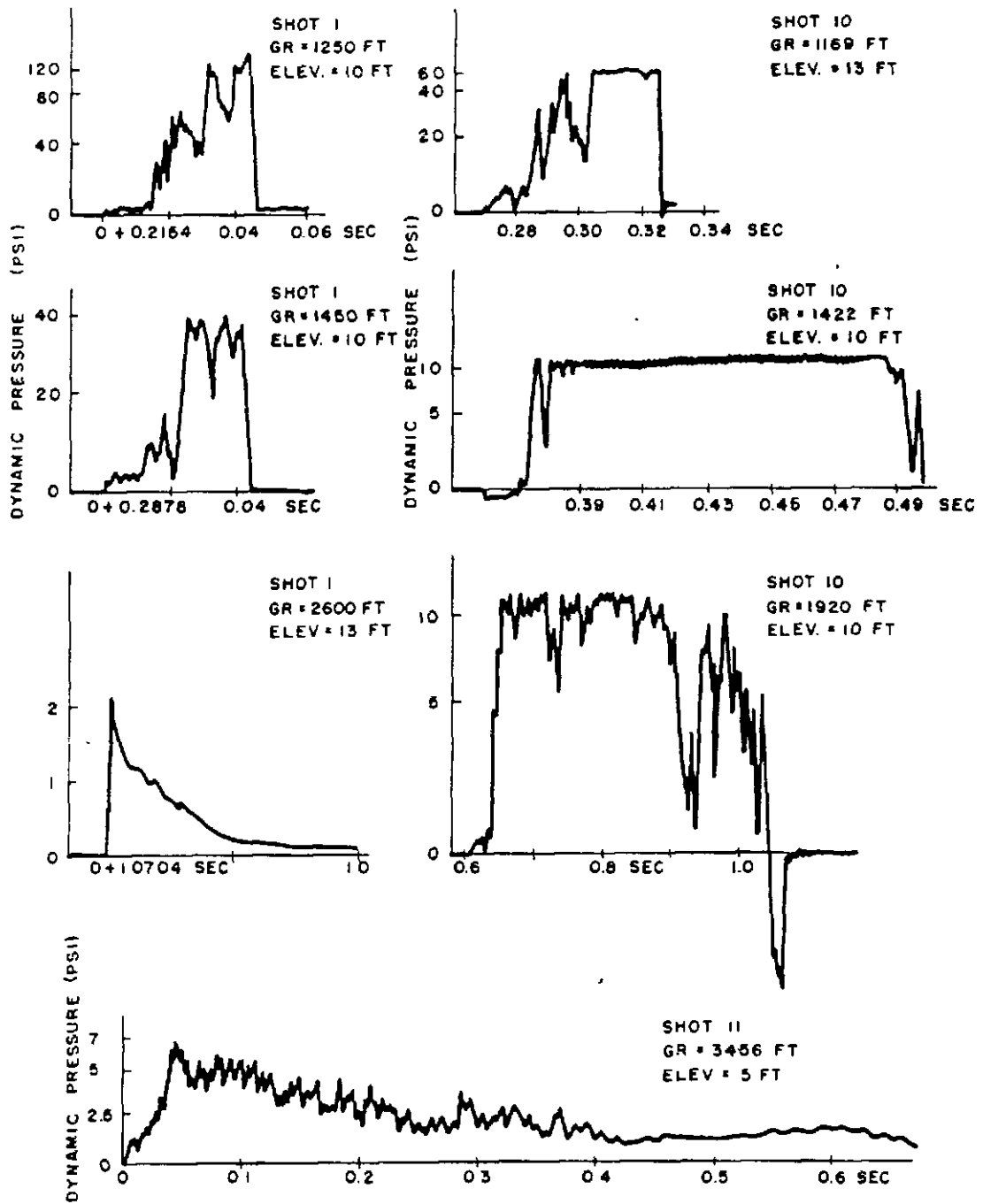


Fig. 2.27—Sample Dynamic Pressure Vs Time Records, Shots 1, 10, and 11.



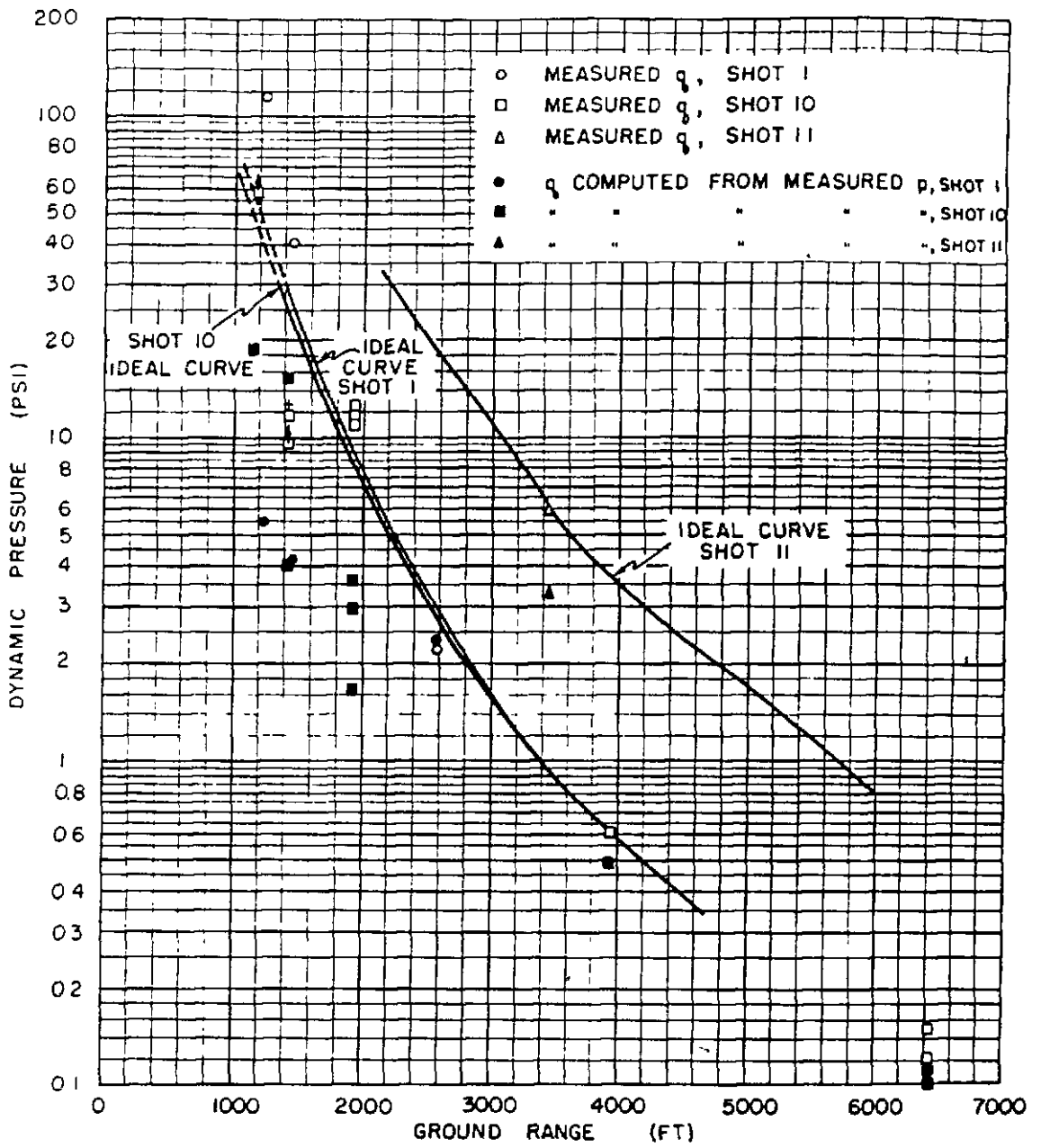


Fig. 2.28—Measured Dynamic Pressure, Shots 1, 10, and 11, Compared to Ideal and to Dynamic Pressure Computed from Measured Peak Overpressure.



Approx. 0.22 sec after
detonation. Just prior
to incident wave strik-
ing Ground Zero.



Approx. 0.25 sec after
detonation. Incident
wave striking Ground
Zero.



Approx. 0.28 sec after
detonation. Appear-
ance of reflected
wave.



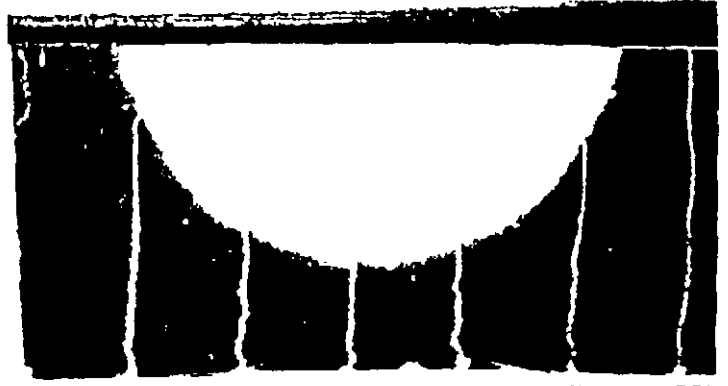
Approx. 0.29 sec after
detonation. Develop-
ment of reflected
wave.

Fig. 2.29 — Precursor Development, Shot 11.

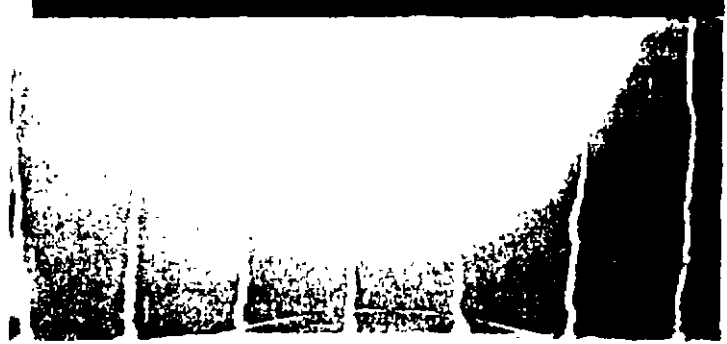
Approx. 0.30 sec after
detonation. Further
development of re-
flected wave--no evi-
dence of precursor
within resolution
limits of photograph.



Approx. 0.31 sec after
detonation. First
evidence of precursor
in advance of reflected
wave at ground level.



Approx. 0.32 sec after
detonation. Develop-
ment of precursor.



Approx. 0.33 sec after
detonation. Further
development of precu-
sor.

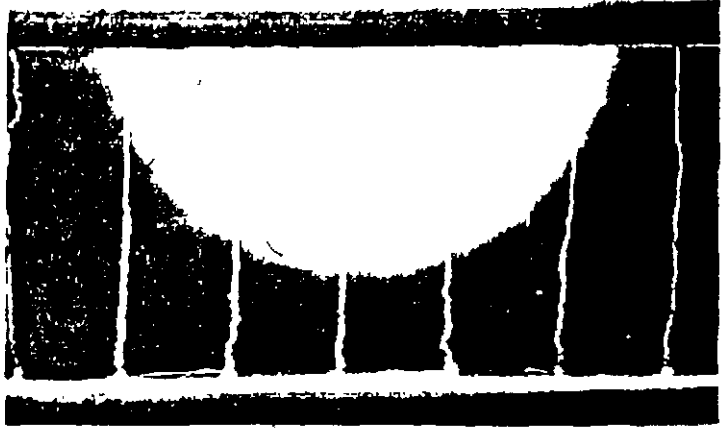


Fig. 2.29—(Continued).

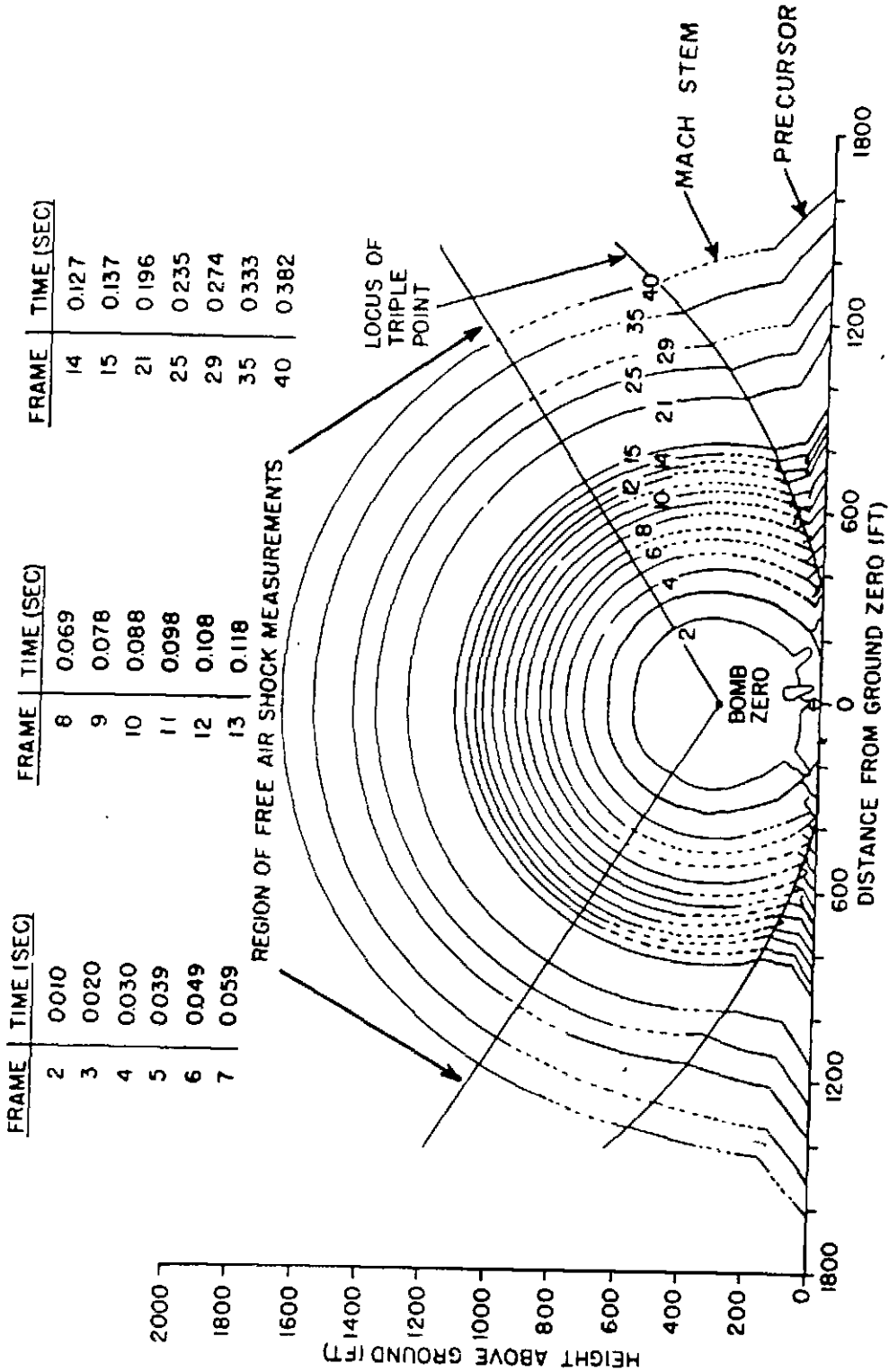


Fig. 2.30—Precursor Shock Contours, Shot 1.

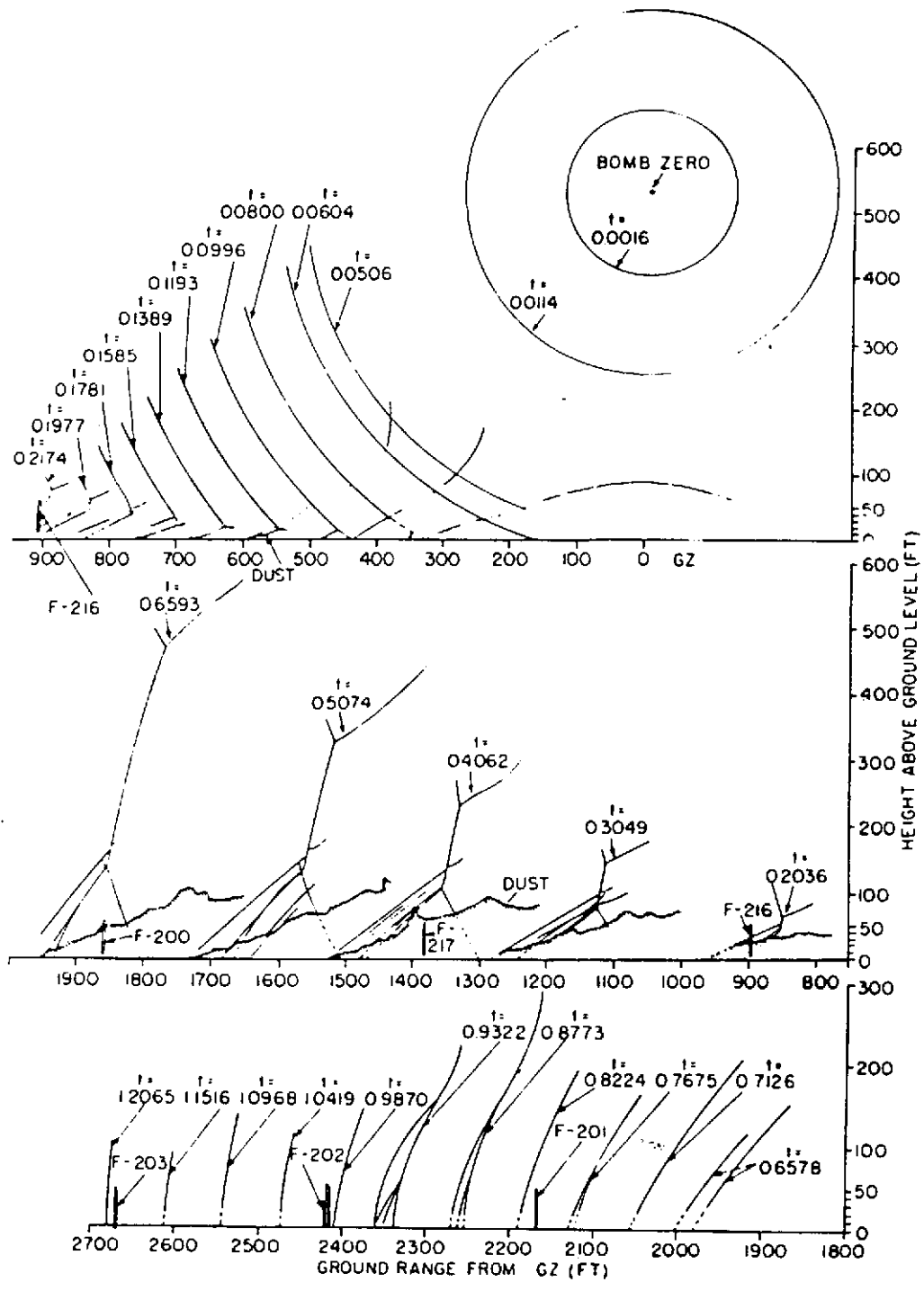


Fig. 2.31 — Precursor Shock Contours, Shot 10.

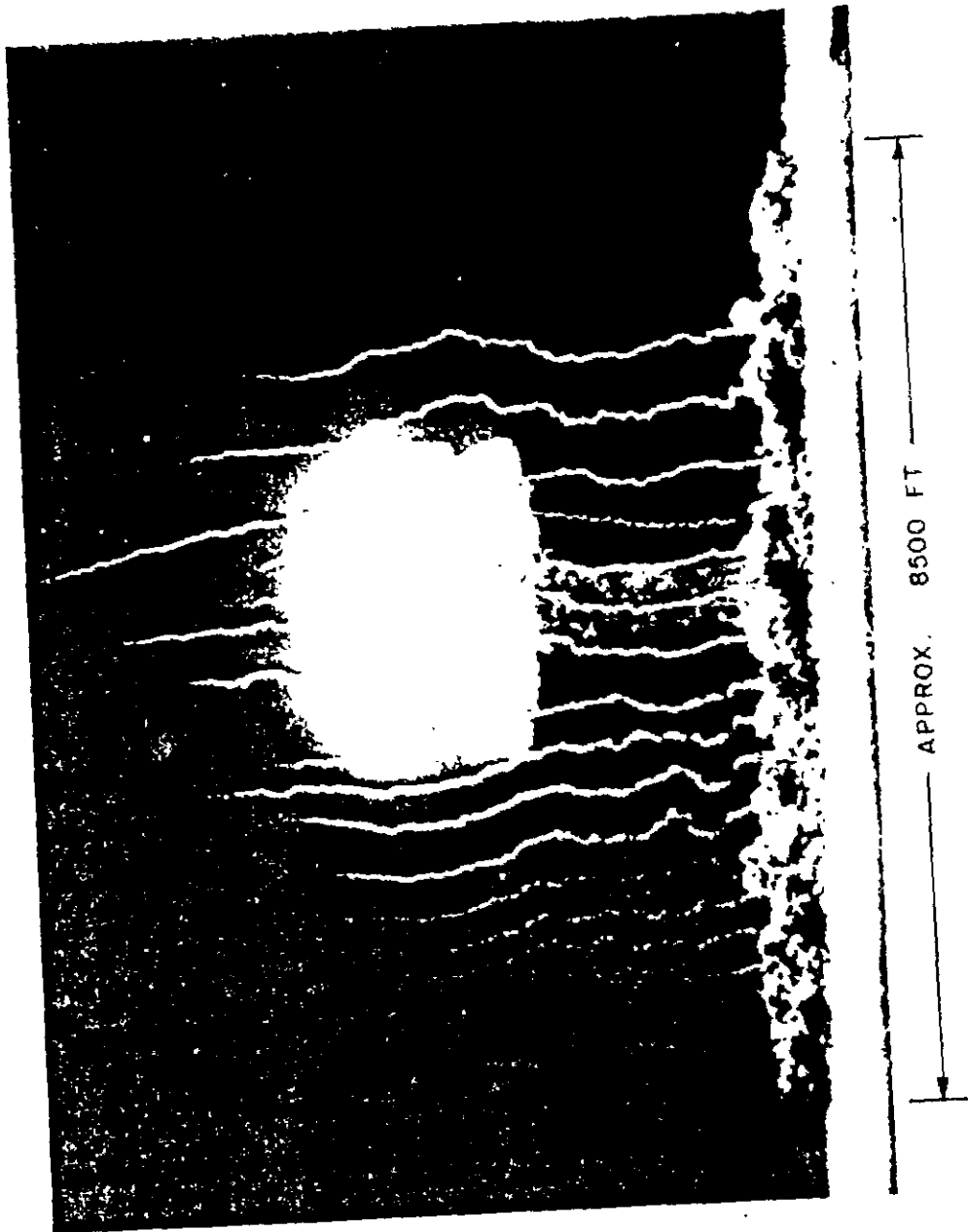


Fig. 2.32—Photograph of Dust Pedestal, Shot 11.

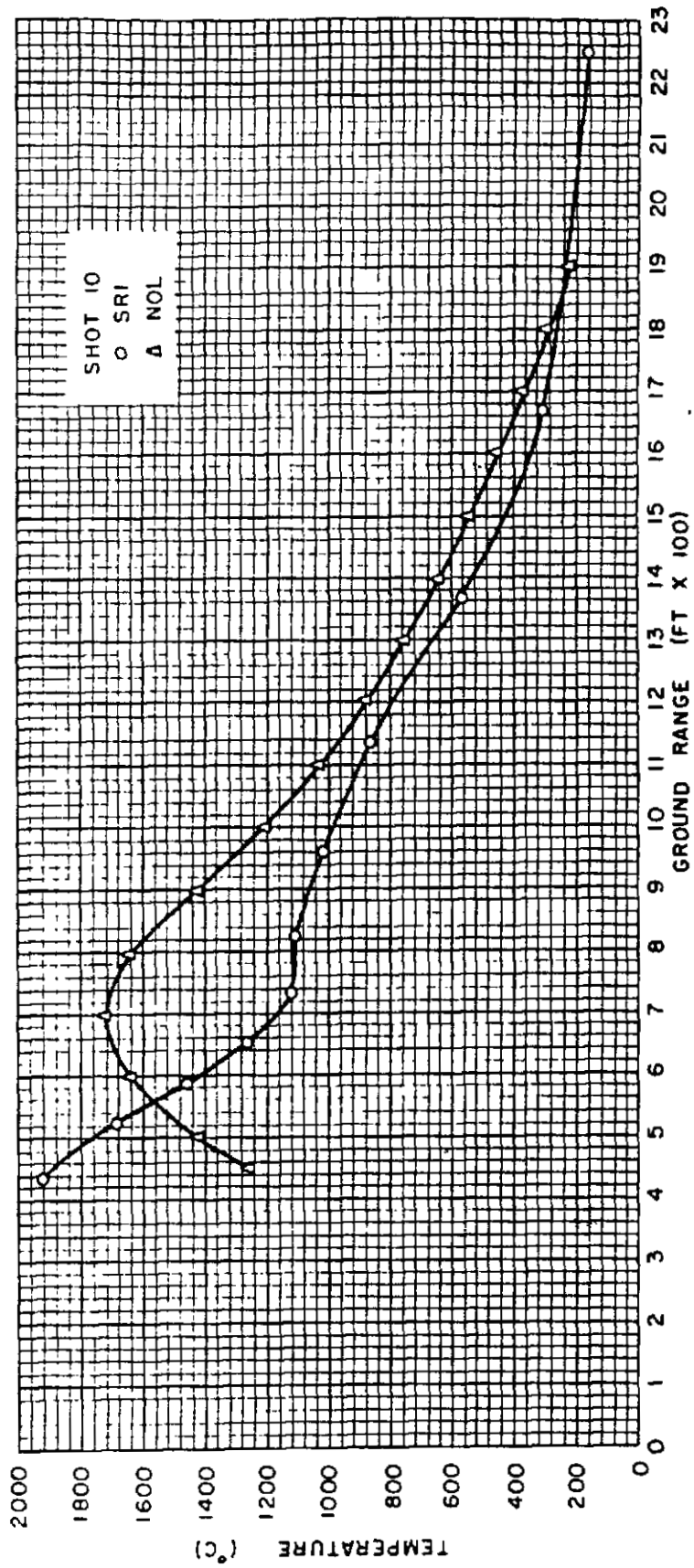


Fig. 2.33 — Preshock Air Temperature, Shot 10.

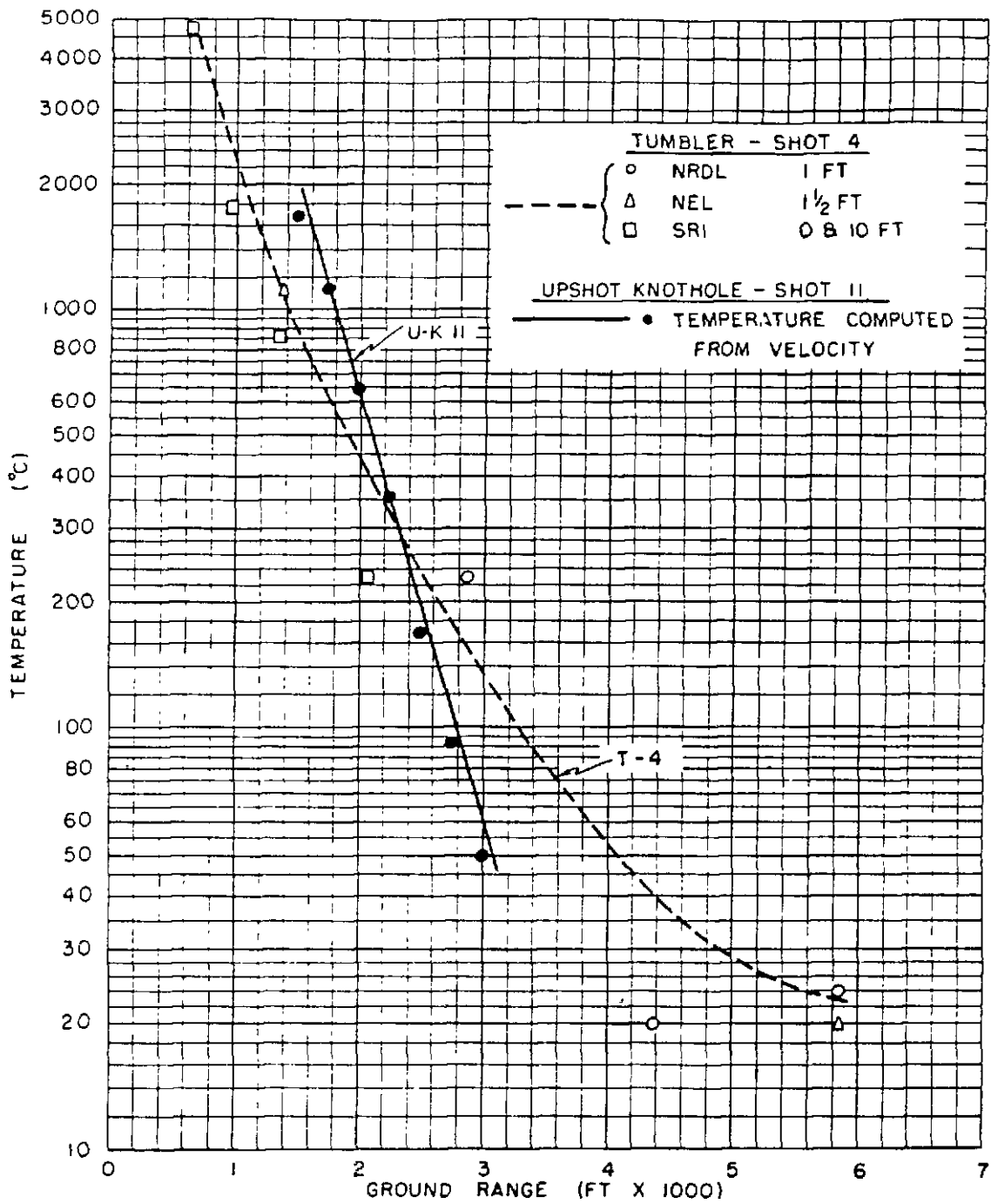


Fig 2.34 — Preshock Air Temperature, Shot 11 and TUMBLER 4.

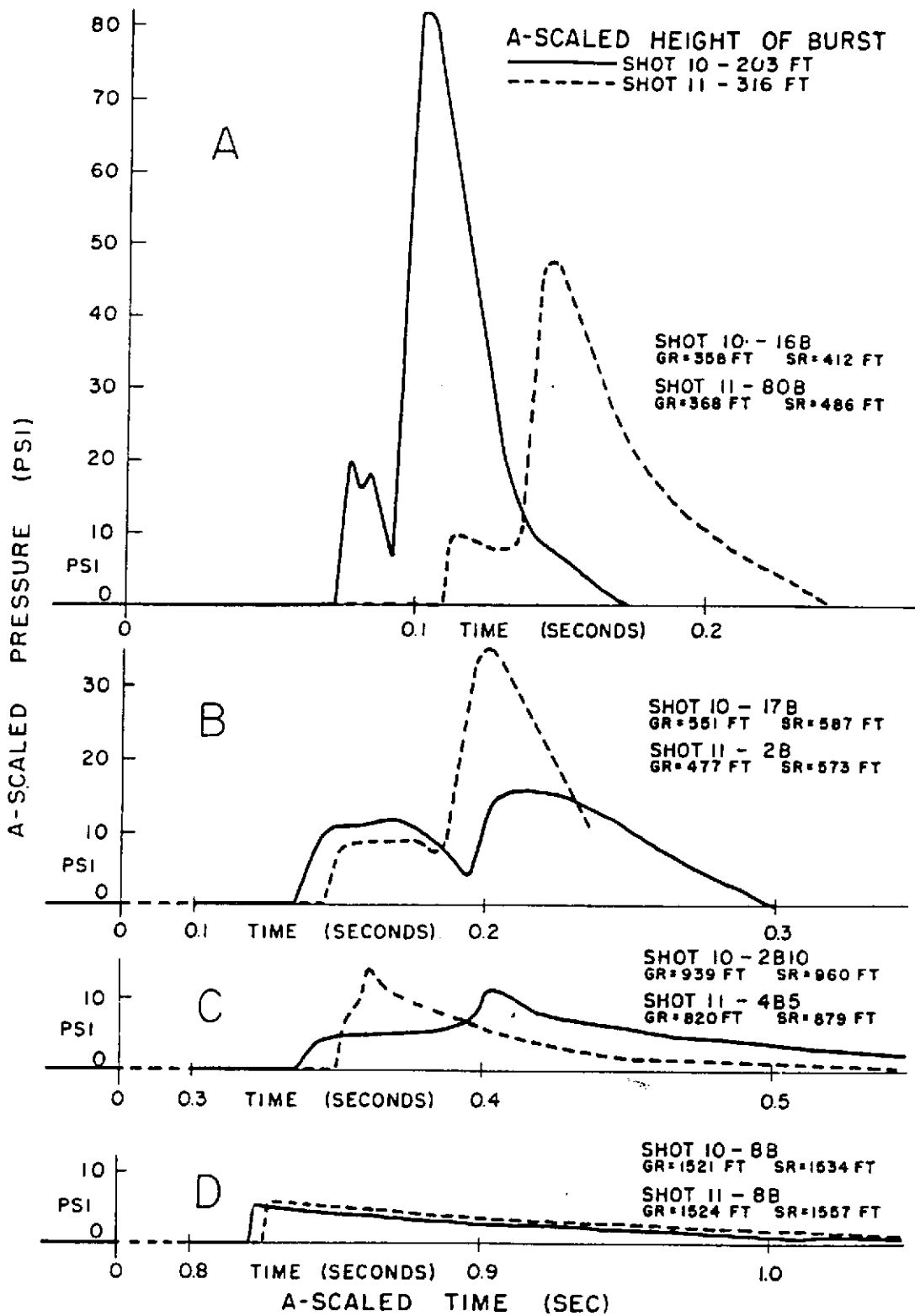


Fig. 2.35 — A-Scaled Overpressure Vs Time Records, Shots 10 and 11.

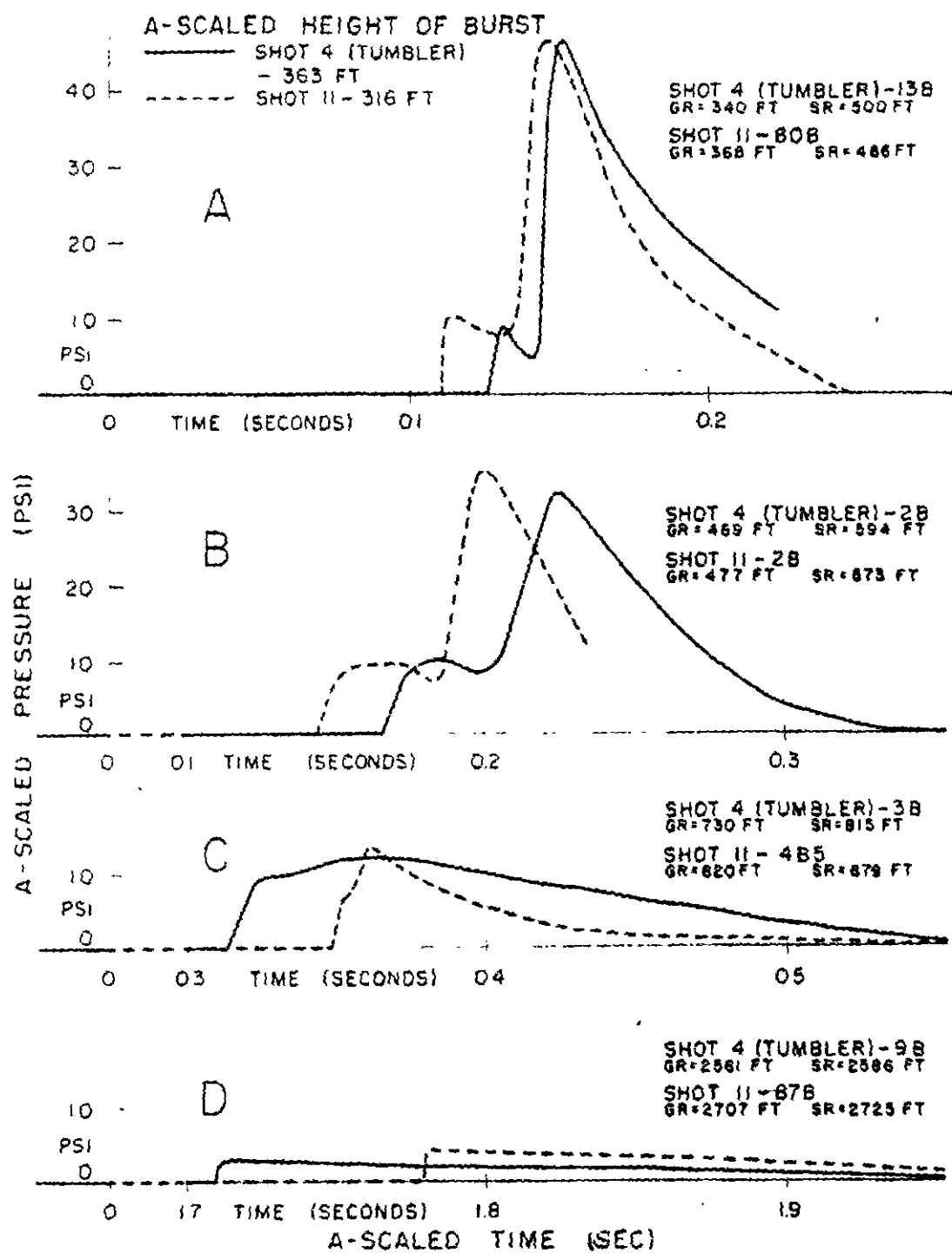


Fig. 2.36—A-Scaled Overpressure Vs Time Records, Shots 11 and TUMBLER 4.

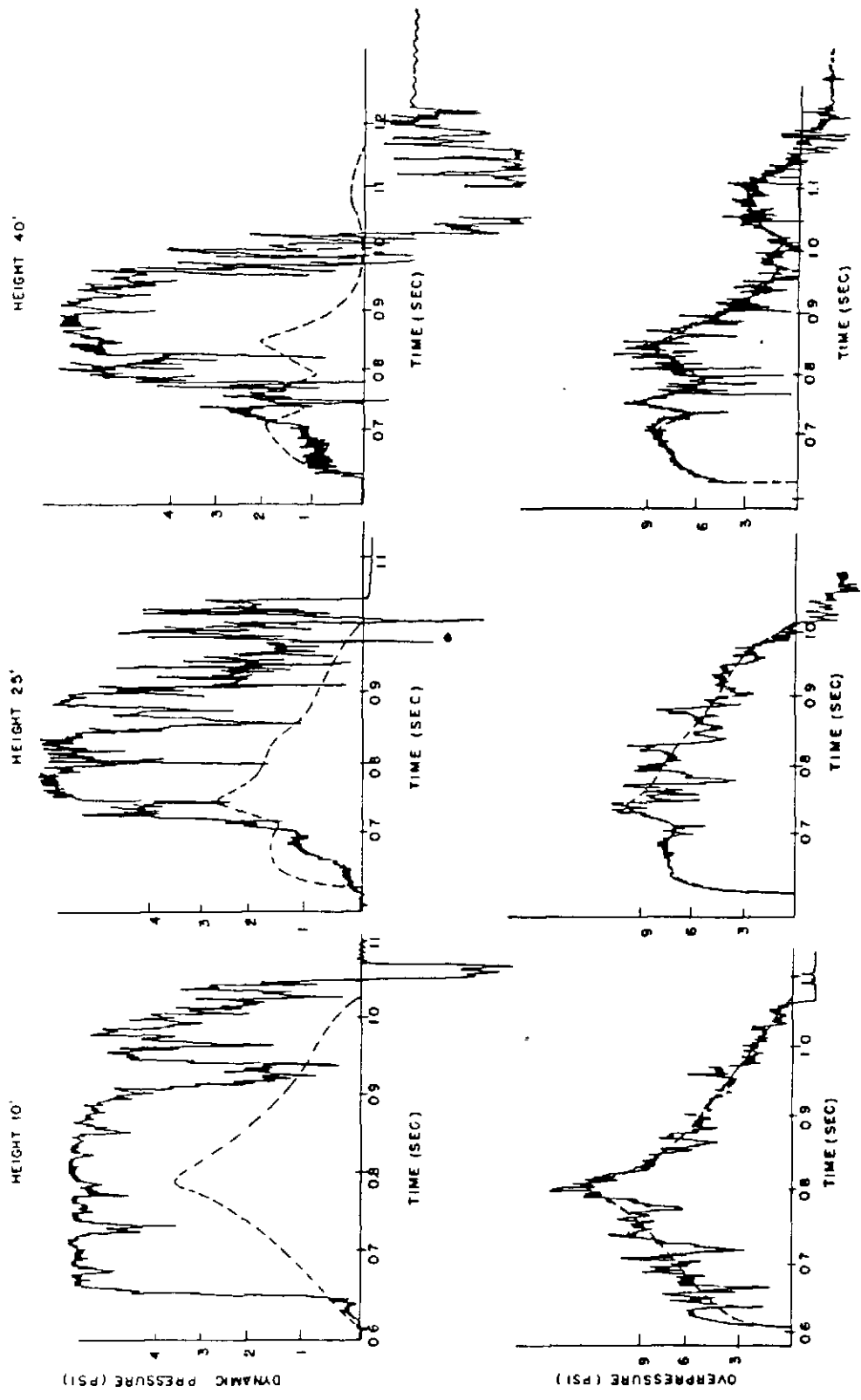


Fig. 2.37 — Dynamic Pressure and Static Overpressure Vs Time, 2000 Ft, Shot 10.

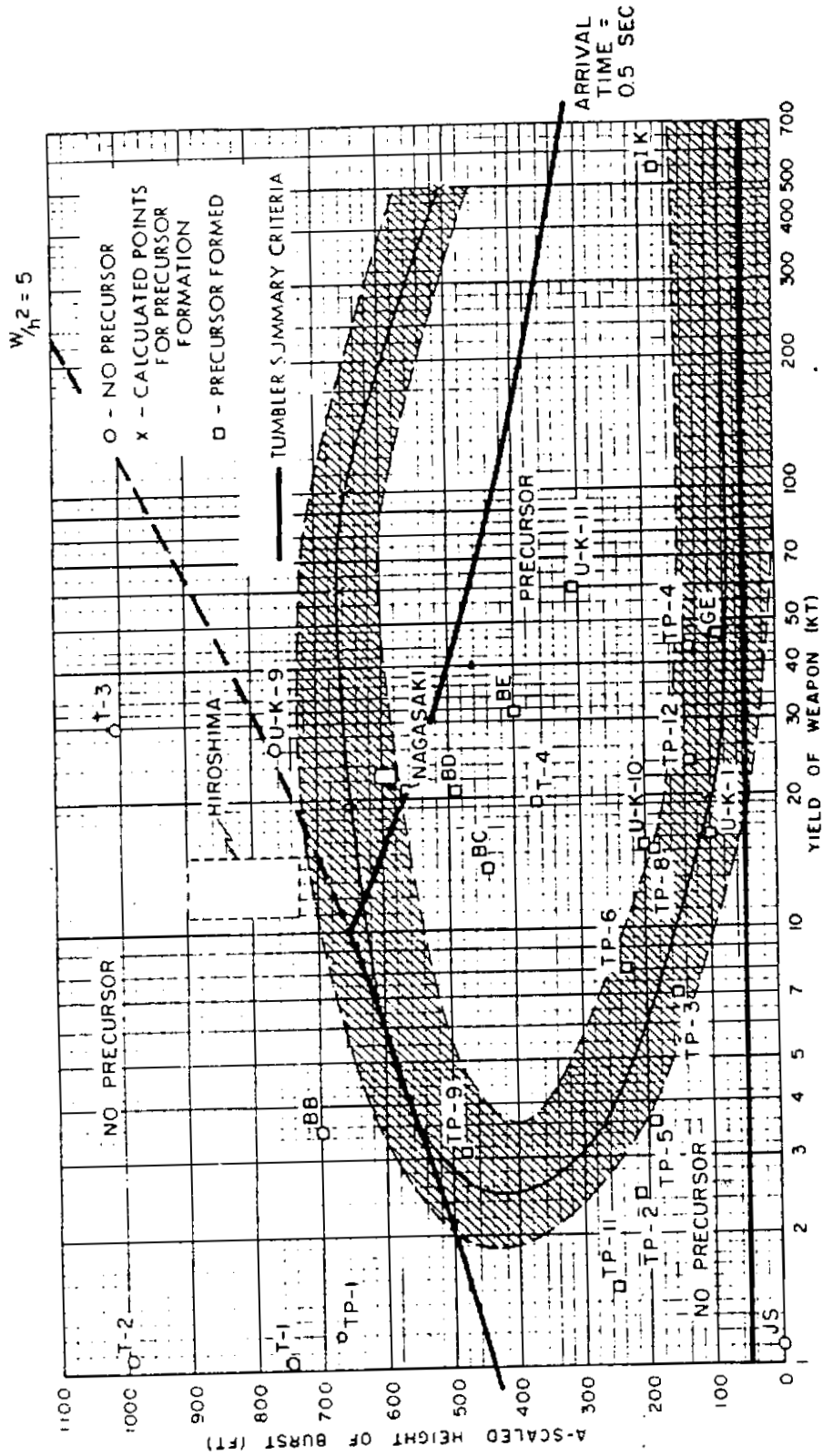


Fig. 2.38—Comparison of Precursor Criteria.

82

BLAST LINE

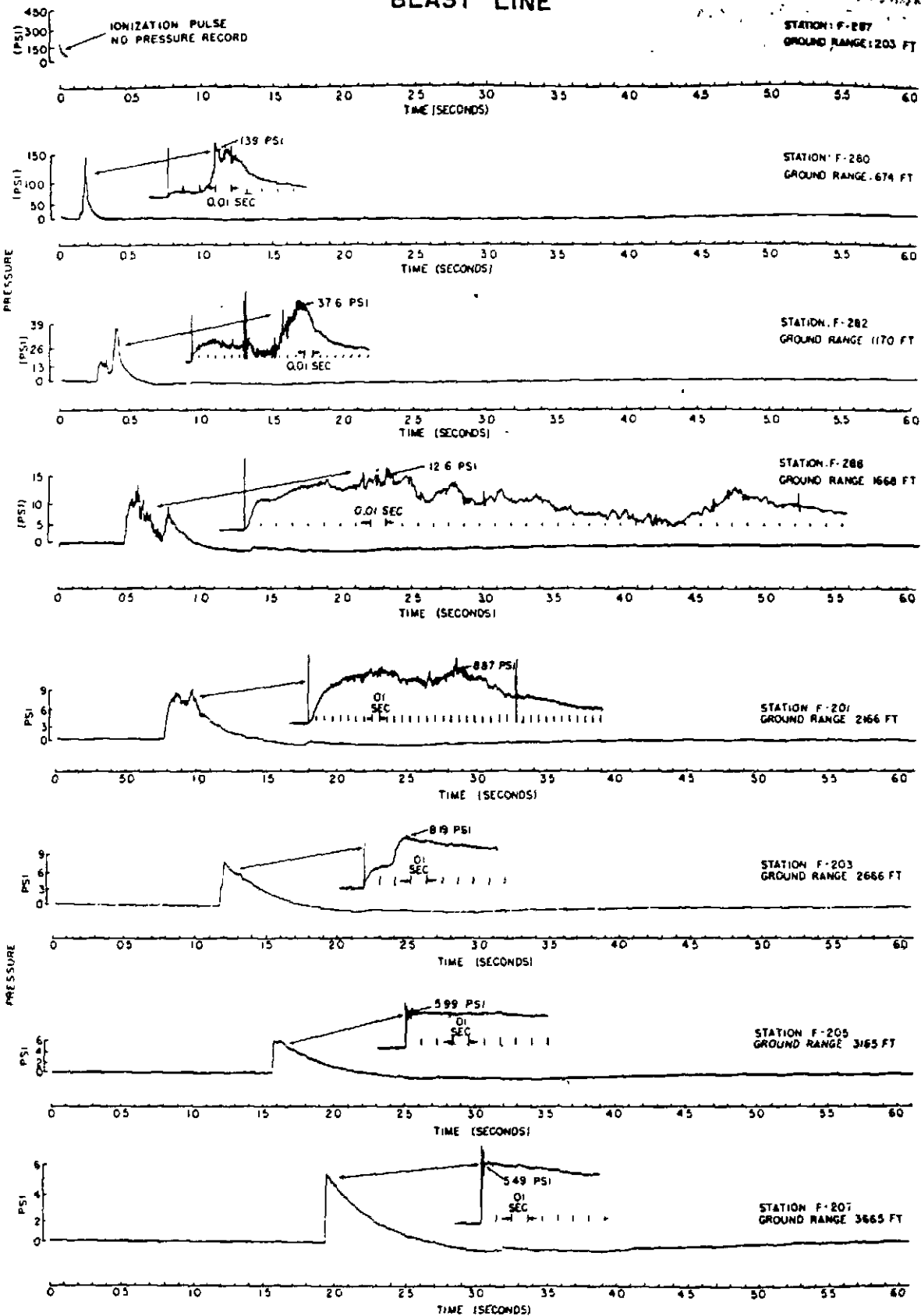
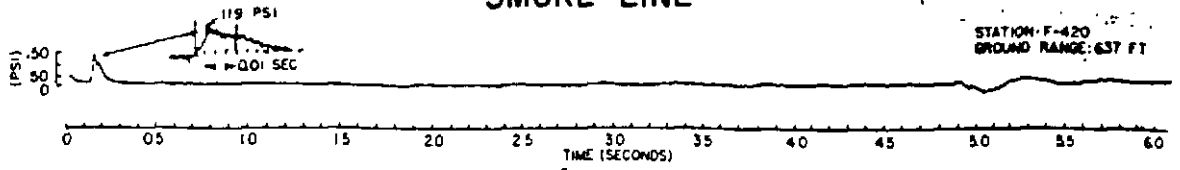


Fig. 2.39—Overpressure Vs Time Records

- P3

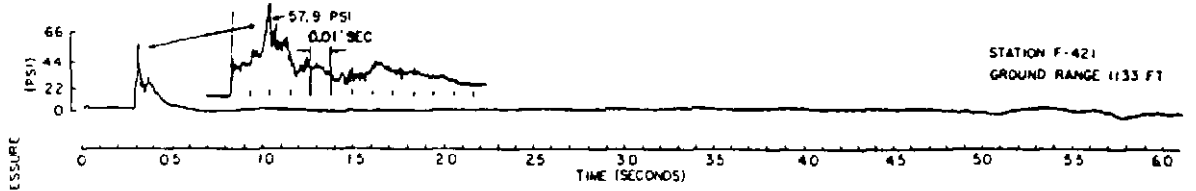
SMOKE LINE

STATION F-287
GROUND RANGE: 203 FT



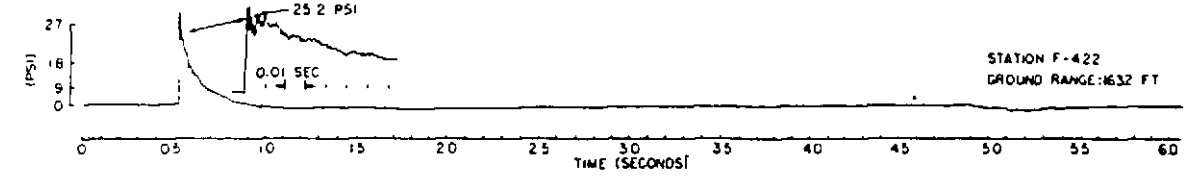
STATION F-420
GROUND RANGE: 637 FT

STATION F-280
GROUND RANGE: 674 FT



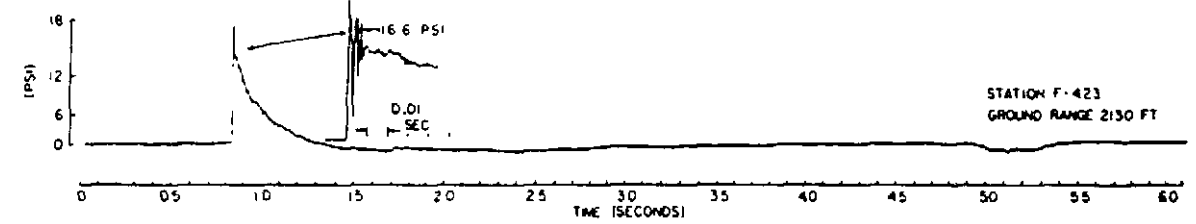
STATION F-421
GROUND RANGE: 1133 FT

STATION F-282
GROUND RANGE: 1170 FT



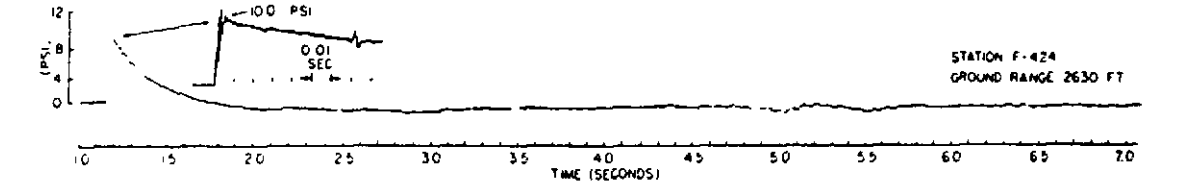
STATION F-422
GROUND RANGE: 1632 FT

STATION F-286
GROUND RANGE: 1666 FT



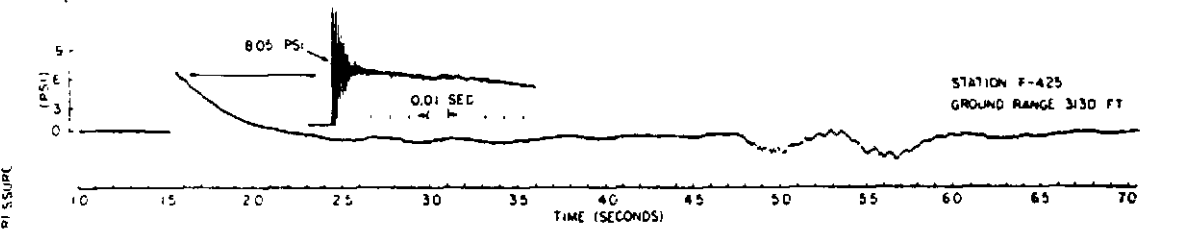
STATION F-423
GROUND RANGE: 2130 FT

STATION F-201
GROUND RANGE: 2166 FT



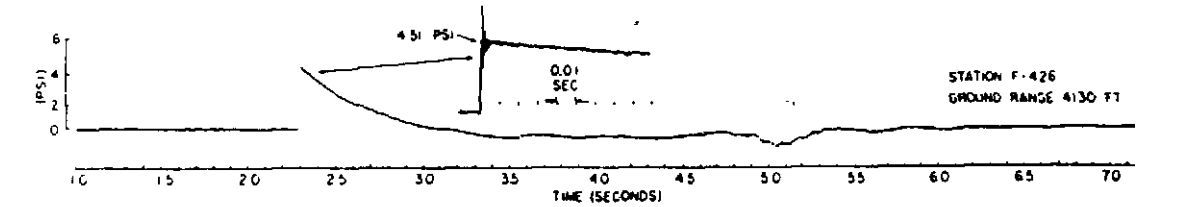
STATION F-424
GROUND RANGE: 2630 FT

STATION F-202
GROUND RANGE: 2666 FT



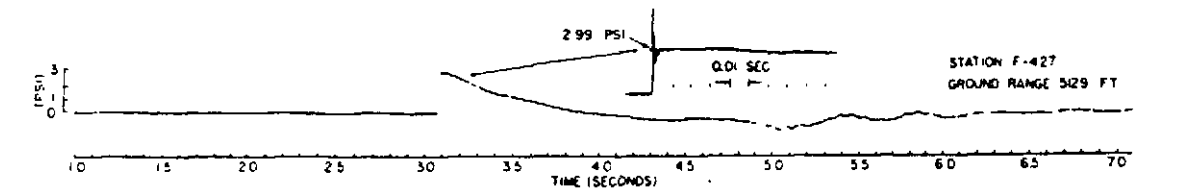
STATION F-425
GROUND RANGE: 3130 FT

STATION F-203
GROUND RANGE: 3163 FT



STATION F-426
GROUND RANGE: 4130 FT

STATION F-204
GROUND RANGE: 3663 FT



STATION F-427
GROUND RANGE: 5129 FT

Vs Time Records Along Main Blast Line and Smoke Line, Shot 10.

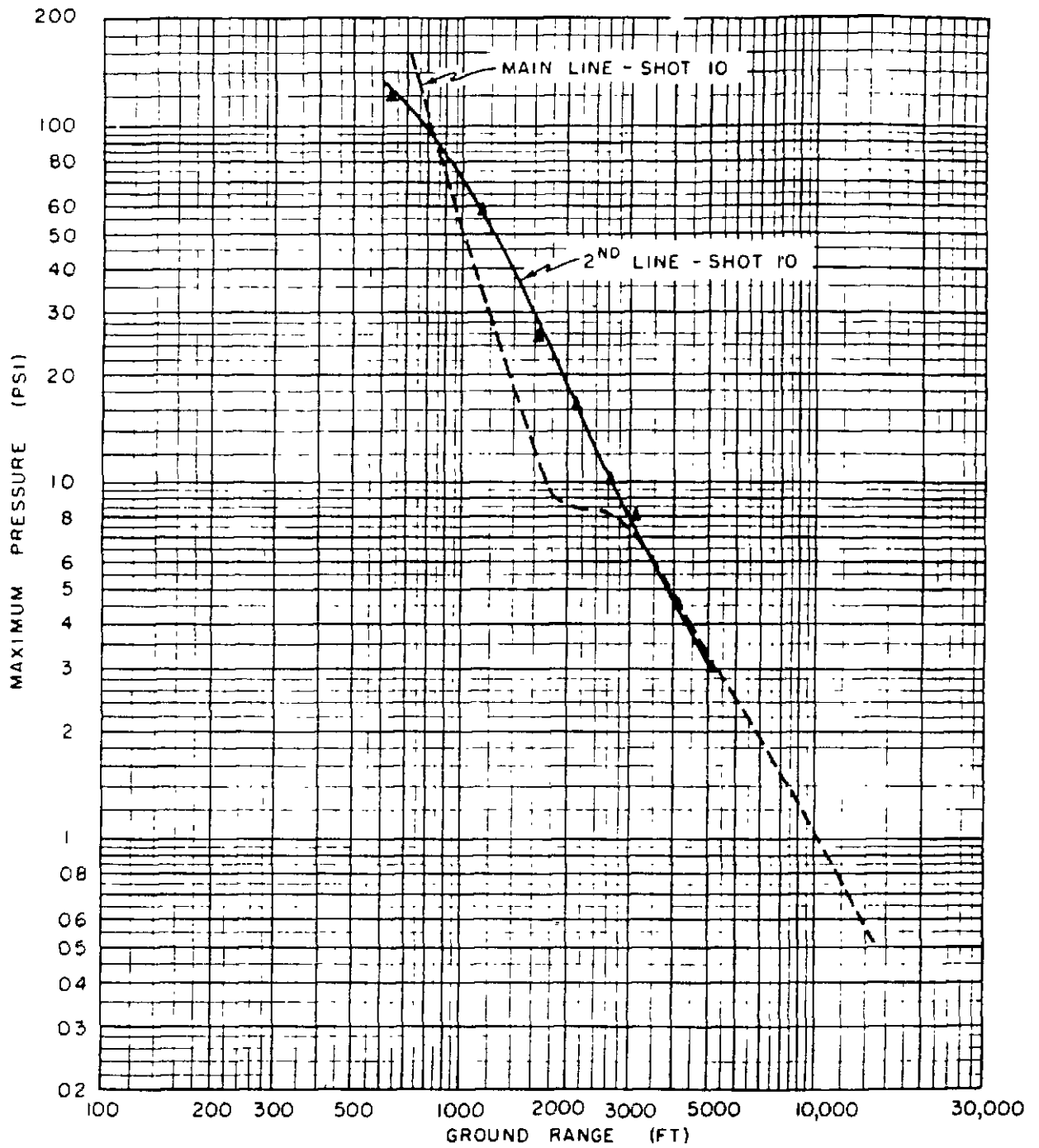


Fig. 2.40—Surface-level Peak Overpressure Vs Ground Range, Main Blast Line and Smoke Line, Shot 10.

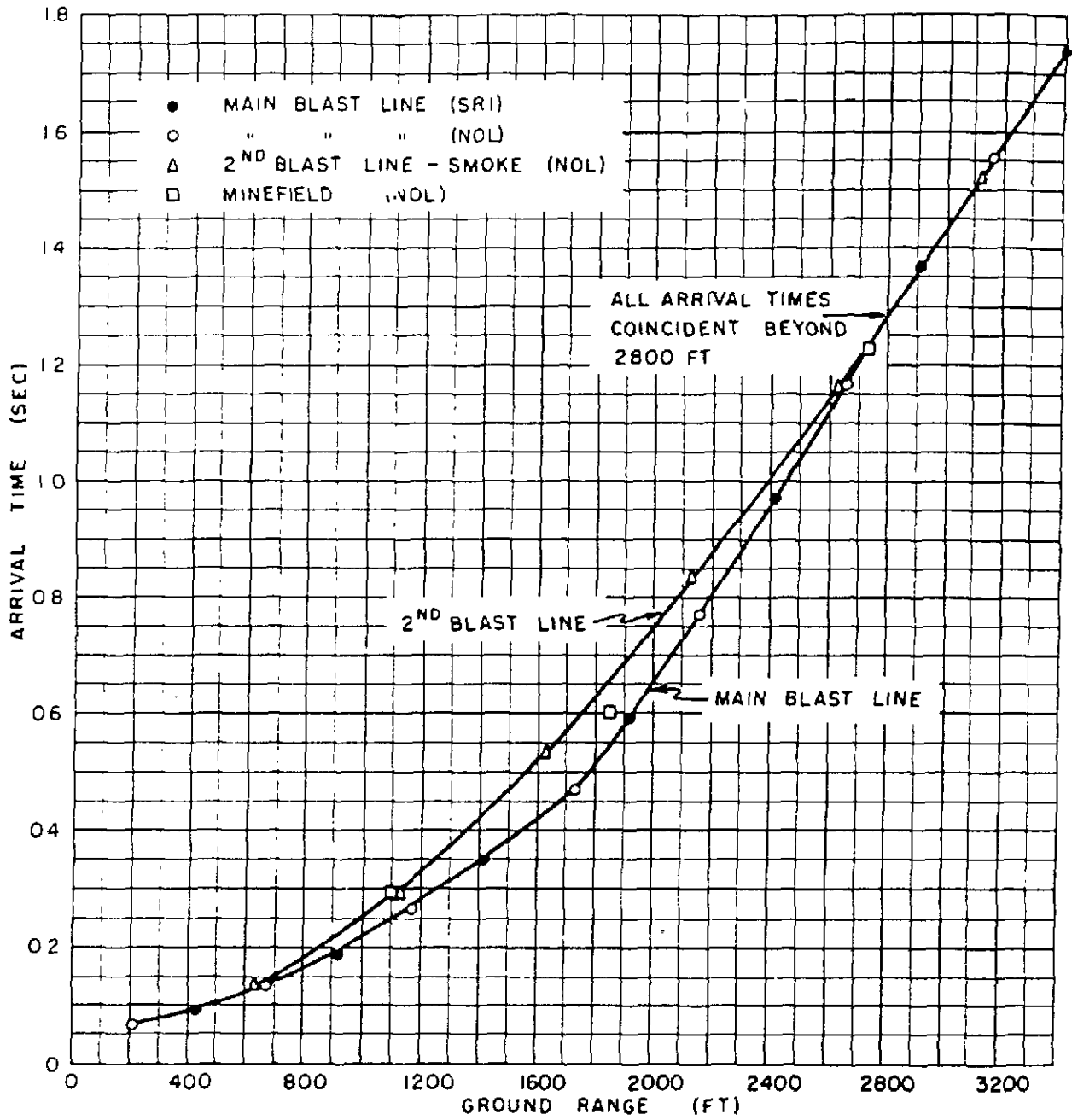


Fig. 2.43 — Arrival Time of Initial Disturbance Along Main Blast Line and Smoke Line, Shot 10.



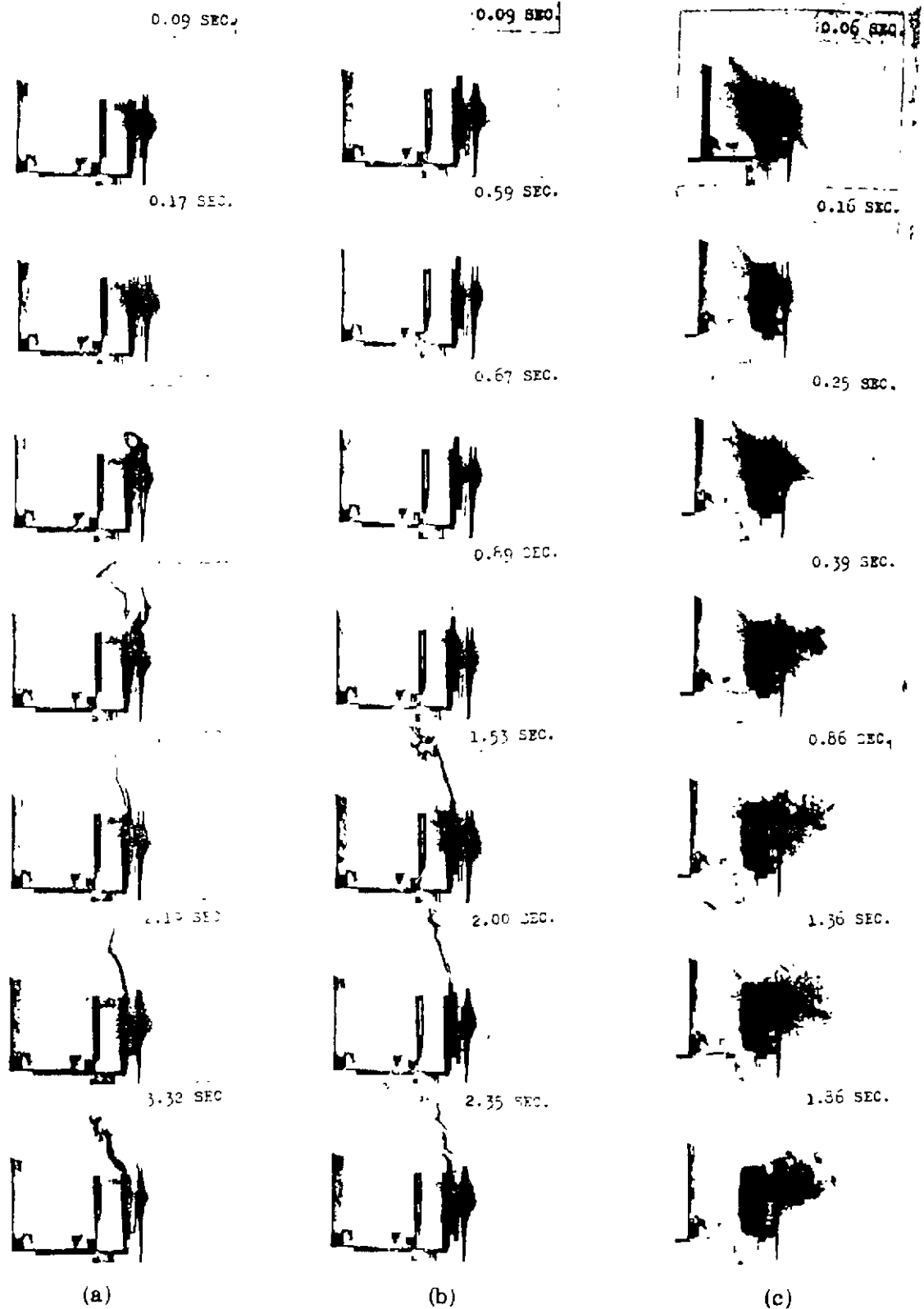


Fig. 2.42—Photographs of Popcornng Phenomenon in the Laboratory. (a) Black Asphalt Roofing Paper. (b) Black Ceramic Tile. (c) Frenchman Flat Adobe.

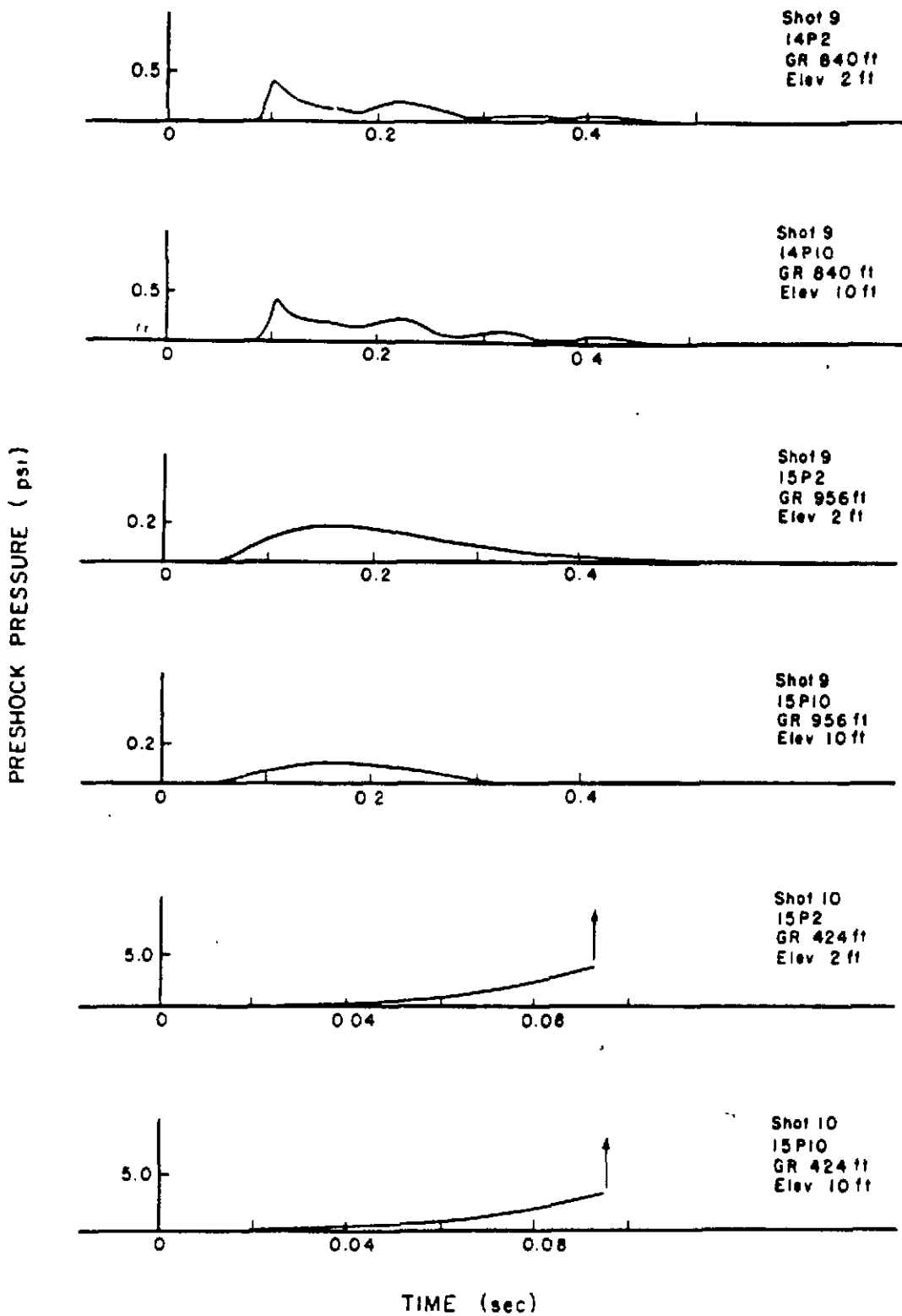


Fig. 2.43—Preshock Pressure Vs Time Records, Shots 9 and 10.



fy

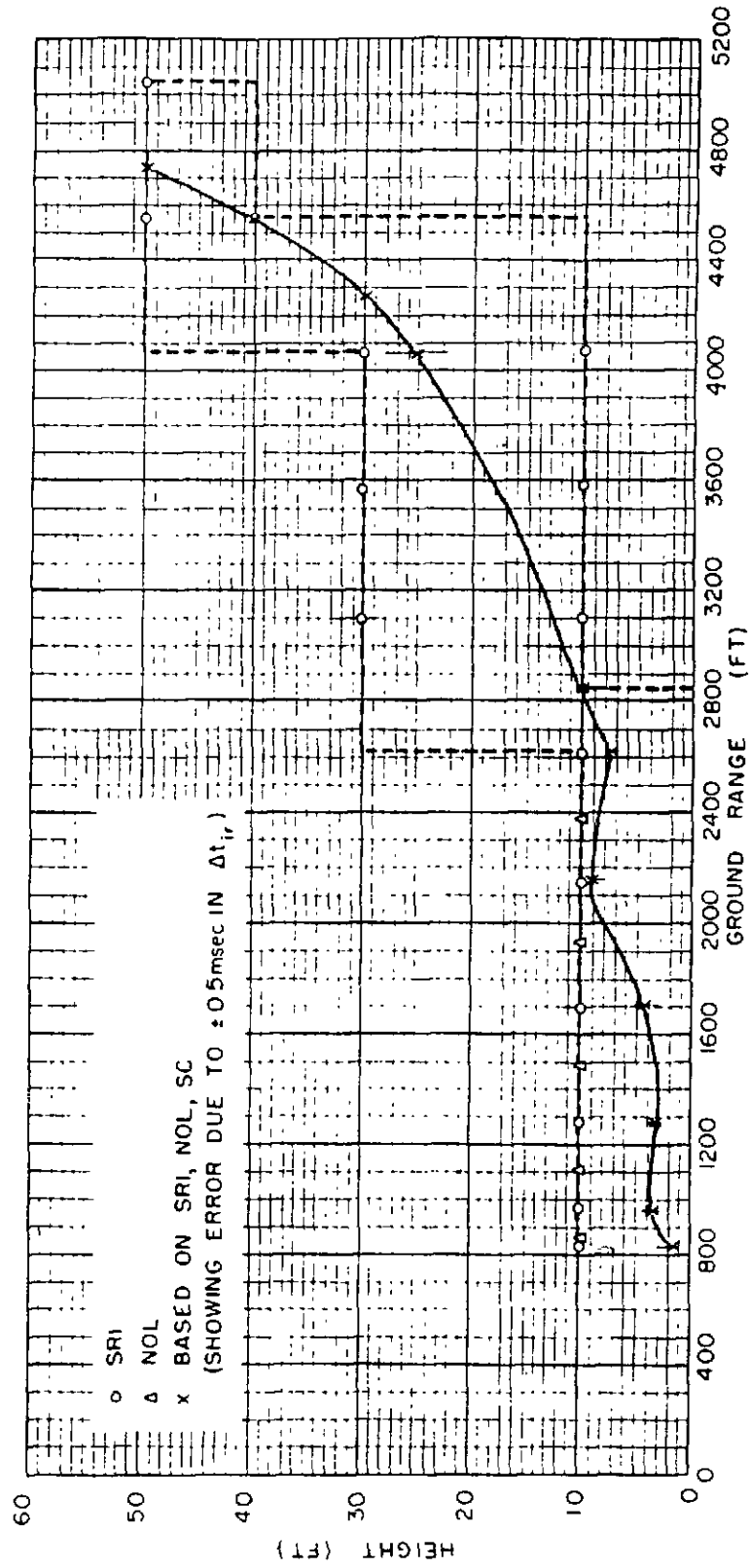


FIG 2.44 — Mach Stem Height Vs Ground Range, Shot 9.

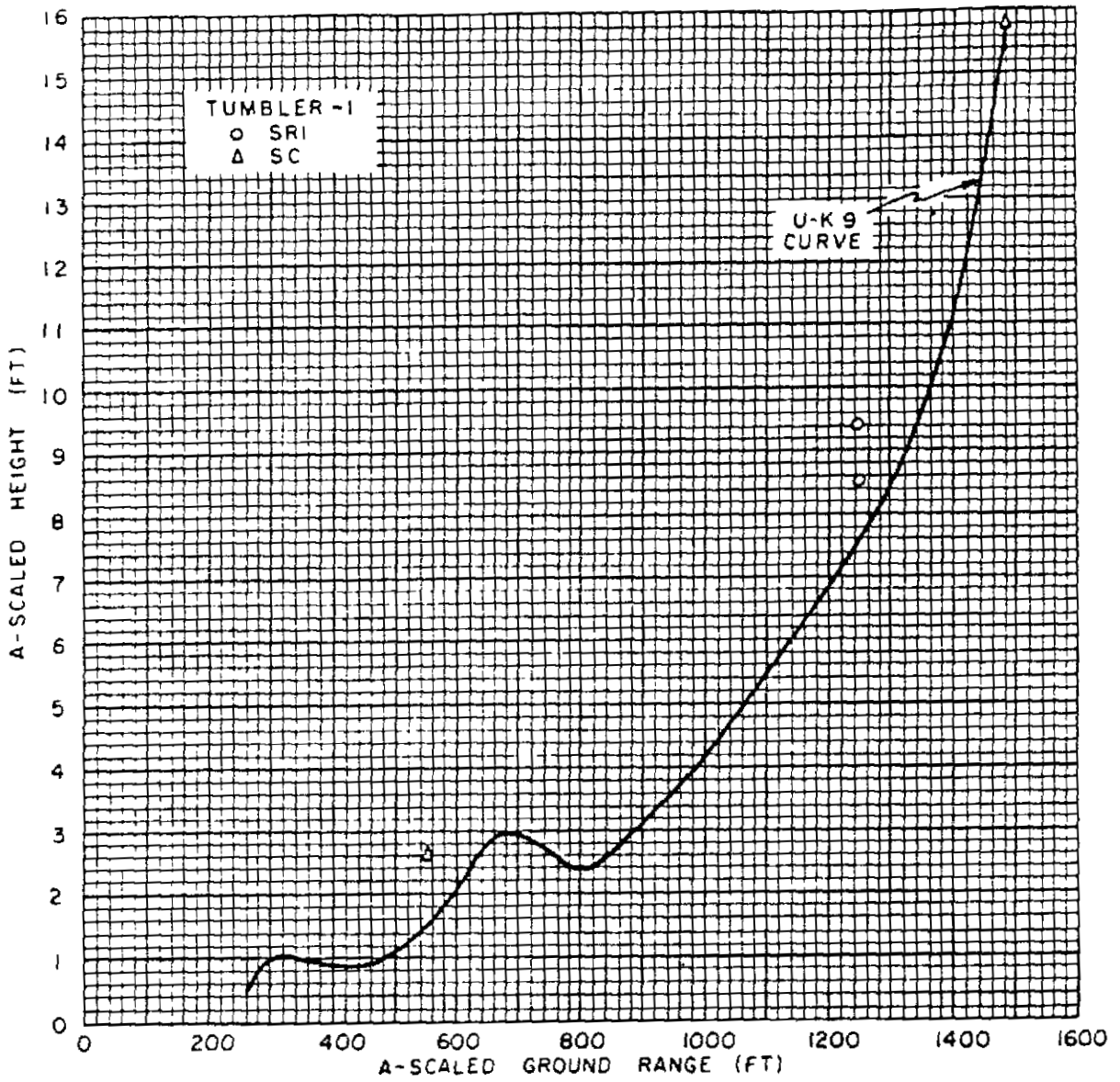


Fig. 2.45 — A-Scaled Mach Stem Height, Comparison of Shot 9 and TUMBLER 1.



92

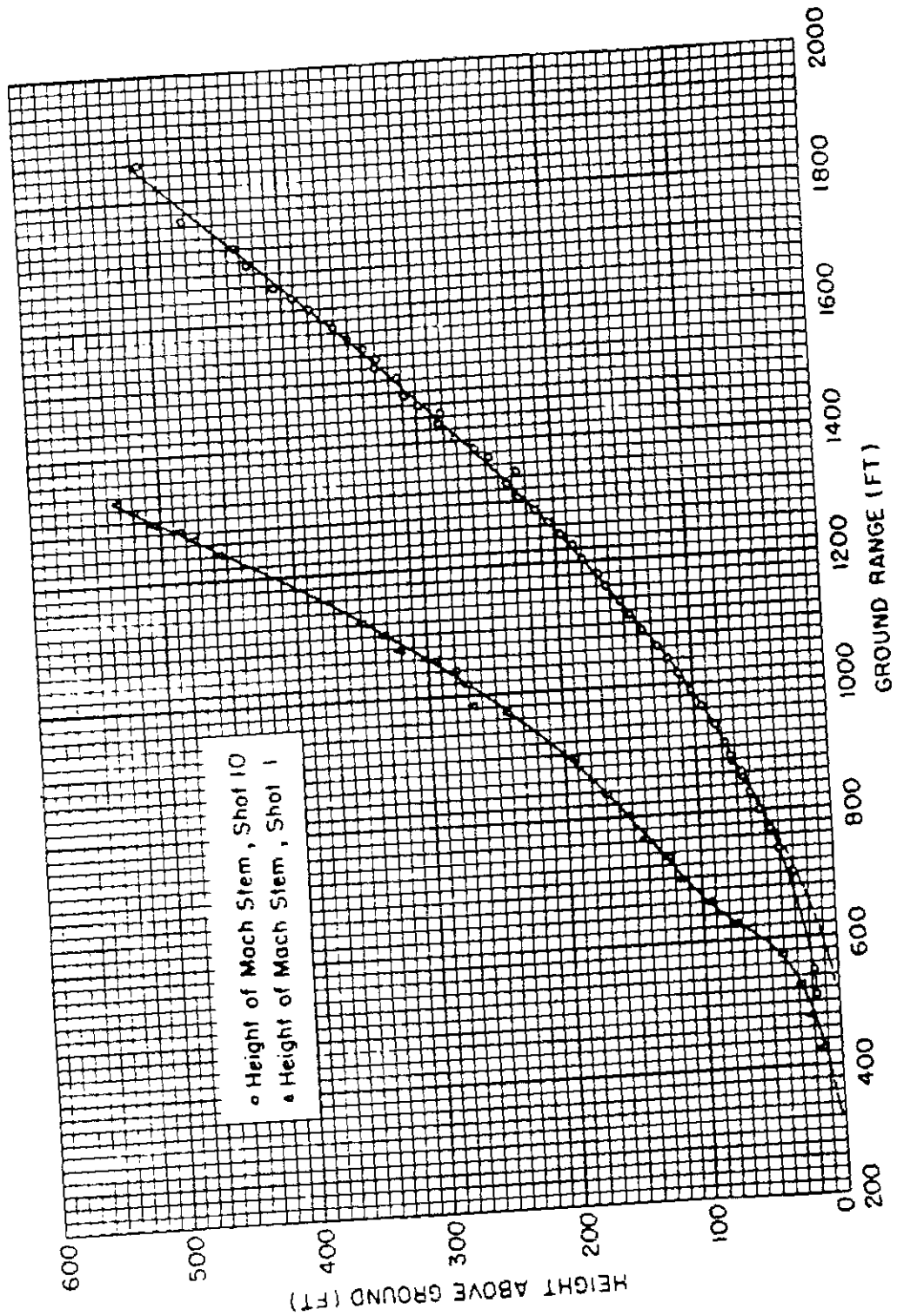


Fig. 2.46 — Mach Stem Height Y_s Ground Range, Shots 1 and 10.

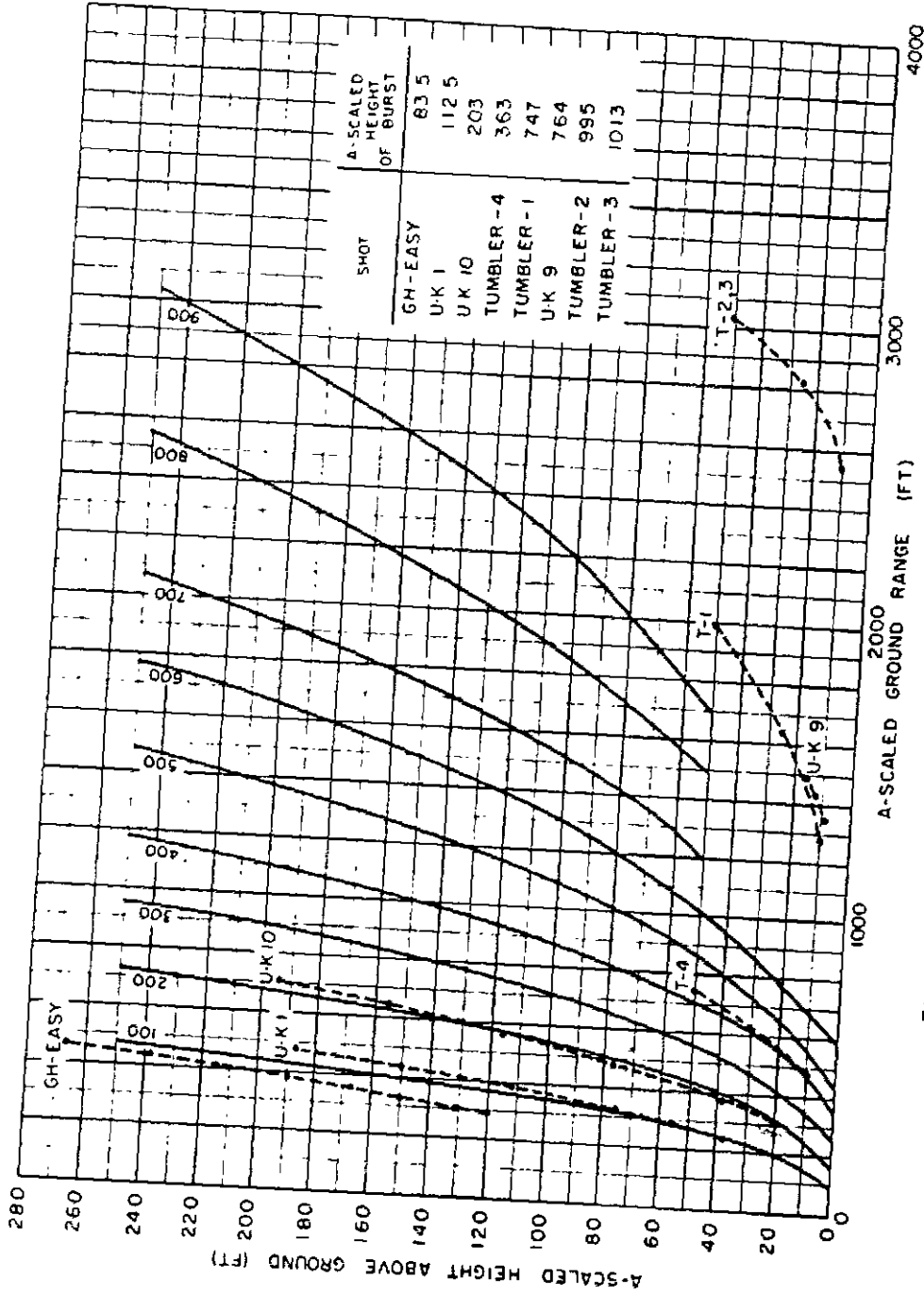


Fig. 2.47—Comparison of Scaled Nuclear and HE Data for Mach Stem Height.

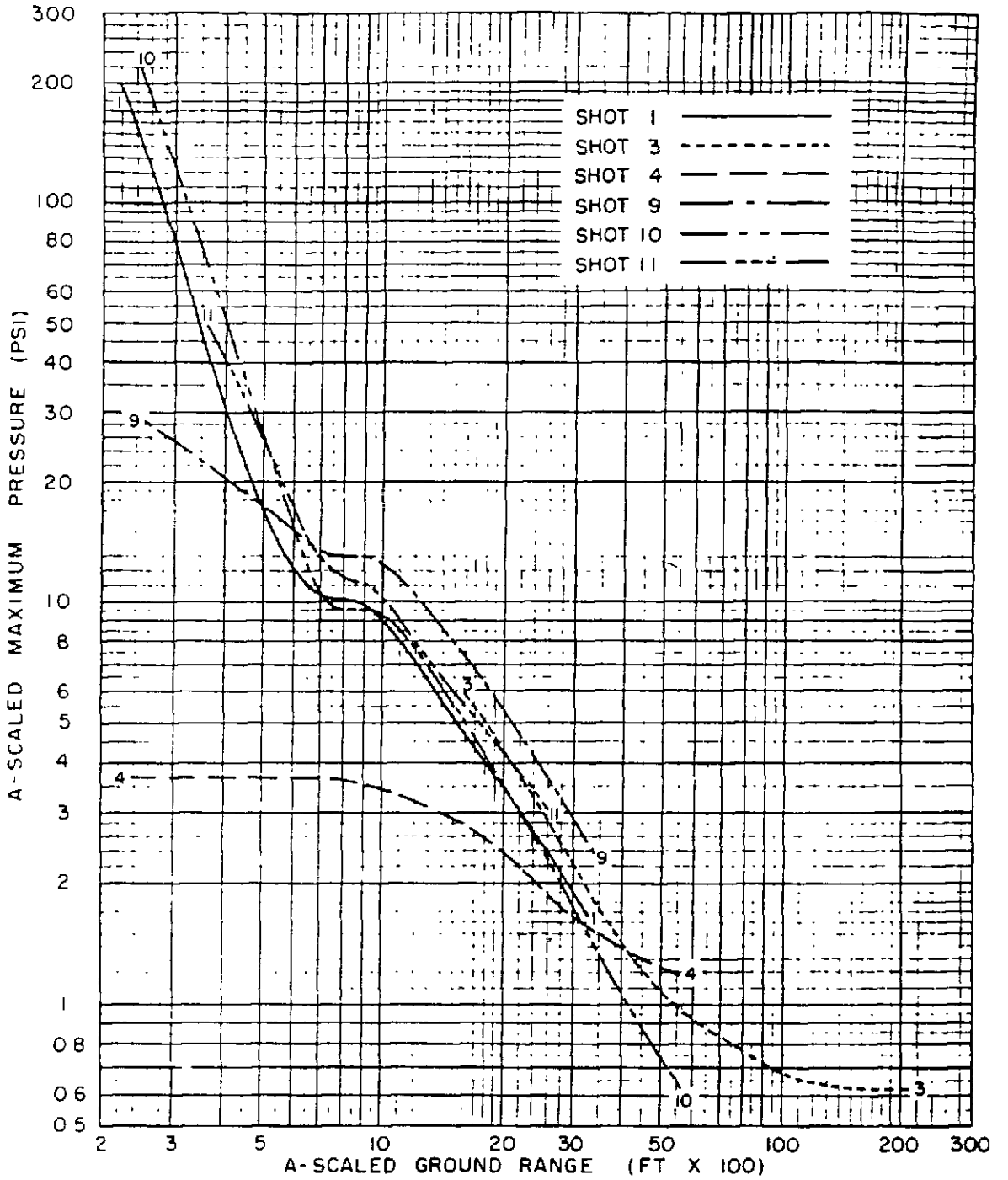


Fig. 2.48—Ground-level Peak Overpressures Vs Ground Range, Shots 1, 3, 4, 9, 10, and 11 (A-Scaled).



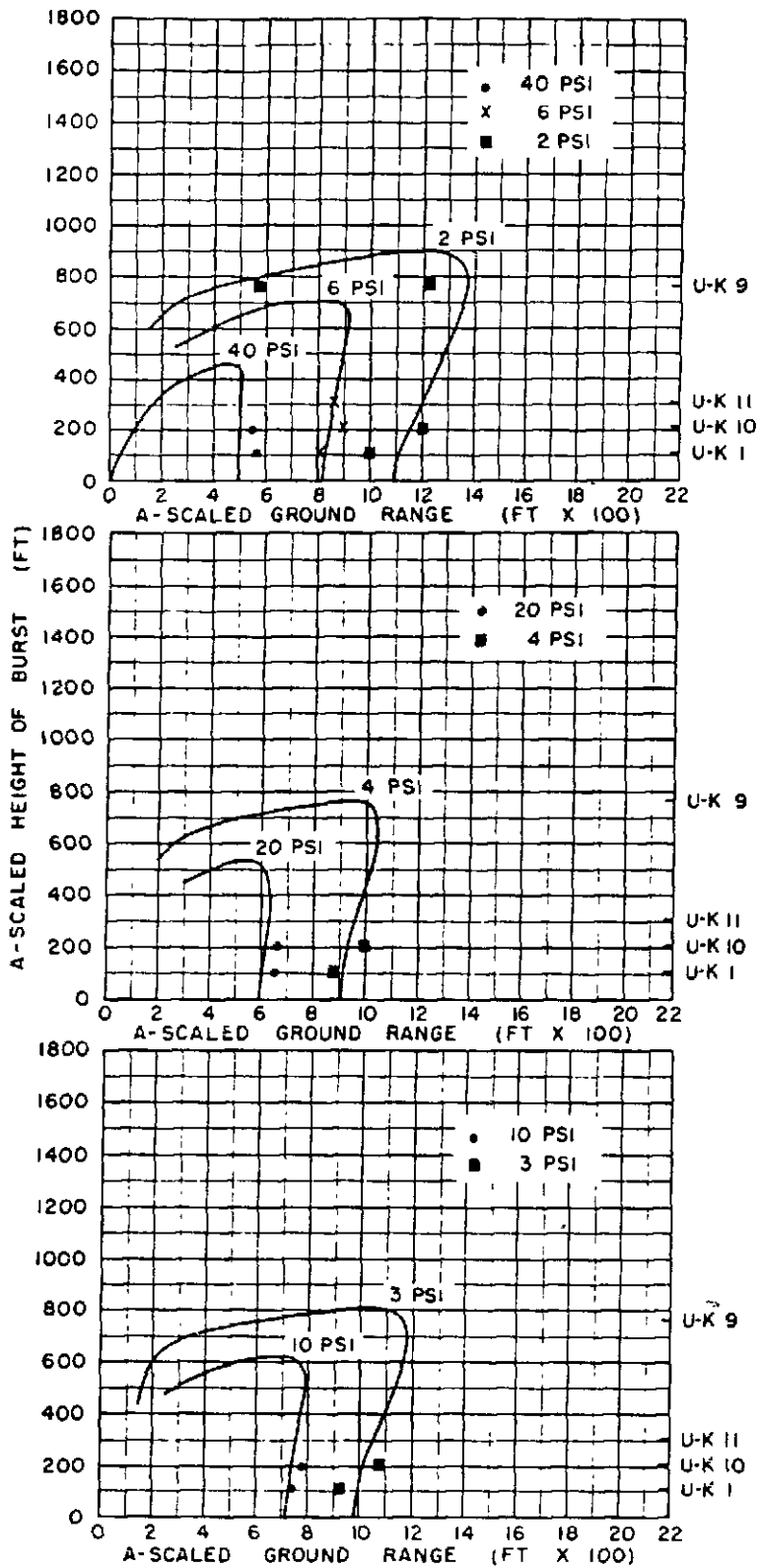


Fig. 2.49—Comparison of Ideal Peak Overpressure Height-of-burst Curves with U-K Data.

98

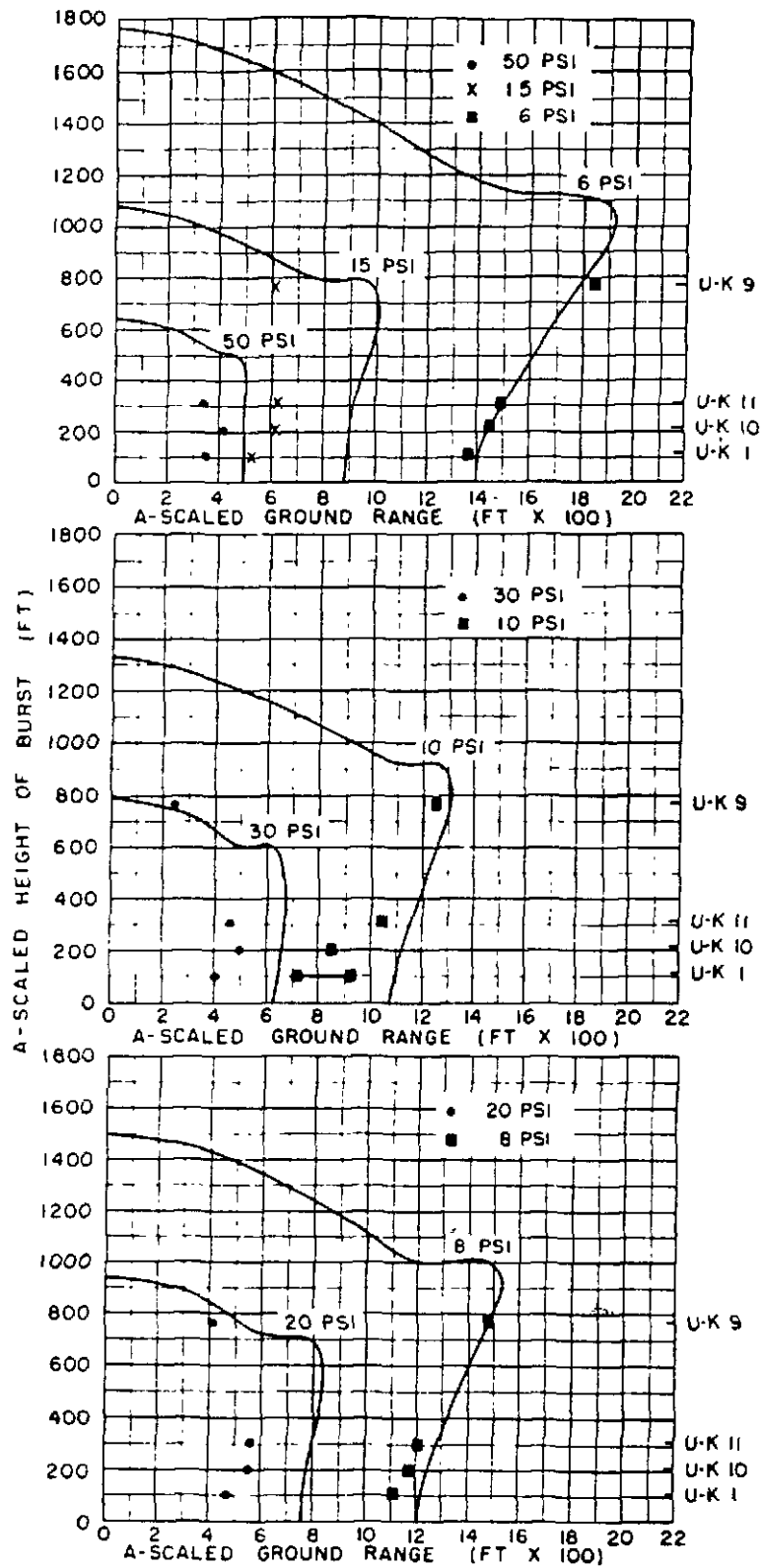


Fig. 2.50—Comparison of Ideal Peak Dynamic Pressure Height-of-burst Curves with U-K Data.

CHAPTER 3

THERMAL-RADIATION MEASUREMENTS

3.1 BACKGROUND

The primary objectives of the basic thermal-radiation measurements program were two-fold: (1) to provide documentation of the thermal characteristics of Shots 9 and 10 for the military effects tests and (2) to obtain data on the basic thermal phenomena of the series of test detonations to supplement related information from previous tests. An additional objective of secondary interest was to obtain thermal data with the AFCRC vacuum capacitor microphone for evaluation of that device as an instrument for measuring thermal phenomena.

Through the efforts of the Naval Research Laboratory (NRL) and Edgerton, Germeshausen & Grier (EG&G), under the Weapons Development Group, and AFCRC and NRDL, under the Military Effects Group, a large quantity of data on thermal phenomena was available for correlation with related information from previous tests. The correlations for the phenomena of interest are presented and discussed in this chapter.

Data on thermal yields and times to minimum and second maximum of the radiant pulse were available from NRL and AFCRC measurements on Shots 1 to 10. Data on times to the minimum were available from EG&G bangmeter measurements on Shots 1 to 11 except for Shots 3 and 6. Data on thermal yields, times to minimum and second maximum, and thermal energy vs distance were available from NRDL measurements on Shots 4, 9, 10, and 11. In addition the Los Alamos Scientific Laboratory (LASL), using NRL equipment, determined the thermal yield of Shot 11.

Supplementing the directly measured quantities enumerated above was a considerable amount of NRDL data related to atmospheric and ground scatter and ground absorption. This latter category of data, although not analyzed, appears potentially attractive for further study and correlation.

3.2 INSTRUMENTATION

3.2.1 Total Thermal Energy and Flux Vs Distance

1. *NRDL disc calorimeters.* These instruments are similar to those used in TUMBLER-SNAPPER and are considered to be the basic thermal instrument (see Project 8.10 Report WT-773).

2. *NRL total energy thermopiles.* These instruments were used in the AEC basic measurements program. (See Project 18.1 Report NRL-4395, RD No. 420.)

3. *Secondary thermal measuring devices.*

(a) *Naval Material Laboratory (NML) cosine-law thermal attenuating calorimeters, rounds.* (See Projects 8.9 and 8.4-1 Reports WT-772 and WT-768.)

(b) *Army Chemical Center (ACC) black ball calorimeters.* These calorimeters are similar to the instruments tested by NRL at BUSTER-JANGLE and were used primarily to measure incident energy over 4 π geometry under the smoke screens (see Project 8.4-1 report).

(c) *AFCRC vacuum capacitor microphone.* Total energy was obtained by integration of time-intensity curves (see Project 8.2 Report WT-767).

3.2.2 Time-Intensity Relations

1. *NRDL foil radiometer.* These instruments are similar to those used in TUMBLER-SNAPPER. Times to the minimum and second maximum of thermal radiation are determined as well as a complete intensity vs time curve (see Project 8.10 Report WT-773).

2. *AFCRC vacuum capacitor microphone.* This instrument, still in the developmental state, yields both time intensity and times to minimum and second maximum (see Project 8.10 Report WT-773).

3. *NRDL calorimeter curves.* Differentiation of the total energy curves as obtained from the disc calorimeters are used as a secondary method of determining time-intensity relations (see Project 8.10 Report WT-773).

4. *EG&G bhangmeters.* The bhangmeter, which is used primarily for diagnostic purposes, produces the time to minimum of thermal radiation with excellent resolution.

5. *NRL spectrographs.* (See NRL Project 18.3 report, when printed.)

3.2.3 Spectral Characteristics

1. *NRDL calorimeter.* Time intensity and total energy in broad spectral bands were determined from basic calorimeters exposed behind broad band pass filters (see Project 8.10 Report WT-773).

2. *NML cosine law attenuating calorimeters.* These devices were exposed behind broad band pass filters to determine as a secondary method the total energy delivered in the same spectral region as those studied by NRDL (see Project 8.9 report).

3. *NRL spectrographs.* (See Project 18.3 report.)

3.2.4 Special Studies

1. *Air scatter.* The contribution of air scatter to total thermal flux received was studied by NRDL using various field of view adaptors on standard calorimeters. In addition, several calorimeters were specially shielded from both the fireball and the ground so that all the energy which reached the sensing element was that which was scattered into the field of view by the air (see Project 8.10 report).

2. *Ground reflectance.* The contribution of ground reflectance to total thermal flux received by aircraft in flight in the vicinity of an atomic-bomb detonation was determined from standard calorimeters placed in manned B-50 aircraft and Navy drones. Specially shielded calorimeters along the ground, which viewed only the ground, were used by NRDL to study ground reflection (see Projects 5.1, WT-748; 5.2, WT-749; and 8.10 reports).

3. *Thermal instrumentation under smoke screens.*

(a) *NRDL calorimeters.* These instruments were oriented so as to measure the goniometry, or spatial distribution, of thermal radiation arriving at a point within the screen (see Projects 8.4-1, 8.4-2, and 8.10 reports).

(b) *NML cosine law thermal attenuating calorimeters.* The roundels were used under the white smoke screen to provide a statistical number of determinations of the spatial distribution of thermal radiation for the construction of polar diagrams of scatter within the smoke screen (see Projects 8.4-1 and 8.9 reports).

(c) *ACC black ball calorimeters.* These calorimeters were used to measure total integrated flux over 4π geometry (see Project 8.4-1 report).

Isolated results from thermal measurements made under the smoke screen may be found in the reports of Projects 8.4-1, 8.4-2, and 8.10. Analysis and discussion of results may be found in reports of Projects 8.4-1 and 8.4-2.

3.3 RESULTS AND DISCUSSION

3.3.1 General

The recent publication of AFSWP-503,¹ which is a digest of all data accumulated on the basic characteristics of thermal radiation from weapons tests through Operation IVY, provides a yardstick against which the thermal data from this operation may be compared. Except for *the times to minimum in the radiant pulse*, the new thermal data from UPSHOT-KNOTHOLE agree with those scaled from AFSWP-503 within the limits of accuracy of the data and the scaling relations. Pending a thorough analysis of forthcoming TEAPOT thermal data and the data from this operation and from prior tests, it is felt that the thermal scaling relations in the AFSWP paper should be continued in use. The various thermal phenomena from this operation, therefore, have been plotted on copies of the appropriate curves from AFSWP-503.

3.3.2 Total Energy Vs Ground Distance

Figure 3.1 presents the results of total thermal flux vs ground distance as obtained by NRDL (Project 8.10) for Shots 4, 9, 10, and 11. The data represent thermal energies incident on surfaces oriented normal to a line of sight to the fireball. The measuring instruments were mounted at heights above the surface sufficient to minimize the effect of obscuration by dust erupted from the surface during the thermal emission period.

For Shots 9 and 10, data are available for total thermal fluxes obtained by Project 8.1 measurements with NRDL type instruments mounted 5 ft above the stabilized areas of that project. The scatter of these data about the curves in Fig. 3.1 constructed from the NRDL data are not considered significant. It is felt that the Project 8.1 results lend credence to the precision with which basic thermal data from air bursts may be applied to effects targets not instrumented with calorimeters, under the ideal conditions prevailing at the NPG, provided the targets are placed over suitably stabilized areas.

3.3.3 Thermal Yields

Table 3.1 summarizes the data on thermal yields, i.e., the energy in kilotons emitted as thermal radiation by the detonation of each weapon. For each shot the air transmissivity in per cent per statute mile, as obtained by NRL, is given.

In the calculation of the thermal yield from measured values of the radiant energy, corrections must be made for absorbed and scattered radiation. In a recent paper by Drummeter,² an approximate method is advanced for correcting observed thermal energies back to those which would obtain in the absence of the atmosphere and the ground. Drummeter has applied his method for calculating the NRL thermal yields as given in Table 3.1. Thus the NRL data have been corrected for the effective temperature of the source, field of view of the receiver, scatter and absorption by the air and ground, and geometry of the ground with respect to the receiver. On the other hand, the NRDL thermal yields have been corrected only for the radiation scattered from the specular path between the source and receiver (i.e., corrected for air transmissivity). Since the NRDL measurements were obtained largely at relatively short ranges, neglecting the other corrections introduces only small differences, less than 10 per cent, in the NRDL thermal yields from yields otherwise calculated. The AFCRC thermal yields

TABLE 3.1 — Total Thermal Energy and Air Transmissivity, All Shots

Shot	Total weapon yield (KT)	Total thermal energy (KT)				Air transmissivity‡
		NRL*†	USNRDL†	AFCRC†	AFSWP-503 (Calculated)	
1	16.2	6.0		7.9§	6.0	94
2	24.5	11		8.7§	8.9	94
3	0.20	0.028	0.020	0.0016¶		95
4	11.0	3.8	4.0	3.3§	4.2	95
				5.0¶		
5	23	9.3		8.9§	8.3	95
6	0.22			0.015¶		96
7	43.4	15		17.6§	15.2	95
				16.7¶		
8	27	11		10.3§	9.7	93
9	26	10	10.1	10.4¶	9.4	92
10	14.9	5.2	5.2	6.5§	5.5	91
				4.7¶		
11	60.8	18.1**	20.3		21	98**

*Data selected from NRL Report No. 4395, RD No. 420, based upon conversation with Dr. L. F. Drummeter, Jr., 7 December 1954.

†See text for explanation of scatter and absorption corrections.

‡NRL results on specular transmissivity in per cent per statute mile for light of 5500Å wave length. See NRL Report 4395, RD No. 420.

§As measured by AFCRC at local stations, 1 to 2 miles from IGZ.

¶As measured by AFCRC at remote stations, 6½ to 14 miles from IGZ.

**As obtained with NRL equipment operated by Dr. Herman Hoerlin of LASL. The value for air transmissivity is doubtful: Rayleigh scattering alone limits the transmission to about 96½ per cent per mile. It should be noted that the thermal yield, as corrected for scatter and absorption, will be low if too high a value is used for transmission, as was in this case.

have been corrected for air transmissivity and field of view of the receiver. Thus the thermal yields in Table 3.1 for the local AFCRC stations are of the order of 10 per cent lower than would be obtained if further corrected for absorption. Thermal yields calculated from the AFCRC data obtained at the more distant remote stations, if further corrected, would be approximately 10 to 15 per cent greater.

The fact that all the elements entering into the calculation of thermal yields have not been considered by NRDL and AFCRC is explained by a certain amount of confusion regarding the method for making the required corrections and also by the relative importance attached by NRDL and AFCRC to each of the correction factors. It appears that it would be of considerable interest to reanalyze the available data on thermal yields, incorporating into the analysis the considerable quantity of data on scatter and absorption obtained, but not analyzed, by NRDL from this operation and at Operation TUMBLER-SNAPPER. Of the calorimeter readings obtained at the two operations, between one-third and one-half of the readings were obtained with calorimeters viewing the ground, with calorimeters shielded from view of the fireball, or with calorimeters having fields of view other than the standard 90 deg. Furthermore, the sensing instruments used by NRL, NRDL, and AFCRC are substantially different one from the other in spectral sensitivity and field of view to warrant examination and further analysis of the data and performance of the instruments. The suggested analysis, it is believed, would test more rigorously Drummeter's method for correcting thermal measurements in Nevada and also might help to clarify parameters entering into the prediction of radiative transfer through real atmospheres. The effort for such an analysis, however, is beyond the scope of this report.

The data on thermal yields are plotted in Fig. 3.2. The straight line log-log relation between thermal yield and radiochemical yield is that published in AFSWP-503, i.e., $E = 0.44W^{0.84}$.

It is seen that the scatter of the NRDL data is least, whereas that of the AFCRC data is greatest. In most cases, however, the agreement between thermal yields as calculated from $E = 0.44W^{0.84}$ is well within ± 15 per cent.

3.3.4 Time Vs Intensity

The characteristic variation of radiant intensity with time from the fireball provides two datum points of interest to effects studies, i.e., time of the minimum and time of the second maximum, the data for which are given in Table 3.2 and plotted in Figs. 3.3 and 3.4.

TABLE 3.2 — Times to First Minimum and Second Maximum, All Shots

Shot	Weapon yield (KT)	Time to minimum (msec)					Time to second maximum (msec)			
		NRL*	AFCRC	USNRDL	EG&G†	AFSWP-503‡	NRL*	AFCRC	USNRDL	AFSWP-503‡
1	16.2	19	14.3		14.5	10.9	180	122		129
2	24.5	15	17.5		18.5	13.4	256	166		159
3	0.20	3.8				1.2	8.5			14
4	11.0		11.2	17	10.5	9.0		117	118	106
5	23	15.5	16.2		17.75	13.0	175	162		154
6	0.22	4.4	5.6			1.3	7.5			15
7	43.4	25.5	19.6		23.25	17.8	225	196		211
8	27	19	16.8		19.2	14.1	125	155		166
9	26		16.8	23	17.8	13.8	265	151	179	163
10	14.9		14.0	17	14.9	10.5		124	138	123
11	60.8			27	27.2	21.2			257	250

*Data extracted from NRL Report 4356, RD No. 393. Times to minimum are indeterminate to 2 or 3 msec; times to maximum to about 25 msec. The times correspond to minima and maxima in black body temperatures of the fireball

†EG&G bhangmeter results. (See Sec. 3.3.).

‡Calculated from the scaling relations given in AFSWP-503.

According to AFSWP-503, the time to the minimum in radiant emission is related to the yield by the expression $t_{min} = 2.7W^{1/2}$, where t_{min} is in milliseconds and W is in kilotons. EG&G bhangmeter times are related to the yield by the expression³ $t_{min} = 3.25W^{1/2}$ (same units). It is apparent on inspection of Fig. 3.3 that the EG&G expression would be a considerably better fit for the data than the AFSWP-503 expression. At this time, however, there are the following arguments for retaining the AFSWP-503 curve. The data used to derive the AFSWP-503 relation for yield and time to the minimum were based upon NRL bolometer (black body receiver with good time resolution) data from Operations GREENHOUSE, TUMBLER-SNAPPER, and IVY. Preliminary bolometer data from Operation CASTLE have also confirmed the AFSWP curve. When the spectral response of the instrument is limited, significantly different times to the minimum are observed.

1. The EG&G times to the minimum correspond to minimum emission in the visible, which is the sensitive range for the bhangmeter. Although the difference between bhangmeter times to minimum and bolometer times to the minimum should not be regarded as detracting from the value of the bhangmeter data, it does introduce a difficulty in correlating times to the minimum obtained with instruments having different or total spectral responses. The effect of spectral response was evident at CASTLE Shot 1, where EG&G found a progressive increase in times to minimum with filtered bhangmeters as the spectral response approached the blue as follows: 350 msec for red light, 450 msec for yellow light, and 650 msec for blue light. The black body bolometer time to minimum obtained by NRL was earlier even than that obtained with the red filtered bhangmeter, being 313 msec. It thus appears that in stating times to the minimum the instrument used in its determination must also be specified.

2. The NRL time to the minimum which was obtained spectrographically corresponds to

the minimum in black body temperature, which, if the entire fireball is in the field of view of the spectrograph, should correspond to the minimum in radiant intensity. Except for the times to the minimum for Shots 3 and 5, where the spectrographs viewed only a few square inches of the fireball surface, the NRL spectrographs saw a substantial proportion of the fireball. Thus the presence of spots, which are discernible in fireball photographs, probably was not a significant factor in the NRL results. Although a dead time of 2 to 3 msec is inherent in the NRL spectrographs due to zero time uncertainty, the values observed, as shown in Table 3.2, exceed this deviation from AFSWP-503. This is not to be considered final due to the preliminary nature of the NRL analysis of the spectrographic records.

3. The NRDL times to the minimum were obtained with radiometers, which have insufficient time resolution for the accuracy desired for study of weapons in the range of yields tested.

4. Since it has been indicated above that the spectral response of a sensing instrument has an effect on the time to the minimum, and since the AFCRC vacuum capacitor microphone is encased in a glass envelope, which is transparent only in the visual range, it is not surprising that the AFCRC times to minimum are different from those which would obtain with a bolometer. However, as with the bhangmeter, the microphone data are self-consistent, as may be seen in Fig 3.3.

According to AFSWP-503, the time to the second maximum in radiant emission is related to the yield by the expression $t_{max} = 32W^{1/2}$, where t_{max} is in milliseconds and W is in kilotons. The data for times to the second maximum are given in Table 3.2 and are plotted in Fig. 3.4. It is seen that the AFCRC data scatter randomly about the line representing the above expression and agree within 10 per cent of the accepted values. Although the NRDL times fall within 10 per cent of the expression for t_{max} , it should be noted that the times all are greater than accepted values, the explanation for which lies in the lack of time response in the radiometers. A reason for the large scatter in the NRL data for times to the second maximum is not apparent. It is possible that in the more fully developed fireball which exists at the second maximum, discrepancies enter due to nonuniformity in shape of the source and to departure of the source from black body characteristics. Since fewer spectral data were reduced for times after 100 msec, due to the preliminary nature of the NRL analysis, there are uncertainties in the time of the second maximum of the order of ± 25 msec. As will be seen from Table 3.2, some of the NRL data deviate from the AFSWP-503 curve by more than ± 25 msec.

3.3.5 Energy Vs Time

NRDL data on the accumulated per cent of total thermal energy delivered as a function of time are plotted in Figs. 3.5 and 3.6 for Shots 4 and 9 and 10 and 11, respectively. The curves in these figures are useful in correlating the phenomena involved in the precursor. Although the accumulated energy vs time data have not been plotted for the other shots of this operation, satisfactory plots may be reconstructed through use of the generalized pulse in AFSWP-503.

3.3.6 Energy Normal to the Ground

In the study of precursor effects, the component of radiant energy normal to the ground is of interest. In Fig. 3.7 the data for the normal component of thermal energy are plotted for Shots 9, 10, and 11 of this operation, for the four shots of BUSTER, and for the first four shots of TUMBLER-SNAPPER. Using the curves in Fig. 3.7, curves of shock arrival time vs distance (such as Figs. 2.24, 2.25, and 2.41), and the curves of per cent thermal energy delivered vs time in Figs. 3.5 and 3.6, the energy normal to the ground prior to shock arrival may be calculated.

3.3.7 Thermal Layer

In a recent paper on the effects of irradiated surfaces on the generation of a precursor, Sauer⁴ has analyzed air temperature, sound velocity, and thermal data from TUMBLER-SNAPPER. Whereas previously it had been thought that popcorning was the principal mechanism for transfer of heat to the air, Sauer's analysis indicates that the operation of conventional convec-

tive processes will probably satisfactorily explain transfer from the heated ground of most of the required energy into the air. Sauer also studied the case of the very high sound velocities over surfaces of fir boughs observed by NEL under Project 8.12a. Recent laboratory results from joint studies by NRDL and the California Forest and Range Experiment Station (CFRES) had indicated that gases initially evolved on intense irradiation of organic surfaces may contain elementary hydrogen. Since the observed NEL sound velocities were considerably higher than could be accounted for by any reasonable flame temperature and since the velocity of sound in hydrogen is four times that in air, Sauer has proposed a combination of convective heat transfer, flaming, and dilution with hydrogen gas as a qualitative explanation of the fir bough data.

3.3.8 [REDACTED]

Shots 5 and 6 were of particularly low yield, approximately 0.2 KT, and there is considerable current interest in the capabilities of weapons in this yield range. The thermal yield for an air-burst weapon of 0.2 KT yield extrapolated from curves based upon data obtained in the range 10 to 30 KT (AFSWP-503) should be about 0.097 KT, the time to the minimum about 1.2 msec, and the time to the second maximum about 14 msec [REDACTED]

3.4 CONCLUSIONS

Results of the basic thermal measurements of time to the second maximum and thermal yields are in good agreement with those calculated from the currently used scaling relations in AFSWP-503. Times to minimum in the thermal pulse were later than those predicted by AFSWP-503. It was concluded that this was due to the limited and different spectral response of the instruments used, thus indicating that when the time to the minimum is quoted the instrument must be specified.

Based upon results of the thermal measurements from this operation and from prior tests in Nevada, there is no further requirement for basic thermal measurements of weapons in the yield range 10 to 100 KT detonated in the air at lower altitudes. For air bursts of this type, presently available thermal scaling relations are sufficiently accurate for thermal effects studies with ground targets, under the ideal conditions prevailing at the NPG, provided the targets are located over suitably stabilized areas.

Further laboratory and field studies of thermal layers established over various types of surfaces (both organic and inorganic) are of interest. Such studies are under way in the laboratory at CFRES and at NRDL and in the field at TEAPOT. [REDACTED]

Further analysis of the thermal data obtained at this operation and from prior tests in Nevada appears to offer an attractive opportunity for evaluating the factors entering into the transfer of radiant energy through the quasi-ideal atmospheres in Nevada and through operationally more real atmospheres. [REDACTED]

3.5 RECOMMENDATIONS

As a step toward relating the propagation of radiant energy through real atmospheres, it is recommended that all the thermal data accumulated by the various agencies from tests in Nevada be correlated and analyzed.

In order to extend or modify, as required, the present scaling relations for thermal phenomena in the yield range below 1 KT, it is recommended that means be found to disassociate the mass associated with the detonation of devices with yields in this range to the extent that the masses approach those contemplated for the stockpile weapons.

REFERENCES

1. L. B. Streets, *Basic Characteristics of Thermal Radiation from an Atomic Detonation*, Report AFSWP-503, November 1953. SECRET RESTRICTED DATA
2. L. F. Drummeter, Jr., *A Method for Estimating Total Atmospheric Transmission of the Nevada Atmosphere*, Report NRL-4379, April 1954, CONFIDENTIAL
3. EG&G Staff, *Bhangmeter Mod II*, Project 12.1, Report WT-788, February 1954. SECRET RESTRICTED DATA
4. F. M. Sauer, *The Preshock Sound Velocity Field over Organic and Inorganic Surfaces*, Report AFSWP-420, December 1954, Division of Fire Research, Forest Service, USDA. SECRET
5. F. B. Porzel, *Preliminary Hydrodynamic Yields of Nuclear Weapons*, Report WT-9001, December 1953, LASL. SECRET RESTRICTED DATA

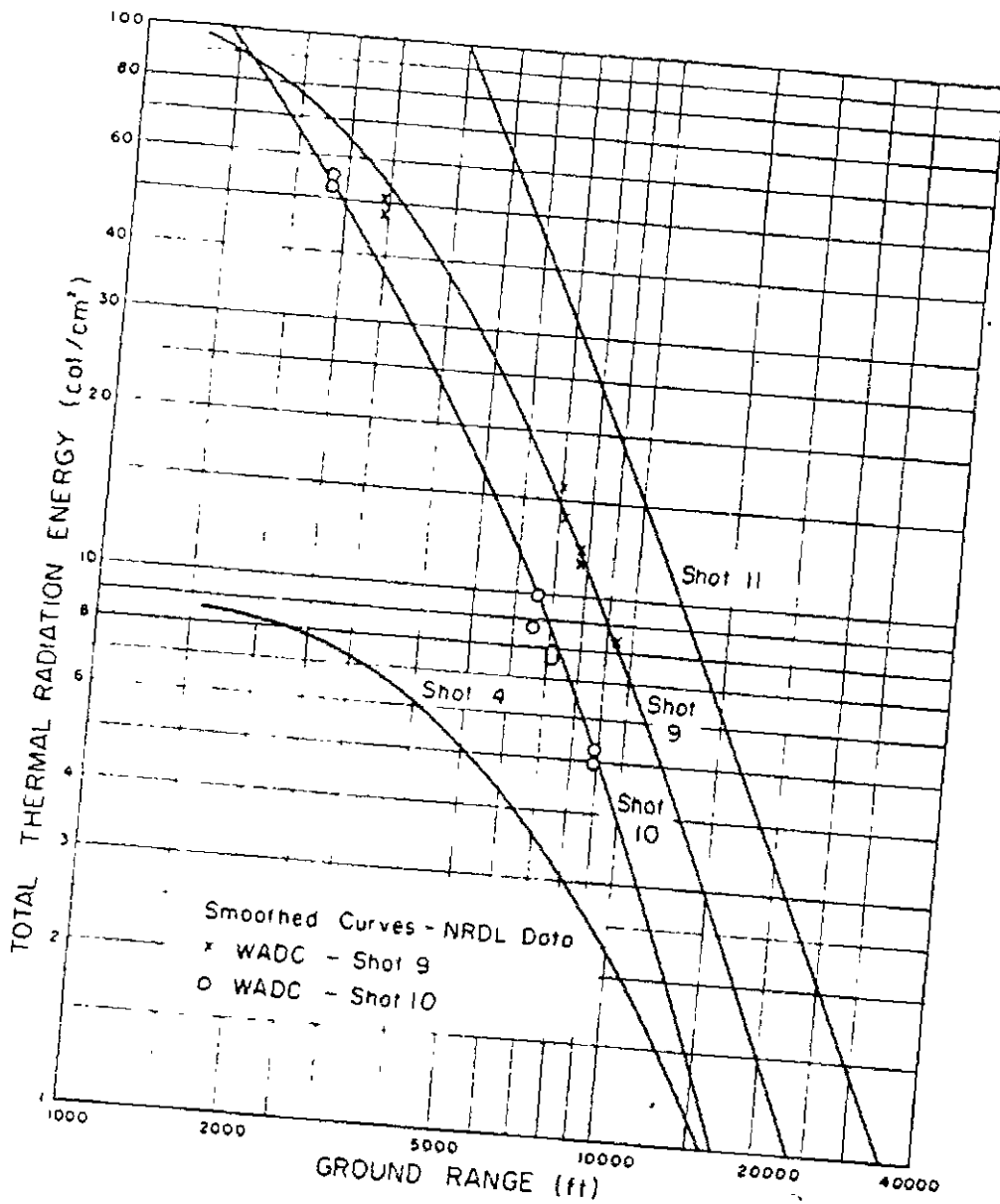


Fig. 3.1 — Total Incident Thermal Energy Vs Ground Distance (NRDL Data).

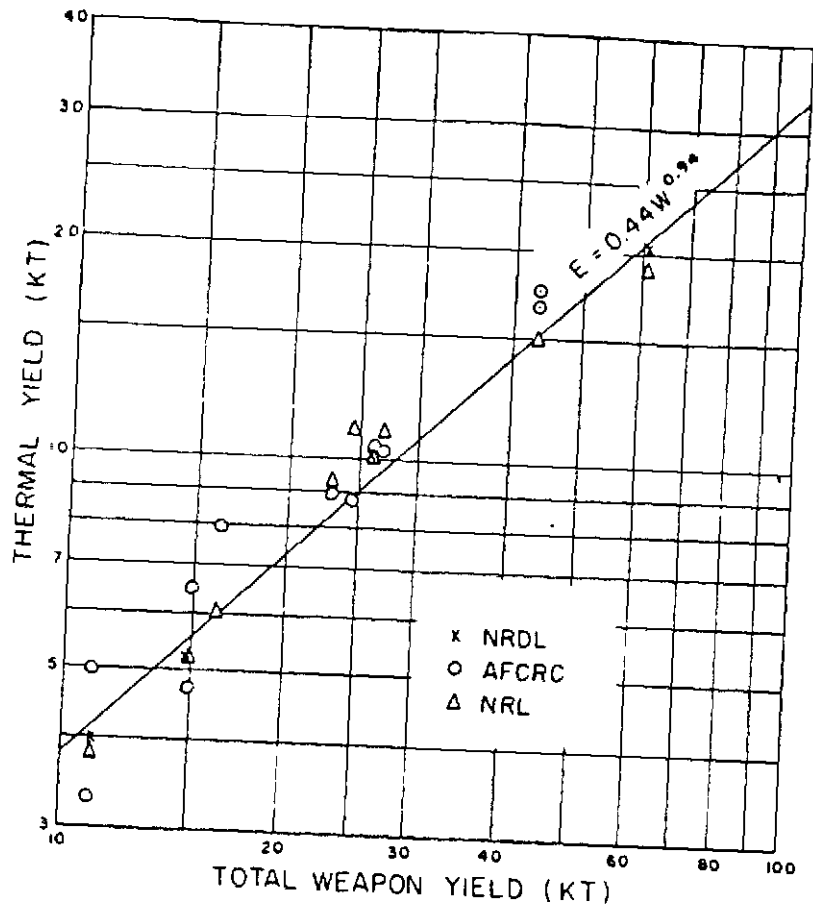


Fig. 3.2—Thermal Yield As a Function of Total Weapon Yield.

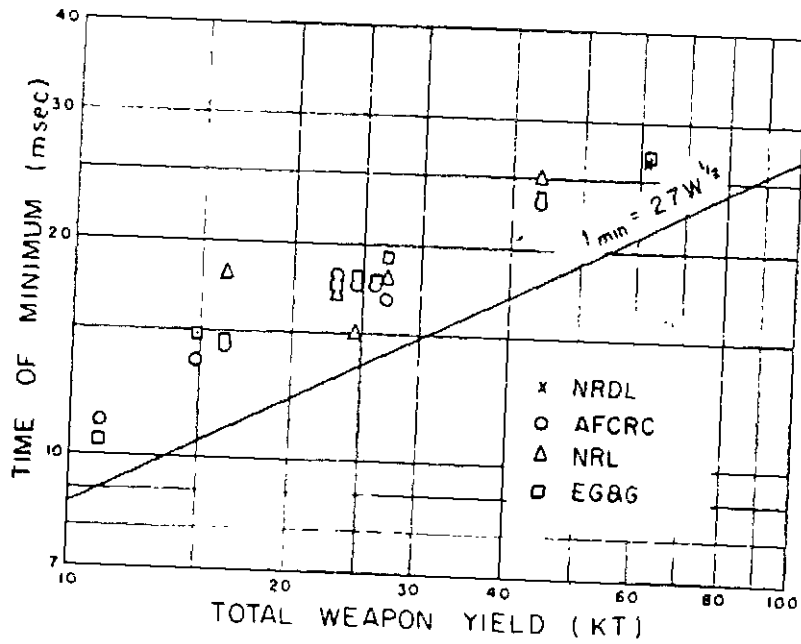


Fig. 3.3—Time of Minimum Vs Total Weapon Yield.

UNCLASSIFIED DATA

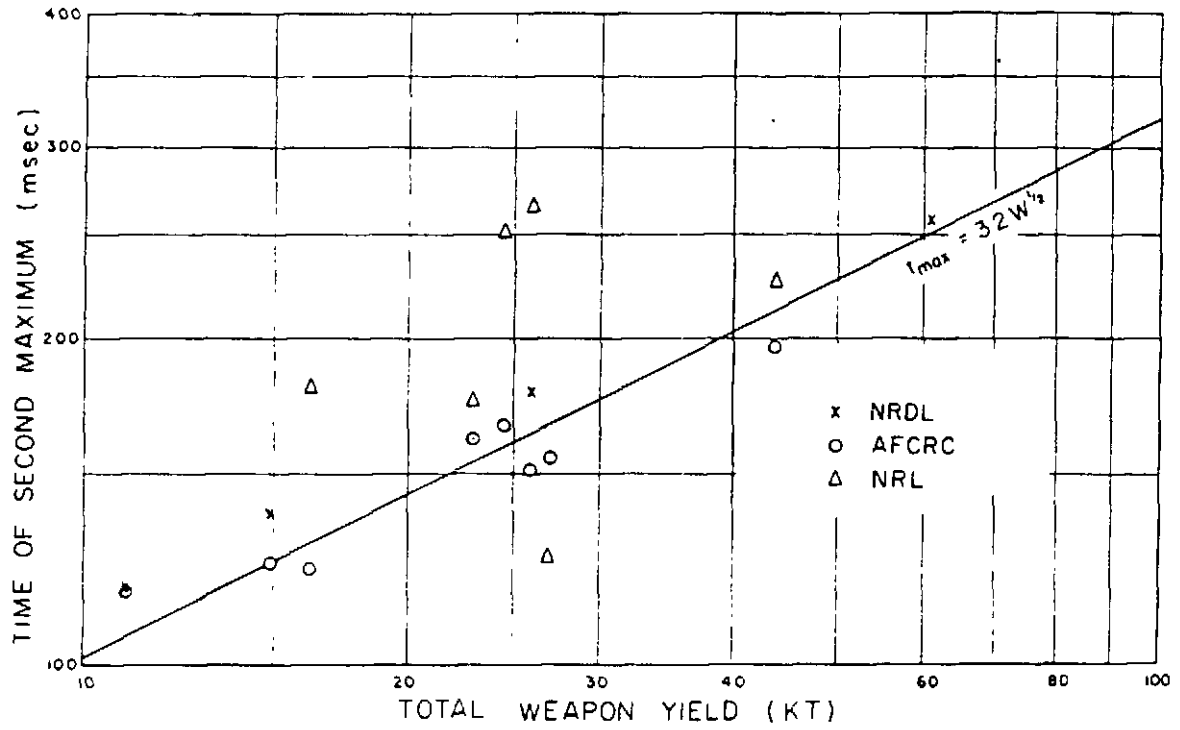


Fig 3.4 — Time of Second Maximum Vs Total Weapon Yield.



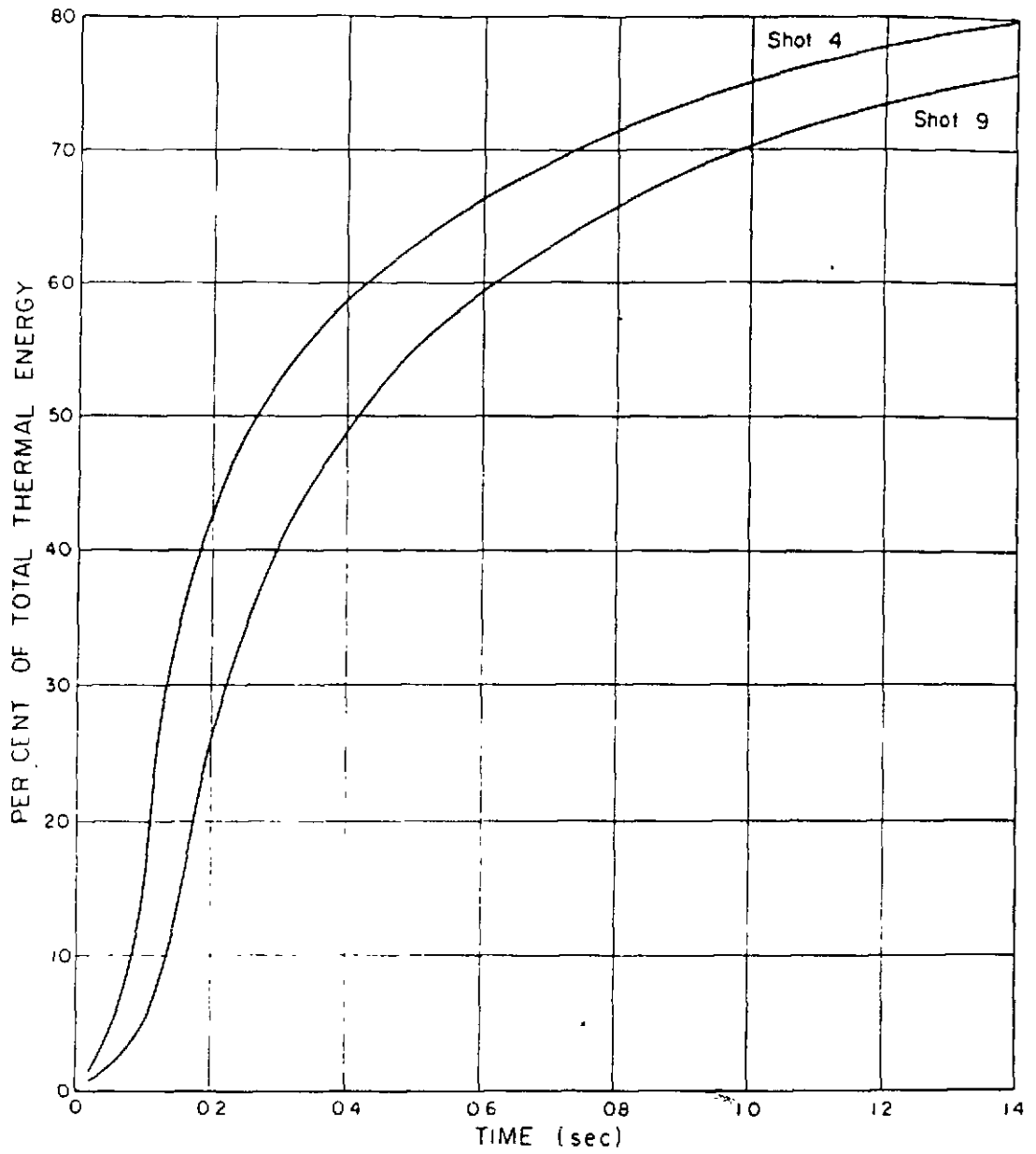


Fig. 3.5—Percentage of Total Thermal Energy Vs Time, Shots 4 and 9.



107

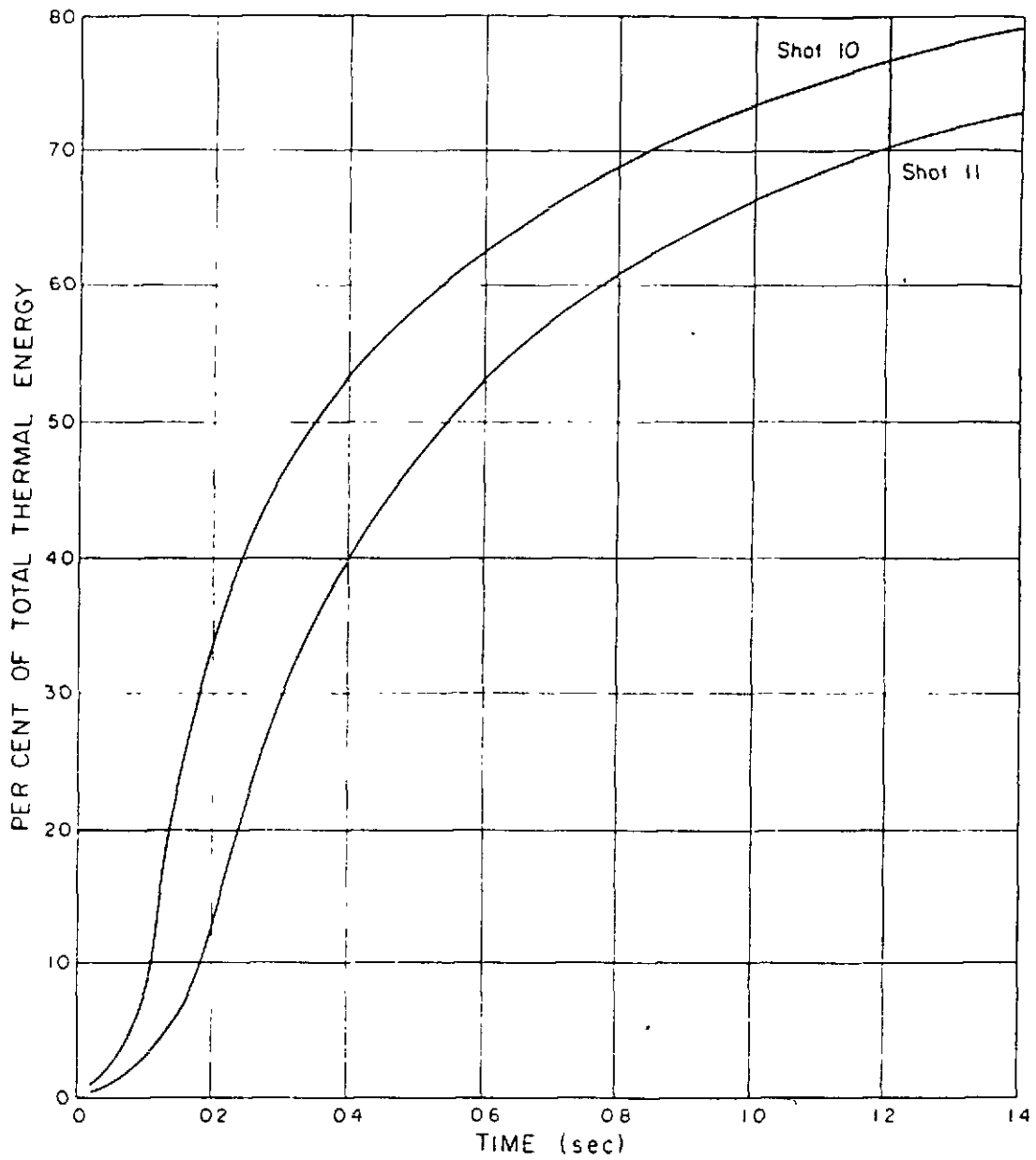


Fig 3.6— Percentage of Total Thermal Energy Vs Time, Shots 10 and 11.



108

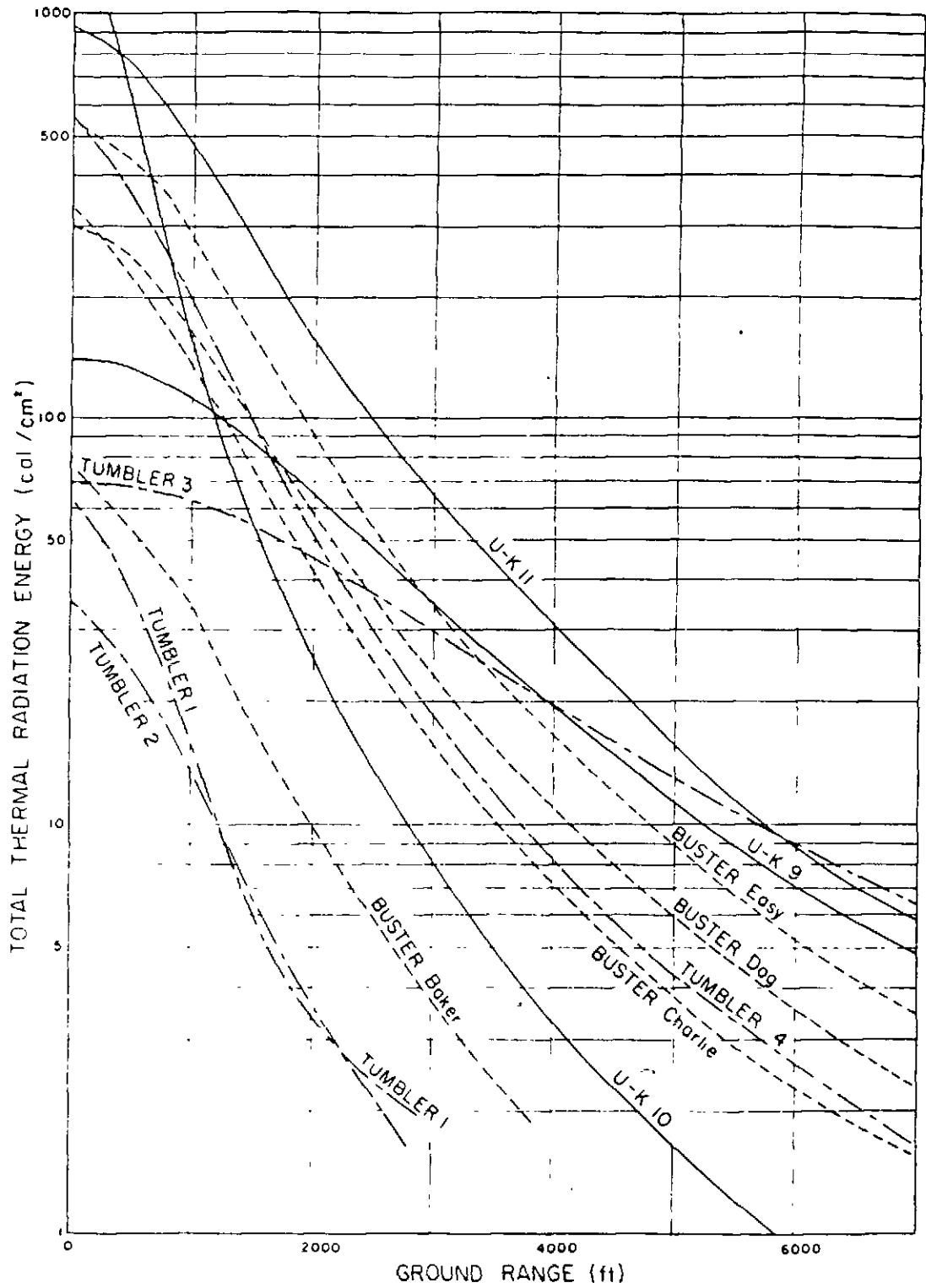


Fig. 3.7— Thermal Energy Normal to Ground Vs Ground Range, BUSTER-TUMBLER-KNOTHOLE Series.

CHAPTER 4

NUCLEAR RADIATION MEASUREMENTS

4.1 INITIAL GAMMA EXPOSURE

Initial gamma-radiation exposure vs distance data were collected by the use of National Bureau of Standards (NBS) type film dosimeters. Data were obtained for all shots in the test series except for Shots 4 and 11.

Figures 4.1 to 4.4 present the total gamma-radiation exposure data in terms of roentgens times distance squared vs distance. All data given have been normalized to an air density of $1.0 \times 10^{-3} \text{ g/cm}^3$. The film emulsions employed were calibrated against Co^{60} sources in the field and were recalibrated against the 10-Mev Naval Ordnance Laboratory betatron. The data presented are based on the latter calibration.

The data for Shot 10, test of the Mk-9 gun assembly device presented in Fig. 4.4, were arbitrarily corrected for a substantial effect of neutrons on the film emulsions. The effect of neutrons on gamma film dosimeter emulsions vs neutron energy is being evaluated at the Brookhaven National Laboratory (BNL) under the direction of Dr. Fred Olsen. Completion of this study should provide correction factors for the neutron effect which, in general, will be significant for thin-skinned devices and high-altitude detonations as well as for gun-assembly devices.

Yield data, together with factors describing the gamma exposure distance data at distance, are summarized in Table 4.1 for purposes of comparison.

The e-fold distance λ and the intercept and the zero intercept of the extrapolated RD^2 vs D plot conveniently summarize the data. Variations in the values of λ and of roentgens per kiloton yield at 2000 yd are a measure of the influence of the nature of the nuclear device tested and of the conditions of detonation on the gamma exposure vs distance.

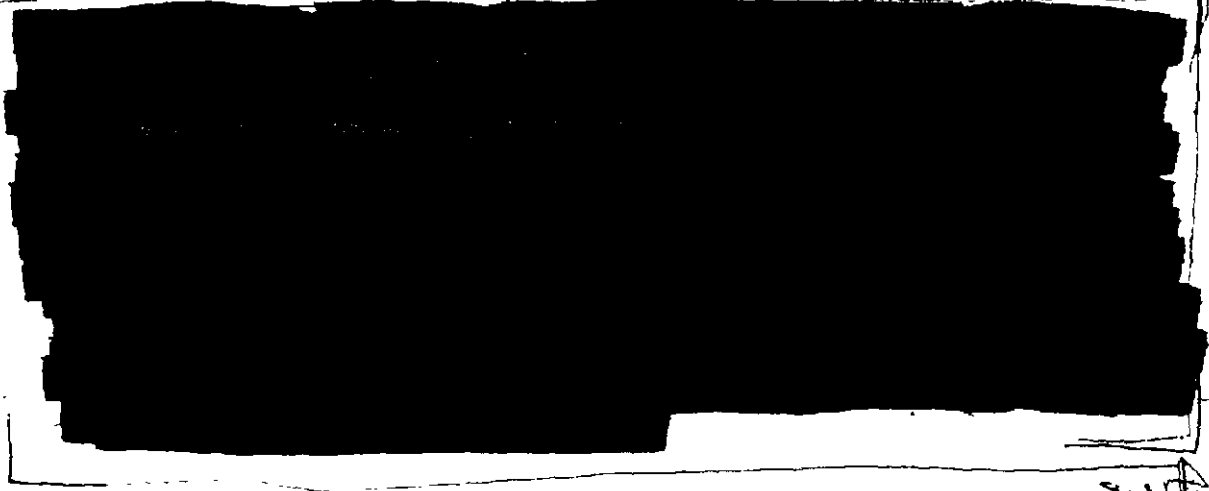


H(3)
DAE



DATA
(b)(3)

TABLE 4.1 - Initial Gamma Data



1247

DNA
1247

4.2 RESIDUAL GAMMA SPECTRUM

The degraded field spectra of the residual radiation was studied following several tower and air shots. Measurements were made using gamma scintillation spectrometer equipment similar to that employed in JANGLE Project 2.4c. Modified radiac instruments which provide for approximate absorption measurement of the gamma radiation were also utilized. The ob-

TABLE 4.2 - Field Measurement Locations

Shot	Approximate time (days after detonation)	Approximate position relative to G2 (ft)	Gamma rate (mr/hr)
7	D + 4	13,200 E	300
	E + 5	13,200 E	290
	D + 10	10,600 E	280
8	D + 0 (H + 3h)	2,000 W	320
	D + 2	1,700 W	220
	D + 3	1,400 W	240
9	D + 0 (H + 2h)	0	180
10	D + 0 (H + 2h)	2,400 W	270
	D + 1	800 W	250
11	D + 4	400 W	230
	D + 0 (H + 3h)	3,000 W	240
	D + 1	1,500 W	280

jectives of the project were to further develop and test spectrometer equipments for field use and to provide a limited portion of the field data which are necessary to establish optimum design parameters for gamma-radiation detection devices.

The scintillation spectrometer provided for the measurement of the gamma energy distribution over the energy range from 40 kev to 3 Mev. Instrument design limitations restricted measurements to positions of low gamma intensity. As a consequence, few data could be obtained on the variation of the spectra with time at a given position or with distance from zero on a given date. Table 4.2 lists the shots and describes the positions for which data were obtained.

Figure 4.5 illustrates the spectra obtained. The ordinate, $6N(E)$, is the number of photons per second entering one cubic centimeter of air from all directions per unit energy (kev) at



114

terval. The data show variation in the low energy part of the spectrum with detector head orientation resulting from some absorption of soft gamma radiation by the detector mounting.

Figure 4.6 shows the air dose rate contribution per unit energy interval corresponding to the spectrum of Fig. 4.5. The relative contribution of soft gamma radiation (below 100 kev) is quite small for the radiation fields measured. The data show increased contribution of higher energy components at the later times of measurement; however, since the locations were not identical, it is not clear whether the difference reflects a change in radiation quality with time or with position.

The results obtained in this study do not necessarily invalidate the results and conclusions of Operation JANGLE Project 2.4c, Report WT-348, which indicated substantial soft gamma contribution, since the nature and distribution of contamination as well as the relative positioning of the measurement points may be quite dissimilar.

Before one can reliably assess the adequacy of present designs of gamma-radiation detection devices, much more information is required on the gamma spectra for residual contamination fields. Instruments which can be employed in fields of higher intensity are required. Future measurements of the field spectra should be augmented with fallout sample collection and analysis so that the spectral data can be evaluated in terms of the nature and distribution of the contaminant. It is also suggested that consideration be given to measurement of the spectra in shielded positions and shelters where the radiation is predominantly highly scattered and thus predominantly of lower energy than is efficiently recorded by most gamma radiac devices.

In addition to the need for better information on the gamma energy distribution, more must be known of the relative biological effectiveness of gamma rays vs energy. Both are necessary for the dependable evaluation of the adequacy of gamma detection devices.

4.3 NEUTRON FLUX

Data are presented for thermal and fast neutron flux vs distance for Shots 8, 9, and 10. The data were obtained using gold and tantalum detectors for thermal neutrons and sulfur threshold detectors for fast (3-Mev threshold) neutrons.

For thermal neutrons the time-integrated flux times the range is plotted against range in Figs. 4.7 to 4.9. For fast neutrons the time-integrated flux times the square of the range is plotted against range in Fig. 4.10. Such plots yield straight lines on semilog paper and represent the neutron flux data at ranges beyond about 600 yd for the yields involved.

The data are summarized in Table 4.3 together with radiochemical yields and zero intercept per kiloton values for other devices for purposes of comparison.

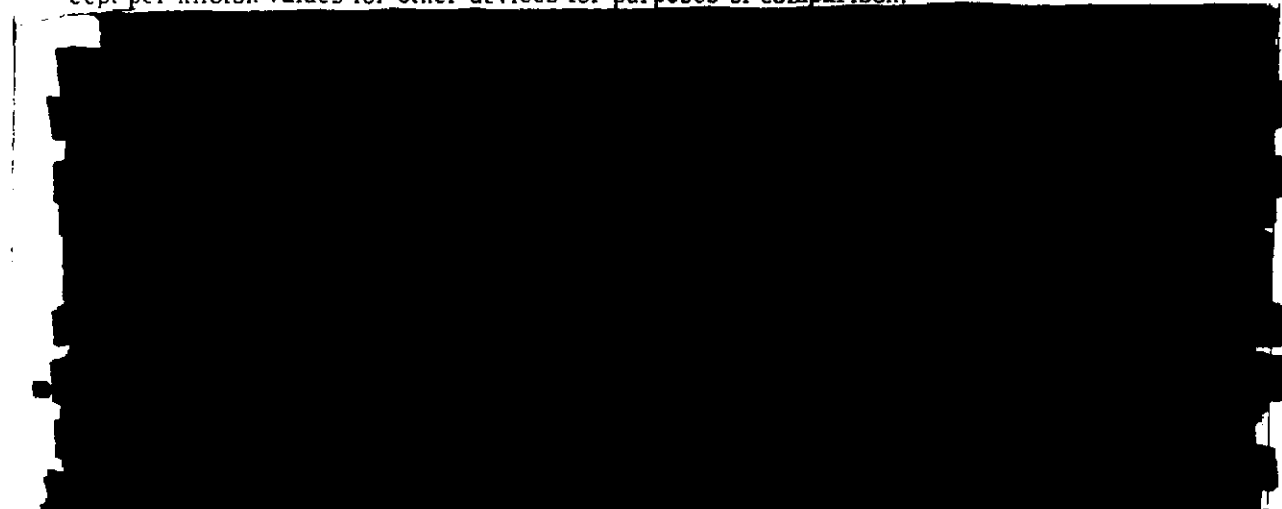
 On the basis of these considerations, more experimental work should be carried out to establish the neutron spectrum and its varia-

TABLE 4.3— Summary of Sulfur and Gold Neutron Data

* From Biggers LAB J 16537-38.

† From AFSWP WT-524.

Note: UPSHOT-KNOTHOLE data not corrected to standard atmosphere. $nvt \times D$ is the ordinate for thermal fluxes; $nvt \times D^2$ for fast neutron fluxes.

tion with distance from the burst point. Both the response of gamma film dosimeters to neutrons vs neutron energy and the biological effectiveness of neutrons vs energy also require further evaluation.

4.4 RADIOACTIVE PARTICLES INSIDE AIRCRAFT

Project 2.1 was concerned with the measurement of the size distribution and concentration of atomic-bomb cloud particulates entering aircraft through the cabin pressurization system. Samples were obtained using cascade impactor equipment connected to the intake manifold of two drone F-80 aircraft. These are the same aircraft instrumented with animals by Project 4.1 to assess biological hazards in aircraft.

The results obtained by particle studies in Project 2.1 support the conclusion of Project 4.1 that the possible hazard from inhalation inside aircraft is of no consequence in relation to the effects of external gamma-radiation exposure.

4.5 RESIDUAL GAMMA-RADIATION DEPTH DOSE IN UNITY DENSITY MATERIAL

Personnel of the Naval Medical Research Institute, Bethesda, Maryland, carried out gamma depth dose measurements in areas of fallout following several shots. Three types of phantoms of unit density material were employed: sets of lucite spheres of varying wall thickness, a large masonite sphere instrumented in depth, and a simulated man, also of masonite. Small Sievert type ionization chambers were used as detectors. Considerable data were obtained which show the dose distribution in depth for unit density materials for the several geometries used.

*Pages 116 through
119 are deleted.*

RESTRICTED

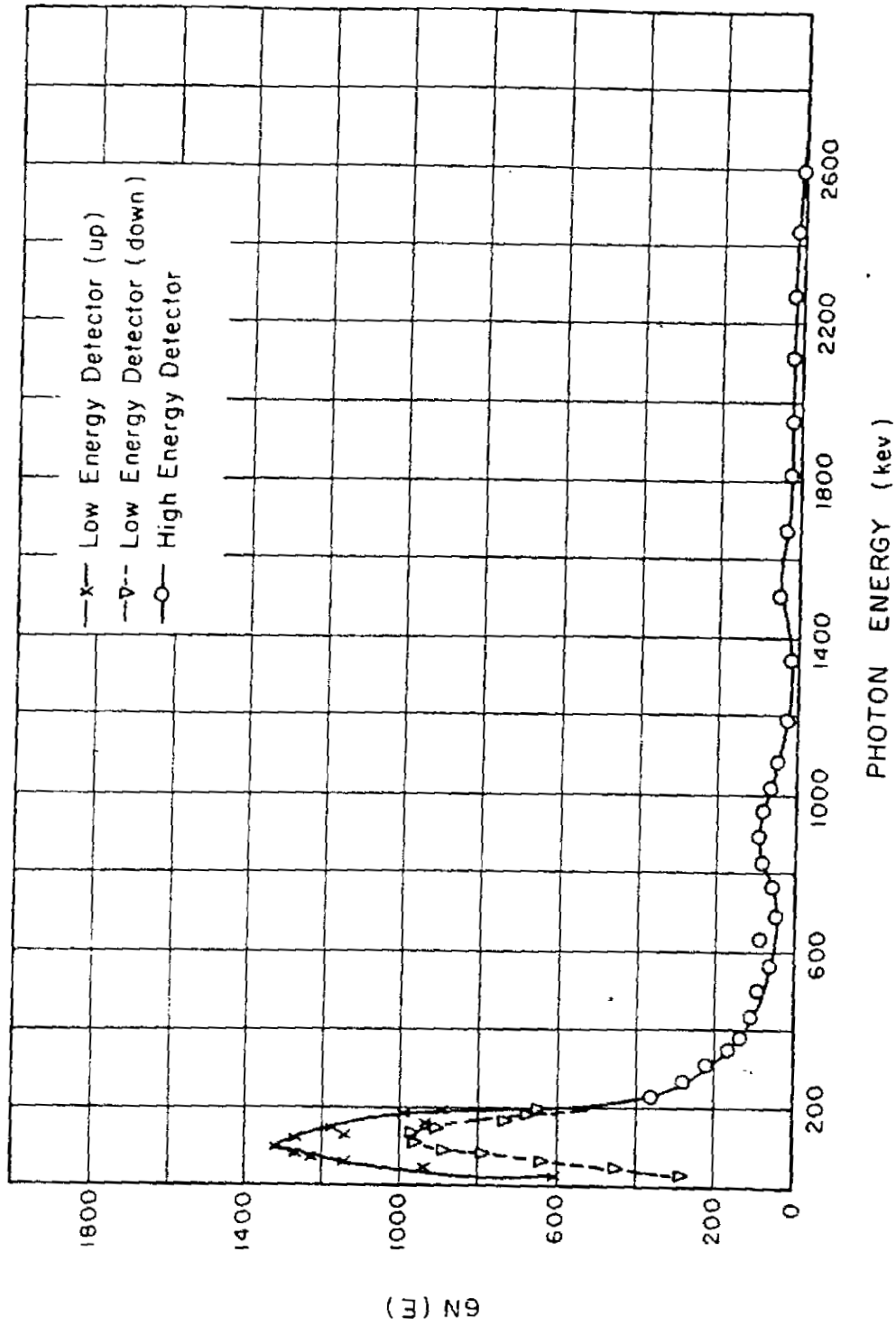


Fig. 4.5—Photon Spectral Distribution, Shot 11 (I1 + 3).

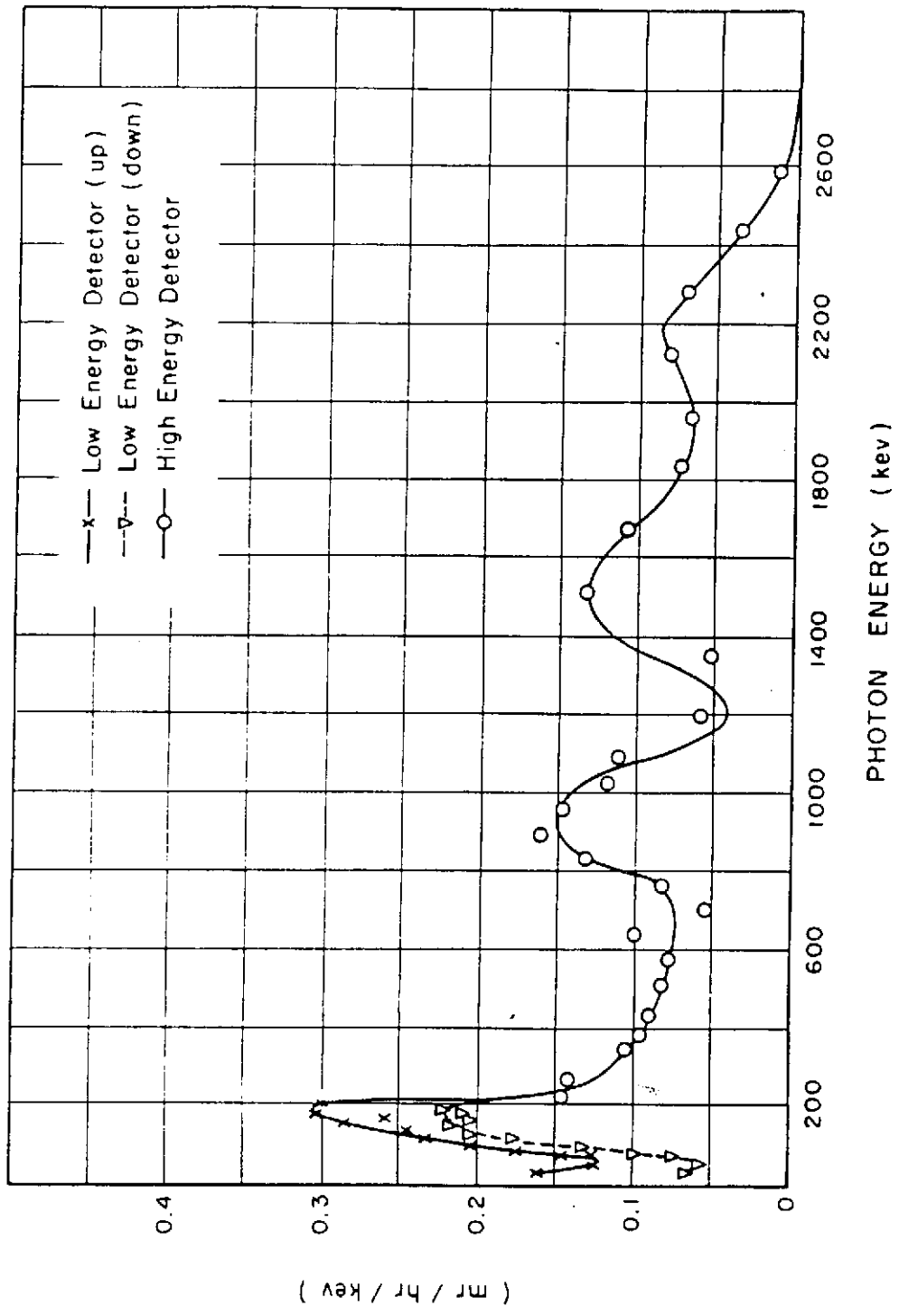


Fig. 4.6—Dose Rate Vs Energy, Shot 11 (H + 3).

Pages 122 through 126 are deleted.



CHAPTER 5

EFFECTS ON STRUCTURES

5.1 INTRODUCTION

It is the intent of this chapter to discuss generally the effects of atomic blasts on structures and installations, with reference primarily to the results of Shots 9 and 10. Included herein are elements or objects tested for the purpose of determining data which can be applied to the prediction of structural effects. These structural effects are related to the effects on equipment and objects of various kinds. Many of the general comments made in this chapter also apply to military targets.

Summaries of projects pertinent to the effects on structures, material, and equipment appear in Appendix B, Section B.3.

5.2 EXPERIMENT DESIGN

The experiments described in this chapter can be divided into two groups: one in which the primary objective was to determine loading or forces on objects of a particular size and shape, and another in which the primary objective was to determine the response of a particular kind of structural element or complete structure. However, many of the tests designed for determination of loading permitted observations of structural response, and conversely. If both the loading and the response are measured, then there is a possibility of extending the test observations to structures or elements of different form and design.

Information concerning both loading and response of structures may be available from sources other than atomic field tests. The applicability of data obtained from such sources can be verified by field tests.

5.2.1 Loading Tests

Although data on loading are available from shock tube and wind tunnel tests, field tests are required for the purpose of considering the effect of variables which cannot be readily reproduced in laboratory tests. In this program, measurements were attempted on rectangular and cylindrical objects in several different positions and at different pressure levels; on bridges and elements of bridges; on aboveground structures with and without earth cover; on roof and wall panels; and on beams covered with various depths of earth. In some of these tests the loading was determinable only from pressure-gage readings on various faces of the objects tested; in other instances loading could be inferred from measured reactions or from structural responses. The tests of wall and roof panels, in particular, were designed to furnish information on the change in loading as a function of the panel response, primarily in the range where break-up or failure of the panel occurred during the loading phase.

5.2.2 Response Tests

Observations were made of structural response for roof and wall panels, for shelters and shelter components, for buildings of various design and type of construction, and for window glazing.

Structural response to dynamic loading is in general a function not only of the loading but also of the resistance parameters of the structure. If the loading is not available from theoretical studies or laboratory experiments, it must be determined by measurements of pressures or net forces if a correlation between prediction and observation is to be achieved. The loading, in magnitude and duration, and the resistance of the structure or structural element are the most important variables affecting the structural response. Some structures are simple enough that their dynamic resistance can be computed or can be measured by means of laboratory tests. However, many other structures are so complicated that information is not available from laboratory tests or theoretical studies to permit the assessment of their dynamic resistance. For these structures, some tests must of necessity be made with the purpose of determining the performance of a particular structure subjected to a particular set of phenomena resulting from the detonation of a given bomb. Such tests have limited applicability unless a theoretical explanation of the response is developed.

5.3 COMMENTS ON INTERPRETATION OF RESULTS

5.3.1 Drag, Diffraction, and Precursor Phenomena

In general, the loading on a structure is a function of its outline and the size of its individual elements, as well as of the general conditions of terrain and the variables pertaining to the height of burst and yield of the weapon. The latter factors determine the intensity of the blast wave and its duration. These are affected by the terrain and particularly by the thermal influences resulting from the thermal radiation interacting with the terrain. These influence both the overpressure, p , and the dynamic pressure, q , which determines the so-called drag pressure resulting from the particle motion of the air. A more general treatment of blast parameters is included in Chapter 2.

The size and makeup of the structure influence the loading transmitted to it by making the structure in some cases particularly susceptible to the loading from diffraction or in other cases to the drag of the dynamic pressures.

All structures are subjected to influences from both phenomena, diffraction and drag. However, the time it takes for the diffraction phase of the loading to clear is dependent on the size of the structure or the structural elements. Therefore, a structure which is relatively very narrow in the dimension parallel to the blast front or made up of parts which are narrow and thin is in general affected primarily by drag. It is called a drag-type structure.

On the other hand, a structure which is moderate or large in size and has walls that do not fail quickly is affected primarily by the diffraction forces which are considerably greater in magnitude than the drag forces. It is not always possible to differentiate clearly between these two types; some structures are of intermediate size where both diffraction and drag are of nearly equal importance. Again, a structure which may be diffraction-type structure in the early stages of loading may become a drag-type structure in the later stages if it has a covering that fails after transmitting some force to the frame. In addition, some structures may be affected primarily by the difference of external and internal pressure or by overall crushing from the external pressure.

Most of the structures in Shots 9 and 10 were clearly of one type or the other, rather than a mixture of both types. In general, the bridges, forest stands, telephone poles, towers, other thin, tall objects, and probably the vehicles of various types were primarily drag-type targets. The wall panels in the various structures in this program were primarily diffraction-type structures. The geometric shapes of Projects 3.1 and 3.3 were in general mixed-type structures

The importance of this distinction of structural type lies primarily in the difference between the effects of Shots 9 and 10 in their overpressure and dynamic-pressure phenomena. Considerable attention is devoted to blast phenomena in Chapter 2. Shot 9, a relatively high burst (2400 ft), essentially represented the ideal case, with no pronounced surface or thermal effects on blast. In the Mach region for ground ranges greater than about 2500 ft, the dynamic and static overpressures followed the conventional Rankine-Hugoniot relationships at the shock front. Consequently, when proper attention is paid to the blast-wave duration, which is a function of the detonation yield, damage to both drag and diffraction targets could be described in terms of either static or dynamic overpressure. In the regular reflection region for ground ranges less than about 2500 ft on Shot 9, simple geometric relationships show that dynamic pressures were substantially less than would be obtained by applying the conventional analytical relationships to calculate them from the static overpressures. Hence, in this region the damage to drag and diffraction targets cannot be described in terms of a single blast parameter but must be related to the dynamic and static overpressures, respectively. Clearly, in the regular reflection region, Shot 9 would be less damaging to drag-type targets than would an equal-yield low burst over an ideal surface at locations having the same peak overpressures.

Shot 10 was a relatively low burst with pronounced surface and thermal effects on the blast wave. These blast-wave perturbation effects, characteristic of a precursor region at the Nevada Proving Grounds, had the effect of reducing the static overpressures below those anticipated in the ideal case. It was clear that the effective dynamic pressures were at least equal to or greater than those to be expected in the ideal case, and the effects of dust loading were not isolated. Consequently, in the precursor region (also the Mach reflection region for all locations of interest) on Shot 10 the effective dynamic overpressures were substantially greater than would have been calculated from the measured static overpressures by the application of conventional analytical relationships. Hence, on Shot 10 in the precursor region the effects on drag-type targets could not be described in terms of the measured peak static overpressures.

The effects of Shots 9 and 10 on drag-type targets at static overpressure levels encountered in the precursor region of Shot 10 cannot be compared on the basis of peak static overpressure but must be compared on the basis of effective dynamic pressures. Consequently, in spite of the fact that Shot 10 was considerably lower in yield than Shot 9, at ground ranges less than about 2500 ft Shot 10 was markedly more damaging to drag-type targets. This result can clearly be ascribed to the effects of Mach reflection and the precursor region of Shot 10, even though the dust effects on Shot 10 were not isolated.

5.3.2 Limiting Conditions

Measurements of structural response in a field test give, at most, only specific results for the particular object tested and for the particular loading conditions applied to it. These data are generally maximum transient deflection determined from appropriate instrumentation, maximum permanent deflection, or type of damage. From these data, inferences can be drawn as to the conditions that would produce a given degree of motion or damage. However, such inferences can be drawn only in those cases where measurements are available or where estimates can be made of both the loading and the structural-resistance parameters. Where such information is not available, inferences as to limiting conditions for failure can still be drawn if results on a number of items, ranging from slight damage to failure, are available. For example, if objects such as vehicles are overturned up to some distance and then from this point on remain essentially unaffected by the blast, a fairly good estimate of the limiting condition for overturning of the objects can be made. It should be emphasized that these limiting conditions of pressure or distance are the most important data which can be determined from structural-response tests.

Unfortunately, the limiting condition for failure or for a given degree of damage is not always easily inferred from field-test data. For structures which are loaded into the plastic range and for loadings which last for even a moderate length of time compared with the fundamental period of the structure or structural element, deflections of structures or structural elements are very sensitive to: minor variations in the magnitude of the peak loading, the

yield-point resistance level, the duration of the entire loading, and particularly the time of rise from the beginning of loading to the peak loading. In some cases, as the rise time of the force on the structure increases, the response first decreases and then increases.

The situation is entirely different for high-explosive bombs. For such bombs, which produce a relatively short positive phase of pressure, the structure is subjected to essentially an impulsive loading, and the deflection is clearly determinable and reliable as a measure of the influence of the loading. However, where the loading is of relatively long duration, as is the case for most of the structures in the UPSHOT-KNOTHOLE program, wide variations in deflection are produced by minor variations in overpressure or dynamic-pressure level. Consequently, very good and consistent data can generally be obtained concerning the overpressure level or dynamic-pressure level which might produce failure, even though it may be impossible to predict the amount of deflection which might be produced under given conditions. The pressure level required for a given degree of damage or failure is the preferable measure of the results of the test because it is less sensitive than the degree of response. In addition, it is a more realistic value for extrapolation to other cases, including other structural types, other sizes of bombs, and especially large-yield weapons in the thermonuclear range.

As an indication of the way in which the various parameters affect the response, the case of an object such as the Bailey bridge, which can move relatively freely except for the resistance offered by friction, may be considered. For such a structure, the amount of motion is roughly proportional to the product of the following two quantities: the square of the difference between the peak dynamic force and the sliding resistance, and the square of the effective duration of the dynamic pressure. If the peak dynamic force is smaller than the sliding resistance, the structure does not move at all. However, when it is only slightly greater than the sliding resistance, even a very small change in the peak dynamic force can cause a tremendous change in the motion. A similar condition applies to other structural types, although the relations are somewhat more complicated. These facts are a good argument against attempting to refine predictions of response to a great degree from the measured input data in a field test, inasmuch as these input data can never be accurately known.

Although there is a difference in the positive-phase durations (both for static overpressure and dynamic pressure) between Shots 9 and 10 because of the difference in yield, corresponding durations are of the same general order of magnitude. Therefore the limiting conditions inferred from these shots can generally be compared in terms of measured static overpressure or dynamic pressure for diffraction or for drag-type targets respectively, owing to the small influence that the duration has on the limiting pressure for failure in either case. If the durations had been significantly different, comparisons in these terms would not have been valid for the drag-type structures.

5.4 RESULTS

5.4.1 General Description of Damage

Summaries of the individual projects are given in Appendix B, Section B.3, and in the individual project reports. The purpose of this section is to give a brief qualitative description of the damage observed in Shots 9 and 10 for those structures which, because of intent or otherwise, were subjected to major deformations from the blast.

The cubicles of Project 3.1 and the cylinders of Project 3.3 were designed primarily to obtain loading information and except for one concrete block suffered no major deformation. The trusses of Project 3.4 were also designed primarily to study loading, but in Shot 9 the truss bridge deformed slightly due primarily to slip of the cable clamps in the bracing. In Shot 10, the upper part of the truss-bridge section failed completely and fell to the ground, even though the cable-clamp detail was strengthened. This failure was at a lower overpressure but probably at a higher dynamic pressure than in Shot 9.

In Shot 9 the wall panels of Project 3.5 failed, except for some of the brick panels.

The railroad equipment of Project 3.6 was tested only on Shot 10. Wooden boxcars, empty or loaded, were severely damaged within 3000 ft. This damage was more severe than expected

and indicates, with other phenomena, a greater dynamic pressure in the precursor region than was expected.

The structures of Project 3.7, which were intended to furnish a study of entrance baffles and ventilation devices, were undamaged by Shot 9 but were destroyed in Shot 10 where the pressures were considerably greater than had been intended.

The buried structure of Project 3.8 indicated, for moderate deflections, that little if any effective attenuation was experienced in the pressures transmitted to a buried structure through an earth cover. This conclusion, of course, is limited to a depth of earth cover about equal to the 8-ft span of the structure. Very little permanent deformation of the elements in the structure was experienced.

In the field fortifications of Project 3.9, failure began in the cover-supporting timbers at moderate overpressures, but no failures occurred in revetments except close in to the blast.

In the light-steel-frame structures of Project 3.11, damage was obtained only in Shot 9. There was an indication that only minor damage occurred at a 1-psi level in the unreinforced building; considerable damage even in the reinforced building occurred at an overpressure level of 2.2 psi. In the brick wall building protected by precast rib panels on the sides and roof (Project 3.12), there were indications of distress in the wall panels from Shot 9 and breakage of about 30 per cent of the wood joists in the roof of the structure from the load transmitted from the deflection of the concrete roof covering.

In the precast gable structures of Project 3.13, only slight cracks and practically no structural damage was noted either in Shot 9 at about 10.7 psi with earth cover, or in Shot 10 with the earth cover removed.

The precast warehouse of Project 3.14 was not tested in its completed condition in Shot 9, but the frame alone suffered no damage. In Shot 10, the roof panel failure was fairly complete at an overpressure of about 2.0 psi.

The Armco steel magazine of Project 3.15, under earth cover, showed no significant damage in either shot except for an entrance-door frame failure in Shot 9.

The glazing and window construction of Project 3.16 showed failure in general at different pressures for the different types of glazing but indicated that in most cases pressure levels greater than 2 psi would break most glass panels.

The forest stand of Project 3.19 showed little attenuation of the static pressure or of the drag pressure, but considerable missile hazard due to flying branches was experienced.

The communications system of Project 3.20 showed little damage in Shot 9 but considerable damage in Shot 10, indicative of the greater dynamic pressures in that shot. A number of poles were broken in Shot 10 up to a limit for dynamic pressure corresponding to about 5-psi overpressure.

The vehicles of Project 3.21 showed a range in results indicating displacements of the order of 6 ft for overpressures of approximately 8.6 psi in Shot 9 but considerably greater effects in Shot 10, with vehicles hurled great distances through the air and frequently broken in-to pieces.

The Bailey bridge of Project 3.22 slid about 4 ft on the steel channel sills at an overpressure of 8 psi in Shot 9 and was moved over 17 ft off the piers and wrecked in Shot 10.

The LVT's of Project 3.24 showed very light damage in Shot 9, in general requiring greater than 22 psi for failure in that shot. These received severe damage in Shot 10.

5.4.2 Discussion

Because of the greater dynamic pressure for a given overpressure in Shot 10 compared with Shot 9, spectacular damage occurred at overpressures in Shot 10 at which little or no damage occurred in Shot 9. Military equipment was broken up and strewn over the landscape in Shot 10, whereas in Shot 9 it was only overturned and in some cases not moved at all. Similarly, the close-in instrument towers on the blast line, undamaged by Shot 9, were thrown down or badly damaged by Shot 10. Slippage of the Crosby clamps used on the guide cables may have contributed to the failure of these towers, but there is evidence that the clamp detail was only slightly weaker than the other connections and the cables themselves. Clearly the effects of

Shots 9 and 10 should not be compared or judged on the basis of equal static overpressure for targets in the precursor region of Shot 10 or in the regular reflection region of Shot 9.

In general, the effect of Shot 10 was greater than Shot 9 only for drag-type structures. Consequently, it is clear that the dynamic pressure must be the factor with which comparisons are to be made for damage to drag-type structures, whereas the static overpressure is the criterion for diffraction-type structures. However, dynamic pressures were not measured at each location. Consequently, in this chapter and in Appendix B, Section B.3, references are often made to values of static overpressure as a measure of dynamic pressure, with the understanding that the dynamic-pressure values are approximately equal to the ideal values for the reported magnitudes of static overpressure.

Simple analytical considerations indicate that the effects on diffraction-type targets in the precursor region characteristic of Shot 10 might be less than for corresponding overpressures in Shot 9, because of the slow rise time of the static overpressure in the precursor region. However, there was insufficient experimental evidence to justify any conclusion of the relative effects of Shots 9 and 10 on diffraction-type targets at corresponding overpressures.

The effects of dynamic loading and of vibrations are important in blast resistance. Details of connections require special consideration in order to resist blast loading.

Earth cover has at least a bonus value in reducing radiation and missile hazard. However, for underground structures beneath a plane ground surface, it appears that unless the deflections are large there is little effective attenuation offered by earth cover of less depth than the short span. Under such conditions, the earth acts as an additional mass and may reduce the response of the structure to very short duration, or impulsive, loading. For long duration loads, the effect of the earth mass is negligible.

For aboveground shelters covered with earth, the influence of the earth is: (1) to change the loading by changing the outline of the structure; and (2) to add mass to the structure, which may increase greatly its resistance to short-duration loads. For long-duration loads, however, the increase in strength is negligible.

5.4.3 General Comments

In atomic field tests, whether for the purpose of determining loading or response, careful planning of the test program is required. Without sufficient advance knowledge of the nature of the response of the structure and the parameters governing its response, it may be impossible to place the structure in a region where the magnitude of the deflections or deformations will be significant. Even in the situation where only loading phenomena are to be studied, unless some prediction as to the magnitudes of the quantities to be measured are available no assurance is possible that the instrument readings will be large enough to provide useful results, because of the necessity for setting the ranges of the instruments carefully.

Because of the many major uncertainties affecting loading and response, it is desirable to make such preliminary observations as are required to determine the properties of the object subjected to test and to insure the proper interpretation of the test records. Furthermore, redundancy in the measurements should be provided in order that reasonable results can be obtained with the normally expected number of failures in the recording channels.

In general, the most successful test program is one in which loading and response are studied at the same time in such a way that some estimate of the loading can also be inferred from the response. In tests of this sort, the various interrelationships among the data permit information to be obtained even under unfavorable conditions.

Finally, in no case should the success or failure of a project hinge on the successful completion of each of a large number of separate readings. Under such circumstances the failure of only one channel may invalidate the whole test.

Care should be used in applying the results of these tests, in terms of specific values of overpressure or dynamic pressure required to produce damage to various targets, to conditions involving weapons of greatly different yields or substantially different heights of burst.

CHAPTER 6

EFFECTS ON AIRCRAFT STRUCTURES .

6.1 INTRODUCTION

Accuracy of bomb delivery is ordinarily a function of the closeness of approach of the delivery aircraft. In the case of atomic-bomb delivery, the nearness of approach of the bomber to the target is severely limited by the effects of the bomb burst upon the delivery aircraft structure. Thus the effectiveness of the atomic bomb in warfare is critically dependent upon accurate knowledge of the reaction of the delivery aircraft structure to the bomb's effects and upon ability to predict the magnitude of the effects. Resolution of these factors naturally leads to improved design criteria for future delivery aircraft. In addition, from the standpoint of both offensive and defensive operations, the effects on aircraft on the ground must be understood.

6.1.1 Background

Extensive instrumented tests of aircraft structures in flight were first attempted at Operation GREENHOUSE, although on previous tests limited qualitative data had been collected. The results of GREENHOUSE provided considerable data which were used in the development of generalized analytical procedures for prediction of effects on aircraft in flight. However, instrumentation failures and limitation in scope left certain gaps in effects information for which further tests were required. Likewise, extensive tests on parked aircraft were conducted on Operation TUMBLER-SNAPPER. The results of these tests indicated further experimental work was required in protection problems for parked aircraft.

6.1.2 Scope

During UPSHOT-KNOTHOLE further attempts were made to determine experimentally the effects of atomic weapons upon various aircraft structures in flight and on the ground. Three different types of aircraft (Navy AD, Air Force B-50, and B-36), thoroughly instrumented to measure loading and response, were flown at various distances from both tower and air-burst detonations. Fighter and bomber type aircraft were exposed on the ground. In addition, various components and idealized structures were exposed on the ground, some in specially constructed mounts designed to separate the blast and thermal magnitude of the loads imposed by these two effects separately and simultaneously.

6.2 THERMAL EFFECTS

Of the many effects observed during the tests, the most spectacular were the thermal effects which in one case led to the loss of a drone aircraft in flight, apparently through weakening

of the structure by heating. From this and other flight tests of this series, it appears well established that in predicting thermal flux at a position in space, ground reflected radiation as well as direct radiation must be considered. This is of greatest importance for bursts occurring relatively near to the ground and/or over ground surfaces with a high reflection coefficient.

It also appears well established that a white heat-resistant paint is by far the best surface finish presently available for the reduction of thermal effects on aircraft structures. The use of such reflective surface finish probably would have prevented loss of the above-mentioned drone, and it follows that reflective surface finishes would be advantageous for delivery aircraft in so far as minimization of thermal effects is concerned.

It is noted that of two different types of white paint tested, one charred after an input of about 25 calories, thereafter becoming a good absorber for remaining thermal radiation, whereas the other, a silicone base heat-resistant paint, remained white at higher temperatures and thus afforded much greater protection at higher thermal inputs.

It is evident that in any study of effects on structures where both thermal and blast effects are appreciable, the modification to the structure resulting from the thermal inputs may influence the effects resulting from the blast inputs. From the ground experiments of Project 8.1, sufficient data were obtained to make possible a reasonably complete study of the blast and thermal coupling effects and of thermoelastic effects on certain types of aircraft structures.

Considerable data were collected concerning thermal effects on various structural components including box beams; tension ties; bonded metal waffle, hat, and honeycomb specimens; B-36 stabilizer assemblies; T-28 stabilizer assemblies; fabric control surface covering; and aircraft undercarriage components. Some noteworthy findings were that bonded metal waffle panels are less vulnerable to permanent skin buckling than bonded metal hat panels for temperatures less than 350°F, that the threshold of permanent skin buckling for bonded metal fixed edge hat panels is as little as about 50°F of temperature rise, and that the failure of the adhesive bond of bonded metal honeycomb core panels occurs at temperatures as low as 300°F. It was found that foil covered fabric can withstand thermal inputs twice that of white painted fabrics before critical damage is encountered.

An interesting, though unexplained, phenomenon was observed from the Project 5.1 flight tests. Metallographic examination of skin specimens indicated microscopically localized areas of high temperatures far in excess of measured or predicted temperatures. Due to the localized character of the thermal damage, it is not considered significant in affecting structural strength. Similar damage did not occur in equivalent specimens exposed on the ground.

The ground and air thermal data verify theoretical procedures for prediction of aerodynamic cooling of heated surfaces as presented in reference 14 of the Project 5.1 report. However, exact thermal properties of the surface concerned must be known in order to obtain quantitative correlation.

Thermal and overpressure damage to parked aircraft was considerably reduced by the use of cloth thermal shields. Strong tie downs also were effective in reducing total damage to fighter aircraft parked nose toward the blast for overpressure levels below that where disintegration of the aircraft takes place. Damage to parked aircraft in the precursor region is considerably higher for a given overpressure level than it is in the region where a clean shock is formed. Unprotected modern aircraft probably would not survive in the precursor region at overpressures above 10 psi.

Some conclusions concerning thermal instrumentation are of interest. Thermal measurements by means of temperature sensitive papers adhered to surfaces generally gave poor accuracy and frequent failures. Thermocouple measurements were reliable. The lack of a high temperature strain gage limited the value of the test. Glass panels gave excellent performance as blast shields for test specimens.

6.3 BLAST EFFECTS

Study of the blast input and loading data leads to a generalized conclusion that center of gravity acceleration and structural stress can now be empirically predicted for the types of

aircraft tested with reasonable accuracy, but further modification of loading theory will be required to produce satisfactory correlation of theory with experiment. Time of shock arrival and magnitude of overpressure can be predicted with acceptable accuracy for a given yield and aircraft position. However, acceleration prediction based on sharp edged gust analysis appears to provide agreement with a sustained acceleration which develops after about 10 msec. Peak structure stresses occur time wise with short duration peak acceleration at about 5 msec for smaller aircraft components (AD wings, B-50 tail) and with the sustained acceleration after 10 msec for larger components (B-50 and B-36 wings and fuselage).

Certain specific conclusions were reached concerning the aircraft tested. AD type aircraft are not adversely affected by overpressures up to 2 psi in conjunction with thermal exposure up to 25 cal/cm². The critical structure in the B-50 type aircraft is the horizontal stabilizer which limits the aircraft to gust loads not greater than those induced in a change in angle of relative wind of 6.2 deg at airspeeds of 190 to 200 mph. The most critical component for B-36 aircraft for tail-on gust loading is either the horizontal tail or after fuselage.

It was noted that accelerations of the nose and tail of aircraft are significantly different from center of gravity acceleration; thus acceleration from a shock loading as read by a pilot at the nose of the aircraft is generally not of structural significance.

An important consideration for large delivery aircraft was noted in the B-36 when wing stresses for a second shock wave exceeded those of the first shock. This was a result of the reflected shock arriving at the aircraft in resonance with the vibrations produced by the first shock. The possibility of such an occurrence should be considered in the analysis of delivery problems.

6.4 CONCLUSIONS

The data collected in these tests will afford satisfactory confirmation or correction of analytical prediction methods for aircraft types similar to those flight tested (B-36, B-50, AD) and will indicate desirable modifications to existing aircraft for improvement of atomic delivery capabilities. The data will be of continuing significance in application to generalized analytical prediction methods and in the establishment of design criteria for future military aircraft.

CHAPTER 7

THERMAL EFFECTS

7.1 GENERAL

The two most important effects of thermal radiation on ground targets are injury (burns) to personnel and the initiation of fires in the target area. Since many important thermal effects are noticed beyond the range of severe blast or nuclear effects, the study of thermal effects has played an important part in past military tests with nuclear weapons. Several modest thermal projects are currently under way at government laboratories. The program of thermal effects at UPSHOT-KNOTHOLE was conceived primarily to satisfy requirements for field checks of laboratory test results.

7.2 FIRE EFFECTS

The problem of predicting the capability of nuclear weapons to set fires within urban areas is complex. The several important factors involved in analyzing a target for fire include prediction of (1) the incidence of kindling fuel ignitions, (2) the probability that such ignitions will initiate fire in more massive combustibles (i.e., buildings), (3) the probability that going fires will merge into a conflagration, and (4) the effects of meteorological conditions on each of the foregoing. Two groups from the Forest Service conducted field checks of kindling fuel ignition energies with a number of different fuels, the results of which established the validity of a larger quantity of laboratory data on ignition energies. Many fuels commonly encountered in urban areas, such as newspaper, dried grass, and tufted cotton, were shown to sustain ignition through the shock wave at thermal energies as small as 2.5 to 4 cal/cm². Although the ignition energies will be greater for higher yield weapons, nevertheless the ranges for such ignitions are quite significant. Based upon the UPSHOT-KNOTHOLE results and upon past work and future planned studies, the development of methods for predicting the incidence of kindling fuel ignitions in urban target areas appears to be possible without further field test work in Nevada. Some limited checks of ignition energies for kindling fuels may be required for large yield detonations. Since kindling fuel ignitions, once established in a target area, may be simulated without employing a nuclear detonation, studies of fire build-up to conflagration size are more economically conducted in the laboratory or at non-nuclear field tests.

7.3 THERMAL BURNS BENEATH FABRICS

Two groups conducted projects for the study of the protection afforded against thermal burns by fabrics. The most significant development which came out of these field studies was to focus attention on a number of parameters to be considered in the design of military uniforms. With the availability now in several laboratories of equipment for duplicating the shape

of the radiant pulse from the bomb, studies with fabrics may be pursued for some time before further field tests become necessary.

7.3.1 Clothed Pigs

In the field tests involving pigs clothed with a limited number of uniform combinations, the results indicated that a four-layer temperate uniform offered protection up to 83 cal/cm². Fire resistant treatment of the outer layers of uniform assemblies was shown to offer superior protection, especially at lower radiant energy levels. Based upon the field and laboratory test results, it is concluded that attention should be devoted to studies of spacing and fit of uniforms, the mechanisms of heat transfer through fabrics to the underlying skin, and to the effects of the shock wave in extinguishing glow or in removing glowing outer layers.

7.3.2 Fabric Damage and Mechanisms of Heat Transfer Through Fabrics

A large variety of fabrics, backed with wood with paper thermometers attached, was studied. Although the ranking of fabric protection was found to be the same as that with the assemblies tested with the pigs, the use of backings other than skin or a proven skin simulant to rank fabrics is thought not to yield valid results. With this cautionary note in mind concerning the experimental technique, combinations of service and developmental uniforms, shoes, body armors, footwear, gas warfare items, ponchos, and aluminized fabrics were ranked as to protection afforded against thermal burns. In addition, factors of reflectance, spacing (fit), flaming, and area of exposed sample were studied. Considering the instrumentation used (paper thermometers on wood backing) for the studies, a firm conclusion can be made only for the area of exposure effect. In this case it is concluded that the area of exposure required for assuring absence of side effects is of the order of 1 to 2 in. in diameter, being closer to the latter for fabrics spaced from skin or for multiple-layer combinations.

7.3.3 Skin Simulant

A requirement for a skin simulant for use in evaluating thermal protective qualities of fabrics has existed for some two years. With the development of a suitable simulant, it was envisioned that a purely physical test technique could replace the less economical technique requiring use of animals for evaluation of uniforms.

At the time of UPSHOT-KNOTHOLE, it was thought that a polyethylene block impregnated with graphite at the surface of which was imbedded a thermocouple showed considerable promise. Traces of temperature vs time of the irradiated block were to be matched against standard laboratory traces calibrated against pigs. Although in the beginning it was recognized that the thermal constants of polyethylene did not match very closely those of skin, it was felt that the deficiencies were not significant. However, further recent laboratory calibrations of polyethylene against pig experiments have shown the departures of the thermal constants for the simulant to be significant. Consequently, further developmental work in skin simulants is being conducted by NML, one of which simulants shows considerable promise.

The time-temperature histories with fabrics over polyethylene were only in fair agreement with those obtained in the laboratory. It is concluded that the area of exposure should be greater for fabrics spaced from the backing and for multiple-layer combinations.

7.4 PROTECTIVE SMOKE

There is interest in providing a means for protection of troops in the open against thermal burns. After considering several possibilities a radiation-scattering white oil-fog smoke was selected as offering the greatest promise for the purpose. The test of smoke at UPSHOT-KNOTHOLE was designed both to demonstrate the capability of smoke and also to provide confirmatory data for extension to the field of theoretical and laboratory studies and of field tests with simulated sources. Due to unfavorable surface winds immediately prior to Shot 9, the

smoke experiment was canceled. In place of the experiment planned for Shot 9, a drastically curtailed smoke test was incorporated into Shot 10. Based upon results from a single instrumented station, it was estimated that the smoke screen, as established, attenuated the thermal radiation by 85 to 90 per cent over that observed in the open. A test of white smoke similar to that planned for Shot 9 is planned for TEAPOT.

CHAPTER 8

BIOMEDICAL EFFECTS

8.1 ATOMIC CLOUD HAZARDS

Data were obtained to define and evaluate the hazards one might encounter in flying through the cloud resulting from an atomic detonation. Dose rates of from 10.6 to 2.1 r/sec were encountered in the clouds 2.7 to 5.2 min after detonation. Applied to a practical situation the data show that personnel in a pressurized aircraft, flying at 400 knots or more, which passes through the cloud of an atomic bomb of 30 KT yield or less and at times greater than 4 min after detonation, will receive an integrated external radiation dose of less than 50 r. A radiation dose of this magnitude is thought to be an acceptable hazard in time of war inasmuch as it will not produce any immediate marked adverse physiological effect on the crew, and it is debatable if any effects of such a dose could be detected in man. However, this dose is in the marginal region above which some physiological effects are to be expected. Combining data from the UPSHOT-KNOTHOLE experiments with those from GREENHOUSE, an empirical expression for average dose rate as a function of time of passage through the cloud has been deduced. For the time interval of 2.7 to 25 min after detonation, the data may be represented by $D = 1.31 \times 10^5 \times t^{-2.00}$, where D is the average dose rate in roentgens per hour and t is minutes after detonation. Although D appears to be independent of yield, there is a factor of 2 in the scatter of data on each side of this empirical expression.

The internal radiation dose resulting from inhalation of fission products by the crew during aircraft passage through an atomic cloud is insignificant both in absolute magnitude and when compared with the external radiation dose. This fact appears to be established so well that further field tests on this aspect of the hazard in the cloud would seem to be entirely unnecessary from the point of view of military requirements. Since the internal hazard is insignificant there appears to be no reason for expenditures of money and time in the design and development of filters or other equipment for protection against an essentially nonexistent hazard.

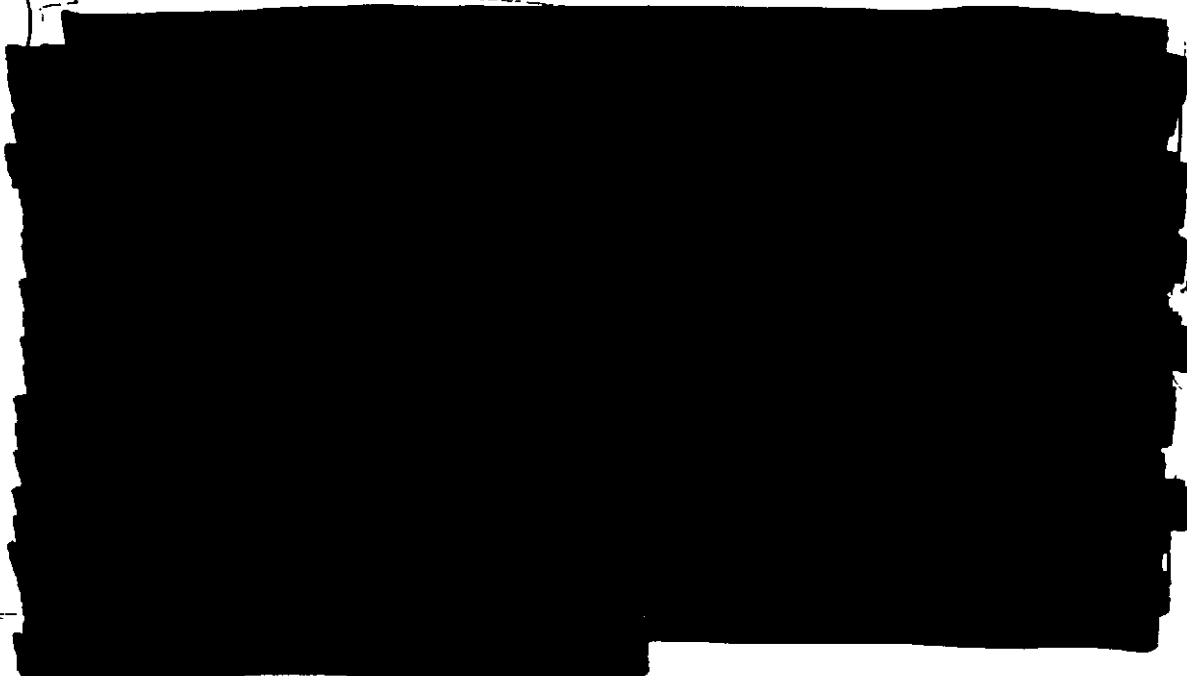
At times longer than 4 min after detonation, the temperature and turbulence in the cloud from a 30 KT bomb do not appear to be sufficiently high to be an appreciable hazard to either the crew or the aircraft. Since it takes about 4 min for the cloud of a 30 KT weapon to reach 30,000 ft when detonation occurs at or near sea level, any aircraft flying above 30,000 ft would not intercept the cloud of a 30 KT weapon until after these hazards had diminished to tolerable levels.

8.2 BETA HAZARD

Prior to the UPSHOT-KNOTHOLE experience the possibility of a beta skin hazard in areas contaminated by fallout remained unresolved. Inability to perfect feasible beta dosimetric equipment for use in the field, because of various theoretical and design considerations, forced

radiological safety control policies to depend solely on gamma dose measurements in contaminated fields. The possibility that the beta hazard was at a nearly critical level under the criteria set for gamma dose hazard control remained untested. The UPSHOT-KNOTHOLE experiment demonstrated quite conclusively that in desert areas contaminated by fallout beta and soft gamma rays present no unacceptable skin hazard to the normally clothed man in the field unless there is an excessive gamma hazard. Thus it was concluded that present dosimetric techniques are adequate from the point of view of radiological safety. This conclusion is valid for distances of 1 cm or more above the contaminated ground. If a man lies on the contaminated ground, it may be that some small areas of the skin would receive high radiation doses from small highly contaminated spots. Since no measurement of distribution of the contamination on the ground was made, it remains to be established whether the above type of exposure presents an unusual hazard. In addition the results do not pertain to the case of direct skin contact with contaminated objects removed from the contaminated field, nor to the possible beta hazard to the skin which might prevail if an individual were in the fallout area at the time of fallout and whose skin and clothing were contaminated by the fallout material. The possibility also remains that fallout over certain types of clean hard surfaces, such as ship decks and clean streets or sidewalks, might demonstrate a greater beta and soft gamma hazard relative to measured gamma hazard than found in the desert, because the mixing of the discrete radioactive fallout particles with the loose desert soil was felt to play an important role in reducing the beta to gamma dose ratios to the levels found in UPSHOT-KNOTHOLE.

8.3 NEUTRON EFFECTS

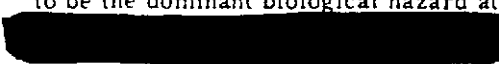


b(3)
DOE

DNA
(3)(3)

(3)
DOE

The biological data from foxhole experiments with mice suggested that at the bottom of standard 42-in. foxholes the attenuation of neutron biological effect was three times the surface dose, but further correction for the effect of the protective lead hemispheres used suggested that the attenuation probably was significantly greater than 3. This compares with a foxhole attenuation factor of 8 to 20 previously measured for gammas at foxhole bottoms and is consonant with physical theory, which predicts that neutrons in air should have a greater ability to scatter than should significantly hard gammas. Hence in foxholes neutron radiation appears to be the dominant biological hazard at all distances of biological interest



DNA
(3)(3)



138

8.4 PRIMARY BLAST INJURY

Results of studies on primary blast injury were inconclusive. Unfortunately, zero-point errors and technical shortcomings of experimental equipment prevented successful bracketing of graded responses to blast injury by the animal species exposed. Furthermore, few conclusions could be drawn from the experiment about the mechanisms of primary blast injury. It was suggested by the presence of typical lung injury in rats exposed to nearly idealized shock waves of Shot 9 and the absence of any blast injury in both rats and dogs exposed to even higher peak overpressures in the region of slow rise times and precursor phenomenology on Shot 10 that abrupt static pressure rise time may be an important criterion of direct blast injury. It was unfortunate that the theoretical possibility of the formation of significant reflected pressure spikes of high intensity and a few milliseconds duration within the animal exposure cylinders on Shot 9 could not be verified or denied because of the low time resolution of the blast gages exposed with animals within the cylinders. Thus the possibility that the exposed animals experienced higher overpressures on Shot 9 than on Shot 10 remains, preventing full confidence in even the tentative conclusion previously drawn about rise-time significance.

The inability to protect animals, exposed in the regions where primary blast injury might be expected, from vastly supralethal radiation doses, even in the face of experimentally designed shielding, suggests that in terms of the effects radii of other damaging nuclear phenomena primary blast injury may not be of important military consequence.

8.5 FLASH BLINDNESS

Men looked at the initial flash of an atomic bomb with the dark-adapted eye for the period of the blink reflex through red filters which screened out most of the visible and infrared radiation except that between 600 and 900 m μ . A total of 55 exposures was made on five shots at distances ranging from 7 to 14 miles. In all instances except one the men received no retinal burns from these exposures, and the vision recovery time for reading red-lighted aircraft instruments after the exposures averaged about 20 sec. This vision recovery time is about 30 per cent less than that which would have been required had exposure been made without filters. Thus the filters offer considerable protection against retinal burns under the conditions of these experiments and reduced appreciably the time required to read aircraft instruments under standard conditions of illumination at night. This type of filter is considered useful for wear as protection for the vision of aircraft crew members in those situations where it may be anticipated that an atomic flash might be viewed at night at distances of a few miles.

In dark-adapted rabbits, unprotected by filters, exposed to the flash of an atomic bomb, burns of the retina were obtained at distances from 2 to 42.5 miles. This does not mean that the retina of a man would necessarily be burned by the flash at these distances. However, retinal burns have sometimes occurred in man on unprotected exposure to the flash at 10 miles or less, and retinal burns at greater distances are considered to be entirely possible. If retinal burns occur at greater distances, the burned area would undoubtedly be small in keeping with the small size of the image of the fireball and likely of limited consequence in so far as impairment of vision is concerned, except in the rare instance where the burn might occur on the macula or area of central photopic vision.

One source of reasonably good data on this problem would seem to be the accidental visual exposures to the flash which take place occasionally on nearly every series of atomic-bomb tests. This source of information has so far been incompletely developed, but it is felt to be entirely feasible to establish a procedure for examination and recording of each case of accidental human exposure to the flash so that eventually a reasonable series of cases could be accumulated from which some valuable conclusion might be drawn.

CHAPTER 9

TECHNICAL PHOTOGRAPHY

9.1 BACKGROUND

Technical photography provided one of the most generally useful tools in the Military Effects Test Program. In general, Program 9 provided services to the technical projects in accordance with their stated needs. Two types of photographic services were rendered:

1. Technical documentary photography; including before-and-after still and motion picture shots, recording construction progress, and static test effects.
2. Zero time technical motion picture photography; defined as a film exposed in the vicinity of zero time, using cameras installed in the test area and controlled by the sequence timing signals utilized to initiate the over-all test program.

Motion picture photography for historical and documentary purposes was performed by the Lookout Mountain Laboratory, USAF, and was not a part of the technical program.

9.2 PHOTOGRAPHY PLAN

The technical documentary photography was performed from time to time throughout the duration of the test series, including the construction period, in accordance with the requests of the interested project officers. Over 10,000 ft of motion picture film and 10,000 still negatives were exposed. A total of 85,000 prints from the still negatives was made for the projects. All processing of these films was done at the test site.

Blast and rocket trail technical motion picture photography was performed on Shots 1, 4, 9, 10, and 11. In addition, a variety of motion picture cameras were utilized for photographing the blast and thermal effects on test targets for Shots 9 and 10. These cameras ranged in operating speed from two frames per minute to 2500 frames per second. The majority of the cameras were simple Gun-Sight-Aiming Point (GSAP) units, utilizing a production aircraft gun sight camera operating at a rate of approximately 64 frames per second. Cameras were mounted on special towers, ranging in height from 5 to 17 ft. A detailed photo plan was prepared following consultation with the interested project officers. This plan included a total of 193 motion picture cameras for Shot 9 and 94 motion picture cameras for Shot 10. One hundred camera towers were used on Shot 9 and 50 camera towers were used on Shot 10. The principal footage utilized black and white film, although on some thermal experiments color film was used. The detailed photography plan will be found in the Project 9.1 Report WT-779.

9.3 STABILIZATION

On previous test series the quality of the technical motion picture photography was seriously reduced due to obscuration by dust. Even without the thermal output of an atomic weapon,

the blast wave would pick up sufficient dust from the ground surface to degrade the photography almost immediately upon shock arrival. Intense thermal radiation has been shown to induce a dust layer by a process sometimes described as "popcorning" (see Fig. 2.42). This thermal dust sometimes causes photographic recording difficulty during the thermal phase prior to shock arrival and provides a very good dust source for the blast wave when it does arrive. In the past some inexpensive stabilization using various tar and asphalt compounds has been used in an attempt to minimize the dust problem. Unfortunately, these materials smoked badly upon thermal irradiation and the photographic results were not completely satisfactory.

Prior to this test series, various stabilizing techniques were tested on a laboratory scale to find a suitable material to reduce the thermal popcorning and at the same time to stabilize the test area. For this test series a low-grade sand cement 2 in. thick was adopted. At each camera location the Frenchman Flat lake bed was stabilized with this soil-cement mixture for distances to the front and rear corresponding to the estimated positive and negative phase particle transport behind the shock front. The stabilization was designed to minimize the thermal dust and to reduce the blast wave dust during the important part of the blast wave transmission past each camera and tower.

9.4 RESULTS

Almost without exception the motion picture cameras operated successfully. Very little difficulty was experienced due to radiation fogging, and in general the difficult problem of exposure was satisfactorily solved. Satisfactory films were obtained except in the strong precursor region of Shot 10, where the camera towers were demolished upon shock arrival. These same camera towers successfully survived equivalent pressures from the more conventional blast wave of Shot 9. Examination of the technical motion picture films indicated satisfactory performance.

The stabilized surfaces were reasonably successful.

Many successful photographic records were obtained throughout the thermal and blast phases where similar efforts had been unsuccessful in the past. Some excellent blast wave photography was also obtained, particularly on Shot 11. On this shot the films show the precursor effect and have been judged to be by far the most satisfactory photographic records of this phenomenon obtained to date.

CHAPTER 10

TESTS OF SERVICE EQUIPMENT AND TECHNIQUES.

10.1 RADIAC EQUIPMENT TESTS

A considerable effort was expended during UPSHOT-KNOTHOLE on the field testing of radiac equipment; this included rate meters, both airborne and ground monitoring, and dosimeters of both administrative and tactical design.

For the past two years development in the field of radiac survey meters has been concentrated on design of light-weight units with a range of 0 to 500 r. Two developmental models, the AN PDR-32 and the IM-71 PD, designed to meet service size, weight, and range requirements, were field tested during UPSHOT-KNOTHOLE. Stringent field tests revealed certain mechanical engineering design defects on both instruments such as poorly designed belt clips and control knobs and cases insufficiently rugged to withstand hard field usage. Defects of this type can be easily rectified with good preproduction engineering. In addition, certain operational problems existed with each instrument which appear to be inherent in the basic design. For example, the AN PDR-32 gave unreliable readings at rates above 300 r/hr due to sporadic effects, and the IM-71 was unreliable due to annoying calibration drift and the difficulty of re-setting it in a high radiation field. The project recommendations should be effected prior to the approval of either equipment for service use.

Of the numerous dosimeters evaluated during UPSHOT-KNOTHOLE, it was determined that two tactical dosimeters, the DT-65 Polaroid film and the type E-1 chemical tactical dosimeter, met service requirements within their design limitations. No further development on these two types is warranted with the exception of minor mechanical changes and possible continued improvement of shelf life. Also, the E-1 will have to have modification of the step values to meet military characteristics as well as a redesigning of the case for better closure and dust proofing. The DT-60 administrative dosimeter, previously tested at BUSTER, proved reliable. However, the Admiral electronic reader designed to read the DT-60 dosimeters proved unreliable and will require additional design and development work. The IM-91, a direct reading 0 to 500 r tactical type quartz fiber dosimeter, was found to be suitable except for a slight rate dependence and air sealing problem. If these two problems can be corrected in accordance with project recommendations, it will readily meet service requirements for a tactical dosimeter.

It was determined that standard radiation rate meters, carried in light aircraft, can be utilized in making rapid aerial surveys of contaminated ground areas. Extrapolation of air readings to the ground introduces many errors and necessitates numerous assumptions. However, approximate but possibly tactically acceptable plots can be accomplished quickly and simply. Complicated self-recording radiac equipment installed in heavier type aircraft and tested during UPSHOT-KNOTHOLE did not improve the accuracy of aerial surveys enough to warrant consideration as tactical equipment. Simple step measuring devices such as droppable

flares or flashing lights designed to indicate ground radiation intensity levels and patterns appear to be practical for certain tactical situations. However, the devices of this type which were tested during UPSHOT-KNOTHOLE were not reliable and will require considerable development and engineering before being subjected to additional field tests.

10.2 TESTS AND DEVELOPMENT OF OPERATIONAL TECHNIQUES

During UPSHOT-KNOTHOLE the Air Force continued the evaluation of equipment and techniques which would best meet the requirements of their Indirect Bomb Damage Assessment (IBDA) program. Specifically, this requirement is for a system that will give a delivery aircraft an all-weather capability for determining gross errors in yield, Ground Zero, and height of burst. This capability would eliminate the need for postshot reconnaissance.

An interim IBDA system was operationally evaluated by Strategic Air Command (SAC) combat crews in fly-over aircraft. This technique utilized a combination of Q-24 radar, K system radar, K-17C aerial cameras, and bhangmeters. Results indicate that the K-17C camera is suitable under visual conditions (day or night) for providing adequate pictorial records to evaluate height of burst and Ground Zero. The Q-24 and K system radars, when operated at the critical setting adjustments established in SAC operating procedures, are suitable for determining Ground Zero and height of burst under all weather conditions for weapons presently in stockpile provided (1) identifiable radar returns exist in the target area and (2) the height-of-burst yield combination gives fairly severe overpressures on the ground in order to generate a detectable radar return. The gain, tilt, and brilliance settings of the radar are quite critical indicating the need for careful training and indoctrination. The bhangmeter was found to be satisfactory for determination of yield under visual conditions. Its reliability for all-weather determination is not yet known. Studies are in progress utilizing all available IBDA records to determine the feasibility and accuracy of determining yield from radar scope time-sequence records of the rate of growth of the shock wave and/or fireball diameter.

In the IBDA equipment development phase, Wright Air Development Center (WADC) utilized both new and modified radar equipment in an attempt to obtain more detailed radar scope pictures of the fireball and cloud shadow phenomena. The ultimate aim is to utilize a simple bombing radar system to meet the IBDA requirement. Developmental models of fast and slow scan Ku-band radar, the APS-48 and APS-43, designed to meet this requirement, were operated in fly-over aircraft. The APS-48 gave the advantage over the APS-43 of better time resolution of fireball and cloud shadow phenomena, but detail was lost due to power and antenna limitations. In addition, a study of the application of airborne moving target indicator equipment was conducted in a fly-over aircraft, but high interference levels prevented obtaining useful results. An attempt was made to record the time difference between the reception of the direct and ground reflected low frequency electromagnetic wave generated by a nuclear detonation, thereby permitting calculation of height of burst from this recorded time interval. The electromagnetic signals were much more complicated than anticipated; as a result it was very difficult to distinguish between direct and reflected signals and resulted in height-of-burst errors too gross to be of any significant value to the height-of-burst determination problem. As a result of the refraction experiments conducted at the NPG, it was concluded that the refraction of the radar beam, which was in close proximity to the fireball cloud, was too small to be measured in the presence of other large-scale effects. Based on these results it can be said that refraction is negligible and can be ignored in IBDA data reduction procedures. Fireball return phenomena, as recorded by the Navy developmental fast scan X-band radar, did not reveal any particular advantage to their type of equipment other than the advantage of recording more scans per unit time than had previously been possible. Missile tracking of the 280-mm projectile was not successful with this radar due to high ground clutter.

The Army Field Forces' capability for short range determination of position of burst and yield was investigated utilizing standard sound ranging equipment, a modified flash ranging system, seismic measurements, and a bhangmeter. Flash ranging proved fairly accurate for burst positioning under line of sight conditions. Sound ranging appears to be satisfactory for

location of Ground Zero for non-line of sight up to distances of 60,000 meters. Seismic techniques for determining height of burst by recording blast induced and thermal induced seismic waves were inconclusive. The bhangmeter yields were accurate to 20 per cent out to distances of 40 miles.

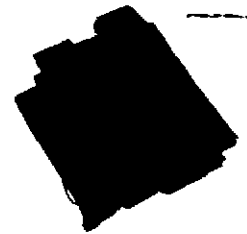
A continuation of the studies of electromagnetic radiation associated with nuclear detonations was conducted by Signal Corps Engineering Laboratories (SEL) as a research experiment to identify and correlate these signals with type and yield of detonations. In the region of 0 to 20 mc, data on polarization, amplitude, and time duration were recorded. The results obtained show a variety of pulse shapes with little indication of characteristic shape. Rough measurements indicated no possibility of correlation in the frequency domain recorded; therefore detailed frequency analysis was not carried out. The results fail to shed any light on the nature of the basic phenomenon.

CHAPTER 11

LONG-RANGE DETECTION

The general objective of Program 7 experiments in this test series was the improvement of present techniques and development of new techniques for the gathering of intelligence concerning foreign atomic-energy events. The experiments were generally designed to accomplish this objective at locations remote from the event; however, measurements for calibration purposes were made within and close to the NPG. Thus the experimental program consisted of both special test efforts and the use of existing atomic-energy detection system equipment and procedures.

STET



APPENDIX A

SHOT PARTICIPATION

Project	Shot											Project	Shot	
	1	2	3	4	5	6	7	8	9	10	11			9
1.1a								x	x	x		3.1	x	x
1.1b			x	x					x	x	x	3.3	x	x
1.1c	x						x					3.4	x	x
1.1d									x	x		3.5	x	
1.2	x			x					x	x	x	3.6		x
1.3				x					x			3.7	x	x
1.4a	x								x	x		3.8	x	x
1.4b									x	x		3.9	x	x
2.1				x					x			3.11	x	
2.2a		x	x	x	x		x	x	x	x	x	3.12	x	
2.2b					x		x		x	x		3.13	x	x
2.3								x	x	x		3.14	x	x
3.30							x	x	x	x	x	3.15	x	x
4.1				x					x			3.16	x	x
4.2								x	x	x		3.18		x
4.5	x	x			x		x	x			x	3.19	x	x
4.7		x						x	x	x	x	3.20	x	x
4.8										x		3.21	x	x
5.1	x	x					x	x	x			3.22	x	x
5.2				x					x			3.24	x	x
5.3									x			3.26.1	x	x
6.2	x	x	x	x	x	x	x	x	x	x	x	3.26.2	x	x
6.3	x	x		x	x		x	x	x	x	x	3.26.3	x	x
6.4							x		x			3.27	x	
6.7	x	x	x	x	x	x	x		x	x	x	3.28.1	x	x
6.8	x	x	x	x	x	x	x	x	x	x		3.28.2	x	x
6.9	x	x	x		x		x					3.28.3	x	x
6.10	x	x	x		x		x	x	x	x		3.29	x	
6.11				x					x					
6.12	x	x	x	x	x	x	x	x	x	x	x			
6.13							x	x	x	x				
Prog. 7	x	x	x	x	x	x	x	x	x	x	x			
8.1	x	x	x	x	x	x	x	x	x	x				
8.2	x	x	x	x	x	x	x	x	x	x				
8.4									x	x				
8.5		x							x	x				
8.6									x	x				
8.9									x	x	x			
8.10			x	x					x	x	x			
8.11a									x	x				
8.11b				x					x	x				
8.12a							x		x	x				
8.12b									x	x				
8.13									x					
9.1	x	x	x	x	x	x	x	x	x	x	x			
9.6									x	x				
9.7									x	x				

~~RESTRICTED~~

146

APPENDIX B

PROJECT SUMMARIES

B.1 PROGRAM 1—BLAST AND SHOCK MEASUREMENTS

Program Director: W. L. Carlson, CDR, USN

The broad objectives set down for Program 1 were (1) to obtain data for other effects programs defining the blast phenomena resulting from Shots 9 and 10 and (2) to add additional knowledge to blast phenomenology, particularly in the region of the precursor. To accomplish the broad objectives, agencies of Program 1 participated in a total of seven shots, placing instruments on the ground surface, near the ground surface, in free air, and underground.

Instruments to measure the various blast parameters on Shots 9 and 10 were placed as indicated in Fig. B.1. Less comprehensive instrumentation lines, Fig. B.2, were installed for Shots 1, 3, 4, 7, and 11. In addition to the instrumentation placements shown in Figs. B.1 and B.2, photography was used as blast instrumentation (both with and without the use of rocket trails), and parachute borne pressure-time gages were deployed in free air.

Specific objectives for each project and the results obtained are outlined in the project summaries.

B.1.1 Projects 1.1a and 1.2: Air Blast Measurements

Agency: Naval Ordnance Laboratory
Report Title: Air Blast Measurements, WT-710
Project Officer: W. E. Morris

The Naval Ordnance Laboratory (NOL) participated in UPSHOT-KNOTHOLE (U-K) with the objective of studying shock wave behavior in free air and along the ground under varied test conditions. The basis for this study was provided by a measurements program conducted by the NOL wherein the smoke rocket photography technique was used to obtain peak shock overpressures as a function of distance in free air; the Wiancko gage FM tape-recorder instrumentation system, along with a newly developed mechanical gage, was used for obtaining pressure-time (p-t) histories on three blast lines along the ground; peak pressures along the ground were measured by modified indenter gages; and direct shock photography was used extensively for the first time to observe shock and dust contours along the ground.

A new pressure-distance curve for free air has been obtained, based on the composite results of TUMBLER Shots 1, 2, 3, and 4, IVY Shot King, and UPSHOT-KNOTHOLE Shots 4, 9, 10, and 11. This new curve, in terms of 1 KT (RC) at sea level, now is considered to be the standard pressure-distance curve down to the 10 psi pressure level for air-dropped weapons ranging from 1 to 500 KT. A TNT efficiency of 45 per cent is assigned to the average of all of these shots. The reason for the departure of the free-air pressure-distance data for the tower shot GREENHOUSE Easy from the previous and new composite curves still is unexplained in

terms of tower effect. U-K Shot 1, which was also a tower shot, departed only insignificantly from the composite curve. On the basis of the results obtained on the high altitude (6022 ft) shot of U-K 4, Sachs' scaling laws for pressure and distance are considered to be valid up to a height of burst of at least 10,000 ft above sea level.

The effects of a thermal layer near the ground are readily apparent in the p-t measurements along the blast line and in the records of the direct shock photography project. On U-K Shot 9, although no precursor was formed, the thermal intensity along the ground was sufficient to produce a noticeable distortion of the wave form, resulting in lower peak pressures at the ground than in the cooler air 10 ft above the ground. The shock photography gave evidences of the formation of a thermal Mach shock in this thermally excited region. (This thermal Mach forms well before the appearance of the true Mach shock.) The U-K Shot 9 blast parameters along the ground scale with those of TUMBLER Shot 1.

On U-K Shot 10, where considerably greater thermal energy was incident on the blast line than on Shot 9, a well-developed precursor wave was formed which radically changed the p-t history in this region. In general, in this precursor region, the pressures were lower, the positive durations were longer, and the impulses were larger than in the ideal nonthermal, nonprecursor region at corresponding distances. On Shot 10, this ideal area was, for the most part, obtained along the smoke line which had a dense black smoke overlay extending several hundred feet into the air. The smoke effectively served as a thermal shield to the ground below, thus minimizing and eliminating thermal effects along the ground.

The theory of precursor formation was reviewed and related to the results obtained, and a theory of thermal Mach formation was proposed by project personnel.

B.1.2 Project 1.1a-1: Evaluation of Wiancko and Vibrotron Gages and Development of New Circuitry for Atomic Blast Measurements

Agency: Naval Ordnance Laboratory

Report Title: Evaluation of Wiancko and Vibrotron Gages and Development of New Circuitry for Atomic Blast Measurements, WT-784

Project Officer: W. E. Morris

A program to test experimental instrumentation was undertaken by the NOL in an endeavor to improve existing blast phenomena measuring equipment and techniques. Four experimental designs were tested: (1) a field unit oscillator-amplifier using transistor circuit elements, (2) a subminiature two-wire field unit, (3) a commercially developed Vibrotron gage and amplifier unit, and (4) a frequency deviation multiplier circuit for obtaining increased signal-to-noise ratios. The operation also provided the opportunity to evaluate more fully the performance of the Wiancko gage.

It was found that transistor circuitry is little, if at all, affected by atomic blast phenomena and holds much promise for further development. The subminiature two-wire system was successful and offers many advantages in economy and adaptability in field use over the present NOL system. The deviation multiplier scheme was completely successful; however, its complexity must be weighed against the freedom from noise required on any particular operation. The Vibrotron gage and oscillator was unstable, not rugged, and in general gave poor results; it requires a good deal of redesign and development before it can be used in atomic effects measuring programs. The NOL modified Wiancko pressure gage proved acceptable, giving results superior to those obtained on previous operations with other inductance type gages. In certain applications the acceleration sensitivity of the gage is excessive and confuses the pressure-time record; also, the damping characteristics of the gage could be improved.

B.1.3 Project 1.1a-2: Development of Mechanical Pressure-Time and Peak Pressure Recorders for Atomic Blast Measurement

Agency: Naval Ordnance Laboratory

Report Title: Development of Mechanical Pressure-Time and Peak Pressure Recorders for Atomic Blast Measurement, WT-785

Project Officer: W. E. Morris

This project evaluated two different mechanical air-blast gages. The first portion concerned the modification, field use, and evaluation of an indenter gage for the measurement of peak pressure. This gage is fully damped and has a response time of from 3 to 5 msec in the pressure range from 1 to 250 psi. The response time can be adjusted as desired. The indenter gage gives true peak pressure for square step and slow rise time shock waves. The gage will not register the maximum pressure of spike type shock waves which have a duration less than the response time of the gage. Under appropriate shock conditions reliable pressure values accurate to within ± 5 per cent were obtained under field conditions when acceleration effects were eliminated by proper mounting.


The second gage designed and evaluated under field conditions was a new self-contained pressure-time recorder. The sensing element is a siphon bellows, and the shock pressure is recorded on a smoked glass plate attached to a sliding table. A one hundred cycle timing signal, regulated by a stop watch, is recorded. Six gages were constructed having response times of 2 and 5 msec and pressure ranges of 25 to 60 psi. When acceleration effects had been eliminated by firmly mounting the gage, good records were obtained which were accurate to ± 0.25 psi.

B.1.4 Project 1.1b: Basic Air Blast Measurements
Agency: Stanford Research Institute
Report Title: Air Pressure and Ground Shock Measurements, WT-711
Project Officer: L. M. Swift

The specific objectives of Project 1.1b included the determination of pressure vs time variations with ground range, at and near the ground surface, for five nuclear shots detonated at very high, intermediate, and relatively low heights of burst, as well as a limited study of the near-surface underground accelerations produced by air-burst explosions. Using these data, the project evaluated present air blast scaling laws, Mach reflection (path of the triple point), precursor characteristics, the empirical height-of-burst chart, and earth accelerations. Some experiments on instrumentation were conducted in conjunction with the project.

Instrumentation performance was highly satisfactory except on Shot 10, during which cables were broken when several towers blew down.

In terms of fulfillment of the objectives of the tests, the following statements may be made. For convenience, the statements are rather positive; the qualifications and assumptions which accompany them are detailed in the project report.

1. On the basis of the comparisons of A-scaled maximum pressures, phase durations, and impulses, the total air blast phenomena of U-K Shot 9 and TUMBLER Shot 1 scale very well. The yield ratio for these two shots was about 26:1 and both were detonated over the same surface  U S A
(b) (3)

2. Shot 9 data indicate that the theoretical analysis of the Mach triple point trajectory near the ground surface is not applicable for this intermediate height of burst. Thermal effects are such that Mach reflection appears to begin at very-short ground ranges and the rise of the triple point shows two plateaus below the 10 ft level.

3. The precursor pressure waves observed on Shots 10 and 11 indicate that precursor effects are increased when the A-scaled burst height is decreased from 300 to 200 ft. Previous observations of the depression of maximum measured surface air pressures in the precursor region were confirmed.

4. Precursor wave front orientations obtained from arrival-time data seem to confirm the heated-layer theory of precursor formation.

5. Additional data for a composite height-of-burst chart were obtained for a number of scaled burst heights. Correspondence with previous data is good in the low pressure region, but not so good in the 10 to 50 psi region.

6. A single measurement of dynamic pressure on Shot 11 indicates that in a region of thermal disturbance the Pitot-tube q-gage measures a peak dynamic pressure which is significantly higher than the value one would compute using the measured side-on pressure and the classical Rankine-Hugoniot relations.

7. The earth acceleration data confirm results obtained on TUMBLER and yield some information on the effect of gage depth upon observations.

B.1.5 Project 1.1c-1: Air Shock Pressure-Time Vs Distance for a Tower Shot

Agency: Sandia Corporation
Report Title: Air Shock Pressure-Time Vs Distance for a Tower Shot, WT-712
Project Officer: J. Harding

Overpressure measurements on UPSHOT-KNOTHOLE Shot 1 (16.2 KT, 300-ft tower) were made along a blast line extending between 700 and 7800 ft from Ground Zero; 16 ground-baffle gages and 12 air-baffle gages 10 ft above ground were used. Full pressure-time histories were recorded for all save the six closest air-baffle stations, which were destroyed by the blast. Wave form anomalies were contrasted with those found on BUSTER Shot Charlie and TUMBLER Shot 4; attenuation rates of double peaks were opposite those usually manifested by precursor wave forms, a behavior that is attributed to the difference in shock interaction with a strong temperature gradient (Shot 1) and a bounded high-temperature layer (usual precursor).

A detailed comparison of overpressure-distance curves reveals that on Shot 1 measured overpressures greater than 10 psi are but half those measured at equal scaled distances on GREENHOUSE Shots Dog and Easy. Dog and Easy data reflect similar wave form anomalies, the second peaks being attenuated at an almost identical rate. Interferometer gage records from Dog shot, scaled to Shot 1, emphasize the similarity. To augment comparison with GREENHOUSE results, thermal energies delivered to the various gage stations prior to blast wave arrival were computed. Calculations indicated considerably higher thermal fluxes for Shot 1 than for either of Shots Dog or Easy. Since the popcorn threshold for Nevada sand is only half that for coral sand, the more extreme blast-thermal interaction seen on Shot 1 is not surprising. Even under these extreme circumstances, positive- and negative-phase impulses seem to remain the same since the scaled impulse-distance curves are reasonably equivalent.

A second experiment was performed to check the expected asymmetry of blast effects on UPSHOT-KNOTHOLE Shot 7; three agencies—the Ballistic Research Laboratories, Naval Ordnance Laboratory, and Sandia Corporation—participated. The device detonated had a massive shield against one face which caused a large fireball protuberance of lesser temperature. Thermal radiation in this direction was reduced considerably and blast asymmetry was marked. At 1650 ft overpressure on the unshielded side was about 25 psi whereas that on the shielded side (shadowed region) was 50 psi. It seems clear that symmetric mass distribution in the device should be a prerequisite when fundamental blast effects studies are to be made.

B.1.6 Project 1.1c-2: Air Shock Pressures As Affected by Hills and Dales

Agency: Sandia Corporation
Report Title: Air Shock Pressures As Affected by Hills and Dales, WT-713
Project Officer: J. Harding

This project was a continuation of the study of the effect of terrain on the blast wave from atomic bombs. The project report discusses the military significance of these effects: how terrain affects target layout as well as blast wave propagation, how choice of the burst point might be influenced by terrain, and how damage susceptibility of various structural elements will change with changes in shock wave form. Terrain effects are more important for large bombs than for small ones because the larger circle of interest will include more terrain features.

Measurements on UPSHOT-KNOTHOLE Shot 7 consisted of ground-level pressures on a ridge to the west of the shot point, the same ridge that was instrumented on Shot 5 of TUMBLER-SNAPPER. Special attention was paid to measuring pressures farther fore and aft of the ridge than before and increasing the number of gages near the crest. Previous observations were confirmed in that pressures on the foreslope were higher (spiked wave forms) and those on the back slope lower (rounded wave forms) than would have been predicted at the same distances over flat terrain. Enough detail was obtained to show that these effects were caused by a compression wave from the initial upslope of the ridge and a rarefaction wave from the downslope at the crest of the ridge

B.1.7 Project 1.1d: Basic Air Blast Supporting Measurements
Agency: Sandia Corporation
Report Title: Dynamic Pressure Vs Time and Supporting Air Blast Measurements,
WT-714
Project Officer: J. Harding

Project 1.1d measured dynamic pressures in the shock wave and preshock pressures. It also conducted a feasibility study of new and modified gages to measure dynamic pressure, density, temperature, and particle velocity.

Measured dynamic pressures can be compared with those calculated from the measured overpressures using the Rankine-Hugoniot shock relations and regular reflection theory. When no precursor is formed, measured dynamic pressures are in reasonable agreement with those calculated although some effects of thermal mechanical interaction are noted. Dynamic pressures measured in the precursor are much higher than those calculated. Laboratory tests have indicated that the Pitot-static instrument used does respond to dust as well as to air, and the quantity measured by these gages is apparently $(\frac{1}{2} \rho u^2)_{\text{air}} + (\rho u^2)_{\text{dust}}$ when dust is present in the shock wave, as is true in the precursor.

Measurements have shown a few instances of real but small preshock increases in air pressure, all apparently caused by thermal radiation alone.

Results of the gage feasibility study indicate that the q-tube (dynamic pressure) and the centripetal density gage are suitable for use on full-scale nuclear tests. Both the modified sonic wind and sound speed indicator and the whistle temperature gage must be subjected to further modification before they are suitable for field use.

B.1.8 Project 1.3. Free Air Blast Pressure Measurements
Agency: Air Force Cambridge Research Center
Report Title: Free Air Atomic Blast Pressure Measurements, WT-715
Project Officer: Lt Col J. O. Vann, USAF

This project was designed to (1) determine the free air peak overpressure vs distance curve for air-burst atomic bombs at overpressures below those covered by existing data, (2) determine the path of the triple point at high altitudes for at least one shot, and (3) measure the relative strengths of the free air and reflected shocks above the triple point and of the Mach shock below the triple point.

The project participated in Shots 4 and 9 because the points of detonation were of sufficient height above terrain to give a good separation of direct and reflected shocks over a wide range of distances. The operation was accomplished by deploying 14 parachute-borne canisters on Shot 4 and 20 canisters on Shot 9. Two B-29's were used in laying down each array. The preliminary positioning of the canisters was determined so as to meet the objectives stated above, and the positions and times of canister release were adjusted to attain these positions at shock arrival time with allowance for wind drift during time of fall.

Each canister contained an altimeter transducer, two differential pressure transducers, and a radiotelemetry transmitter. The telemetered pressure and altimeter data were recorded at a ground station.

Complete data were received from all canisters in both tests. In Shot 4 all canisters were in the region of regular reflection. In Shot 9, 14 canisters were in the region of regular reflection and six were in the Mach region. In addition to the main direct and reflected shocks, a small secondary shock and its ground reflection were received at nearly all canisters on Shot 9.

The free air values were normalized to 1 KT in a homogeneous sea-level atmosphere and used to extend the TUMBLER composite free air curve down to overpressures of about 0.07 psi. A comparison of this curve with the results of previous tests at low heights of burst was made to determine the effective reflection factor for these earlier shots. The path of the triple point was determined for Shot 9 over the range of altitudes between 6500 and 10,500 ft, and some tentative conclusions were reached on the distribution of peak overpressures in the reflected and Mach shocks in the neighborhood of the triple point.

B.1.9 Project 1.4: Earth Measurements
Agency: Sandia Corporation
Report Title: Free-field Measurements of Earth Stress, Strain, and Ground Motion,
WT-716
Project Officer: J. Harding

Part I— Project 1.4a

Earth cover provides protection to underground structures against the effects of air shock loading. Part of this protection may result from attenuation of stress with thickness of the cover. Measurements of vertical earth stress at three depths and at five ground ranges were made during Shots 9 and 10 to detect and evaluate stress attenuation with depth. Data fit equally well the empirical equations

$$P = P_1 \exp - (d - d_1) 0.07$$

and

$$P = P_1 \left(\frac{d}{d_1} \right)^{-0.34}$$

in which P and P₁ are the stresses in psi at depths d and d₁ in ft, d₁ being the shallower. Precision in each case is better than ±25 per cent.

Part II— Project 1.4b

A practical system for measuring free-field earth stresses and strains resulting from transient loads has been tested with sufficient thoroughness to establish its feasibility. Arrays of directionally sensitive earth stress and strain gages and accelerometers were installed 5 ft deep to record these parameters during Shots 1, 9, and 10. Duplicate instrumentation showed that stress measurements were reproducible with average deviations of 16 per cent and strain measurements with average deviations of 35 per cent. This test disregards the presently unknown factors related to perturbations of the stress field by gages. Stress-strain graphs demonstrate hysteresis. Plastic deformation of the soil resulted in rates of energy dissipation as high as 300 μ ft-lb/ft³. Data from Shot 10 defined the stress tensor in terms of magnitudes and directions of the three principal stresses as a function of time.

B.1.10 Project 1.5: Test Procedures and Instrumentation for Projects 1.1c, 1.1d, 1.4a, and 1.4b
Agency: Sandia Corporation
Report Title: Test Procedures and Instrumentation for Projects 1.1c, 1.1d, 1.4a, and 1.4b, WT-787
Project Officer: J. Harding

Operationally, Sandia Corporation's Blast Instrumentation Program consisted of shelter installations, gage installations, and the associated liaison and logistics for Projects 1.1c, 1.1d, 1.4a, and 1.4b. These projects were concerned with air blast pressures, dynamic pressures, and supporting measurements and with pressures, strains, and accelerations in the earth.

These measurements were made in three different areas at the NPG and covered four shots. A total of 273 electronic information channels were attempted. A tentative score is as follows:

- Shot 1: 65 channels attempted; 49 good, 12 partial, 4 bad.
- Shot 7: 39 channels attempted; 38 good, 1 bad.
- Shot 9: 90 channels attempted; 82 good, 3 partial, 5 bad.
- Shot 10: 79 channels attempted; 57 good, 17 partial, 5 bad.

In almost every instance when only partial information was obtained, the gages failed

because the tower on which they were mounted blew away. In many cases when no information was obtained, experimental gages of unproved design were involved.

B.2 PROGRAM 2—NUCLEAR MEASUREMENTS AND EFFECTS

Program Director: E. A. Martel

B.2.1 Project 2.1: Studies of Airborne Particulate Material
Agency: Army Chemical Center
Report Title: Radioactive Particle Studies Inside an Aircraft, WT-717
Project Officer: Maj J. M. Roady, USA

This project was conducted to study radioactive particles in the inhalation size range to which crews of pressurized aircraft might be exposed as a result of flying through an atomic cloud. The objective of the study was the evaluation of potential inhalation hazard relative to the associated external radiation exposure. The study was carried out in association with biomedical investigations with the same objective conducted under Project 4.1.

Instrumentation was placed in two QF-80 drone aircraft (operated under Project 4.1) which were flown through the cloud a short time after two air-burst detonations. Samples of the contaminated intake air were collected on the slides of a five-stage cascade impactor, which was backed by a millipore filter.

Laboratory analysis of the samples is complete, but extensive revisions required on the Project 2.1 final report have delayed its publication. The results indicate, however, that the internal hazard associated with contaminated cockpit air is negligible when compared to the accompanying whole body external dose received during the penetration of the cloud.

B.2.2 Project 2.2a: Measurement of Gamma Radiation of Fission Products
Agency: Signal Corps Engineering Laboratories
Report Title: Gamma-ray Spectrum of Residual Contamination, WT-718
Project Officer: R. C. Bass

The object of this project was to determine the gamma-ray spectral distribution of the residual contamination resulting from tower and air detonations of several nuclear devices. Information of this nature is required to furnish optimum design parameters for various radiation detection devices as well as to determine the biological significance of the gamma radiation associated with the residual contamination.

While data were obtained utilizing two types of instrumentation, primary emphasis was placed on the use of a scintillation spectrometer. The measurements consisted of a determination of the spectral distribution of the secondary electrons produced by the incident photons in two different scintillating phosphors. The light pulses produced within the phosphors were detected with photomultiplier tubes, and the count rate as a function of pulse height was recorded. This was done using a preamplifier, linear amplifier, pulse-height analyzer, and scaler. These data were then analyzed to determine the spectral distribution of the incident photons. The secondary method utilized five radiac instruments, one of which was air equivalent. The other four were modified by lining the lucite walls of the ionization chambers respectively with aluminum, copper, tin, and lead. This method enabled only a determination of the approximate percentages of the dose rate contributed by the portions of the gamma-ray spectrum below and above 200 kev and of the approximate spectral extent.

Measurements were made at times varying from 1 hr to 10 days following detonation at positions near Ground Zero for air bursts and at ranges from 1000 yd to 3 miles from Ground Zero for tower shots. The locations at which readings were taken were limited inasmuch as the techniques used were reliable only at gamma-ray intensities of less than 500 mr hr. An analysis of the data obtained during UPSHOT-KNOTHOLE indicated that the major contribution to the gamma radiation associated with the residual contamination is from gamma rays of energy greater than 200 kev and that little radiation lies above 2 Mev in energy. The results of the two types of instrumentation used are in good agreement both as to spectral quality and

approximate spectral extent, and results obtained with the lined chambers appear to be in agreement with those obtained during SNAPPER. Results obtained from the scintillation spectrometer measurements are presented in the form of plots of gamma photon flux and gamma-radiation intensity in milliroentgens per hour as a function of energy between 40 keV and 3 MeV at different times after detonation for various locations in the residual contamination field. Results obtained from the lined ionization chambers and comparison of these results with those of the scintillation spectrometer measurements are presented in tabular form in the project report.

It is felt that future efforts should be directed toward an analysis of the gamma-ray residual spectral distribution subsequent to a surface or underground detonation and that measurements include high-intensity areas. Indications are that the associated spectral quality is sufficiently softer, warranting further efforts in this direction. The present technique of instrumentation and analysis is considered adequate in conducting rapid measurements in the field. Three lined chambers enable an almost instantaneous determination of the approximate percentages of the dose contributed by the portions of the gamma-ray spectrum below and above 200 keV for the spectral distributions for which comparisons were made. For a more precise determination of the energy spectrum, the use of a total absorption spectrometer employing a large NaI-Tl crystal is recommended.

B.2.3 Project 2.2b: Residual Gamma Depth Dose Measurements in Unit Density Material
Agency: Naval Medical Research Institute
Report Title: Residual Gamma Depth Dose Measurements in Unit Density Material, WT-719
Project Officer: CDR F. W. Chambers, USN

Gamma-radiation absorption measurements were made, employing small energy-independent ion chambers in several types of unit density phantoms, to study the characteristics of residual contamination radiation. Such measurements are of value in the interpretation of the biological significance of various regions of residual gamma energy distributions measured by Project 2.2a.

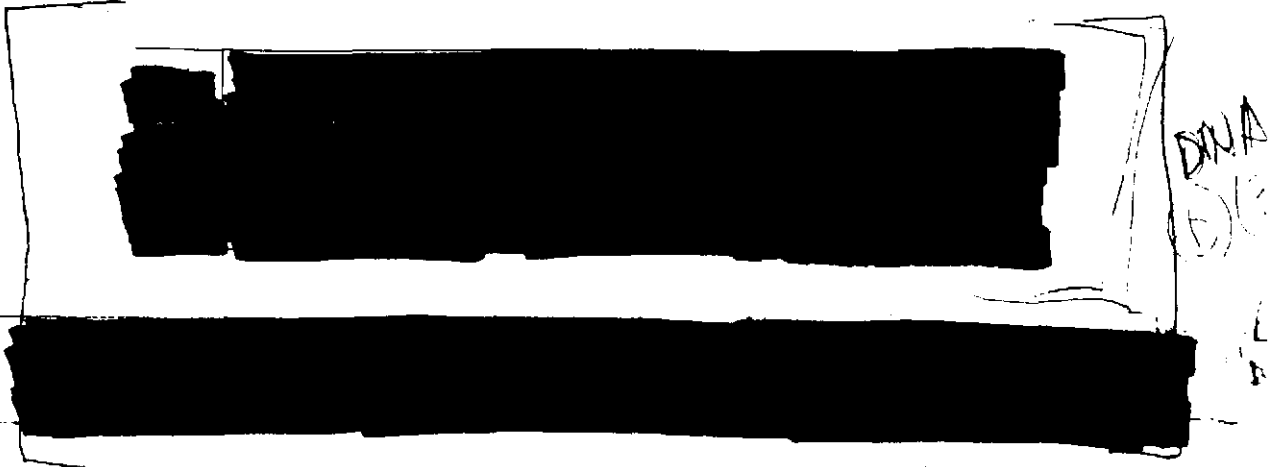
Three types of unit density phantoms were employed. In addition to sets of lucite spheres of various wall thicknesses that had been used in the study of initial gamma radiation, a masonite sphere and a masonite man were used in this study. These latter type phantoms, with dosimeters distributed in depth and direction, more nearly approximate the geometry of the body configuration.

Examination of the residual radiation field data from these measurements reveals a readily absorbed component present in the residual radiation that is not present in the initial radiation and that the depth dose curve for the high-energy component in the case of a fallout area 3.5 miles from Ground Zero is not very different from that obtained from the initial radiation.

B.2.4 Project 2.3: Neutron Flux and Spectrum Vs Range
Agency: Naval Research Laboratory
Report Title: Neutron Flux Measurements, WT-720
Project Officer: T. D. Hanscome

The measurement of neutron flux vs range at UPSHOT-KNOTHOLE was a continuation of the work done at SNAPPER, as far as techniques are concerned. Most of the methods used in SNAPPER were used again in UPSHOT-KNOTHOLE. There was no modification in the use of the thermal and threshold detectors—gold, tantalum, and sulfur. The proton recoil films were not used on this operation because of the shortage of personnel and the lack of facilities for reading the plates. Additional emphasis was given to the use of fission threshold detectors and nuclear track emulsions of appropriate sensitivity to record the fission fragments. This method is a modification of past work in which the fission fragments were caught on aluminum foils and counted.

The results of the project may be summarized by giving the attenuation factors (the so-called e-fold distance) and range = 0-intercept as measured with each of the detectors:



B.3 PROGRAM 3—STRUCTURES, MATERIAL, AND EQUIPMENT

Program Director: CDR C. E. Langlois

B.3.1 Project 3.1: Tests on the Loading of Building and Equipment Shapes
Agency: Air Materiel Command
Report Title: Tests on the Loading of Building and Equipment Shapes, WT-721
Project Officer: B. J. O'Brien

The objective of this test was to determine how the loading on a rigid rectangular block is influenced by changes in blast parameters and in structural size and shape. Specifically, the effects of the following variables were desired:

1. Effect of shock strength.
2. Effect of two-dimensional compared with three-dimensional loading.
3. Effect of absolute size of obstacles of similar shape.
4. Effect of orientation of obstacles of the same shape.
5. Effect of varying absolute length of an obstacle whose height and width dimensions are kept constant.
6. Effect of multiple ground reflections as a function of distance from the bottom of an elevated structure to the ground.
7. Effect of shielding as a function of distance between obstacles.
8. Effect of multiple reflection and clearance caused by various types of re-entrant corners and cavities.
9. A comparison between loading in the Mach region and that in the regular reflection region.

A series of 17 reinforced-concrete blocks was designed for exposure to Shots 9 and 10. The structures were anchored to the ground and were expected to withstand the effects of the shock wave without permanent deformation. Two of the structures were located in the expected regular reflection region of Shot 9 and the others in the expected Mach reflection region for that shot. In Shot 10 two of the structures were located in the precursor region.

The array of structures consisted of control blocks 6 ft high, 12 ft wide, and 6 ft deep in the direction of the blast, together with other blocks having proportional dimensions and specially designed structures to attain the other objectives of shielding, orientation, elevation above ground, etc. A view of some of the blocks is shown in Fig. B.3. A total of 214 channels of pressure-time instrumentation was operated for each shot. The soil was stabilized for a space of 200 ft in front of the array at 4900 ft to help in obtaining a clean shock wave.



The structures were located as follows:

[REDACTED]

Success in obtaining pressure-time records on most gages was achieved. Structure 3.1b, located in the precursor region of Shot 10, overturned and was thrown back about 20 ft. No other structures suffered any permanent deformation or displacement.

The pressure-gage data provided sufficient information to satisfy most of the test objectives. Diffraction phenomena, in general, were consistent with pretest expectations, but drag coefficients did not turn out to be constant as was expected. Pretest diffraction-impulse predictions were, on the average, high. The largest discrepancies in diffraction impulse between predictions and test results appeared on one of the skew-oriented structures and on the structures elevated above the ground.

There seems to be a nearly linear decay in drag forces during the positive phase of the blast wave. The drag forces observed were not in agreement with the pretest method of prediction, which was based on simple one-dimensional wave theory. Uncertainties in instrumentation made the determination of drag forces doubtful, and the possibility exists that the increased drag force observed was not a real phenomenon.

The test was designed primarily to study diffraction phenomena. A comparison between measured and predicted diffraction loads served to confirm certain aspects of the pretest methods and led to revisions of others. In the remaining instances, the form of the data was inadequate to either confirm or revise the methods. This latter category includes those cases in which the test data were clearly in disagreement with pretest predictions. However, it was not possible to revise the prediction scheme, and further study is recommended.

The pretest load-prediction methods were revised in three instances: (1) the value of the buildup coefficient, n , was modified to yield a more-rapid pressure buildup on rear surfaces, (2) a correction factor was developed which effectively decreases the predicted diffraction impulses on obliquely loaded surfaces, and (3) the method of loading on the underside of elevated structures was changed to give loads which are lower than previously predicted but still somewhat higher than free-stream.

The pretest predictions were confirmed with regard to: (1) peak average pressure on semi-front oblique surfaces, (2) loadings on the top and rear of very wide (i.e. nearly two-dimensional) structures, (3) time-scaling on the top and rear surfaces of geometrically similar structures, (4) occurrence of a so-called peaked shock effect which leads to reduced pressures on the front of large structures (i.e. those which are large in terms of the ratio of structure height-to-blast wavelength), and (5) diffraction impulse on surfaces of irregularly shaped structures.

If the increased drag force is accepted as a real phenomenon, it can be explained in terms of an analytical solution for the free-air blast parameters, which results in a dynamic pressure-time curve differing from that obtained by one-dimensional wave theory.

A method of predicting loadings on rectangular parallelepipeds in the precursor region was developed from the pressure data on Structure 3.1t. This load-time variation consists of a linear rise of net force on the structure to a maximum value given by the product of a drag coefficient and the peak ideal dynamic pressure (i.e. the dynamic pressure over an ideal surface in the absence of a precursor), followed by a linear decay to zero at the end of the positive phase. The time of rise to maximum load is about 100 msec and is probably independent of the building geometry. Inasmuch as this empirically determined loading is based on only one set of data, it may vary considerably for other precursor shot conditions and for other building shapes.

USAF
(b)(3)
11

B.3.2 Project 3.1u: Shock Diffraction Study
Agency: U. S. Naval Ordnance Laboratory
Report Title: Shock Diffraction in the Vicinity of a Structure, WT-786
Project Officer: W. E. Morris

The objective of Project 3.1u was to determine the shock diffraction in the vicinity of a structure. An array of 14 pressure-time gages at ground level and at a height of 5 ft were located behind and to the side of the 3.1t structure. The instrumentation employed Wiancko inductance type pressure gages and the NOL FM transmission and magnetic tape recording system.

On Shot 9, the 3.1t structure and the 3.1u diffraction measurements were in the region traversed by a conventional Mach shock wave. Diffraction effects were observed in the form of a 50-msec duration spike superimposed on the free-field side-on pressures both behind the structure and to the side of the structure. Directly behind the structure the magnitude of this spike was 40 per cent higher than the free-field peak pressure at the ground level gage closest to the structure (6 ft). The 5-ft high gage showed less of an increase (about 15 per cent) in pressure than the ground level gages. The magnitudes and shapes of the pressure-time records of the gages located behind the structures were quite similar to the pressure-time records from gages on the 3.1t structure located along the center line and at corresponding heights on the back face of the structure. The magnitude of the pressure spike to the side of the 3.1t structure was 20 per cent greater than the free-field peak pressure at the closest station (9 ft). Diffraction effects were observed 24 ft both to the side and in back of the structure. At 48 ft an effect had about disappeared. Since the largest dimension (L) of the 3.1t structure was 12 ft, diffraction effects appear to exist out to about 4L. Therefore, if shielding effects are to be avoided, a minimum distance of at least 4L should be maintained both to the side and behind a structure.

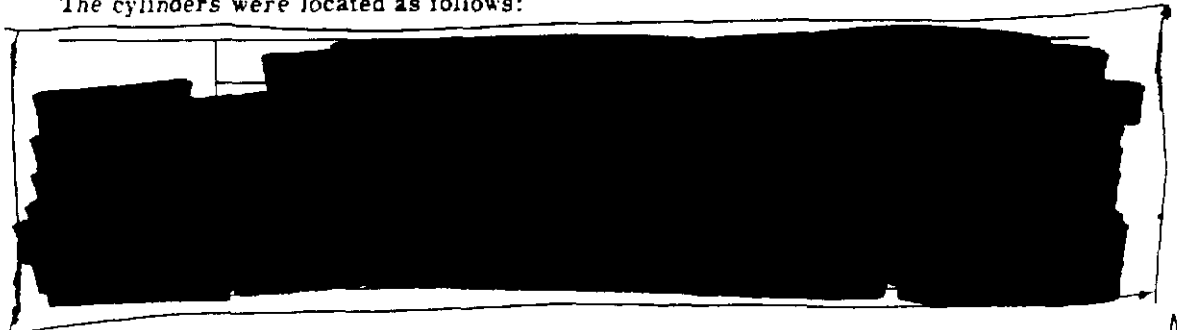
On Shot 10, the 3.1t structure was in the well-developed precursor region. No strong diffraction effects should be expected in this region where a slow rise-time pressure pulse was observed rather than a true shock wave. No diffraction effects were observed in the records of the 3.1u array, and the pressure-time records followed closely the free-field pressures. In contrast to the Shot 9 results, the peak pressures of the gages closest to the structure showed decreased pressures (35 per cent in back and 15 per cent to the side). These decreased pressures may be ascribed to the effect of the influence of the drag loading phase since they persist over a large portion of the pressure-time history.

B.3.3 Project 3.3: Tests on Horizontal Cylindrical Shapes
Agency: Air Materiel Command
Report Title: Tests on the Loading of Horizontal Cylindrical Shapes, WT-722
Project Officer: B. J. O'Brien

The objectives of this experiment were to determine the blast loading on horizontal cylinders, with particular reference to the effects of shock strength, the effects of target size on the net loads, and the effect of distance above ground.

Five steel cylinders closed at both ends and supported at varying distances above the ground were located at two stations in both Shots 9 and 10. Four of the cylinders were 6 ft in diameter and 20 ft long, and one was at one-quarter scale of these dimensions. The heights above ground varied from 4 to 36 in. A typical cylinder is shown in Fig. B.4.

The cylinders were located as follows:



The cylinders were subjected to clean, well-defined blast waves in both Shots 9 and 10. The pressure-gage data provided the loading on a cylinder one radius above the ground. There is some uncertainty as to the pressure scale, but the buildup and clearing times were found to be essentially the same as for a cylinder in free space, with the exception of the clearing time on the front face. The predicted clearing time on the front face of an isolated cylinder was between 4 and 5 r/U time units (r = radius of cylinder, U = shock-front velocity); the test results indicate a clearing time of between 8 and 10 r/U time units.

The remaining test objectives could not be realized from the pressure records, since these data exhibited a considerable and generally random spread from which no trends could be established. In addition, no quantitative information was obtained from strain records, because of inability to interpret these data properly. The data-reduction schemes, as applied, did not yield a satisfactory interpretation of the data; however, computations were not carried to the point where definite conclusions could be reached as to the feasibility of the various methods employed.

No definite conclusions have been reached for this test, although some information of value concerning the scaling of time details and the loads on one cylinder configuration was obtained. The interpretation of the strain data most probably would have been enhanced had the dynamic characteristics of the test items been determined by independent means either before or after the tests. It is also clear that much additional work remains to be done with respect to the design of net-force-measurement systems and, in particular, associated problems of data interpretation.

B.3.4 Project 3.4: Tests of Truss Systems Common to Open-Framed Structures
Agency: Air Materiel Command
Report Title: Tests on the Loading of Truss Systems Common to Open-Framed Structures, WT-723
Project Officer: B. J. O'Brien

The objective of this project was to determine the drag forces applied to open frame structures, such as bridges. Specific objectives were to determine the relative amounts of diffraction and drag impulses, to find the effects of drag loading due to the shielding of component parts, and to obtain data for comparison with wind tunnel data obtained under steady-state flow conditions.

The basic structure was a duplicate of the center section of a through-type, open-deck, single-track, truss railway bridge. Duplicate sections of the top chord assembly, the bottom chord assembly, and a single beam from the bottom chord assembly were also included. The fifth test item was a section of a through-type, open-deck, plate-girder railroad bridge. Each of the sections except for the single beam was mounted upon simulated bridge piers of concrete about 15 ft high, with the test sections fastened to steel sensor bars which were in turn welded to base plates bolted to the piers. A view of the plate-girder section is shown in Fig. B.5. The design of the reaction structure was intended to be such that forces on the bridge elements could be determined from strain-gage readings on the sensor bars.

In the prototype bridge, lateral stability of the top chord was maintained by a top lateral system extending to portal bracing at each end. Because this system was unavailable in the test specimen, which consisted only of one panel of the bridge, a cable-bracing system was added to prevent lateral deflection of the top chord.

All the objects tested were located in the range of 2200 to 2330 ft from actual Ground Zero for Shot 9, and 1950 ft from actual Ground Zero for Shot 10. The peak side-on pressure levels for these ranges were, respectively, about 11.5 psi for Shot 9, and 9 psi for Shot 10.

The effects of the blast in Shot 9 caused little damage to the test items. The cracking of two sensor bars at the weld of the plate-girder section was observed. A small permanent set of approximately 3 in. at the top of the truss section resulted from the guy cables being loosened, apparently due to the slippage of the cable clamps. After the shot the cables were tightened and five clamps were installed on each cable end, instead of three.

The damage of the test items on Shot 10 was considerably more severe than had been ex-

pected. The upper part of the truss-bridge section failed completely and fell to the ground. The cable clamps again slipped, but it is not known whether the forces would have been sufficient to break the cable had the clamps held. A small permanent set was observed in the top-chord component. The bottom-chord component appeared to have sustained damage from flying debris. A view of the structure after failure is shown in Fig. B.6.

Five strain records on Shot 9 and all eighteen records on Shot 10 were considered to be unusable. The Shot 10 records consisted entirely of what might be termed high-frequency hash; many of these show predominant zero shifts and off-scale readings. Even the Shot 9 strain records gave some indication of base-line shifts and calibration errors. For the most part the strain data did not yield interpretable results, and therefore none of the stated objectives have been achieved. However, in view of the limited and uncertain nature of the experimental data obtained, it is very doubtful that all the test objectives could have been realized anyway. The data-reduction techniques employed were similar to those used in Project 3.3, and in general the same negative results were obtained. Perhaps the most important results of the test have come about through consideration of the damage sustained by the truss-bridge section. It was found that a simplified dynamic-response analysis, incorporating the pretest predicted loading for the regular reflection region on Shot 9 and a tentative load-prediction scheme applicable to the precursor region on Shot 10, provided an adequate estimate of the damage sustained by the bridge in these two shots. While there is sufficient uncertainty in the assumptions of the response analysis to invalidate this agreement as a check on the essential accuracy of the load-prediction methods, confidence in the utilization of existing methods for damage-prediction estimates of open-frame structures is certainly increased as a result of this test.

No conclusions regarding the principal objectives of the test are possible from the sensor-bar data as reported. The best available data for the dynamic pressures at the distances of the bridge truss members indicate a value of about [REDACTED] for Shot 10, compared with about [REDACTED] or Shot 9. Even with the shorter duration in Shot 10, because of the smaller yield, the increased pressure is sufficient to account for the difference in deformation observed in the bridge truss in the two tests. It can be concluded that the deformations observed are consistent with the forces.

Sufficient redundancy should be provided in the planning of instrumentation for field experiments to permit the interpretation of data obtained from the tests, even when parts of the data are missing.

B.3.5 Project 3.5: Tests of Wall and Roof Panels
Agency: Air Materiel Command
Report Title: Tests on the Response of Wall and Roof Panels and the Transmission of Load to Supporting Structure, WT-724
Project Officer: B. J. O'Brien

The general objective of this experiment was to determine the load transmitted to building frames through various common types of panel wall and roof construction. Other objectives concerned the determination of modes of failure of common types of wall and roof construction, and the changes in magnitude and type of loading on the various parts of a structure as affected by the failure sequence of parts of different strength.

Reinforced-concrete test cells were built to support the wall and roof panels. A view of some typical roof panels is shown in Fig. B.7. Each of 10 test walls measured 8 ft, 9 in. high by 13 ft, 9 in. wide and was supported in a channel frame attached to sensor bars to measure the load transmitted to the supports. Each of the seven test roofs measured approximately 29 ft long by 14 ft wide. The cells supporting the roofs had openings in front and rear of about 16 per cent of their frontal area. A description of each of the types of wall and roof panels is contained in Tables B.1 and B.2. The 3.5c wall panels are shown in Fig. B.8.

Instrumentation consisted of 21 pressure measurements primarily on inside surface of roofs, 69 strain-gage channels to measure loading transmitted by the roof and wall panels to the supports, time-of-break gages on four roof panels, and motion-picture photography.

TABLE B.1—Summary of Test Data, Wall Panels

[REDACTED]	[REDACTED]	[REDACTED]	[REDACTED]	[REDACTED]
------------	------------	------------	------------	------------

TABLE B.2—Summary of Test Data, Roof Panels

[REDACTED]	[REDACTED]	[REDACTED]	[REDACTED]
------------	------------	------------	------------

USAF
(b)(3)
(1)

Groups of test cells were located at 6700 ft, 4500 ft, and 2200 ft, to give data at three pressure levels. Because nearly all items failed in Shot 9, as intended, no instrumentation was provided for Shot 10.

The description of the test items, the overpressure levels recorded, and a brief summary of the damage resulting from the test are summarized in Tables B.1 and B.2.

The results of this test should be viewed with caution as indicative of general trends for other sizes of panel or type of supporting structure. In particular, the brick walls acted more or less as arches, and even after initial failure occurred in the panel they had a considerable resistance. Such a resistance might not be mobilized in an actual building.

USAF
(b)(3)
(1)

Even though a wall fails structurally quite early in the loading period, the debris may take a relatively long period of time to clear from the opening. In such cases, the peak forces and their dynamic effects in the interior of the building are expected to be considerably lower than if the wall debris had cleared away more rapidly. The effect of wall debris may therefore be of considerably greater importance than had been previously anticipated in reducing the loading on interior equipment, downstream walls, columns, and trusswork.

Early structural failure of the roof does not necessarily imply that interior pressures are altered quickly from what would occur with no roof failure, at least for the geometries considered. In fact, for the six instrumented roof panels it appears that roofing was removed by the blast too slowly to have a large effect at any time on the interior pressures.

The effect of purlins on pressures on the undersides of roofs are probably confined to areas closer to the purlins than about one purlin height. The effects of longitudinal trusswork on pressure are also indicated to be small. In fact, the later (pseudo steady-state) pressures on the undersides of all roof shapes which were tested appear to be unaffected by the geometric differences between these roofs, including pitched and arched shapes.

Comparison of measured pressures with predicted loadings on the roofs tested indicates that the predictions are fair to good in most respects for the Mach reflection region but are poor in certain respects for the regular reflection region.

The masonry and reinforced-concrete panels appeared to fail as two-way slabs. The test results seem to support an arching-action theory. The lightweight wall and roof covering appeared to fail in bending as one-way slabs.

B.3.6 Project 3.6: Tests of Railroad Equipment
 Agency: U. S. Army Transportation Corps—Air Materiel Command
 Report Title: Tests on the Loading and Response of Railroad Equipment, WT-725
 Project Officer: Lt Col D. G. Dow, TC, USA

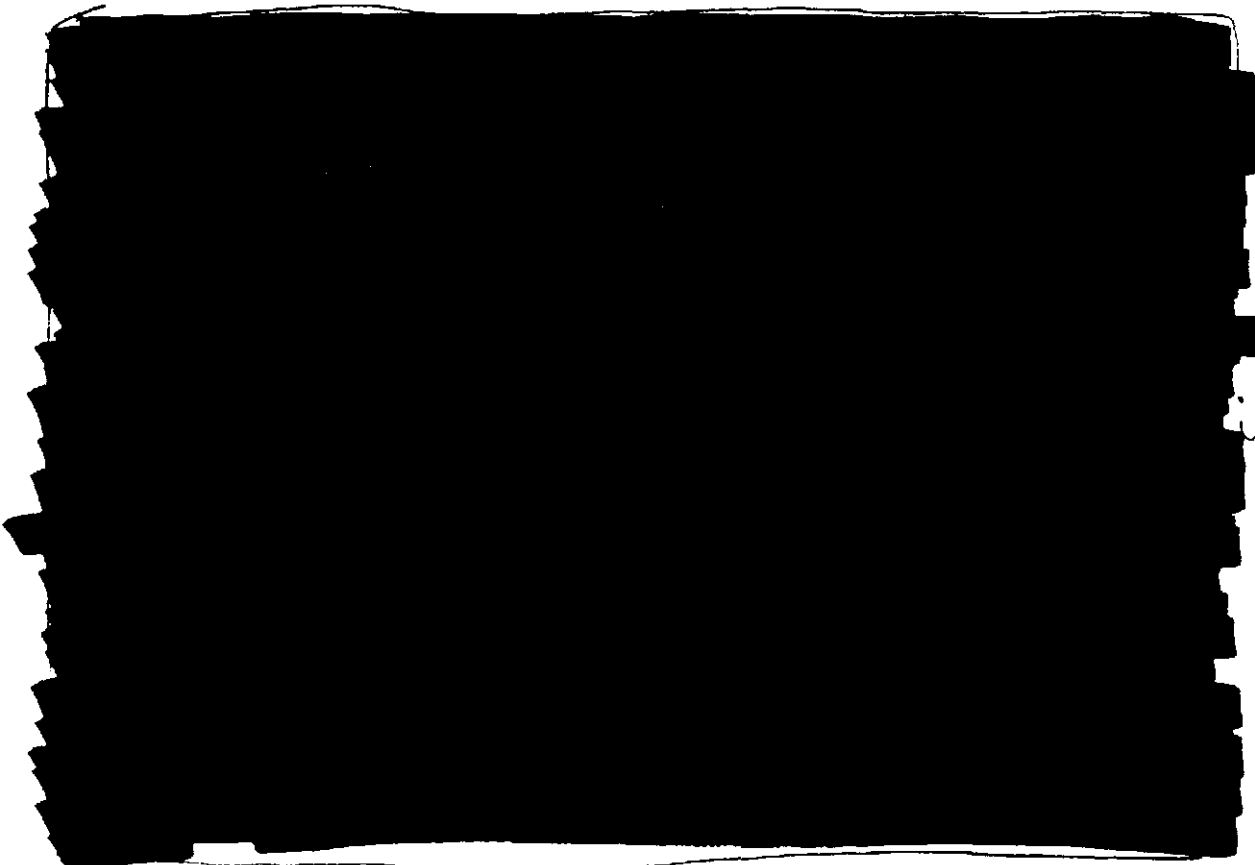
The objective of this test was to study the vulnerability of the various types of railroad equipment to the blast and thermal effects associated with an atomic explosion. The specific objectives were concerned with general damage to railroad cars, both loaded and empty; the bracketing of the shock overpressure causing damage; the gathering of data relating to blast loading, response, and dispersion criteria; and correlation of response with damage and thermal effects.

Sixteen items of standard Transportation Corps equipment, consisting of several types of boxcars, tank cars, and one diesel locomotive, were included in Shot 10. The boxcars included five empty and five loaded wooden boxcars, one empty steel boxcar, and two empty plywood boxcars. The tank cars included one empty welded tank car and one empty riveted tank car. Each piece of equipment was installed on a 126-ft section of track. Loading consisted of sandbags stacked to a height of about 3 ft above the floor.

This equipment was located as follows:

Item	Distance from Actual GZ (ft)	Peak Side-on Pressure (psi)
Wooden boxcar (empty)	6600	1.9
Wooden boxcars (empty and loaded)	4400	4.0
Diesel locomotive	3400	6.0
Wooden boxcars (empty and loaded)	3400	6.0
Plywood boxcar (empty)	3400	6.0
Wooden boxcars (empty and loaded)	2820	7.5
Steel boxcar (empty)	2820	7.5
Wooden boxcars (empty and loaded)	1870	9.3
Plywood boxcar (empty)	1870	9.3
Wooden boxcar (loaded)	1520	13.3
Steel tank cars (riveted and welded)	1520	13.3

STEEL



USANCA
~~1~~ 1

B.3.7 Project 3.7: Effectiveness of Blast Baffles at Shelter Entrances, Air Intakes, and Outlets
 Agency: Office of the Chief of Engineers, U. S. Army
 Report Title: ~~an~~ Blast Effects on Entrances and Air Intakes of Underground Installations, WT-726
 Project Officer: W. J. Matthews

The objectives of this project were to obtain, under field conditions in an atomic blast, data on various devices suitable for use as air intake and ventilation ducts and data on the blast-attenuating performance of entranceways of two simple designs.

All of the elements tested were contained in two independently reinforced-concrete cells in a single structure, located about 2 ft under the surface of the ground. Two large cells 18 ft by 8 ft by 7 ft high and six independent plenum chambers of 3 ft by 4 ft by 7 ft height were provided, to which ventilating ducts of various kinds led. Various ventilating ducts were provided with protective devices at their entry of the following types: (1) straight pipe with T-shaped entry, (2) straight pipe with 180°-bend entry, (3) heavy-duty muffler-type blast baffle, (4) Swedish rock grille, (5) Chemical Corps filter, and (6) Chemical Corps anti-blast closure valve. Each large chamber was equipped with a ventilating blower protected with a Swedish rock grille in one chamber and a T-shaped entry in the other. The exhaust vent in the chamber with the Swedish rock grille was also protected with an anti-blast valve. The entryway to one chamber was the T-section type and on the other the entryway was protected with blast-arresting details in the form of right-angle bends. Thirty-four channels of air pressure measurements were provided for both Shots 9 and 10. The test chamber in process of construction is shown in Fig. B.9.

The range of the structure for Shot 9 was 963 ft, and the overpressure recorded was approximately 20 psi. The range for Shot 10 was 765 ft and the overpressure recorded was considerably in excess of the expected value, reaching approximately 110 psi or more.



Complete records were obtained on Shot 9 for all of the vents and the entryways. In Shot 10 only six pressure-time records were obtained. The results of Shot 10 were of particular interest because of the failure which occurred in the roof of the structure in one large cell of the test shelter. This roof had been designed for a pressure of 60 psi, with design values that corresponded to a factor of safety of slightly less than two. The conditions of failure were somewhat unusual, in that only the roof over one cell failed, apparently primarily in shear, and the other showed no important deformation.

Practically all of the ventilating-duct devices lengthened the rise time of the pressures in their plenum chambers and in some cases reduced the peak pressures greatly. In general, the pressures measured in the ducts were in agreement with analyses developed.

Both entryways showed indications of peak pressures, reached early in the shot, of magnitudes nearly twice the incident overpressure level. After some clearing time of approximately 1 to 1.5 times the period for the shock to travel through the entranceway to the farthest point and back out again, the pressures in the entranceway passages appeared to be practically the same as those outside the structure in the general shock region.

B.3.8 Project 3.8: Effects of Air Blast on Buried Structures
Agency: Office of the Chief of Engineers, U. S. Army
Report Title: Air Blast Effects on Underground Structures, WT-727
Project Officer: W. J. Matthews

The general objective of this program was to obtain some of the necessary basic data from which to develop criteria for the economical and efficient design of underground protection from air blast forces. The specific objectives were: (1) to investigate the nature of the forces transmitted from an air burst of an atomic bomb through the earth to underground structures; (2) to determine the variation of these forces with the depth of transmission through the earth and with the flexibility of the structural elements subjected to the forces; and (3) to study the response of simple structural elements of different stiffnesses subjected to the transmitted dynamic forces.

The structures subjected to test were primarily reinforced-concrete boxes having a large number of simply supported steel-beam strips forming their roofs. Three identical reinforced-concrete cells were designed to support roof structures at three depths of burial: 1 ft, 4 ft, and 8 ft. Each of the structures had a number of individual beam strips, with three or four strips of each of three different degrees of flexibility. All of the beam strips had a span of 8 ft and were composed of two closely spaced I-beams welded to a common $\frac{1}{2}$ -in. steel coverplate. One set of beam strips for each depth was designed to develop plastic strains even for low pressures; another set was intended to develop plastic strains at relatively high overpressures; and a third set was designed to remain in the elastic range even for very high overpressures.

The test beams were instrumented with strain, deflection, and earth pressure gages on the central beam of each group. Air pressure measurements were also recorded both inside and outside the structure. A total of 99 channels of information were operated. Placing of earth cover and backfill was carefully controlled. Physical properties of the test beam strips were measured on control specimens and on duplicates of the strips tested in the laboratory. A view of a test chamber and of individual beam strips is given in Fig. B.10.

The structures were located in a group at approximately 1425 ft from the actual Ground Zero of Shot 9 (pressure level, about 15 psi) and at about 900 ft from the actual Ground Zero of Shot 10 (pressure level, about 63 psi).

No damage or permanent deformation was expected in Shot 9 and none was observed. The pressures obtained in this shot, because of the bombing error, were considerably smaller than expected and the records obtained provided only qualitative information in most cases. In Shot 10, the pressures were of about the order of magnitude expected in the design with a definite precursor pulse. Only small permanent deflections were obtained in the test, although the transient deflections were of an order of magnitude sufficient to give appreciable readings.

In well-compacted silty subsoil of the type at the test site, there is no effective attenuation of a pressure pulse applied at the surface with depth through the subsoil under the following

conditions: (1) when the pressure is transmitted to a structure in the soil; (2) when the structure is buried at a depth not more than the span of the structure, and (3) if the deflections are less than 0.5 per cent of the span. The transient, as well as the permanent, strains and deformations of the beam strips were of about the same order of magnitude at all three depths of burial. Apparently the dynamic arching phenomenon is negligible unless the deflections are large or the depth of cover is greater than the span; the beneficial effect of added cover under these circumstances is primarily due to the added mass of such a cover. Although attenuation of pressure with depth was noted in free earth measurements in this project and in Project 1.4, there was no indication on the structures of such attenuation, either from pressure measurements, reaction measurements, or deflections and strains.

For underground structures having a net density less than that of the displaced soil, the overall accelerations of the structure act to reduce the influence of the pressures applied to the top. However, this influence is not large.

The lateral pressures exerted on vertical faces of a buried structure, compared with the pressures applied at the top surface, are quite small in the subsoil at the Nevada Proving Grounds.

The pressures exerted upward on the base and floor slab of buried structures are very nearly of the same magnitude as the downward pressures on the ground surface.

B.3.9 Project 3.9: Design and Location of Field Fortifications
Agency: Engineer Research and Development Laboratory
Report Title: Field Fortifications, WT-728
Project Officer: Capt V. S. Adkins, USA

The test had four objectives: (1) to obtain evidence supporting a detailed qualitative discussion of atomic effects on field fortifications with overhead cover and revetment; (2) to make air-pressure measurements inside various fortifications and compare them with the air pressures in the open at ground level; (3) to make measurements of the reflected thermal radiation within open two-man foxholes and determine a method of scaling to a range of possible situations; and (4) to determine the dependence of gamma radiation measurements upon the angular orientation of film badges inside an open two-man foxhole.

To study blast effects, various types of covers, revetments, and reinforcements were added to standard command posts, two-man foxholes, and machine gun positions (see Fig. B.11), which were situated at three different positions (500, 1500, and 4600 ft from planned Ground Zero). Indenter pressure gages were used to obtain pressure measurements within the emplacements. Preshot and postshot photography was also employed. Results indicate that failure began in the cover-supporting timbers at 8 psi. Almost no failures occurred in revetments up to 20 psi. Covers on emplacements must be well anchored and very strong, or flexible, to withstand pressures in the 20-psi region. Conventional sandbags are unsatisfactory for entrance revetments subjected to an atomic explosion, since they catch on fire and spill their contents before the blast arrives.

For overpressure multiplication, five two-man foxholes, two at 4100 ft and three at 7000 ft, were instrumented with Wiancko pressure-time gages, self-recording scratch-type pressure-time gages, and indenter pressure gages. The results show that pressures inside foxholes can reach values as high as twice the peak pressure at ground level, and that the addition of covers to emplacements can effectively reduce pressure buildup inside foxholes to any desired extent. Results of Project 3.7 provide corollary information on this subject.

To determine thermal reflection, a series of 22 two-man foxholes lined with aluminum sheeting and oriented at various angles in the ground was exposed to Shots 9 and 10. The aluminum sheeting was designed to act as a diffuse reflector (see Fig. B.12). Each foxhole was lined with an array of passive indicators to measure thermal energy for each orientation and in various positions within the foxholes. Calorimeters were employed as a check on the passive indicators. By representing passive-indicator reaction energy as a fraction of direct thermal energy, predictions may be made at any point in a foxhole for any condition of bomb yield, height of burst, distance from Ground Zero, and soil reflectance. For aluminum-lined fox-

holes, the results indicate that thermal energies up to 40 per cent of the incident energies may be present at 1 ft from the top of the foxhole, with a rapid decrease to 10 per cent or less as the depth is increased to 3 ft. Since reflectance of most soils is considerably less than that of aluminum, the percentage of the incident energies present in the foxholes under actual conditions will be much less than the above figures. Comparisons of aluminum and soil reflectance are presented in the project report.

In the absence of any theoretical basis for the performance of field fortifications, extreme caution should be used in applying the specific results of these tests to situations involving substantially different yields or heights of burst.

B.3.10 Project 3.11: Protective Measures for Existing Constructional Light Steel Frame Structures

Agency: Bureau of Yards and Docks, USN
Report Title: Navy Structures, WT-729
Project Officer: LTJG P. J. McEleney, USN

The objectives of this experiment were to determine the blast resistance inherent in a standard steel-frame warehouse of a type proposed for Navy use and to determine the practicability of obtaining a greater blast resistance through closer spacing of standard components.

The overall dimensions of the structures were 40 ft by 100 ft in plan, 14 ft to the eave, and 19 ft, 6 in. to the ridge. Two structures were tested, one with twice as many framing members (bents, purlins, and girts) as the other. The stronger structure, designated 3.11-a, was designed to resist a 150-mph wind at an allowable stress of 20,000 psi. The weaker (standard) structure, 3.11-b, was designed for the combined effect of a 70-mph wind and 20-psf snow load. The weaker building was placed at a distance of 20,000 ft from Ground Zero and the stronger at 12,000 ft, for both Shots 9 and 10.

Structure 3.11-a was subjected to a peak overpressure of 2.2 psi from Shot 9, and was displaced 5 in. at the crown. The main frames suffered light damage due to buckling of windward rafters. The sheeting was relatively undamaged except near the door, which was completely damaged. Window glass breakage was complete. Purlins and girts were generally undamaged.

Structure 3.11-b received 1.0 psi from Shot 9. The frames were displaced 1 $\frac{1}{2}$ in. at the crown, and the leeward rafters were buckled. The door of this structure was only lightly damaged, and window breakage was minor in extent. The front-wall sheeting suffered up to 6 in. of permanent displacements. A postshot view of this structure is shown in Fig. B.13.

With a strengthened door and door-framing system and a few minor modifications, Structure 3.11-a could probably withstand pressure levels up to 2.2 psi with only light damage and be completely serviceable as a warehouse after the blast with only minor repairs. With similar modifications, Structure 3.11-b could probably resist a 1.0-psi overpressure with only minor damage resulting.

B.3.11 Project 3.12: Protective Measures for Existing Construction; External Protective Measures

Agency: Bureau of Yards and Docks, USN
Report Title: Navy Structures, WT-729
Project Officer: LTJG P. J. McEleney, USN

The objective of this project was to test the effectiveness of protecting a brick, bearing-wall, timber-decked structure with precast reinforced-concrete panels. A secondary objective was to test dynamically isolated panels mounted flush with the ground surface in specially constructed foundations.

The brick structure to be protected was 44 ft by 21 ft, 4 in. in plan and 11 ft, 6 in. high. The roof consisted of 3 by 12 joists at 16 in. on centers spanning the short direction with 1-in. diagonal timber sheeting. The brick walls were 12 in. thick. The panels used to cover the roof were about 10 ft, 8 in. wide and spanned the short direction. The panels consisted of a 2-in.

slab with 12-in. edge beams and a 12-in. center beam with 6-in. sub-beams parallel to the short side at 3 ft, 4 in. on centers. Wall panels had 8-in. edge beams with 6-in. sub-beams. All wall panels were 11 ft in height and were of four different widths. The panels were connected to the roof-framing system and the brick walls by means of bolts, and were connected to each other and the curbing by welded splice plates. Structure 3.12 is shown in Fig. B.14.

The secondary test panels (3.12-b and 3.12-c) were 5 ft by 20 ft and 10 ft by 20 ft in overall dimensions, and had 8-in. edge beams. These panels were mounted in pairs, one of each size, in foundations designed to receive them flush with the ground surface. The panels were connected at the ends to the foundation by means of welded splice plates, but were free to deflect independently of each other.

Two 5-ft by 20-ft panels (3.12-f) were tested statically at the U. S. Navy Civil Engineering Research and Evaluation Laboratory, Port Hueneme, California. In this test the yield resistance was about 1.5 psi at about 3-in. deflection, and the ultimate strength was about 2.5 psi.

The 3.12-a structure was exposed to an overpressure of 6.4 psi from Shot 9 at a distance of 4900 ft from Ground Zero.

The panels of 3.12-b were subjected to an overpressure of 3.4 psi from Shot 9, while the 3.12-c panels received 2.5 psi from the same shot. The 3.12-c panels were retested in Shot 10 in the precursor region at a range where the overpressure was 8.1 psi.

The panels of 3.12-a were slightly damaged, with a maximum permanent deflection of 0.14 ft in the roof. However, the panel deflections were large enough to produce failure in about 30 per cent of the joists. The brick walls were relatively undamaged, with only minor cracking of the front wall resulting from the deflection of the front-wall panels.

The panels of 3.12-b and 3.12-c were deflected permanently about 5 in. and 3 in., respectively. The corresponding maximum transient deflections were roughly 8 in. and 6 in. The damage was confined to the edge beams, with minor cracking in the sub-beams.

The 3.12-c panels tested in Shot 10 were placed directly against the ground in such a manner that the main and sub-beams could not deflect. The edges were sealed with earth to prevent pressure application on the underside of the slab. These panels were lifted bodily and transported 130 ft and 25 ft, respectively, by the blast in the precursor region.

The precast panels may have performed the task assigned to them; viz., protection of the brick structure against blast effects associated with a 6.4-psi overpressure. However, it is not possible to determine the efficiency of this method of protecting the given structure from this test alone, since the unprotected strength of the structure is unknown.

B.3.12 Project 3.13a and 3.13b: Precast Gable Shelters

Agency: Bureau of Yards and Docks, USN
Report Title: Navy Structures, WT-729
Project Officer: LTJG P. J. McElenny, USN

The primary objective of this experiment was to determine the structural adequacy of a precast shelter intended for use at Naval shore establishments. Secondary objectives were to test the effectiveness of a pressurization system, to verify the validity of a method of dynamic structural analysis developed by BuDocks, and to check the reduction of radiation intensity offered by these structures.

These structures were personnel shelters designed to accommodate 100 persons. Interior dimensions were 22 ft by 48 ft in plan and 13½ ft high. The buildings, one of which is shown in Fig. B.15, were divided into three compartments by precast concrete partitions.

Structure 3.13-a had 3 ft of earth cover for Shot 9 and no cover in Shot 10. Entry was provided through a T-shaped tunnel lined with a corrugated-metal pipe. Structure 3.13-b was identical with 3.13-a except no cover was provided, and the door was protected by a blast wall.

Various types of instrumentation were provided to measure transient effects, such as air-pressure gages, earth-pressure gages, and deflection gages

These structures were located as follows:

Structure	Shot 9		Shot 10	
	Distance from Actual GZ (ft)	Peak Side-on Pressure (psi)	Distance from Actual GZ (ft)	Peak Side-on Pressure (psi)
3.13-a	2700	10.8	2300	8.2
3.13-b	4900	6.2	4900	3.7

For the structure with 3 ft of cover, the natural frequency of vibration measured from a vertical pull test was 12 cps.

The overpressure level was 10.8 psi at the location of Structure 3.13-a for Shot 9. The structure itself remained essentially elastic at this level of pressure.

The air pressure measured at the surface of the earth cover near the crown was approximately 12 psi on the windward side and approximately 8 psi on the leeward side. Near the door in the tunnel entrance, a pressure of about 8 psi was measured.

The earth-pressure gages placed at the structure-earth interface gave the following results. On the windward side of the building, the pressures were between 13 and 20 psi, except for an unreasonably low value of 5 psi recorded at the top of the nearly vertical leg. On the leeward side of the building the pressures ranged between 5 and 14 psi.

The deflection gages indicated that the crown of the structure moved down and the haunches moved out when the dynamic load was applied. The airlock was destroyed by the blast, and the interior partition was slightly damaged.

Structure 3.13-b was located in a 6.4-psi overpressure range. The frame was essentially undamaged. Minor cracking was observed in the end panels, but the interior partitions were heavily damaged owing to the blast entering through the ventilation openings.

For Shot 10, the uncovered Structure 3.13-a was at the 8.2-psi range. Air pressure measured on the periphery of the structure varied between 5 and 7 psi except for a reading of 15 psi at about the mid-height on the windward side. The values obtained on the windward side near the toe and crown were unreasonably low. Damage inflicted on the structure by the air blast was unimportant. There was a slight permanent deflection at the crown of 0.3 in. up and a general leeward motion of 0.2 in. The cracks in the panels and ribs were found widened. The structure was punctured by a missile which resulted in a large hole in a panel.

It is concluded that this building is structurally safe for the overpressures indicated, and that earth cover is valuable in reducing missile damage and radiation on thin-walled concrete buildings. Whether or not this is a preferable type of shelter would depend on economics, priorities, and logistics at the time of construction. The end walls are relatively weaker than the sides and roof. This weakness would become even more important if the end were oriented to face Ground Zero. The ventilating system needs re-study.

B.3.13 Project 3.13c: Model of Blast-Resistant Panel
 Agency: Bureau of Yards and Docks, USN
 Report Title: Navy Structures, WT-729
 Project Officer: LTJG P. J. McEleney, USN

This project was designed to study the action of a panel designed as a torsion pendulum. It was expected that the panel mounted in this manner would provide time delay, as well as shock absorption and reduction in the load transferred to the frame.

One panel, 3 by 6 by $\frac{1}{2}$ ft mounted in the front face of a T-6 Pontoon, was tested in both Shots 9 and 10. The Pontoon was anchored to a 2- by 2- by 12-ft concrete slab. The panel framework was welded to a 4.0-in.-OD, 3.563-in.-ID steel torque tube positioned at the bottom edge of the panel. A concentric, inner torque tube was welded to the 4-in. tube at the mid-length. This inner torque tube was 3.5 in. OD and 2.25 in. ID for Shot 9, and 3.5 in. OD and 2.75 in. ID for Shot 10.



The measured overpressures during Shots 9 and 10 were 10.8 psi and 8.1 psi, respectively. The permanent deflection from Shots 9 and 10 were $1\frac{3}{8}$ in. and $\frac{1}{4}$ in., respectively. Because of instrumentation failure and lack of pressure measurements on the panel, the reduction of load transmitted to the frame, as effected by the torque tubes, was not determined.

B.3.14 Project 3.14: Precast Warehouse
Agency: Bureau of Yards and Docks, USN
Report Title: Navy Structures, WT-729
Project Officer: LTJG P. J. McEleney, USN

The objective of this experiment was to observe the behavior of a precast warehouse similar to those now being provided at Navy shore establishments.

The structure tested was quite similar in the type and arrangement of the framing to actual warehouses which are larger. Seven 2-span bents made up of hollow, precast columns and girders were spaced at 20 ft. Precast concrete struts were employed between bays at column locations. The roof consisted of precast panels approximately 10 ft by 20 ft with 8-in. edge beams and 6-in. sub-beams at approximately 5 ft on centers. The front and rear wall panels were similar to the roof panels, except that the horizontal and vertical sub-beams were 8 in. instead of 6 in. deep. The side wall panels were similar to the front and rear wall panels, except that the horizontal ribs were 6 in. deep. The foundation consisted of a continuous footing under the walls 3 ft, 2 in. wide by 1 ft, 6 in. deep and 5- by 5- by 2-ft footings under each column tied in the transverse direction with 1- by 1-ft struts.

The structure was designed for a roof live load of 40 psf and a 90-mph wind. However, the connections to the slabs and reinforcing steel of the bents were increased in strength above that required by the analysis for static loads, to provide for blast effects.

Five pressure gages and three displacement gages were installed to obtain dynamic measurements.

For Shot 9 the frame was tested uncovered with the panels laid on the ground with the ribs down (see Fig. B.16). The complete structure was tested in Shot 10. The actual distance from Ground Zero was 6500 ft in each shot. The overpressure levels were about 4.3 psi for Shot 9 and 1.9 psi for Shot 10.

The skeleton structure exposed to Shot 9 was undamaged. The panels, left lying on the ground with ribs down, were damaged by cracking of sub-ribs and dishing of skin up to 1.5 in. The main ribs were uncracked. These deformed panels were forced into position on the frames for Shot 10, so that the completed structure was initially stressed an unknown amount.

For Shot 10 the structure was exposed to an overpressure of 1.9 psi. The frame was again undamaged. The roof panels, however, were almost completely destroyed, with approximately 50 per cent of them falling to the floor. The vertical ribs of the wall panels were heavily cracked; otherwise they were relatively intact. A postshot view is shown in Fig. B.17.

The total destruction of the roof panels was initiated by the failure of the end connections and consequent removal of end restraint, followed by failure of the panels themselves near the location where reinforcing steel was bent up.

Because of the premature failure of the roof panels, the structure probably did not receive the maximum load associated with a 1.9-psi overpressure. Thus it is not possible to conclude that the structure is safe at that overpressure when the roof panels do not fail.

B.3.15 Project 3.15: Armco Steel Magazine
Agency: Bureau of Yards and Docks, USN
Report Title: Navy Structures, WT-729
Project Officer: LTJG P. J. McEleney, USN

The objectives of this experiment were to: (1) evaluate the effectiveness of earth cover against air blast in protecting aboveground structures in general, and a corrugated-steel-arch ammunition magazine in particular; (2) determine the adequacy of this structure for use as a personnel shelter; (3) gain information leading toward optimum design of earth-covered structures; and (4) develop analytical methods for the prediction of response of earth-covered structures.

Two structures were tested in this project. The first, designated Armco II, was tested statically at the U. S. Naval Civil Engineering Research and Evaluation Laboratory at Port Hueneme. The second structure was exposed to Shots 9 and 10 with 3 ft of earth cover.

Structure 3.15 was a semi-circular, corrugated-steel arch (10 gage), 25 by 48 ft in plan, manufactured by the Armco Drainage and Metal Products, Inc. The semi-circular sections were bolted at the edges to longitudinal base channels. The front and rear walls were built up of corrugated panels (3 gage) bolted to curved channels which were attached to the inner surface of the arch and to base angles at the foundation. A T-shaped entry made of Armco multi-plate 84-in. pipe (10 gage) bolted to the front wall was provided (see Fig. B.18). Armco II was essentially the same as Structure 3.15, except that 12-gage steel was used in the arch sections instead of 10-gage steel. Structure 3.15 was located 2700 ft from Ground Zero for Shot 9 and 2300 ft from Ground Zero for Shot 10.

Elaborate instrumentation was provided to measure deflections (with respect to ground), strain, and earth and air pressures.

As for Structure 3.13-a, elaborate pull and drop tests were performed on both of these structures. For Structure 3.15, the horizontal and vertical pull tests were performed for no cover, 0, 1, 2, and 3 ft of earth over crown, and 30 days after the test, again for the 3-ft-cover case. At this time, the drop test was conducted by dropping a 1500-lb clamshell on the crown. For the case of no cover, the vertical pull test indicated that the natural frequency of the structure was about 6.7 cps.

Similar tests were conducted on Armco II at Port Hueneme. There, earth cover over crown up to 5 ft was used. For the case of no cover, the natural frequency of the system obtained by the vertical pull test was about 6.25 cps. For the case of 3 ft of earth cover, the frequency was down slightly to 6.15 cps. The complete results of these tests are reported in: J. R. Allgood, *Static and Dynamic Studies of Three Personnel Shelters*, NAVCERELAB Technical Note N-159.

Structure 3.15 was exposed to an overpressure of 10.8 psi in Shot 9. Air pressure measured on the windward incline was about 18 psi and about 12 psi at the crown. In the tunnel entrance near the door, spikes in the pressure record of about 11 psi were measured. The earth pressures were generally between 10 and 20 psi on the arch, with a low of 2 psi near the leeward bottom edge. The maximum pressure was recorded near the crown on the leeward side. The leeward deflection of the arch is assumed to be responsible for this high pressure.

The major structural response for this shot was essentially elastic. The door was ripped off and hurled about 30 ft into the structure. This might account for the relatively low pressure in the entry. The entrance bulkhead was deformed and the bulkhead-to-tunnel connection failed. There is evidence that during the first 50 to 100 msec the windward foundation settled about 1.2 in. Some slippage along the laps of the corrugated sheet metal was noticed.

For Shot 10, the structure was located in the 8.1-psi overpressure range. The earth pressure over the front half of the structure was approximately 8 psi. Records from the gages in the leeward side were lost. The air pressure in the tunnel entrance near the door was only 4.5 psi. The door, which was redesigned after the failure that occurred in Shot 9, proved satisfactory. Unfortunately, deflection records were not obtained for Shot 10. The structure remained essentially elastic.

The end wall without entrance sustained serious deflection and probably represents the weakest component of the structure.

Except for the failure of the door in Shot 9, the structure remained operational and provided protection.

B.3.16 Project 3.16: Tests of Glazing and Window Construction
Agency: Bureau of Yards and Docks, USN
Report Title: Navy Structures, WT-729
Project Officer: LTJG P. J. McEleney, USN

The objectives of this project were: to determine the comparative resistance to blast of different types of window design, glazing, screens, inside curtains, and outside shields; and to

develop a window design with improved resistance or one that will swing open without damage when struck by blast.

The test items were located in three identical wooden structures at three ranges in Shot 9. The closest building was reglazed and tested in Shot 10. Each building contained a skylight and seven cubicles approximately 8 by 8 by 10 ft, three of which were partitioned to isolate partially the rear windows from the front windows. The buildings were anchored to deadmen by cables to provide restraint against blast loading and were painted with fire-retardant paint.

Glazing included: tempered safety glass, 1/4-in. plate glass, 3/16-in. window glass, double-strength wire glass, and double glass; 1/8-in., 3/16-in., and 1/4-in. plastic; and corrugated-wire glass. Windows were of double-hung, inswinging-casement, architectural-projected, pivoted, and inswinging hopper-vent types. Jalousies were installed on the exterior of some windows, while venetian blinds and curtains of different materials were hung inside. Instrumentation consisted of ordinary and high speed motion picture photography.

These structures were located as follows:

Structure	Shot 9		Shot 10	
	Distance from Actual GZ (ft)	Peak Side-on Pressure (psi)	Distance from Actual GZ (ft)	Peak Side-on Pressure (psi)
3.16a	7,600	3.3	7600	1.5
3.16b	12,500	1.5		
3.16c	20,000	0.6		

The structures themselves were undamaged when subjected to the blast from Shots 9 and 10, except for some loosened cables and slight scorching (see Fig. B.19). No convenient summary of the damage to the glazing and other elements can be given here because of the very large number and difference in character of the test items. Detailed information regarding the performance of the test items must be obtained from the project report.

The results of very-broad comparisons and evaluation of the test data are presented below as conclusions.

1. Of all glazing materials tested, 1/4-in. plastic and tempered glass offer the greatest resistance to blast when mounted in fixed, unprotected sash.
2. Jalousies mounted on the outside of windows give some protection, although some of the blast passes through the slats and damages the window without permanently deforming the jalousie.
3. The 1/4-in. wire mesh (hardware cloth) offered the best interior protection for stopping flying glass fragments. Heavy curtains made of tough fibers like cotton or wool may prove more effective in stopping fragments than fabrics made of glass fibers.
4. The advantages of inswinging sash were not definitely determined, although this type of sash seems to prevent glass breakage under certain conditions.

B.3.17 Project 3.18: Minefield Clearance
 Agency: Engineer Research and Development Laboratory
 Report Title: Minefield Clearance, WT-730
 Project Officer: Capt V. S. Adkins, USA

The general objective of this project was to study the detonation of pressure-activated land mines caused by the blast from atomic weapons. Specific objectives were: (1) to determine the applicability of the standard Universal indicator-mine probability constants to live mines; (2) to study the effect of sympathetic detonation of live mines; (3) to supplement the present knowledge of the effect of depth of burial on detonation; and (4) to correlate the actual mine-detonation patterns with the basic blast parameters.

Two thousand Universal indicator mines and 1200 live mines (the M6-antitank, the M15-antitank, and the M14-antipersonnel mines) were exposed to Shot 10 in various special patterns



extending out to 2700 ft from the intended Ground Zero. The antitank and indicator mines were buried at the following depths: 0, 1, 3, 6, 9, and 15 in. The antipersonnel mines were placed flush with the ground surface. The test area consisted of a strip 620 ft wide and 2100 ft long extending radially 600 ft from the intended Ground Zero. The indicator mines were placed in panels along the entire length of the field beside the live mine panels so that the indicator-mine readings and live-mine detonations could be correlated. To study the effect of sympathetic detonation, M6 mines were placed at a conventional spacing of 18 ft and a depth of burial of 1 in. in a belt extending almost the entire length of the field. To study the effect of the superposition of the pressure waves due to the long-duration air blast and the detonation of the mines, several rosette patterns consisting of single M6 mines surrounded by indicator mines at various radii were also tested.

As a result of this test, all antitank mines detonated out to a distance of approximately 1300 ft from actual Ground Zero. At roughly 1540 ft, all antitank mines buried at depths up to 6 in. detonated, while 40 to 80 per cent of the mines at the 9-in. depth and only 20 to 60 per cent of the mines at the 15-in. depth detonated at this range. At the next range, roughly 1790 ft, 20 per cent of the M6 mines at the 15-in. depth detonated, while none of the other M6 mines exploded. On the other hand, about half of the M15 mines at 0-in. and 1-in. depths detonated, with all others unexploded. No detonations occurred in the next panels at 2030 ft and the subsequent panels. One hundred per cent of the antipersonnel mines detonated out to 1645 ft, but at the next panel at 1900 ft, only 3 per cent of the mines detonated.

The indicator-mine readings did not correlate with actual incidence of detonation on the basis of calibration constants obtained from high-explosive (HE) tests. For example, for the M6 mines at 1-in. depths, the indicator mine results using HE-calibration constants would predict 100 per cent detonations at about 1100 ft, while the actual distance for 100 per cent detonation was about 1540 ft. The corresponding distances for 0 per cent detonation were roughly 1400 ft and 1800 ft.

The indicator mines also showed that out to about 1300 ft the response of all mines was essentially the same, except for the mines at 15-in. depths, which responded less; i.e. the deflection of the pressure plate was less. Beyond 1300 ft the response of the indicators at 6 in. seemed to be greatest.

The M6 mines placed in the continuous belt suffered incidence of detonation higher than that at corresponding distances in the isolated panels, thus indicating that sympathetic detonations did occur. In general, the range for a given percentage of detonation was extended about 200 ft beyond that given by the isolated panels.

The rise times of the pressure on the mines were very long compared to the response times of the mines assuming an immovable base; thus the mines probably felt essentially a static load. Correlation of incidence of detonation with known static behavior of mines is very good. Assuming static behavior, the pressures inferred from the indicator mine results compare favorably with measured pressures at the ground surface.

The indicator mine constants determined from HE tests cannot be used directly for nuclear bursts unless response characteristics of the live mines are very similar to those of the indicators. However, mathematical models can be used in conjunction with expected pressure functions to predict minefield clearance with good accuracy for many types of mines.

There will be a considerable decrease in mine response with increasing depth when the incident pressure wave has a sharp front and short duration; however, this condition occurs in regions of very high pressures so that blast-vulnerable mines like the M6 and M15 will be cleared, even when buried 15 in. below ground surface. In regions where the rise time is slow, no significant difference should be found with depths of burial down to 6 in., but a gradual reduction in response at deeper burial depths should occur. In the region where the incident wave is a sharp shock of long duration, the reduction in mine response with increasing depths of burial will be considerably less than in the short-duration case. This region is usually a region of low pressure so that mines may not be affected, i.e., this occurs beyond the precursor.

The radius of detonation of mines in conventional minefield patterns will be increased by sympathetic detonation. The effect of the increased detonation can be predicted with fair accuracy for a given mine at a given spacing by superimposing the blast wave from the mine upon

the nuclear blast wave and calculating the response on a spring model of the mine.

The clearance of pressure-activated mines can be determined with very good accuracy from the static-response characteristics of the mines and the expected incident pressure waves. In precursor regions the pressures required to detonate mines will be the static pressures (about 13 psi for M6 and M15 antitank mines, and about 11 psi for the M14 antipersonnel mines). In regions of long-duration pressure waves and sharp shock fronts, the required detonation pressures will theoretically be reduced to one-half of these values (7 psi for the M6 and M15 and 6 psi for the M14). Since infinitely sharp shock fronts will never actually be realized, a more realistic value would be two-thirds of the static pressures; i.e., 9 psi for the M6 and M15 and 7 psi for the M14.

B.3.18 Project 3.19: Effects of an Atomic Explosion on Trees in a Forest Stand
 Agency: U. S. Department of Agriculture
 Report Title: Blast Damage to Coniferous Tree Stands by Atomic Explosions, WT-731
 Project Officer: W. L. Fons

The objectives of this experiment were to: (1) determine the effects of atomic explosions on a stand of trees and isolated trees; (2) correlate experimental data with analytical methods of breakage prediction; and (3) study the shielding effects of a stand of trees upon the effects of an atomic explosion.

A stand of 145 ponderosa pine trees covering an area 160 by 320 ft was placed at approximately 6500 ft from Ground Zero. Isolated trees at 500-ft intervals in two radial rows 100 ft apart were installed from 5000 to 8000 ft. Tree pairs at each station were of substantially different periods. In addition a pair of trees was installed at 1500 ft, and a pair of pendulums at 5000 and 8000 ft. Average tree height was 51 ft and average diameter at the base was 15 in.

Instrumentation consisted of ground-level, 10-ft, and 60-ft pressure gages; pitot-type dynamic-pressure measurements; snubber-wire arrangements for the determination of deflections; accelerometers; strain gages; time-recording anemometers; and a wind-direction indicator. Still and motion-picture photography was also employed. See Fig. B.20.

Stations were located as follows:

Station	Shot 9		Shot 10	
	Distance from Actual GZ (ft)	Peak Dynamic Pressure* (psi)	Distance from Actual GZ (ft)	Peak Dynamic Pressure* (psi)
5000	4740	1.13	4850	0.30
5500	5240	0.90		
6000	5730	0.72		
6500	6230	0.58		
Stand	6460	0.52	6390	0.11
7000	6720	0.46		
7500	7220	0.37		
8000	7710	0.30	7850	0.055

*Computed from ground-level-measured, side-on pressure values.

On Shot 9 incidence of breakage of the isolated trees (31 out of 145) was about twice as great as predicted. No breakage occurred on Shot 10. The forest stand afforded complete thermal shielding beyond the fourth row of trees.

Close correlation between calculated and measured deflections for the isolated trees and between their predicted and actual breakage substantiates the generalized method of breakage prediction for isolated trees. Breakage and tree deflections within the stand were approxi-



mately twice the value predicted on an isolated tree basis. Consequently breakage predictions based on isolated trees appear to underestimate the actual incidence of breakage for small forested areas. A postshot view of the stand is shown in Fig. B.21.

Within the limits of instrumentation there is apparently very little or no attenuation of peak overpressure, peak dynamic pressure, or their respective impulse in stands several acres in area.

Tree and pendulum deflections, dynamic pressure measurements, and the close correlation of deflection results on a dynamic-impulse basis indicate that greater damage to certain drag-type targets will accompany low burst heights at the Nevada Proving Grounds for pressure levels below that at which the precursor disappears and extending to overpressures of at least 1.5 psi.

B.3.19 Project 3.20: Vulnerability of a Typical Tactical Communications System to Atomic Attack

Agency: Signal Corps Engineering Laboratories

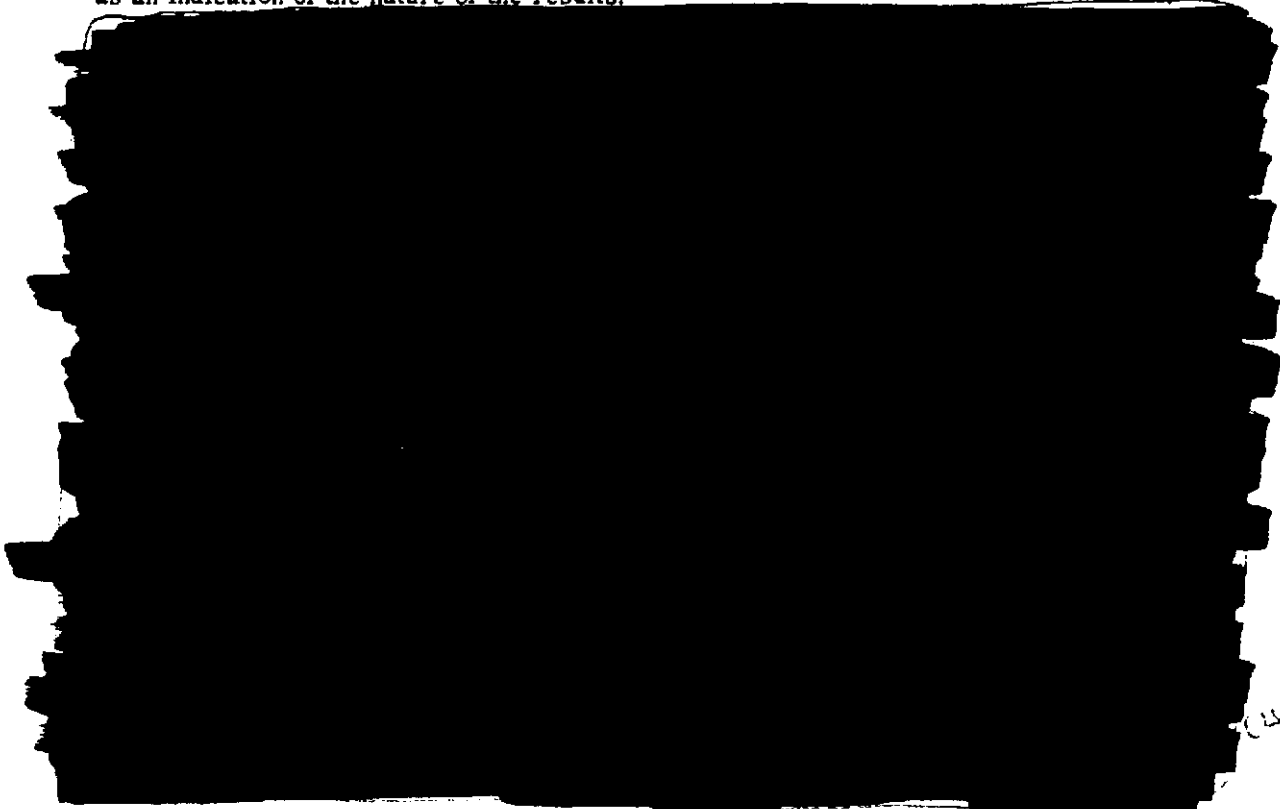
Report Title: Blast and Thermal Effects of an Atomic Bomb on Typical Tactical Communication Systems, WT-732

Project Officer: J. Eggert

The objective of this project was to subject selected items of Signal communications electronics equipment and material to air burst atomic weapons to determine the effects thereon.

Typical items of this equipment and material were exposed to blast, 93 test groups to Shot 9, and 17 to Shot 10. The test items included radial pole lines, transverse pole lines, separate poles without crossarms (both guyed and unguyed), 120-ft and 200-ft aluminum Signal towers, antenna systems, masts, buried and surface-laid wires and cables, and other items at various distances from Ground Zero. Several of the test items appear in Fig. B.22.

Reference should be made to the project report for a description of the test results, because of the vast number of individual items and the details of the different elements and the respective damage thereto. A brief description of damage to selected items is given here only as an indication of the nature of the results.



CLASSIFIED
1



USANCA
1

B.3.20 Project 3.21: Statistical Determination of Damage Criteria for Critical Items of Military Equipment and Supplies
 Agency: Ballistic Research Laboratories
 Report Title: Statistical Estimation of Damage to Ordnance Equipment Exposed to Nuclear Blasts, WT-733
 Project Officer: E. Bryant

The objectives of this project were to obtain statistical data on damage to certain ordnance equipment and to use this information to verify methods of damage prediction.

The equipment exposed in Shot 9 consisted of twenty-seven 1/4-ton trucks (Jeeps) (M38A1), twenty-seven 2 1/2-ton trucks (M35), and two 90-mm AA guns (M1A1). For Shot 10, eleven 1/4-ton trucks and eleven 2 1/2-ton trucks, twenty-seven 57-mm guns (M1), five 105-mm howitzers (M3), seven tanks (M3, M4, M7, and M24), and two 90-mm AA guns (M1A1) were tested. The test items were in general oriented side-on, face-on, and rear-on to the blast. The guns and howitzers were tactically emplaced.

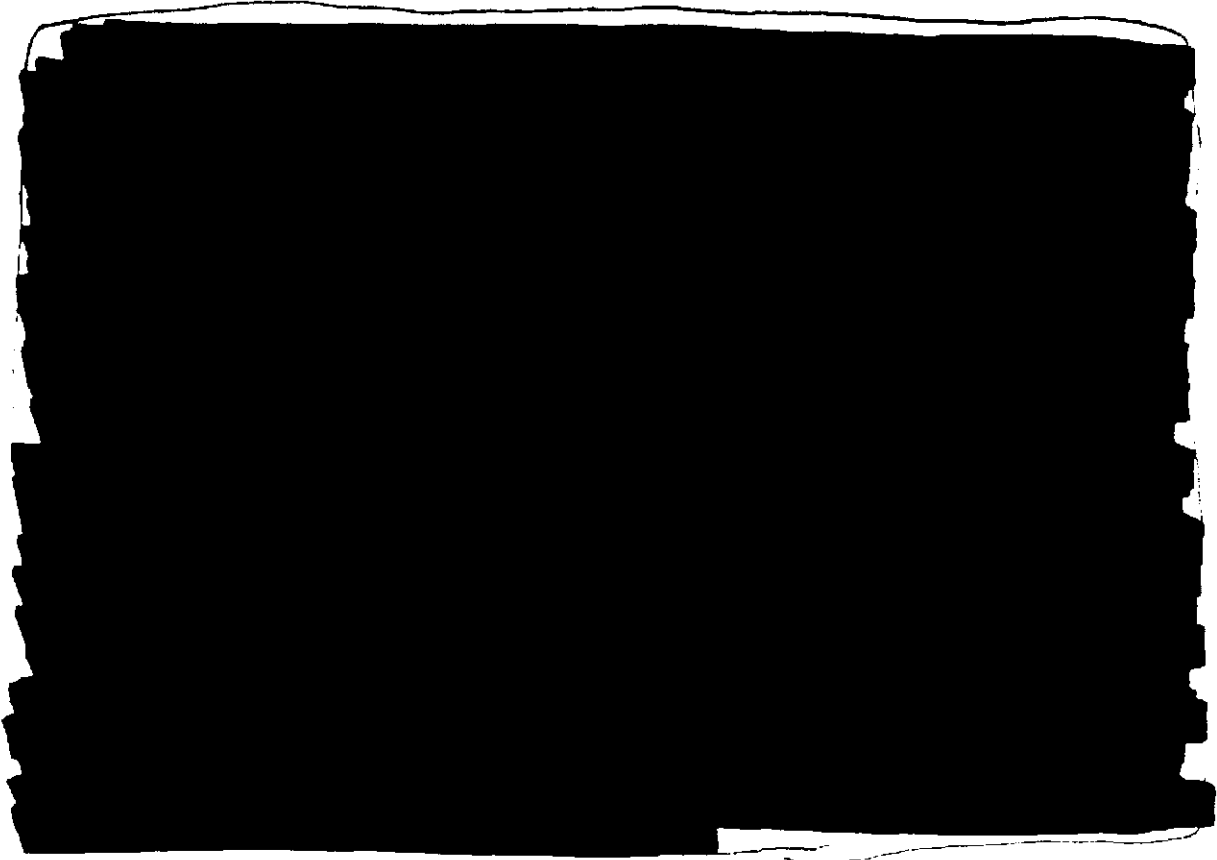
Instrumentation was provided to measure linear acceleration and angular velocity of several vehicles to determine their response. In addition, limited motion-picture coverage was provided for both shots.

The equipment was located as follows:

Test Items	Shot 9		Shot 10	
	Distance From Actual GZ (ft)	Peak Dynamic Pressure* (psi)	Distance From Actual GZ (ft)	Peak Dynamic Pressure* (psi)
1/4-ton truck (M38A1)	875-6550	2.6 max 0.5 min	900-4380	126-0.5
2 1/2-ton truck (M35)	875-6550	2.8 max 0.5 min	900-4380	126-0.5
90-mm AA gun (M1A1)	1500, 5200	1.7, 0.9	715, 3000	290, 1.9
57-mm gun (M1)			645-1240	430-4.9
105-mm howitzer (M3)			720-1265	290-36
Tank (M3)			1045	73
Tank (M4)			380-570	
Tank (M7-SP)			1415	23
Tank (M24)			715	290

*Estimated values.

UNCLASSIFIED



B.3.21 Project 3.22: Effects on Engineer Bridging Equipment
 Agency: Engineer Research and Development Laboratory
 Report Title: Effects on Engineer Bridging Equipment, WT-734
 Project Officer: Capt V. S. Adkins, USA

The purpose of this test was to determine the effects of an atomic-bomb blast on military-type, prefabricated, fixed bridging. The specific objectives were to: (1) determine the loading due to blast; (2) determine the weakest structural component in the bridges; (3) determine what level of damage may be tolerated without causing progressive failure; (4) establish a general analytical method to calculate the response of truss structures to atomic-bomb blast; and (5) investigate practical methods of limiting the structural response of a Bailey bridge to blast loading.

Two 100-ft-span, double-truss, single-story Bailey bridges were tested, one in Shot 9 and both in Shot 10. In Shot 9, the bridge was free to slide except for frictional resistance developed at the support; for Shot 10, the bridge at the greater distance from Ground Zero was welded to supports to increase the deformation in the truss, and the nearer bridge was again free to slide except for frictional resistance. These were mounted on piers so that the bottom chords were about 22 ft above the ground surface. See Fig. B.23.

In addition, two single-bay sections of a Bailey bridge and a T6 bridge were exposed to both shots. They were placed on the ground surface, unanchored.

In order to determine experimentally the resistance offered by the frictional forces to the sliding motion of the bridge, a pull test was conducted on a bridge section. The skids and channels actually used later in the field test of the bridge, which was allowed to slide in Shot 9, were so tested. The static coefficient of friction was found to vary between 0.5 and 0.6, while the dynamic coefficient (velocity of bridge with respect to support was about 1 ft/sec) varied between 0.25 and 0.3.

 RESTRICTED DATA

The results of the tests are summarized below:

Bridge	Shot	Distance to GZ (ft)	Peak Overpressure (psi)	Peak Dynamic Pressure (psi)	Average Rigid-Body Response (in.)	Remarks
100-ft Bailey	9	4100	7.75	1.52	43.5	No structural damage
1-Bay Bailey	9	1050	19.0	1.10		No structural damage
1-Bay T6	9	1050	19.0	1.10		No structural damage
100-ft Bailey	10	2000	10.6	>6	>240	Severe damage
100-ft Bailey	10	4250	4.1		*	No structural damage
1-Bay Bailey	10	1500	14.0		≈240	Severe damage
1-Bay T6	10	1500	14.0		≈120	Light damage

*This bridge was welded to supports.

For Shot 9 the 100-ft bridge was entirely within the Mach stem, so that the blast load was essentially horizontal. The ends of the bridge moved 30 in. and 57 in., or an average of 43.5 in. Skid marks indicate that there was no recovery, i.e. the motion was away from Ground Zero only. No plastic deformation was found in any of the bridge components. The single-bay sections of the Bailey and T6 bridges were also undamaged structurally, but were displaced as rigid bodies.

For Shot 10 the bridge at the greater distance, which was welded to the support, was undamaged. However, the bridge closer in was pushed completely off the piers. Evidence left by the skid marks indicate that the bridge was subjected to lift forces great enough to lift the windward side of the bridge from the support almost immediately and finally to lift a third corner of the bridge off the supports. Structural damage to the bridge was severe, but the direct effects of the blast cannot be separated from the effects of the 20-ft fall. See Fig. B.24.

The single bay Bailey bridge was moved about 20 ft and suffered severe damage to the components. The T6 bridge was moved about 10 ft and suffered only slight damage.

It was concluded that truss-type structures are drag sensitive; thus, predictions of damage should be stated in terms of dynamic pressure rather than peak overpressure, since dynamic pressure is not always uniquely related to peak overpressure. Damage from thermal radiation is not important for the size of weapon used in these tests.

Results from Shot 10 indicate that significant lift forces may be applied to bridges. Therefore a frictional-restraint anchorage alone is not satisfactory. An anchor cable that will give after a certain tension is reached appears to be a more satisfactory answer, and has the additional advantage that it can be connected to the bridge several feet out from the end, thus reducing the effective span.

The analysis indicates that the end-bay sway braces will be damaged before other components for single-story bridges of moderate or great spans. Rupture of the end-bay sway braces will, in general, result in the progressive collapse of the bridge. For double- or triple-story bridges, transom-clamp seats and rakers may be limiting factors, since their failure would allow the windward truss to lay over, thus causing collapse.

The sliding analysis of the bridge gave satisfactory results for the values of the parameters used.



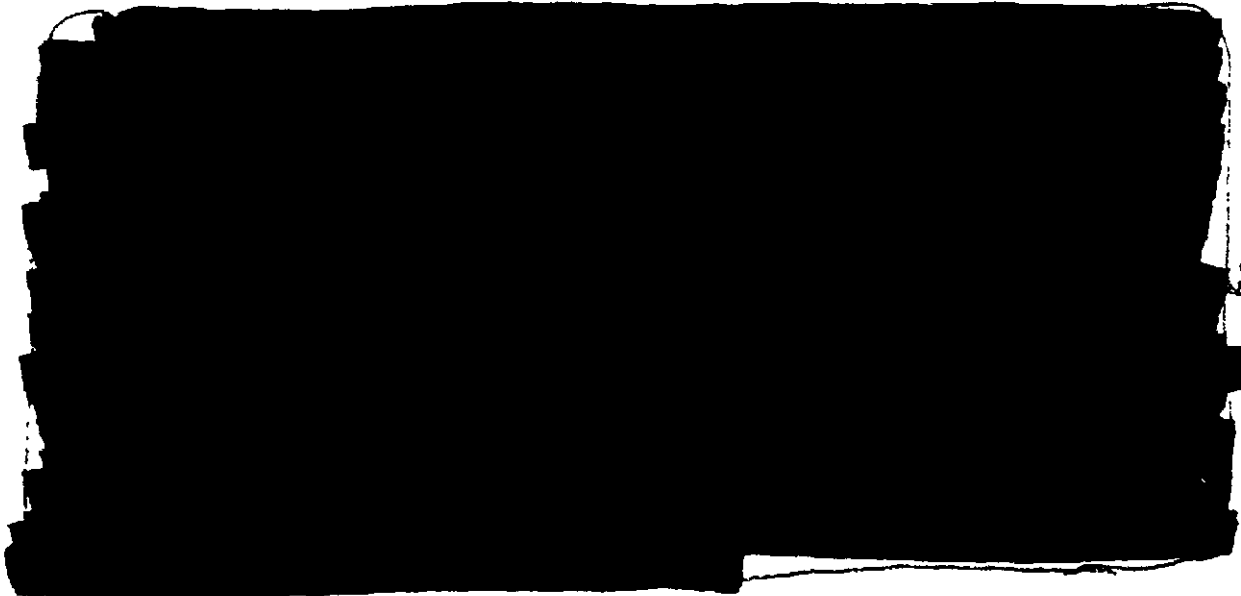
B.3.22 Project 3.24: Blast Effects on LVT's
 Agency: Naval Radiological Defense Laboratory
 Report Title: Effects of an Air Burst Atomic Explosion on Landing Vehicles Tracked (LVT's), WT-735
 Project Officer: Lt Col M. R. Olson, USMC

The objectives of the test were to determine the degree of blast damage which LVT's would sustain from an atomic air explosion and to determine, qualitatively, the degree of protection which these vehicles afford from the effects of such an explosion.

Six LVT's were exposed to Shots 9 and 10 at various distances and orientations (see Fig. B.25). Dosimeters were installed on the exterior and in the interior of each vehicle to obtain data on gamma-radiation-dose-reduction factor for these vehicles. For Shot 10 only, the two most-remote vehicles were instrumented with four Taylor maximum-minimum thermometers and four sets of thermal temperature-indicating papers to indicate the temperature rise within the vehicles. Motion-picture coverage was obtained for one vehicle for each shot.

The vehicles were located as follows:

Vehicle Position	Shot 9		Shot 10	
	Distance from Actual GZ (ft)	Peak Side-on Pressure (psi)	Distance from Actual GZ (ft)	Peak Side-on Pressure (psi)
1	775	22.3	1030	52.0
2	935	20.3	1210	30.5
3	1705	14.0	1525	14.0
4	2410	11.1	1880	9.1
5	2420	11.1	2575	8.1
6	4510	7.1	3450	5.8



USANC
1

B.3.23 Project 3.26.1: Test of the Effects on POL Installations
 Agency: Air Materiel Command
 Report Title: Test of the Effects on POL Installations, WT-736
 Project Officer: B. J. O'Brien

The objective of this project was to study blast and thermal effects of an atomic detonation on gasoline and oil storage depots and on containers.

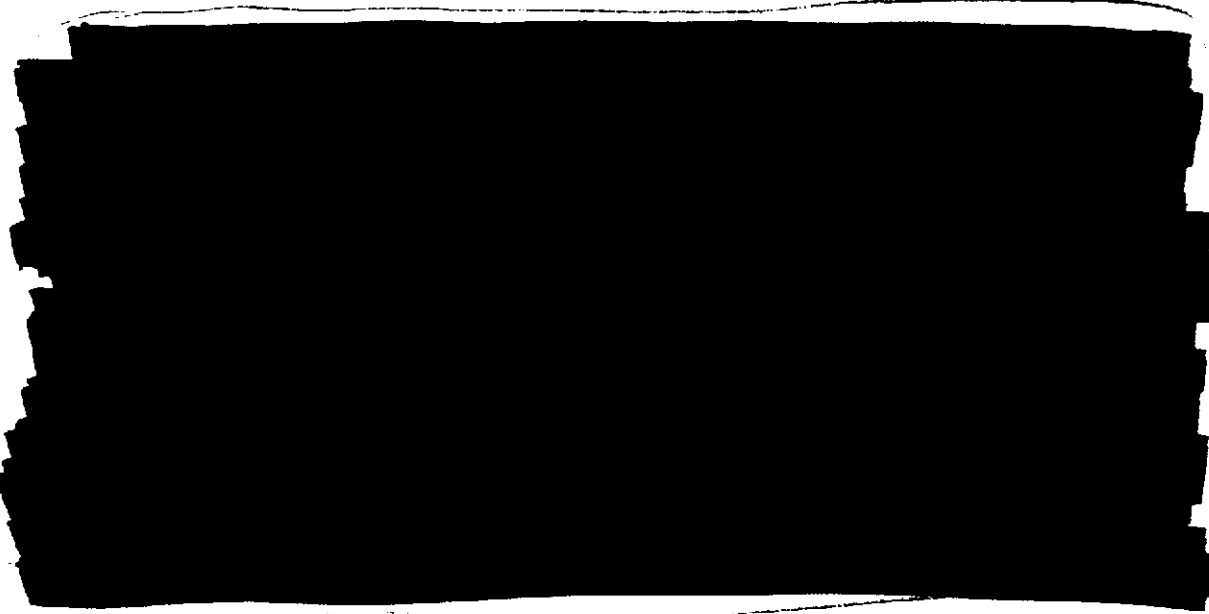


Test items included in Shot 9 and Shot 10 consisted of three categories: (1) groupings of standard 55-gal. storage drums filled with diesel fuel; (2) storage tanks filled with diesel oil or aviation gasoline, especially designed so that the fuel would either seep or flow rapidly from the damaged tank; and (3) vertical storage tanks of either welded or bolted construction; the roof-section of the welded tanks was designed to model the roof action of prototype storage tanks of the 120-ft diameter class, while the bolted tanks represented standard Army equipment. The number of items is too large for individual listing here; however, the extreme ranges and corresponding blast and damage phenomena are given.

The test items were located as follows:

USANCA 1

Item	Distance to GZ (ft)	Peak Overpressure (psi)	Thermal Energy (at normal incidence) (cal/cm ²)	Remarks
Stacked drums	1080-4590	18.7-7.1	122-32	Shot 9
Stacked drums	750-1570	118-13	510-160	Shot 10
Quick-opening tanks	244-4640	30-6.9	146-31	Shot 9
Storage tank, welded	1990-15,000	13-1		Shot 9, tanks 70 per cent full
Storage tank, welded	1640-15,000	12-0.7		Shot 10, tanks empty
Storage tanks, bolted	3560, 9920	9, 3		Shot 9, tanks 70 per cent full
Storage tanks bolted	4010, 9110	5, 1		Shot 10, tanks empty



USANCA
1

USANCA
I



B.3.24 Project 3.26.2: Effects of Atomic Weapons on a POL Supply Point
Agency: Quartermaster Corps, USA
Report Title: Tests of the Effects on POL Installations, WT-736
Project Officer: H. A. Stiles

The objective of this project was to determine the effects of an atomic explosion upon the following POL equipment: (1) cans and drums stored in the conventional manner for Quartermaster fuel dump; (2) cans and drums of gasoline protected by revetments, tie downs, and clamps; (3) collapsible gasoline storage tanks; and (4) can-cleaning equipment.

Each of the following items was exposed to Shot 9 at four different stations: (1) 55-gal. drums with and without protective cover, filled with gasoline or empty; (2) 5-gal. gasoline cans without protective cover, filled with gasoline; (3) two 900-gal. collapsible tanks filled with water, without protective cover, one of Marine Corps design and the other of Quartermaster Corps design, and (4) a 50-gpm pump circulating gasoline through a can-cleaning machine, without protective cover. A preshot view of the test items is shown in Fig. B.27

The 55-gal. drums, 5-gal. gasoline cans, and a Marine Corps 900-gal. collapsible tank were retested in Shot 10, the first two items at three stations and the Marine Corps tank at a fourth station

The locations were as follows

Station	Shot 9			Shot 10		
	Distance from Actual GZ (ft)	Peak Side-on Pressure (psi)	Thermal Flux (cal cm ²)	Distance from Actual GZ (ft)	Peak Side-on Pressure (psi)	Thermal Flux (cal cm ²)
1	2600	11	68	750*	140	≈400
2	3150	7.6	38	1080*	40	≈250
3	6800	4.3	16	1590*	11	125
4	10,000	2.7	7	2160†	8	92

*Drums and cans only
†900-gal. collapsible tank only (Marine Corps design).



USANCA
I





UJAN 1
1

B.3.25: Project 3.26.3: Effects of an Atomic Explosion upon an Amphibious Assault Fuel Handling System (Shore Phase)

Agency: U. S. Marine Corps
Report Title: Tests of the Effects on POL Installations, WT-736
Project Officer: Lt Col H. W. Sharpenberg, USMC

The objective of the experiment was to determine the resistance of equipment and materials of an Amphibious Assault Fuel Handling System to thermal and blast damage of an atomic explosion.

Equipment and materials of an Amphibious Assault Fuel Handling System were selected for testing. The components of the system are LVT-transported fuel tanks, shore unloading equipment, shore transfer equipment, dispensing equipment, and storage equipment. Some of the test items were rigid-aluminum and collapsible-synthetic-rubber tanks, hose, pumps, meters, nozzles, strainers, etc. A typical array is shown in Fig. B.28.

The equipment was located as follows:

Station	Shot 9			Shot 10		
	Distance from Actual GZ (ft)	Peak Side-on Pressure (psi)	Thermal Flux (cal cm ²)	Distance from Actual GZ (ft)	Peak Side-on Pressure (psi)	Thermal Flux (cal cm ²)
1	2675	10.8	66	750	135	300
2	4700	6.6	32	1080	37	235
3	5585	5.1		1590	10.7	125
4	7825	3.6				
5	10,150	2.7				



UJAN 1
1



WANCA
1

B.3.26 Project 3.27: Effects of Atomic Weapons on Field Medical Installations
Agency: U. S. Army Medical Field Service School
Report Title: Effects of Atomic Explosions on Field Medical Installations Equipment, WT-737
Project Officer: Lt Col E. S. Chapman, USA

The major objective of this project was to determine the effects of an atomic explosion on field medical installations, equipment, and personnel (as normally employed) and to determine the degree of protection which is afforded by placing such installations in dug-in positions.

Two types of composite field medical installations were displayed for Shot 9 at three distances from Ground Zero both in a standard aboveground position and in a dug-in position.

Unit Type A, a composite battalion aid station and regimental collecting station was established at Sites 1 and 2; unit Type B, a composite division clearing station, mobile army surgical hospitals, and evacuation hospitals, was established at all three sites. Each unit was established in the standard tentage authorized and contained all representative items of equipment authorized for those units. All of the equipment was arranged functionally within the installations and some of the equipment was operational at the time of the blast.

The location was as follows:

Installation	Distance from Actual GZ (ft)	Thermal Flux (cal/cm ²)	Peak Overpressure (psi)
1	4164	40	7.8
2	9000	8	2.7
3	15,000	1-2	1.0

Results of the test were highly satisfactory and demonstrated that casualty production and damage was severe at the most-forward site, moderate at the intermediate site, and mild to slight at the rear site. Pre- and postshot views are shown in Figs. B.29 and B.30.

Casualty incidence from all causes in medical installations of the types tested would have been about 98 per cent in both the above-ground and below-ground installations at Site 1, 10 to 27 per cent in the above-ground and 5 to 10 per cent in the below-ground installations at Site 2, and below 5 per cent for both types of installations at Site 3. At the site nearest to Ground Zero, the gamma radiation, thermal radiation, and burns from secondary fires would have contributed greatly to the high incidence of casualties. However, at the site furthest from Ground Zero, almost all of the casualties would have been due to flying missiles.

Medical-equipment maintenance personnel evaluated the key items of each site both before and after the blast. The general results of their study were:

Average Percentages of Equipment Undamaged or Repairable within the Unit

Unit	Site	Above ground	Below ground
A	1	50	25
A	2	95	100
B	1	64	55
B	2	66	96
B	3	99	100

A comparative analysis at each site indicated that 30 to 50 per cent greater protection for personnel and approximately 40 per cent greater protection for equipment is afforded by having these installations dug in or revetted. However if fires should occur, the percentage of casualties and damage to equipment may be greater for a dug-in installation.

B.3.27 Project 3.28.1: Structures Instrumentation
Agency: Ballistic Research Laboratories
Report Title: Structures Instrumentation, WT-738
Project Officer: J. J. Meszaros

For the purpose of obtaining structural loading data in connection with Program 3 of Operation UPSHOT-KNOTHOLE, Project 3.28.1 was given the responsibility of measuring transient physical phenomena associated with the blast loading of specially designed structures and a variety of test items. On Shots 9 and 10, a total of 892 channels of instrumentation were provided to secure information on air pressure, earth pressure, structural strain, displacement, acceleration, panel-time-of break, and angular velocity. Projects instrumented were those of the Army, Navy, Air Force, and Federal Civil Defense Administration.

An electronic system based on referenced phase modulation was used as the principal method of instrumentation, in conjunction with Wiancko air pressure, earth pressure and acceleration gages, and Baldwin SR4 strain gages. Originally designed by the Webster-Chicago Corp. for use by the Sandia Corporation on GREENHOUSE, this equipment required considerable modification before being put into operation on UPSHOT-KNOTHOLE. Twenty-seven of these magnetic tape recording systems, each capable of supplying 20 channels of information, were needed for the number of measurements made. In this manner a total of 798 channels of information were provided, of which 703 yielded readable records; the remaining 95 were lost because of damage to some of the test items and electrical failures in the recording equipment.

Forty-three self-recording accelerometers designed by Engineering Research Associates were used as backup measurements for the Wiancko electronically recorded accelerometers. With a potential of 86 channels, these instruments provided 42 channels of readable data.

In addition to four panel break measurements made for the Federal Civil Defense Administration on Shots 9 and 10, displacement measurements were successfully attempted using two different types of self-recording gages.

To determine the extent to which certain structural members were strained beyond their elastic limits, 1152 measurements were made with a 2 in. Whittemore strain indicator.

From the results of this and previous tests of a similar nature, it is evident that an electronic system based on the recording of phase modulated signals on magnetic tape is feasible for this type of instrumentation. However, the present Webster-Chicago system should be improved upon in several respects. First, it is doubtful that the limited frequency response of such a system justifies its use, considering its cost and bulk, and the number of skilled technicians required to operate it. In addition to improving the frequency response, it would be highly desirable to provide a more linear playback system.

For future operations, it is apparent that a development program is needed to explore the potentialities of self-recording mechanical type gages and to investigate the development of an electronic system combining the flexibility of magnetic tape recording with the reliability and simplicity of the conventional 3-kc carrier type instrumentation.

B.3.28 Project 3.28.2: Structures Instrumentation
Agency: Naval Ordnance Laboratory
Report Title: Pressure Measurements for Various Projects of Program 3, WT-739
Project Officer: W. E. Morris

The Naval Ordnance Laboratory instrumented various Program 3 projects for pressure-time histories. The instrumentation system consisted of Wiancko inductance gages, FM intelligence generation, and magnetic tape data storage. Pressure measurements were made on three aboveground structures, one underground structure, five foxholes, a diffraction study

layout around one of the aboveground structures, and a tree stand. The results of Shot 9 were excellent; 127 complete pressure-time records were obtained from the total of 128 stations instrumented. On Shot 10, forty-eight complete records and 48 partial records were obtained from the 105 stations instrumented. Broken cables caused by displacement of the structures accounted for most of the partial and total loss of records on this shot. The records were reproduced as pressure-time curves with pressure scales added and, along with instructions for record analysis and interpretation, were presented to the cognizant agencies for their analysis.

B.3.29 Project 3.28.3: Structures Instrumentation
Agency: Stanford Research Institute
Report Title: Pressure Measurements on Structures, WT-740
Project Officer: L. M. Swift

Project 3.28.3 of Operation UPSHOT-KNOTHOLE was concerned with the measurement of pressures existing on the surfaces of various nonresponsive structures from Shots 9 and 10. The experiment plan and the analysis of data were not a portion of this project, but the data were used in computation of structural loading and response under air blast. A secondary portion of the project was the definition of air blast conditions existing at the time of measurement.

A total of 143 satisfactory records were obtained from the two shots, a 99.3 per cent performance. Secondary air blast records were analyzed, and the results were published for the use of other projects.

B.3.30 Project 3.29: Tests of Four FCDA Curtain Wall and Partition Structures
Agency: Federal Civil Defense Administration
Report Title: Blast Effects of Atomic Weapons upon Curtain Walls and Partitions of Masonry and Other Materials, WT-741
Project Officer: B. C. Taylor

The objective of this test was to observe and determine the absolute and relative blast resistance of exterior and interior wall panels.

A group of continuous test cells were built with concrete floor slabs and reinforced concrete walls and roofs. Some idea of the cells may be obtained from Figs. B.31 and B.32. The front walls of three cells at the extreme right were used for panels under Project 3.5. The panels were 10 ft high and varied in length from 10 to 20 ft, the majority being 16 ft long; a large group contained steel sash. Test panels were installed on both the windward and leeward faces, and the cells also contained one or two interior partitions.

The exterior panels were reinforced concrete, reinforced and unreinforced brick, unreinforced cinder block, and various combinations of brick, clay tile, and cinder block. The interior partitions were cinder block, stud and plaster on metal lath, solid plaster, and removable steel. Various types of edge support were used.

Instrumentation included air pressure gages, displacement gages, and time-of-break gages on selected panels. In addition, the entire project was covered with 40 motion picture cameras.

This experiment was successful to the extent that the damage was substantially greater at the forward location than at the rear, permitting a bracketing of the range of pressure likely to damage much of the construction involved.

There was some additional damage due to Shot 10, mostly to rear walls where the front wall had been blown out previously, or to panels for which some damage had been noted after Shot 9.

Detailed evaluation of results has not been completed, but a few generalizations are possible. Walls with 20 per cent window openings (where the glass breaks) are much more blast resistant than walls without openings. Walls with these openings allow sufficient pressure to enter to wreck interior partitions of normal construction.

B.3.31 Project 3.30: Air Blast Gage Studies
Agency: Ballistic Research Laboratories
Report Title: Air Blast Gage Studies, WT-742
Project Officer: J. J. Meszaros

The purpose of Project 3.30 of Operation UPSHOT-KNOTHOLE was to test self-recording gages for the measurement of pressure-time and peak pressure in connection with air blast waves from nuclear explosions.

To accomplish this purpose, prototypes were manufactured for three types in quantities of 10 to 30 (see Fig. B.33). They were employed in numerous ways to determine their characteristics, limitations, and capabilities. A nylon arcing initiation device was used on the pressure-time gages to start the recording time after the detonation of the device.

The pressure-time gages were accurate to ± 10 per cent and recorded pressure-time curves similar to those obtained by more expensive electronic instrumentation. The pressure-time gages were accurate to ± 10 per cent, and no initiation device was needed.

The components of the gages tested form a basis for other gages to measure pressure-time phenomena, underwater pressure, ground shock, acceleration, and temperature. It was concluded that gages of the type tested can give useful data, on tests requiring shorter and longer blast lines, with sufficient accuracy and for less expenditure of money than possible with other types of instrumentation.

E.4 PROGRAM 4—BIOMEDICAL EFFECTS

Program Director: E. Pinson, Col, USAF

E.4.1 Project 4.1: Evaluation of the Hazard of Flying Through the Atomic Cloud
Agency: Air Force Cambridge Research Center
Report Title: The Radiation Hazard to Personnel Within an Atomic Cloud
Project Officer: Capt P. M. Crumley, USAF

The general objective of Project 4.1 was to define and evaluate the importance of the various potential hazards to which a flight crew in a military aircraft would be exposed upon flying through the atomic cloud from an atomic explosion minutes after detonation. The specific objectives were to measure (1) the radiation dose and dose rate by means of various dosimeters and ionization chambers in the atomic cloud in parachute-borne canisters and in QF-80 (drone) aircraft, (2) the radiation dose due to inhalation of fission products received by monkeys and mice flown in a ventilated pressurized compartment in these drone aircraft, and (3) the nature of the pressure variations, and turbulence in the cloud during passage of the drone aircraft. The procedure to attain these objectives was (1) to drop canisters through the atomic cloud when the cloud was at approximately 25,000 ft mean sea level (MSL) and at ± 8 minutes after detonation, (2) to stabilize the aircraft at the altitude, and (3) to fly drones through the cloud at 30,000 and 32,000 ft between +3 min and -7 min, the exact time of penetration being determined by the time the cloud was at these altitudes. The most uncertain aspect of the operation was the rate of rise and position of the cloud with sufficient accuracy to permit dropping canisters and drones. Participation in three shots was planned, but weather conditions permitted participation in only two shots; namely, Shot 4 of 10 KT yield and Shot 9 of 28,000 ft MSL.

Two of the canisters passing through the cloud at about 28,000 ft MSL in Shot 9 registered a maximum dose rate of 7.5 r/sec and 10.6 r/sec, respectively. The other canisters were not obtained due to failure in hitting the cloud or to failure of the telemetering equipment. Integrated radiation doses obtained by a film badge on the canisters hitting various parts of the Shot 9 cloud at the altitude and time were 77, 120, 180, and 200 r. The latter value was obtained on a canister passing through the center of the cloud. Since the canisters passed through the cloud vertically at a rate of 150 ft/sec at this altitude, it is estimated that an aircraft traveling 400

STET

through the cloud horizontally at this time would accumulate a radiation dose between one-half and one-third that registered on the canisters.

One drone passing through the Shot 4 cloud at 30,000 ft (MSL) at +4.5 min showed a maximum radiation dose rate of 2.1 r/sec and received an integrated dose of 11.3 r. A similar 30,000 ft (MSL) penetration on Shot 9 at +6.8 min showed an integrated dose of 29 r, the rate meter being malfunctional. A 32,000 ft (MSL) penetration on Shot 9 at +5.2 min gave a maximum rate of 2.8 r/sec and an integrated dose of 21.3 r. The length of time inside the visible cloud was not accurately known.

Although there is a factor of about two in the scatter of data, the combined GREENHOUSE and UPSHOT-KNOTHOLE experience on cloud and stem penetration at relatively early times suggests that the average dose rate in flying through an atomic cloud is independent of yield. For the time interval of 2.7 to 25 min after detonation, the data may be represented by $D = 1.31 \times 10^5 \times t^{-2.06}$, where D is the average dose rate in roentgens per hour and where t is the minutes after detonation.

The internal radiation dose to the lungs of a man due to inhalation of fission products during cloud passage in the three penetrations mentioned above amounted to an upper limit value of only 240 mr and, therefore, would have been insignificant both in actual amount and in comparison with the external dose received. It was shown that the alpha radiation hazard from unfissioned Pu²³⁹ and U²³⁵ and long-lived, bone-seeking fission products was also insignificant.

Temp tapes on the skin of the drones did not reach 65°C, the minimum recordable temperature during cloud passage. Pressure changes and associated turbulence of sufficient magnitude to endanger the crew or the aircraft did not exist in the cloud at the times of drone penetration on these tests.

The above results suggest that personnel in a pressurized aircraft flying at 400 knots or more which passes through the cloud of an atomic bomb of 30 KT yield or less at times greater than 4 min after detonation will receive a total external integrated radiation dose of less than 50 r. The internal radiation dose due to inhalation of fission products during such a passage is insignificant even when the air passing through the pressurized compartment is unfiltered and the crew members are not wearing oxygen masks. Any provision of filters in the aircraft cabin air intake or on the individuals' oxygen equipment appears to be an unwarranted precaution against an essentially nonexistent hazard.

B.4.2 Project 4.2: Air Blast Injuries
Agency: Naval Medical Research Institute
Report Title: Direct Air Blast Exposure Effects in Animals, WT-744
Project Officer: Capt R. H. Draeger, USN

Project 4.2 was designed to study direct air blast injury from atomic weapons in animals in the pressure range of 20 to 50 psi.

Two animal species of widely different sizes (rats and dogs) were selected in an attempt to compare levels of direct blast injury in small and large animals. It was expected that the comparative tolerances of such different exposure subjects to atomic air blast would help differentiate the roles played in blast injury by abrupt shock fronts and high peak overpressures as opposed to positive phase duration and impulse loading, whose relative importance was not clear from previous experience with high explosive (HE) blast experiments.

For test exposure purposes the animals were placed in 26-in.-diameter aluminum cylinders open at both ends in order to provide limited protection against missiles, thermal radiation, and ionizing radiation while permitting relatively free access to the air blast wave. Although it was realized that some attenuation of the external pressure-time relations might be expected to occur within the exposure cylinders, it was anticipated that actual measurement of the air pressure histories to which the animals were subjected would provide satisfactory data for analytical correlation. For this purpose small self-recording air pressure recorders whose action was initiated by a timing signal and which utilized sensitive diaphragm pressure detecting elements with a time resolution estimated to be approximately 4 msec were alongside the animals in a number of exposure cylinders.

UNCLASSIFIED DATA

Two hundred rats were exposed to 24 to 30 psi overpressures in this manner on Shot 9, where the air blast physical measurements described clean cut blast waves approaching idealized shock wave form in the region of the biomedical blast exposure equipment. Autopsy findings showed moderate lung hemorrhage in most animals undoubtedly due to direct air blast, as the pathological findings were consistent with those seen after primary blast injury suffered from high explosive concussion waves in the laboratory.

On Shot 10, 700 rats and 56 dogs were similarly exposed. In the precursor region measured values of dynamic pressure were higher than those which would be calculated from measured values of peak overpressure using normal shock relations. The exact relations between the various parameters of the blast wave under precursor conditions have not yet been established. However, it appears that the measured dynamic pressures in the dusty region were at least equal to those which would have been predicted for low heights of burst over surfaces free of thermal effects. Due to drag forces many of the cylinders were displaced or damaged, and their contents were destroyed. Because of this and a further error of underestimating the effect of gamma and especially neutron fluxes received at the close-in distances of the biomedical cylinders, most of the animals were dead upon recovery (H + 4 hr), and those living were in a state of severe shock. Only 12 rats found scattered in the exposure area were recovered, and autopsy of these and of 50 recovered dogs revealed no trauma or lung hemorrhage indicative of direct air blast injury despite the rough treatment and high overpressures to which the animal specimens were subjected.

Examination of the pressure recordings taken within the cylinders and a review of pressure records made at equivalent ranges by other projects on Shot 10 confirmed the presence in that shot of a marked precursor pressure wave and of a slow rise time with serious perturbations of the idealized shock wave in the region of animal exposure. Peak pressures ranged from 105 psi at the innermost animal station to 16 psi at the outermost station on Shot 10.

Comparison of the pressure records and autopsy findings from Shots 9 and 10 led to the tentative conclusion that exposure to a pressure wave of slow rise time at a given pressure level under the conditions of blast exposure experienced in Shot 10 does not produce as much lung (blast) injury as the same peak pressure associated with an abrupt rise time, such as was experienced in Shot 9 and in experimental exposures to HE blast waves. However, a possibility that the more dramatic results of Shot 9 might have been due to a reflected pressure peak within the exposure cylinders could not be ruled out because of the low time resolution of the self-recording pressure gages placed in the cylinders with the animals.

B.4.3 Project 4.5: Flash Blindness
Agency: USAF School of Aviation Medicine
Report Title: Flash Blindness, WT-745
Project Officer: Col V. A. Byrnes, USAF

One objective of Project 4.5 was that of evaluating the efficacy of a filter system, which might be used as a lens in a sun glass or spectacles frame, for protecting the dark-adapted eye of man against retinal burns and reducing the time of flash blindness on exposure to an atomic-bomb flash. These filters have a negligible transmissivity for electromagnetic radiation of wave length less than 6000 Angstroms and more than 9000 Angstroms. Visible light is transmitted through these filters mainly in the red and orange region of the visible spectrum. Red-lighted cockpit instruments can be easily read through these filters. At the same time the filters, when worn, will reduce by about 75 to 80 per cent the energy in the combined visible and infrared region of the bomb spectrum which reaches the eye. When looking at the initial flash of an atomic bomb through these filters, burning of the retina may be prevented in instances where it might otherwise occur if the eye were not so protected. These filters also reduce the time of temporary flash blindness by about 25 per cent. For this latter purpose the filters appear less efficacious than for preventing retinal burns. Temporary flash blindness is associated with the bleaching effect of light on visual purple in the retina, a reversible chemical reaction. Reducing the amount of light entering the eye by means of the filters does not reduce proportionally the length of the time required for recovery of normal visual functions. Thus

the filters are useful in reducing or avoiding retinal burns from atom bombs and are helpful in reducing the time of recovery from flash blindness.

Another objective of this project was to determine the threshold distance and/or thermal flux intensity which would produce a burn on the retina of dark-adapted rabbit eyes exposed to an atomic-bomb flash. Retinal burns were obtained in the eyes of rabbits exposed at distances from 2 to 42.5 miles from Ground Zero. The size and severity of the retinal burns obtained appeared to vary with the yield of the bomb and inversely with the distance of the animals from Ground Zero. The burn injuries to the rabbit retinæ were assessed by clinical, photographic, histologic, and biochemical means.

Although differences in the physical and physiological factors between rabbit eyes and human eyes suggest that rabbits might experience retinal burns more readily than man, the data presented indicate that the retinal burn hazard of the bomb flash to man extends out to considerable distances. Retinal burns have been observed to occur in the unprotected eyes of man when exposed to the flash of an atomic bomb at distances up to 10 miles in SNAPPER and in an accidental exposure in UPSHOT-KNOTHOLE. That such burns may occur at greater distances is a distinct possibility. At distances greater than 10 miles the image of the fireball is small, and, consequently, the retinal area subjected to possible burning is small and likely of limited consequence in so far as impairment of vision is concerned, except in the rare instance where it might occur on the macula or area of central scotopic vision.

B.4.4 Project 4.7: Measurement of Beta Hazard in Bomb Contaminated Areas
Agency: USA, Office of the Surgeon General
Report Title: Beta-Gamma Ratio in the Postshot Contaminated Area, WT-746
Project Officer: Lt Col J. T. Brennan, USA

The objective of Project 4.7 was to determine the military significance of certain theoretical calculations based on idealized geometries which indicated that, in a bomb-contaminated area, the beta radiation dose to the skin should far exceed the gamma dose at all points in air less than about 2 meters above ground level. Because technical and theoretical considerations have mitigated against the feasibility of constructing a quantitatively accurate beta survey dosimeter for field use, it was felt that a direct measurement technique was required in order to determine whether current permissible radiation schedules and hazard control policies, based essentially on the measurement of gamma dose only, are acceptable.

The present experiment was designed to measure the beta and soft gamma radiation dose that would be received by the sensitive layers of skin that underlie the dead and unresponsive cornified outer skin surface always present. Measurements were made in several areas in Frenchman Flat and Yucca Flat contaminated by fallout from nuclear detonations from 4 hr to 40 days previously. Specially constructed ion chambers with thin walls designed to be equivalent in absorbing power to the epidermal layer of the skin were used to detect all beta particles and gamma rays that could penetrate to the sensitive layers of skin. These chambers were employed at various heights above ground in free air, and their readings were compared with readings similarly taken with conventional Victoreen chambers, whose thick walls discriminate against betas and soft gammas and allow an estimate to be made of the beta difference, which may be compared with the theoretical predictions. Chambers also were exposed in grooves along the sides of a masonite "phantom" of man to determine the shielding effect of man's body on the skin dose of soft radiations. Similar exposures with the chambers covered with thicknesses of conventional military clothing then demonstrated the protective effects of clothing against the beta and soft gamma flux. Further placement of chambers within shoes was designed to evaluate the protection afforded by shoes against the relatively high beta radiation expected near the ground surface.

It was found that although there is an increase in the radiation dose received by the thin-walled chambers in free air at points near the ground, the very large beta hazard predicted by theory does not actually occur in the field. The most probable explanation is that the theoretical calculations necessarily deal with a uniformly contaminated perfectly plane surface in which there is no masking of beta radiation by surface irregularities, whereas this is not the case in

the field. Furthermore, some of the betas predicted by theory (probably a small portion) are soft enough to be absorbed in the walls of even the thin-walled chambers, although they presumably carry no beta hazard to the skin either. In addition, the walls of even the conventional Victoreen chambers allow passage of some of the more energetic beta rays, and they further allow passage of some Bremsstrahlung radiation, which is a reflection of the beta field. As a result of these latter considerations, the ratio of dose measured with the thin-walled chamber minus that measured with the conventional chamber divided by that measured with the conventional chamber (thin-thick/thick) will be less than the true beta-to-gamma dose ratio at the location of the measurements. The data showed a maximum soft radiation dose in free air near the ground about 5 times the dose measured with Victoreen chambers, and the effect of the man phantom was to cut this soft radiation dose to about one-half the free air value at any given height. The further protection of field clothing was on the average a factor of 2, whereas shoes protected by three or more times. The result of the decreasing soft radiation dose with increasing elevation combined with these protective effects located the point of maximum soft radiation hazard in the normally clothed man as on the lower leg just above the shoe top.

Because the erythema dose of skin for betas (or very soft gammas) is about three times the median lethal dose of gammas for humans, it was concluded that the maximum beta dose of two and one half times the gamma dose recorded with the use of the "naked" man phantom did not warrant the development of further personnel external radiation monitoring devices beyond the existing devices sensitive predominantly to gammas. This conclusion was further supported by the knowledge that in most actual field exposure conditions the additional protection afforded by clothing against betas and soft gammas would be present.

The conclusions drawn from this experiment apply only to the situation measured, namely, the soft radiation hazard in the air over a desert surface contaminated with fallout. Other geometries, such as city streets or ship decks, and other surfaces, such as metals or pavement, may give rise to higher ratios of soft radiation to hard radiation than are indicated by these data. Furthermore, this experiment in no way attempts to define the contact beta skin hazard that may arise when radioactive fallout particles fall directly onto the skin or are pressed directly against it, nor does it consider the problem of the relative hazards from hard and soft radiations emanating from a contaminated object removed from the fallout radiation field.

B.4.5 Project 4.8: Biological Effects of Neutrons
Agency: Naval Radiological Defense Laboratory
Report Title: Biological Effectiveness of Neutron Radiation from the Nuclear Artillery Shell in Free Air and in Foxholes, WT-747
Project Officer: Lt R. E. Carter, USN

Project 4.8 was designed to determine the biological effectiveness of neutron radiation from the gun type assembly nuclear device, detonated in Shot 10, both on the surface of the ground as a function of distance from the burst point and in conventional-sized foxholes as a similar function of distance.

Biological measurements were made on mice according to the techniques previously used at GREENHOUSE and TUMBLER-SNAPPER and included studies of organ weight loss, changes in the total white blood cell count, changes in the uptake of radioactive iron in erythrocytes, and determination of mortality as a function of time after exposure. Animals were shielded from gamma radiation by ventilated hemispherical lead shields of 7-in. wall thickness. Estimates by AFSWP indicate that animals within these shields may demonstrate 50 per cent or less of the neutron effect they would show had they been exposed to the neutron radiation from the weapon in free air. The attenuation of the biological effect by the lead shields may also vary with the neutron spectrum and hence with distance from Ground Zero. Animal exposure units were placed at varying distances from the indicated Ground Zero along the surface of the ground and also in foxholes, where the animals beneath the shields were positioned 42 in. below the ground surface.

Results indicated that the shielding afforded by the foxholes reduced the biologically recorded neutron dose by a factor of 3 as compared with ground surface measurements, but con-

STET

sideration of the role played by the lead shields suggests the foxhole protection factor may be significantly greater than 3. Satisfactory data were obtained for all biological parameters, both in the foxhole stations and in the stations on the ground surface. The value of rem per sulfur-measured neutron obtained from the artillery-shell device was lower than that previously obtained from similar animal exposures to 30-in. implosion type fission weapons, where rem was taken as "roentgen equivalent mammal" as determined by the various biological indicators used. This suggested possible neutron spectral differences from the more conventional weapons over the distances studied, which was to be expected from the nature of the gun device.

For the ground surface stations over the gamma radiation range of 100 to 800 r, the neutron radiation effect in rem, calculated with the assumption that the mice "saw" 50 per cent of the external neutron biological effect, appeared to about equal that of the gamma radiation dose in roentgens. The mean survival time of the neutron-irradiated animals was short (average of 3 days), and a relative protection of the bone marrow as compared with soft tissue structures was apparent. These findings are in keeping with previous observations.

In the foxholes neutron radiation appeared to be the dominant biological hazard at all distances of biological interest. Here the neutron radiation effect in rem, assuming that the mice inside the lead shield "saw" 50 per cent of the external neutron biological effect, appeared to equal about three or four times the gamma radiation effect to be expected in the bottom of these foxholes.

It was suggested by the project authors that although data obtained in this experiment and in previous experiments using the mouse have served as a valuable initial survey of weapon neutron radiation effect, large animal neutron studies are required in order to extrapolate animal data quantitatively to man, the point of ultimate interest.

B.5 PROGRAM 5—AIRCRAFT STRUCTURES TESTS

Program Director: K. H. Stefan, CDR, USN

B.5.1 Project 5.1: Naval Aircraft Structures

Agency: Bureau of Aeronautics

Report Title: Atomic Weapons Effects on AD Type Aircraft in Flight, WT-748

Project Officer: CDR K. H. Stefan, USN

The objective of Project 5.1 was to study the blast and thermal effects of atomic weapons on AD type aircraft in flight. Data covering weapons effects and airplane structural response to these effects were collected for the aircraft in level flight attitude, tail toward the blast in a vertical plane containing the burst point. This orientation represents an escape configuration of an AD type aircraft following delivery of an atomic weapon.

One or the other of two Navy Model AD's converted to drone configuration was flown on Shots 1, 2, 7, 8, and 9. The slant ranges at burst time involved in these shots varied from 14,400 ft for the AD-2 piloted flight of Shot 1 to 6200 ft for the AD-2 pilotless flight of Shot 7. In Shot 7 the actual yield exceeded the planned yield by greater than 30 per cent. The drone aircraft was positioned for near critical weapons effects, and the higher thermal radiation severely weakened all the blue painted skin on the underside of the wing. Both the port and starboard wing panels were torn off at the time of shock arrival as a result of the weakened skin and combined overpressure and gust effects. A considerable amount of valuable information on thermal damage was obtained from these panels, which were recovered after the test. Visual inspection of the structural failures indicated that the aircraft might have survived had the bottom skin of the wing been bare aluminum or painted with heat resistant white instead of standard blue.

In addition to the above flight tests, aluminum alloy panels of various thicknesses and paint finishes were exposed at three different stations on the ground during Shot 9 to obtain supplemental information on the effects of thermal radiation. Effective thermal absorptivity coefficients obtained ranged from 0.12 to 0.16.

Measured overpressures were in agreement with the theoretical values. Measured thermal radiation was observed to be appreciably greater than predicted as a result of ground re-

flectivity. Thermal calculations using $\beta = 0.55$ (albedo) provided good correlation with test measurements. Peak aircraft accelerations were approximately double the calculated values, although measured wing and tail loads were in close agreement with the loads calculated using rigid body relations.

No direct correlation between measured and calculated aircraft skin temperature rise was established, although the effects of heat received, skin thickness, and surface finish were apparent. Results of metallurgical studies on aircraft skin specimens, begun in an attempt to determine skin temperature rise on Shot 7, indicated effects normally associated with temperatures far in excess of those recorded. This effect was so localized that no serious structural consequences in excess of those normally associated with the thermal intensities experienced are expected.

B.5.2 Project 5.2: Blast, Thermal, and Gust Effects of Aircraft in Flight
Agency: Wright Air Development Center
Report Title: Atomic Weapon Effects on B-50 Type Aircraft in Flight, WT-749
Project Officer: R. C. Lenz

Project 5.2 was established to determine minimum operational parameters for delivery of atomic weapons from medium bombardment aircraft. Three B-50D airplanes were selected and instrumented for the measurement of peak overpressure, thermal radiation, and wing tip deflection. One of the airplanes was further instrumented for the measurement of wing, fuselage, and stabilizer bending moments; angular and linear accelerations; and elevator positions.

A flight pattern was established so that the positions of the three B-50's simulated the position which would be occupied by a bomb-dropping airplane relative to the point of detonation of the weapon. Attainment of this position was confirmed by aerial mapping techniques from the test aircraft.

Gust loading of the horizontal stabilizer was determined to be the limiting structural parameter of the B-50 airplane for delivery of atomic weapons. The extent of this limit was closely defined by the attainment of 79 per cent of design limit bending moment at Station 98 of the horizontal stabilizer on Shot 9.

Sufficiently precise and extensive data concerning the effects of atomic weapons on the B-50 were obtained to enable accurate definitions of general operational parameters for delivery of atomic weapons with this airplane. In addition, the information is of such nature that it may be used in the correlation and correction of theoretical analyses which serve to extend the results to generalized problems of atomic weapon delivery involving other types of aircraft, positions in space, and other ranges of weapon yield.

Wing bending moments predicted on the basis of the current theoretical analysis were found to be consistently twice as large as the actual wing bending moments measured in this experiment.

B.5.3 Project 5.3. Blast and Gust Effects on B-36 in Flight
Agency: Wright Air Development Center
Report Title: Blast Effects on B-36 Type Aircraft in Flight, WT-750
Project Officer: G. F. Purkey

Project 5.3 obtained data on the blast response of a B-36D aircraft flown in the proximity of Shot 9. The test aircraft was the same B-36D aircraft utilized for similar testing by Project 6.10 during IVY. The instrumentation was modified to include additional measurements on the horizontal tail. Response measurements included nose, tail, wing tip, and center of gravity accelerations; wing fuselage and horizontal stabilizer bending moments; and horizontal stabilizer shear. Peak overpressure at the aircraft was also measured.

The purpose of the program was to supplement the blast response data obtained during the IVY tests and particularly to investigate more fully the aft fuselage and horizontal stabilizer response characteristics. The purpose was accomplished even though the peak loads obtained were not as high as desired. The peak stabilizer bending moment measured was 34 per cent

of limit load. Peak wing bending moments were somewhat higher than those measured during IVY but were still only a fraction of the limit allowable. The data obtained by Project 5.3, combined with previous data, will allow a complete check of the present blast/load theory in the low and medium load ranges. Theoretical extrapolation to loads approaching design limit should be confirmed by additional experimental data.

The position of the aircraft at blast arrival was such that the reflected shock wave arrived 4.44 sec after the direct shock wave; and, because of fortuitous phasing with low amplitude vibrations initiated by the direct shock, the peak loads produced by the reflected shock were slightly higher than would be predicted from a single shock with the strength of the reflected shock. However, with proper phasing and shorter time interval between shocks, the reflected shock could induce peak loads considerably higher than those obtained from the direct shock.

The data obtained by Project 6.10 in IVY are included in the report of this project.

B.6 PROGRAM 6—TESTS OF SERVICE EQUIPMENT AND OPERATIONS

Program Director: D. I. Prickett, Lt Col, USAF

B.6.1 Project 6.2: Test of Radar Techniques for Accomplishing IBDA
Agency: Wright Air Development Center
Report Title: IBDA Phenomena and Techniques, WT-751
Project Officer: F. E. James

The objective of this project was to evaluate current experimental techniques and equipment designed to accomplish Indirect Bomb Damage Assessment (IBDA). Specific objectives were as follows:

1. To determine the amount by which a radar beam is refracted by the fireball.
2. To compare the relative merits of Ku-band fast scan radar to Ku-band and X-band slow scan equipment.
3. To determine the adaptability of Airborne Moving Target Indicator (AMTI) equipment to the IBDA problem.
4. To evaluate a system of computing height of burst utilizing the time difference between arrival of a direct and ground reflected low frequency electromagnetic signal generated by the detonation and received in an aircraft.

The refraction experiment, conducted on Yucca Flat, utilized a main radar transmitter, 15 receiver stations, and a synchronizing radar station for remote control of the main radar transmitter. The receivers and synchronization station were located for each tower shot along a line perpendicular to a line from the main radar transmitter through the shot tower. The amount of refraction caused by the growth of the fireball was indicated by a shift of the main radar beam along the receiver line. It was determined that the amount of refraction was not significant and could be ignored in IBDA reduction procedures.

The fast and slow scan Ku-band radar, AMTI radar, electromagnetic receivers, and bhang-meters were operated from three B-29 aircraft oriented for each shot in the same relative positions to Ground Zero. The fast scan radar gave better time resolution to fireball return phenomena, but detail was lost due to antenna and power limitations. High interference levels prevented the obtaining of useful results with the AMTI equipment. The radar techniques tested, such as fast scan and AMTI, are all desirable and could probably be used in an IBDA system to assist in obtaining the required Ground Zero parameter. However, none of the techniques individually or collectively can be considered important enough to warrant the development of a special system for IBDA utilizing these techniques. When future bombing equipments include these techniques as part of their system, Ground Zero will probably be obtained with greater ease and accuracy than with the present AN/APQ-24 and K series bombing systems. The use of the electromagnetic wave is not considered practical for height-of-burst determination at this time. However, when more is known about the characteristics of electromagnetic pulse from an atomic detonation, further development and refinement of techniques might prove productive.

B.6.2 Project 6.3: Field Test of IBDA
Agency: Strategic Air Command
Report Title: Interim IBDA Capabilities of Strategic Air Command, WT-752
Project Officer: Capt R. E. J. Scott, USAF

This project was a corollary to Project 6.2 in that an interim IBDA system, installed in operational SAC aircraft, was evaluated in connection with simulated strike missions. These simulated strike missions, flown by B-50, B-47, B-36, and F-84 type aircraft, also served to provide valuable and realistic indoctrination for SAC air crews.

Ten to 12 SAC aircraft participated in nine shots. Each aircraft carried current type radar bombing equipment and K-17 cameras. Several bhangmeters were also utilized. Photographic records and interpretation techniques employed by SAC show that they have satisfactorily developed an IBDA capability for determining height of burst and Ground Zero from the K-17C camera, i.e., photography during day or night visual conditions. Yield determination for this system can be obtained by utilizing bhangmeters. Their radar technique studies indicate that radar photography has the potential to supply Ground Zero and height of burst regardless of visibility conditions. The limiting factors are, for Ground Zero, adequate crew training in techniques; for height of burst, the yield and altitude combination must be such that there is adequate ground disturbance from the shock wave, and the cloud shadow effect must be discernible. Present stockpile weapons, if detonated at reasonable heights, should provide the necessary phenomena. The possibility of developing a technique to determine yield from radar records of the shock front or fireball growth time history are still under study by both WADC and SAC.

B.6.3 Project 6.4: Evaluation of the Chemical Dosimeter
Agency: Chemical Corps Chemical and Radiological Laboratory
Report Title: Evaluation of Chemical Dosimeters, WT-753
Project Officer: J. Johnston

The objective of this project was to evaluate, under field conditions, the E-1 tactical dosimeter, which is the latest version of the Taplin chemical dosimeter.

On Shots 7 and 8 a total of some 250 dosimeters were placed at eight separate thermal and blast shielded stations along the Project 6.8 dosimeter line at distances calculated to cover the entire range of the dosimeter. Results were evaluated against film exposed in National Bureau of Standards film holders. Dosimeters were recovered at H + 30 hr on Shot 7 and H + 2 hr on Shot 8. Field results combined with laboratory findings show that the E-1 dosimeters indicated within the correct range, were rugged, consistent, and showed little if any rate dependence. This dosimeter is considered to have reached its full state of development with the exception of mechanical and step range modifications.

B.6.4 Project 6.7: Electromagnetic Radiation over the Radio Spectrum
Agency: Signal Corps Engineering Laboratory
Report Title: Measurements and Analysis of Electromagnetic Radiation from Nuclear Detonations, WT-754
Project Officer: Lt W. T. Kertulla, USA

This project had two main objectives: (1) to determine the characteristics of electromagnetic radiation from nuclear detonations and (2) to determine the feasibility of detecting electromagnetic radiation from prenuclear detonations (Oxcart I).

Both experiments were performed primarily for information on scientific phenomena, with the knowledge that there exists practical military applications if any reliable characteristics can be systematically recorded and explained.

Results of previous experiments of related design have shown the 0 to 20 mc band to be the area of strongest signal return. Antennas, oscilloscopes, and related equipment were designed to permit evaluation of polarization, pulse amplitude, and time duration of the recorded signals in this low frequency band. The Oxcart I phase utilized pulse delay lines between antenna and

oscilloscope, which, when triggered on a Blue Box, would record any prenuclear electromagnetic signals occurring immediately prior to the detonation.

The data when analyzed did not indicate any correlation between pulse characteristics, such as amplitude, duration, shape, etc., and yield. Neither did there appear to be any common characteristic which could be said to be typical of the pulse from a nuclear explosion. Polarization data were insufficient to determine a definite plane of polarization; however, the available data do not support the idea that the plane of polarization is vertical. No definite conclusions were drawn from the Oxcart I data obtained at Nevada; however, subsequent experiments with high explosives demonstrated that no HE signals of interest exist prior to the main nuclear signal because of their low signal strength and time resolution relative to the nuclear signal.

B.6.5 Project 6.8: Evaluation of Radiac Instrumentation, Equipment, and Operational Techniques

Agencies: Signal Corps Engineering Laboratory and Bureau of Ships

Report Title: Evaluation of Military Radiac Equipment, WT-755.

Project Officer: J. M. Johnston

The purpose of this project was to test under field conditions the accuracy, reliability, practicability, and desirability of various service sponsored radiac instruments. These included rate meters and dosimeters, the majority of which were in the final developmental stage. In addition the project provided radiac instrument repair support for the Rad-Safe organization, film badges developing for Desert Rock, and instrument calibration facilities.

Radiac instruments were evaluated by conducting ground surveys in radiation fields up to 500 r/hr. Some 150 qualified service personnel were employed and rotated in weekly increments of 12 to 15 after attaining their maximum radiation exposure. Their comments, observations, and recorded data along with maintenance, repair, and modification records were utilized in the final evaluation of the instruments. In addition, numerous instruments were utilized by Desert Rock troops and by air crews of participating aircraft and their evaluation duly recognized.

Dosimeters were exposed in the prompt radiation fields of all shots. Some 12 to 14 stations located to cover the range of the dosimeters were utilized. These portable stations were designed with aluminum thermal and blast shields. All dosimeters were compared to film exposed in NBS film holders. The film standards were calibrated against a known calibration source of Co⁶⁰. Dosimeter readings were accomplished by numerous personnel, and results were cross-checked. All dosimeters were recovered about H + 2 hr, with the exception of one or two shots where fallout prevented recovery for several additional hours.

The two survey instruments of primary interest, the AN/PDR-32 and IM-71/PD, were found to require additional development and engineering work. The AN/PDR-32 models were preproduction units, and changes were recommended to improve the instrument before full-scale production is attempted. The IM-71 was found to require some development work, but, primarily, the IM-71 requires production engineering. It was recommended, however, that, following the development changes, preproduction engineered models of the IM-71 be procured and submitted for service testing by Army Field Forces. No further field testing of radiac instruments at NPG is warranted until preproduction test models, completely engineered, are available and have been accepted by the interested service laboratory.

The dosimeter evaluation indicated that two tactical and one administrative dosimeter have reached developmental maturity and are ready for final production engineering and package design. The DT-65 Polaroid and E-1 chemical tactical dosimeters were found to have reached an acceptable state of development, within the limitations of the device. If some difficulties with rate dependence and pressure sensitivity can be corrected, the IM-91 tactical dosimeter would be a good tactical dosimeter for service use. The DT-60 administrative dosimeter was tested on BUSTER. During UPHOT-KNOTHOLE an attempt was made to evaluate the Admiral reader for the DT-60. It was found that the reader requires additional design and development work before being accepted. Some of these deficiencies had been corrected at the time of writing of the project report. One significant recommendation for future dosimeter testing is that more

care be taken to evaluate the dosimeter accuracy in residual fields and that future dosimeter evaluation programs include a comprehensive analysis of dosimeter response to residual radiation fields.

B.6.6 Project 6.8a: Gamma Exposure Vs Distance
Agency: Signal Corps Engineering Laboratories
Report Title: Gamma Exposure Vs Distance, WT-756
Project Officer: Peter Brown

The objective of this report was to measure prompt gamma radiation as a function of distance. In addition, gamma measurements were made for any requesting project.

Data were obtained from film packs in NBS energy corrected film holders and were calibrated against a Co⁶⁰ source. To obtain normalizing factors from a Co⁶⁰ source to an atomic explosion, film was exposed to the Co⁶⁰ field calibration unit and then to a 10 Mev betatron whose radiation spectrum is believed to approach that of an atomic detonation. Corrections for neutron flux effects on film badges were made for Shot 10 data out to 2000 yd. from Ground Zero. Neutron flux effects on other shots were less than 5 per cent; therefore no corrections were made. No measurements were made on Shots 4 and 11, and Shot 2 data are felt to be low due to absorption caused by a concrete mass in the cab on the gamma line side of the tower. It is felt the results as presented in the 6.8a report are accurate to within ±20 per cent.

B.6.7 Project 6.9: Evaluation of Airborne Radiac Equipment
Agency: Bureau of Aeronautics
Report Title: Evaluation of Naval Airborne Radiac Equipment, WT-757
Project Officer: CDR J. H. Terry, USN

The purpose of this project was to re-evaluate Naval Airborne Radiac equipment which had been modified in accordance with BUSTER-JANGLE recommendations. This equipment was designed to record radiation levels above terrain, correct for variables, and permit rapid extrapolation to the ground for the plotting of ground contamination contours. In addition, new ideas in droppable flares, telemetering units, and flashing lights to indicate ground radiation levels were tested.

On all contaminating events a P2V aircraft with the permanently installed instrumentation made aerial surveys over the contaminated areas at H + 1 hr. Telemetering units were dropped on the evening of D Day and morning of D + 1 on three shots. Flares and flashing lights were tested at H + 1 on one shot only.

Results indicate that the airborne equipment functioned as designed, but operational techniques and equipment are much too complicated for the accuracy of the results obtained. Insufficient results were obtained from the flares, telemetering units, and flashing lights to make a firm conclusion, but the system of flares or flashing lights appears to be a practical approach to the problem of indicating high radiation levels on the ground from air observation.

B.6.8 Project 6.10: Rapid Aerial Radiological Survey
Agency: Signal Corps Engineering Laboratories
Report Title: Evaluation of Rapid Aerial Radiological Survey Techniques, WT-758
Project Officer: Lt J. R. Price, USA

This project had the objective of developing a system of estimating ground contamination from aerial survey by utilizing standard portable rate meters in light aircraft.

Standard portable survey meters were carried in both helicopters and fixed wing light aircraft. A clover-leaf pattern was flown over the contaminated area at H + 1 hr on all events having extensive contaminated areas. The flight pattern developed during JANGLE and SNAPPER was simplified and refined to permit a more rapid survey.

It was shown that ground contamination levels can be plotted from the air, using light aircraft and standard radiac survey equipment, with the results obtained being accurate within a factor of 10. No further work on this system is considered justified at this time.

B.6.9 Project 6.11: Operational Training for TAC Crews
Agency: Tactical Air Command
Report Title: Indoctrination of TAC Air Crews in the Delivery and Effects of Atomic Weapons, WT-759
Project Officer: Lt Col J. W. Rawlings, USAF

The objective of TAC participation was to indoctrinate air crews in the problems of tactical delivery of atomic weapons and direct bomb damage assessment using aerial photography techniques. In addition, an attempt was made to obtain data on aircraft skin temperature rise utilizing temp tapes on the skin of the aircraft.

To indoctrinate the air crews, T-33 aircraft were positioned and flown to simulate recommended escape maneuvers. RF-80 aircraft were used to fly a standard photo reconnaissance mission to evaluate direct bomb assessment techniques.

Satisfactory indoctrination was obtained on one of the two shots in which TAC participated. The photo reconnaissance mission was performed satisfactorily, and photographic results were excellent for bomb damage assessment studies. The temp tapes were evaluated by WADC; however, no conclusive results were obtained since temperature rise was not greater than that which could have been caused by direct and reflected solar rays.

B.6.10 Project 6.12: Determination of Height of Burst and Ground Zero
Agencies: Army Field Forces and Evans Signal Laboratory
Report Title: Determination of Height of Burst and Ground Zero, WT-760
Project Officer: Lt Col R. V. Tiede, USA

With the advent of tactical support of ground troops by atomic weapons, the Army Field Forces indicated a need for a system to determine location and yield of nuclear weapons. The objective of this project was to evaluate the following systems in ability to fulfill this requirement:

1. Artillery sound ranging equipment for location of Ground Zero.
2. Seismic wave velocity determination of height of burst.
3. Flash ranging for location of Ground Zero and determination of height of burst.

Sound ranging stations were located up to 60,000 meters from Ground Zero. The system was comprised of three separate microphone arrays several miles apart along a line perpendicular to the line from the center of the array to the burst point. The sound ranging provided better results for air burst than for near surface detonations. For air bursts at ranges of 20,000 to 60,000 meters, an angular standard deviation of 13.8 min of arc and radial location error of 0.61 per cent were obtained. Calculation of the burst point required approximately 30 min after sound arrival.

Seismic geophones were operated approximately 8 to 10 miles from Ground Zero on all shots. An attempt was made to record a thermal induced seismic wave as well as the blast induced signal. Results were inconclusive.

Flash ranging cameras were located on a line roughly perpendicular to the lines of sight to the various Ground Zeros at a range of 8 to 12 miles. Pinhole cameras and Polaroid film were used to photograph the fireball. By triangulation from the surveyed camera locations, points of burst within an average accuracy of 0.75 miles were obtained; this required 5 to 10 min of calculation after removing the Polaroid film from the cameras.

Conventional bhangmeters gave yields within 20 per cent to distances of 40 miles.

B.6.11 Project 6.13: Effectiveness of Fast Scan Radar
Agency: Navy Electronics Laboratory
Report Title: Effectiveness of Fast Scan Radar for Fireball Studies and Weapons Tracking, WT-761
Project Officer: R. B. Keeran

The objective of this project was to evaluate the effectiveness of a new developmental fast scan X-band radar for phenomenology studies of nuclear detonations and to attempt to track the 280-mm projectile.

This Naval radar gave 20 antenna revolutions per second and provided excellent time resolutions for fireball shadow studies. The van-mounted equipment was tested on Shots 7 to 10. Presentation of radar return was made on a PPI and B scope and photographed.

The familiar "horse-shoe" shaped pattern was noted in some shots, whereas in others the pattern was missing, there being a complete blanking of all targets in the immediate area of the fireball. It was recommended that any future developmental radar designed for fireball phenomena studies have a higher bearing resolution of approximately 45° azimuth coverage and at least 50 scans per second.

Missile tracking on the gun shot was not possible due to the high ground clutter.

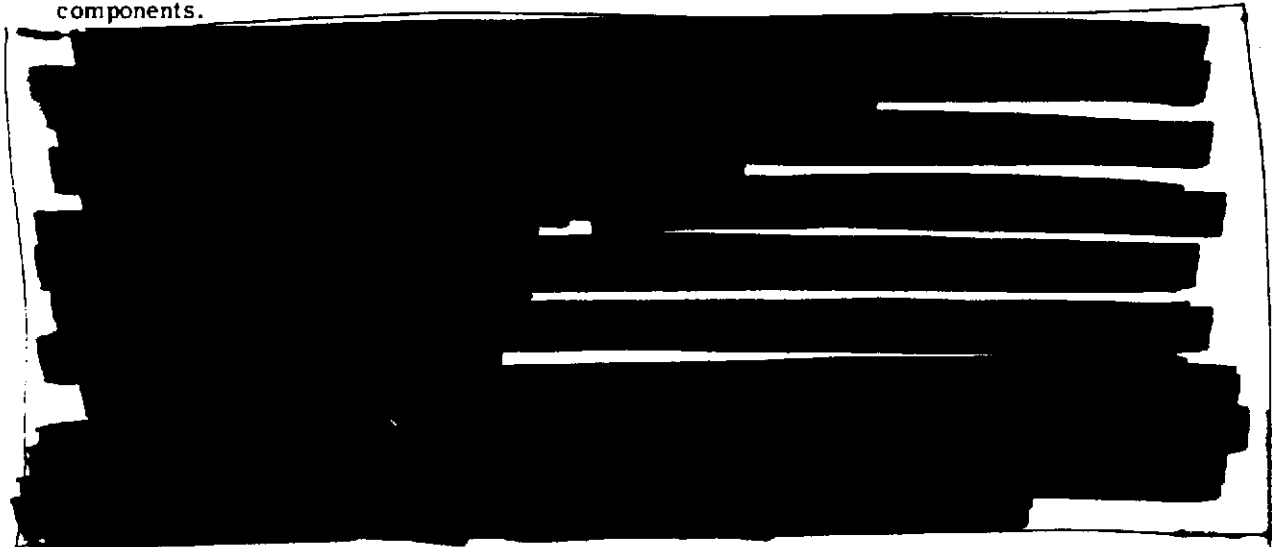
B.7 PROGRAM 8—THERMAL MEASUREMENTS AND EFFECTS

Program Director: R. G. Preston

B.7.1 Project 8.1a: Aircraft Structures Tests
Agency: Wright Air Development Center
Report Title: Effects of Thermal and Blast Forces from Nuclear Detonations on Basic Aircraft Structures and Components, WT-766
Project Officer: Capt G. T. James, USAF

The objective of this project was twofold. Primarily, it was designed as an integral part of the long-range WADC research and development program to establish design criteria for future atomic weapons delivery aircraft. The secondary, and more immediate, objective was to improve the state of knowledge pertaining to the delivery capability of present day delivery aircraft and to effect modifications to increase this capability.

The experimental procedure followed was to expose, at various ranges from Shots 9 and 10, basic and critical aircraft structures and components for obtaining their time history of temperature and strain responses. Specimens tested were 8 box beams, 8 tension ties, 13 horizontal stabilizer and elevator assemblies, and 6 aircraft panels. Additional measurements for peak temperature only were made on 31 aircraft panels, a B-36 stabilizer and elevator assembly, a B-36 wing section, 212 control surface protective coverings, and 89 undercarriage components.



B.7.2 Project 8.1b: Aircraft Structures Tests
Agency: Wright Air Development Center
Report Title: Additional Data on the Vulnerability of Parked Aircraft to Atomic Bombs, WT-809
Project Officer: Capt G. T. James, USAF

USAF
(b)(3)
(u)

This project was specifically aimed at the determination of the protection afforded parked aircraft exposed to atomic detonation by thermal radiation shields and strong tie-downs, and to



obtain additional data on certain fighter and bomber aircraft in the nose-on orientation.

A B-17, B-29, B-45, F-86, and four F-47's, all of which had been used in previous tests except the B-29, were exposed in six shots for a total of 16 aircraft exposures. The instrumentation included extensive temperature determination on all exposures as well as considerable high-speed motion picture photography.

The more obvious conclusions obtained from this experiment were:

1. In those high overpressure regions where a relatively high degree of damage is sustained, strong tie-downs apparently reduce the amount of damage to fighter aircraft in the nose-on orientation.

2. Cloth thermal shields were observed to have provided protection from thermal radiation and thermal-blast coupling. It is anticipated that these shields will be far more effective protection against higher yield weapons where thermal radiation becomes relatively more critical than blast energy.

3. Data obtained in this test provide further confirmation of related data from TUMBLER-SNAPPER.

B.7.3 Project 8.2: Measurements of Thermal Radiation by Means of Radiation Pressure Phenomenon
Agency: Air Force Cambridge Research Center
Report Title: Measurement of Thermal Radiation with a Vacuum Microphone, WT-767
Project Officer: M. D. O'Day

The objective of this project was to evaluate a vacuum capacitor microphone as a device for measuring thermal radiation from the bomb. Signals generated in the microphone by the pressure of the radiant energy, which is related to the radiant intensity, are amplified electronically, fed to an oscilloscope, and recorded on magnetic tape. Overheating of the capacitor diaphragm by the incident thermal radiation is avoided by the use of a chopper operated at 1400 cycles/sec and, if the assembly is close to the detonation, by the use of neutral density filters interposed before the microphone. The amplitude of the output is related to the intensity of the radiant energy. Total thermal energies may be obtained by integrating the curves of intensity vs time.

Project 8.2 participated in Shots 1 to 10. The recording equipment was contained in two vans which were manned and located within view of the detonations. Sensing equipment was located at distances from 1 to 14 miles from the burst point.

As the result of the extensive participation of this project, a large amount of thermal data was obtained. Calculated thermal yields for this project correlate well with those of NRDL and NRL. Project 8.2 times to the minimum agree well with EG&G bhangmeter times (see Secs. 3.3.3 and 3.3.4).

Since the chopping rate of the vacuum microphone may be quite high, the instrument may be designed to yield values for times to minimum and second maximum in the radiant pulse. Further analysis of thermal yield data for this and past Nevada tests is necessary before the accuracy of the instrument for measuring thermal yield may be judged (see Sec. 3.3.3).

B.7.4 Project 8.4-1: Attenuation of Thermal Radiation by White Scattering Smoke
Agency: Chemical and Radiological Laboratories
Report Title: Protection Afforded by Operational Smoke Screens Against Thermal Radiation, WT-768
Project Officer: E. H. Engquist

The objectives of this project were dual: first, to evaluate the attenuation of thermal radiation by an operational fog oil smoke screen and, second, to collect data to verify theoretical predictions concerning the attenuation expected.

It was planned to conduct the field test of the white smoke (scattering smoke) on Shot 9. When it became necessary to delete the white smoke experiment at the last minute, due to unfavorable surface winds, a limited experiment using a single instrumented station surrounded by smoke pots was incorporated into Shot 10. Instrumentation for the attenuated ther-

mal radiation employed NML roundels, NRDL disc calorimeters, Chemical Corps black ball calorimeters (these three types of instruments were arranged for detecting spherical dissymmetry), and photographic coverage for the determination of the volume-density characteristics of the screen.

As the result of the drastically curtailed experiment incorporated into Shot 10, the objectives of this project were only partially attained. Based upon the thermal energies measured beneath the smoke and after due allowance was made for the shielding of the scattering smoke by the Project 8.4-2 black smoke, interference by which was shown through analysis of the photographic records, it was estimated that the oil-fog smoke screen, as established, was attenuated by 85 to 90 per cent. Edge effects due to the limited size of the screen were not evaluated. Also, verification of theoretical predictions concerning the attenuation was not possible.

B.7.5 Project 8.4-2 Effects of Black Absorbing Smoke on Thermal Radiation and Blast
Agency: Chemical and Radiological Laboratories
Report Title: Evaluation of a Thermal Absorbing Carbon Smoke Screen, WT-769
Project Officer: E. H. Engquist

The objective of this experiment was to provide a relatively thick heated layer of air over a blast measurement line. This was accomplished by laying a carbon black thermally absorbing smoke over a line east of target zero for Shot 10 between 500 and 4600 ft from the target point. It was intended to study the effect of the heated layer on the shock wave, particularly the precursor pressure wave.

Instrumentation of the black smoke line was similar to that of the white smoke described in Sec. B.7.4 except that roundels were not used because they would be rendered useless by deposition of smoke particles on the energy sensitive papers. In addition to thermal radiation instrumentation, the smoke line was instrumented for blast and for the velocity of sound to measure air temperature. Two poles, one set at 2600 ft and the other at 3500 ft from intended Ground Zero, were equipped with shielded, temperature-sensitive papers at vertical intervals of 5 ft up to 72 ft in an additional effort to measure air temperature.

Due to the absence of a low capping inversion, which might have been attained with a shot time set for earlier in the morning, diffusion upward of the thermally absorbing smoke was greater than was desired for the comparatively low burst height for Shot 10. Ideally, it would have been desirable for the screen to have been capped strongly and uniformly at a height well below the height of the bottom of the fireball. In spite of this deficiency the shielding of the ground from significant thermal fluxes and the absorption of radiant energy in the relatively nonuniform smoke layer resulted in profoundly altering the shock front characteristics over those observed in the open.

The net effect of the smoke screen was to modify the precursor type wave under the absorbing layer and to reduce comparatively the range over which the precursor effect was observed in the open. The reduced thermal effect on the shielded ground surface resulted in peak pressures and arrival times of the shock wave more nearly like that which would be predicted for a thermally reflecting surface. At the instrumented stations between 2630 and 5630 ft from Ground Zero, the thermal energy observed was less than 3 per cent of that which would have been observed without smoke. Air temperatures in the screen at 2600 and 3500 ft ground ranges at heights up to 72 ft above the surface did not rise to the minimum detectable value of 60°C. At this height, however, it was calculated that the temperature rise should have been less than 1°C.

B.7.6 Project 8.5 Degree and Extent of Burns Under Service Uniforms
Agency: Quartermaster Research and Development Laboratories, USA
Report Title: Thermal Radiation Protection Afforded Test Animals by Fabric Assemblies, WT-770
Project Officer: J. F. Oesterling

The objectives of Project 8.5 were to obtain immediate information on the skin burn protection value of a limited number of service and experimental clothing combinations, and to

provide data which can be used to establish a relation between fabric protective characteristics as determined in the field and protective characteristics as measured in the laboratory. It is anticipated that the results of these experiments, coupled with results of related laboratory programs, will lead to the development of a technique whereby the protective value of clothing may be assessed by physical means directly in the laboratory without resorting to physiological experiments or field tests.

In order to accomplish the above objectives, two types of animal exposure were made. In the major effort animals were exposed to the thermal pulse and ensuing blast wave in clothing of standard or experimental armed services uniforms. In the other case animals were exposed in cylinders provided with fabric-covered portholes, which duplicated the exposure arrangement used in the laboratory.

Of the several summer and winter uniform assemblies evaluated at Shots 9 and 10, two exhibited substantial degrees of protection, one of which assemblies, the four-layer temperate, provided protection against thermal burns up to 83 cal/cm². Fire resistant combinations were superior, especially at lower thermal energies, to untreated fabric assemblies. Increased fabric spacing (loose-fitting) and greater number of fabric layers contribute significantly to higher degrees of thermal protection afforded by uniforms.

Based upon the field and laboratory studies of protection afforded by uniforms against thermal burns, it is considered that attention in future laboratory studies should be devoted to spacing and fitting of garments, to mechanisms of heat transfer through fabrics as it affects burns to the underlying skin, to effects of pulse duration (weapon yield) on burns, and to effects of the subsequent arrival of the shock wave in snuffing out flame and removing glowing outer fabric layers.

Considering as a whole the results of this project and the related results of Projects 8.6 and 8.9, it is concluded that significant progress has been made in the evaluation of protection offered by fabrics against thermal burns and in delineating the factors to consider in the development of physical methods for the evaluation.

B.7.7 Project 8.6 Thermal Effects on Clothing Materials
Agency: Quartermaster Research and Development Laboratories, USA
Report Title: Performance Characteristics of Clothing Materials Exposed to Thermal Radiation, WT-771
Project Officer: J. F. Oesterling

The objectives of Project 8.6, which were closely associated with the animal exposure experiment (Project 8.5), were:

1. To determine field performance characteristics of standard armed services clothing and experimental fabric assemblies by means of panels exposed to the thermal radiation of a nuclear weapon.
2. To relate the data thus obtained to that developed through the field exposure of clothed pigs (Project 8.5).
3. To determine whether or not flaming may occur between the end of the thermal pulse and the arrival of the blast wave.
4. To utilize these data in establishing laboratory evaluation methods which can be used as screening techniques for determining the relative merits of protective fabric assemblies which may be used in the development of combat or field uniforms.

In addition, certain items of equipment of interest to the Chemical Corps and certain packaged materials, which are not amenable to laboratory study, were exposed to both thermal radiation and blast in order to obtain field evaluation of the resistance of the materials to the effects of a nuclear detonation.

The effectiveness of the protection provided by the various panel materials was estimated by means of the temperature reached on the panel backing as determined by passive temperature indicators. The effect of the presence of an air space between the backing and the material was also studied.

Results from the panel experiments with the same fabric assemblies as were used with the pigs (Project 8.5) indicated a ranking of the fabrics, with respect to degree of protection, the same as that obtained with the clothed pigs. Other fabric combinations not tested with the pigs were ranked as to degree of protection from the results of the panel tests.

No conclusive results were obtained from panel tests designed to study the effects of fabric reflectance and spacing. It was concluded that destruction of the outer layer in a large proportion of the test samples introduced the factor of glow and sustained exothermic reactions which complicated analysis of the results.

Although results of panel tests on the effects of flaming and sustained glowing of irradiated fabrics led to no quantitative conclusions, the results indicated definitely the beneficial effect of using an outer fabric layer treated with a fire retardant agent.

The effect of the area of fabrics exposed in contact and spaced from the backing indicated that areas of the order of 1 or 2 in. in diameter, closer to the latter for spaced fabrics or multiple layer combinations, are necessary to avoid excessive edge effects from smaller exposure areas. Results from tests at Shot 10 of Quartermaster items of packaged rations and clothing indicated damage to be attributable primarily to blast effects. A single bale of clothing exposed to 12.5 cal/cm² was consumed by fire. The origin of the primary ignition in this case was not evident.

The test results of other Quartermaster items and Chemical Corps items were essentially as expected.

The ranking of fabric combinations with respect to protective characteristics was accomplished in this project by instrumenting oak veneer backing with temperature indicators (paper thermometers) adhered to the exposed side of the backing. These papers served to indicate the maximum temperature attained by the system comprising the surface of the backing and the paper. It should not be presumed that the temperature attained with the papers (and the ranking of the fabric) bears a relation to degrees of burns to skin. The National Bureau of Standards has shown, theoretically, that the temperature indicators have properties which prevent their thermal behavior from simulating that of human skin. For this reason, the results of this project, except for the exposure area studies, should be interpreted with caution. As is noted in Sec. B.7.8, the status of physical methods for evaluating fabric protective qualities is unsatisfactory at the present time; and it appears that a reliable physical method must await the development of an improved skin simulant.

B.7.8 Project 8.9: Effects of Thermal Radiation on Materials
Agency: Naval Material Laboratory
Report Title: Effects of Thermal Radiation on Materials, WT-772
Project Officer: T. I. Monahan

The general objective of this experiment was to obtain field checks of material damage studies currently being conducted in the laboratory with a simulated radiant energy source of small size. Of interest was the establishment of check points for cloth-skin simulant studies, for material damage as a function of the variable time-intensity of the energy from the bomb, for evaluation of temperature-sensitive passive indicators behind clothing, and for evaluation of certain material parameters influencing the protective value of fabrics and paints.

The development of a purely physical laboratory method for evaluating the protection offered by clothing is an objective which, if attained, would be of considerably wide interest. With the present state of the art, experimentation to evaluate clothing with animals in the laboratory is difficult and expensive when compared to a physical method. It has been shown that burns on skin behind cloth barriers cannot be correlated with damage to the cloth. It has also been shown that the shape and amplitude of time-temperature curves obtained on the skin surface upon irradiation are rough indications of the degree of burn. The NML experiments on plastic skin simulants behind cloth employing thermocouples were designed to utilize the latter fact.

It has been demonstrated that thermal damage does not follow a reciprocity relation as the time of delivery is indefinitely decreased for the same total energy delivered. The radiant energy necessary to effect an observed damage, i.e., the critical energy, however, is a useful

quantity for correlating such effects. In the NML experiment thermal damage as a function of the period in the period of radiant emission during which sensitive materials were exposed was accomplished by a calibrated spring-loaded cover which traveled down a slotted frame and successively exposed and covered up the materials once the cover was triggered by a zero time signal.

The time-temperature histories of the polyethylene skin simulant with various cloth barriers in contact with the simulant irradiated in the field were only in fair agreement with laboratory tests. It was found that the area of cloth exposed becomes important as spacing of the fabric from the backing is increased, important with multiple layer systems and important where flaming of the outer layer occurs.

Temperature-sensitive papers attached to polyethylene skin simulant show little promise as a tool for evaluating protection offered by cloth barriers. Temperature-sensitive plastics painted on the polyethylene show some promise for gross-ranking of the protective qualities of fabric (see Sec. B.7.7.)

Due to partial failure of equipment at shot time, insufficient data were obtained from the devices which exposed materials either to the initial or latter portion of the thermal pulse. Consequently, no quantitative conclusions, based upon field results, could be made concerning the failure of reciprocity for thermal damage. However, with the shaped thermal pulse simulators now available at NML and NRDL, loss of the field data should not materially hamper thermal effects studies.

Although the time-temperature histories of the polyethylene skin simulant were in fair agreement with NML laboratory tests, a recent AFSWP review of the status of the skin simulant studies indicates that the polyethylene is significantly lacking in the desired characteristics of a simulant. Increased emphasis is planned toward development of materials which will more closely simulate the conductivity, absorptivity, and heat capacity of human skin. Results from recent work at NML with other simulants are encouraging.

B.7.9 Project 8.10: Measurement of Basic Characteristics of Thermal Radiation
Agency: Naval Radiological Defense Laboratory
Report Title: Physical Characteristics of Thermal Radiation from an Atomic Bomb Detonation, WT-773
Project Officer: A. Guthrie

The objectives of this project were to supplement definitive information on the basic thermal radiation phenomena associated with small yield weapons (below 100 KT) for extension and corroboration of scaling laws and effects prediction methods, and to provide documentation of the radiant energy characteristics of Shots 9 and 10 for use with the large effects test program. The NRDL calorimeters and radiometers employed by this project are considered the basic instruments for effects test studies of thermal radiation.

Any instrument employed to measure thermal radiation which has a finite field of view always receives, in addition to direct collimated radiation from the bomb source, some energy scattered from the atmosphere. Any instrument which sees, in addition to the fireball, any portion of the ground below the burst point receives energy over that coming directly from the fireball through ground reflection.

It has been demonstrated, qualitatively, that, at a given point in the air above the ground in the vicinity of the burst point, the radiant energy received at that point may be substantially in excess of that predicted from the inverse square relation. The albedo (or scattering coefficient) of the ground and the specific geometry of the burst point with respect to the ground and the point of interest in space are factors which influence the enhancement of the radiant energy.

In order to obtain the necessary field data for checking theoretical approaches to the problem of calculating scattered radiation, ground stations at Shots 4, 9, 10, and 11 were generously instrumented with field-of-view, air-scatter, and albedo calorimeters as well as total energy calorimeters directly viewing the fireball. In addition, at Shots 4 and 9, two SAC B-50 planes flying formation with the drop plane were instrumented with calorimeters for albedo and total energy determinations.

Limited instrumentation for total energy and spectral distribution was accomplished under this project for the black and white smoke patterns under Project 8.4.

At Shot 10, special efforts were made to instrument two ground stations with both NRL and NRDL calorimeters so that direct comparisons of results could be made.

Measurements under this project were also conducted at Shot 3; but since the weapon went far below the anticipated yield and due to failure of some of the recorders, no reliable data were obtained. Other than the failure of the instruments on Shot 3, all instruments functioned satisfactorily, and essentially all channels gave useful information.

The thermal yields calculated from the measurements of this project agree closely with those in AFSWP-503. Due to inherently slow time resolution, times to minimum as measured with NRDL radiometers are greater than those calculated from AFSWP-503. Times to the second maximum suffer similarly but to a lesser extent.

The large quantity of data on reflection and scattering of radiation which were obtained by NRDL at this operation and at TUMBLER-SNAPPER is yet to be analyzed.

B.7.10 Project 8.11a: Initiation and Resistance of Primary Fires (Structures and Interior of Structures)

Agency: Forest Products Laboratory, Forest Service, USDA

Report Title: Incendiary Effects on Buildings and Interior Kindling Fuels, WT-774

Project Officer: H. D. Bruce

Both this project and Project 8.11b were concerned with the study of urban vulnerability to primary ignitions resulting from the radiant energy of atomic weapons. The probability that mass-fires, fire storms, and conflagrations will occur following an atomic attack on urban areas depends to some extent upon the frequency of occurrence of the primary ignitions. Methods for predicting the frequency of ignitions are important in making target analyses for offensive and defensive military operations. Studies under this project were devoted to kindling fuels found either as a part of a combustible building itself or found within a building. Studies under Project 8.11b were devoted to kindling fuels found exterior to buildings.

Kindling fuels which are commonly encountered in American cities were known to the two Forest Service groups conducting Projects 8.11a and 8.11b. Minimum ignition energies for each of the fuels had been determined in the laboratory with a simulated radiant source. In the field minimum ignition energies were determined by exposure of representative fuels placed at several predicted thermal energy levels expected to bracket the desired effect. Only those fuels which ignited in laboratory tests at thermal energies below 20 cal/cm² were studied.

In addition to the study of urban vulnerability to fire under Project 8.11a, five miniature houses were constructed to provide illustrative footage of time-technical photography for use in demonstrating fire hazards from atomic weapons. Three of the houses were intended to demonstrate ignition from exterior kindling fuels and two from interior fuels.

Several experimenters have shown that thermal radiation from atomic weapons causes only transient flames in massive wood or on exterior surfaces of appreciably thick combustible material. These flames usually die out with the fading of the radiant pulse. If not, the flames are always snuffed out by the passing shock wave. The case is quite different, however, with thin kindling fuels, especially fuels such as crumpled newspaper, dead vegetation, folded curtains, oily waste, excelsior, and the like. In compacted fine fuels the contrast is so great that, in many cases, the subsequent arrival of the shock wave actually drives the persistent flame into the mass of fuel and enhances greatly the probability that the flames will persist through the blast. It has also been shown that decayed massive wood, if unprotected by paint, irradiated by thermal radiation may ignite, continue to glow through the shock wave, and subsequently burst into flame.

Fuels in which flame is likely to persist through the passing shock wave are potential sources of disastrous fires if the ignitions are established in the vicinity of more massive combustible fuels, such as the interiors or exteriors of houses, fences, interiors of automobiles, and military supply dumps. One of the objectives of this project and of Project 8.11b was to develop methods, based upon laboratory and field results, for predicting the incidence

~~RESTRICTED DATA~~

762

in urban areas of the primary ignitions which may occur and persist through the shock wave.

For the some 20 kindling fuels exposed under Project 8.11a in Shots 9 and 10, the minimum ignition energies as found with the laboratory source averaged 29 per cent higher than the energies found in the field. Using this conversion factor, ignition energies may be predicted from data obtained with the laboratory source for other kindling fuels not tested in the field. It is anticipated that with further laboratory tests employing a suitably modified radiant source, the results from this project may be satisfactorily extended, without significant additional field work, for application to weapons with yields larger than 10 to 100 KT (i.e., weapons with longer and lower average intensity pulses) which is the present limit for application of the Project 8.11a results.

The timed-technical photography of the five miniature houses exposed at Shot 9, together with supplementary off-site footage, was incorporated into two FCDA films, each entitled *House in the Middle*, one a 6-min film, the other a 13-min film.

B.7.11 Project 8.11b: Initiation and Persistence of Primary Fires (Ignitable Litter)
Agency: Division of Fire Research, Forest Service, USDA
Report Title: Ignition and Persistent Fires Resulting from Atomic Explosions - Exterior Kindling Fuels, WT-775
Project Officer: W. L. Fons

The close relation between this project and Project 8.11a has been noted. The results of laboratory and field studies under both Projects 8.11a and 8.11b are important to the over-all problem of target analysis for fire probability in urban areas for offensive and defensive military operations.

The techniques used in the field for this project were the same as those described for Project 8.11a. Among the kindling fuels tested were various types of waste paper, mops, rags, pine needles, car seats (in automobiles and separately exposed), and awning canvas. This project participated in Shots 4, 9, and 10.

Minimum ignition energies were established for those exterior kindling fuels which are encountered in urban areas in this country. The conditions under which ignitions of these fuels will occur with lower yield weapons (10 to 100 KT) have been firmly established as the result of field studies under this project and related laboratory studies. It is anticipated that ignition energies may be extended through appropriate laboratory studies to the larger yield weapons with characteristically longer radiant pulses, thus obviating any need for further extensive field studies.

The establishment of primary ignitions in automobiles from thermal radiation was shown to be relatively an unimportant hazard.

B.7.12 Project 8.12a: Measurement of Velocity of Sound
Agency: Navy Electronics Laboratory
Report Title: Sound Velocities near the Ground in the Vicinity of an Atomic Explosion, WT-776
Project Officer: H. C. Silent

The primary objective of this project was to determine the velocity of sound near the ground before arrival of the shock wave as a function of distance for Shots 9 and 10. Secondary objectives of the project were to determine the effects of different surfaces and of white and black smoke on the preshock sound velocities and, also, to measure the velocity of the wind behind the shock front. Data on sound velocities close to the surface prior to shock arrival are a useful tool for correlating precursor pressure wave studies since shock wave behavior is dependent upon sonic velocity.

The basic instrumentation consisted of transducer pairs mounted 3½ and 10 ft above the ground at Intended Ground Zero (IGZ) and at several intermediate stations out to 5000 ft along the blast line and to an equal distance along the smoke line. Each pair of transducers consisted of one speaker and one microphone separated by an 8-ft path length.

For the wind velocity measurements two stations, one at 2000 ft and the other at 3500 ft from IGZ on the blast line, were equipped with three mutually perpendicular transducer pairs to measure the vectorial components of the wind. In the experiment on surface effects on Shot 9, transducer pairs, with the 8-ft sound path, were mounted $3\frac{1}{4}$ ft above surfaces of mat of white fir boughs and of Frenchman Flat soil at distances of 1000 and 2000 ft from IGZ on the blast line. For Shot 10 the fir boughs were replaced with surfaces of blackened sheet iron.

On Shot 9 sound velocities attained prior to shock arrival over Frenchman Flat soil at $3\frac{1}{2}$ and 10 ft elevations ranged up to 2000 ft/sec and 1400 ft/sec (ambient velocity 1100 ft/sec), respectively. Above fir boughs the velocities attained were considerably higher than over sand, being 3000 ft/sec or more at $3\frac{1}{4}$ ft elevation. Over the sand coated with a thin cover of asphalt (around IGZ), instruments at $3\frac{1}{2}$ ft elevation indicated that the sonic velocity was lower than that over sand. Since the smoke was not activated on Shot 9, no data on sonic velocities beneath scattering white smoke were obtained.

On Shot 10 the destructive effect of the blast forced the NEL shelter located at 500 ft from IGZ into the ground, severing all the instrument cables running from this point through Ground Zero to the smoke line. Also the early arrival of the shock wave prevented recovery of the closer-in instruments from the electromagnetic transients induced at zero time. In general, very few reliable data on sonic velocities were obtained from Shot 10. A single sound velocity result over blackened iron on this shot seemed to indicate, as anticipated, that the velocity is lower over metal due to dependence upon the conductive process only for transfer of heat to the air.

Due to failure of instruments to recover sufficiently soon after shock arrival, data on sonic velocities with the particle velocity meters could not be reduced to yield particle velocities within the shock wave.

The NEL sound velocity data on surface influences (fir boughs, asphalt, sheet iron, and sand) were, perhaps, the most significant finding from this project.

It does not appear advisable, at least with the present design of NEL velocity meters, to utilize the NEL equipment for postshock measurements. The NEL equipment should be modified so as to reduce greatly or eliminate the electromagnetic transient effect if the NEL technique is to be employed again at field tests.

B.7.13 Project 8.12b: Precursor Shock Study
Agency: David Taylor Model Basin
Report Title: Supplementary Pressure Measurements, WT-777
Project Officer: G. W. Cook

The objective of this project was to determine whether a shock wave may be generated prior to the arrival of the main shock by exposure of a surface to thermal radiation from an atomic weapon. Although the hot air boundary layer hypothesis was generally accepted as the mechanism for precursor generation, this experiment was designed to record the possible existence of a significant thermal shock.

Sensitive capacitance type pressure gages were used to measure pressures at the center of 10×10 thermal panels inclined toward the point of detonation on Shots 9 and 10 at ranges of 1500 and 3000 ft from IGZ. These inclined surfaces consisted of black asphalt roofing paper (a highly absorbing, smoke-producing surface), black ceramic tile (an absorbing but nonreactive surface), and Frenchman Flat soil molded with water (an absorbing, popcorning surface). A fourth gage was mounted at ground level at each of the two stations for reference purposes. These panels were inclined at angles such that they were approximately perpendicular to the thermal radiation from both of these air bursts in order to enhance the values of the incident radiant energy.

No significant preshock pressures were observed on Shots 9 and 10 that would substantiate the thermal shock hypothesis as a mechanism for precursor generation. Several minor preshock signals were observed on Shot 10 which occurred at the time of the thermal pulse. There is evidence to believe that this gage response was due to the effect of electromagnetic and thermal radiation. There appear to be conflicting results on thermal shock phenomena from

other projects. Project 1.1a and 1.2 reports no preshock measurements with either mechanical or electronic gages in this region, whereas Project 1.1d reports small preshock pressures for both Shots 9 and 10 as recorded on electronic gages. It is not presently known whether such preshock pressures are real or whether they are within the uncertainties of the instrumentation system.

It is possible that under certain conditions preshock pressures may result from thermal shock in those regions which are close to Ground Zero. However, it does not appear that there is sufficient energy available for purposes of precursor formation or propagation. Furthermore, thermal shock is not considered significant since it may be expected to occur only under those conditions favorable to the formation of a thermal layer at the surface and the subsequent development of a precursor at slightly greater ranges. It is considered that this project has demonstrated that further study of thermal shock phenomena is not warranted.

B.7.14 Project 8.13: A Study of Fire Retardant Paints
Agency: Engineer Research and Development Laboratories
Report Title: Study of Fire Retardant Paint, WT-778
Project Officer: H. Miller

The objective of this project was to obtain exposure of a number of test paint panels to the radiant energy of the bomb. The paints exposed were fire retardant paints which, subsequently, were tested in the laboratory to determine residual fire retardancy of the exposed surfaces.

Although such paints are not proposed for inhibiting primary ignitions from the weapon, they may have application for retarding combustion of massive fuels (see Project 8.11a) from nearby ignition points established either in kindling fuels (primary ignitions) or in fuels ignited by broken gas lines, electrical lines, etc. (secondary fires). In such cases the residual fire retardancy of the irradiated surfaces would be of interest.

Wood panels painted with three fire retardant paints and two non-fire retardant paints were successfully exposed on Shot 9 to three different levels of thermal energy. Subsequent tests at ERDL of the residual fire retardancy of the exposed panels indicated no serious decrease in the fire retardant properties of the exposed panels even at the highest energy of exposure, i.e., 31 cal/cm². The results indicate that the role of fire retardant paints in inhibiting the spread of fire will not be seriously affected by exposure to thermal radiation in most cases. The project was not designed, however, to indicate the enhanced ignitability of irradiated wood surfaces adjacent to kindling fuels ignited by the thermal radiation.

There are no recommendations for future field tests.

B.8 PROGRAM 9— TECHNICAL PHOTOGRAPHY
Program Director: W. R. Greer

B.8.1 Project 9.1: Technical Photography
Agencies: Edgerton, Germeshausen & Grier and U. S. Signal Corps
Report Title: Technical Photography, WT-779
Project Officer: Maj W. R. Greer, USA

Project 9.1 was established to provide a centralized organization responsible for all photography, other than documentary and historical, required by the various military effects projects participating under the direction of Programs 1 to 9. Documentary and historical motion picture photography was performed by Lookout Mountain Laboratory.

The still photography and the pre- and post-test motion picture photography of this project was performed by personnel and equipment furnished by the U. S. Army Signal Corps. This photography was done for the various projects for record purposes. Over 85,000 prints were processed from approximately 10,000 ft of exposed motion picture film.

The motion picture technical photography at shot time was performed by Edgerton, Germeshausen & Grier, under contract, and included all zero time photography desired by the projects. This phase was accomplished by the use of motion picture cameras operating be-

tween the limits of 2 frames per minute and 2500 frames per second. A total of 193 cameras on 100 steel towers of various heights were used on Shot 9. A lesser, but still considerable, number of cameras were used on Shot 10; 94 cameras and 50 towers. The towers ranged in heights from 5 to 25 ft.

In general, the technical photography gave exceedingly good results, and those camera targets which were beyond 2500 ft from Ground Zero and several feet above the ground gave outstanding results. Those targets which were closer than 2500 ft or near the ground gave fair to poor results.

B.8.2 Project 9.6: Stabilization (Production)
Agency: Field Command, Armed Forces Special Weapons Project
Report Title: Production Stabilization, WT-780
Project Officer: Capt C. S. Adler, USA

The objective of Project 9.6 was to provide stabilized areas for the photographic stations used on Shots 9 and 10 in order to eliminate the thermal and blast dust.

Designated areas were stabilized with a sand-cement mixture approximately 2 in. thick, the exact area stabilized depending on the distance the camera stations were from Ground Zero. These various distances were derived from curves showing estimated particle transport vs blast pressures or ground ranges. Approximately 700,000 sq yd of the Frenchman Flat lake bed were stabilized. The stabilization specification was established by the U. S. Corps of Engineers at the request of AFSWP.

The results from this production stabilization were excellent at all distances over 2000 ft from Ground Zero. It may be said that the success of the technical motion picture photography was dependent to a large extent on the success of this stabilization program.

B.8.3 Project 9.7: Stabilization (Experimental)
Agency: U. S. Corps of Engineers
Report Title: Experimental Soil Stabilization, WT-781
Project Officer: Capt C. S. Adler, USA

Project 9.7 was established to test the resistance of several types of surfaces to the effects of thermal and blast from nuclear detonation using specifications which were not used in the production stabilization effort.

On the basis of previously conducted laboratory studies, several promising stabilizing agents were tested. Tests included sand-cement, sodium silicate, and lignin in various solutions. The experimental stabilized surfaces were photographed with zero time photography so as to record the effects of thermal radiation. In addition the stabilized surfaces were exposed for prolonged periods of time to test their perviousness to the elements of Frenchman Flat.

The sodium silicate worked well with incident thermal energies up to 50 cal/cm² as did the cement mixture. Up to peak overpressures of 50 psi, the cement mixture was quite satisfactory, whereas the sodium silicate solution withstood pressures up to only 15 psi. No materials tested are recommended for over 60 psi. In addition, it is to be noted that the sodium silicate stabilization will not support traffic.

SHOT NO	STATION		ELEVATION IN FEET																						
	LINE	DISTANCE FROM I.G.Z (FT)	F-206	F-207	F-208	F-209	F-209	F-209	F-210	F-210	F-211	F-211	F-211	F-211	F-211	F-211	F-211	F-211	F-211	F-211	F-296	F-297			
PROJECT	AGENCY	MEASUREMENT																							
9 MAIN	110	NOL	3500	3750	4000	4250	4500	4750	5000	5500	6000	6500	7000	7500	8000	8500	9000	9500	10000	11000	15000				
		MECH GAGE P		2 of 0	0,10				0,10		0,10				0	0	0	0	0	0	0	0	0	0	0
		INDENT GAGE P		9 of 0							9 of 0														6 of 0
	11b	SRI		0,10,35	10,40,50	0,10,30				0,10,50		0	0,10,35		0										
		VERT ERTH ACC	-1																						
	11d	SC				2 of 10																			
		AIR P-1																							
		AIR PRSHCK																							
		AIR P-1				10																			
		AIR TEMP				10																			
		SWASSI				10																			
	14	SC																							
		VERT ERTH STRESS																							
	812a 812b DTMB	NEL		10																					
		SOUND VELOCITY														10									
P-1																									
P-1																									
10 MAIN	110	NOL																							
		MECH GAGE P		0,10																					
		INDENT GAGE P		23 of 0																					
	11b	SRI		0,10,30	10,40,50	0,10,30				0,10,50		0	0,10,35		0										
		VERT ERTH ACC	-1																						
	11d	SC				2 of 10																			
		AIR P-1																							
		AIR PRSHCK																							
		AIR P-1				10																			
		AIR TEMP				10																			
		SWASSI				10																			
14	SC																								
	VERT ERTH STRESS																								
812a 812b DTMB	NEL		10																						
	SOUND VELOCITY														10										
	P-1																								
	P-1																								

Fig. B.1—Instrumentation Chart, Shots 9 and 10.

SHOT NO	LINE	STATION	F-214	F-215	F-216	F-217	F-218	F-219	F-220	F-221	F-222	F-223	F-224	F-225	F-226	F-227	F-228	F-229	F-230			
		DISTANCE FROM I G Z (FT)	0	500	1000	1500	2000	2500	3000	3500	4000	4500	5000	5500	6000	6500	7000	7500	8000			
		PROXIMITY MEASUREMENT	GAGE ELEVATION IN FEET																			
9 MAIN	11a	NOL	0.10	0.10	0.10	0.10	0.10	0.10	0.10	0.10	0.10	0.10	0.10	0.10	0.10	0.10	0.10	0.10	0.10	0.10		
	11b	SRI	0.10, 30, 50	0.10, 30, 50	0.10, 30, 50	0.10, 30, 50	0.10, 30, 50	0.10, 30, 50	0.10, 30, 50	0.10, 30, 50	0.10, 30, 50	0.10, 30, 50	0.10, 30, 50	0.10, 30, 50	0.10, 30, 50	0.10, 30, 50	0.10, 30, 50	0.10, 30, 50	0.10, 30, 50	0.10, 30, 50	0.10, 30, 50	
	11c	SC	2.10	2.10	2.10	2.10	2.10	2.10	2.10	2.10	2.10	2.10	2.10	2.10	2.10	2.10	2.10	2.10	2.10	2.10	2.10	
	14	SC																				
	B12a	NEL	10	10	10	10	10	10	10	10	10	10	10	10	10	10	10	10	10	10	10	
	B12b	DTMB	P-1	0.3 at 35	0.3 at 35	0.3 at 35	0.3 at 35	0.3 at 35	0.3 at 35	0.3 at 35	0.3 at 35	0.3 at 35	0.3 at 35	0.3 at 35	0.3 at 35	0.3 at 35	0.3 at 35	0.3 at 35	0.3 at 35	0.3 at 35	0.3 at 35	0.3 at 35
	11a	NOL	0.10	0.10	0.10	0.10	0.10	0.10	0.10	0.10	0.10	0.10	0.10	0.10	0.10	0.10	0.10	0.10	0.10	0.10	0.10	0.10
	11b	SRI	0.10, 30, 50	0.10, 30, 50	0.10, 30, 50	0.10, 30, 50	0.10, 30, 50	0.10, 30, 50	0.10, 30, 50	0.10, 30, 50	0.10, 30, 50	0.10, 30, 50	0.10, 30, 50	0.10, 30, 50	0.10, 30, 50	0.10, 30, 50	0.10, 30, 50	0.10, 30, 50	0.10, 30, 50	0.10, 30, 50	0.10, 30, 50	0.10, 30, 50
	11c	SC	2.10	2.10	2.10	2.10	2.10	2.10	2.10	2.10	2.10	2.10	2.10	2.10	2.10	2.10	2.10	2.10	2.10	2.10	2.10	2.10
	14	SC																				
B12a	NEL	10	10	10	10	10	10	10	10	10	10	10	10	10	10	10	10	10	10	10	10	
B12b	DTMB	P-1	0.3 at 35	0.3 at 35	0.3 at 35	0.3 at 35	0.3 at 35	0.3 at 35	0.3 at 35	0.3 at 35	0.3 at 35	0.3 at 35	0.3 at 35	0.3 at 35	0.3 at 35	0.3 at 35	0.3 at 35	0.3 at 35	0.3 at 35	0.3 at 35	0.3 at 35	

SHOT NO	LINE	STATION	F-420	F-421	F-422	F-423	F-424	F-425	F-426	F-427	F-428	F-429	F-430	F-431	F-432	F-433
		DISTANCE FROM I G Z (FT)	500	1000	1500	2000	2500	3000	3500	4000	4500	5000	5500	6000	6500	7000
		PROXIMITY MEASUREMENT	GAGE ELEVATION IN FEET													
9 MAIN	11a	NOL	0.10	0.10	0.10	0.10	0.10	0.10	0.10	0.10	0.10	0.10	0.10	0.10	0.10	0.10
	11b	SRI	0.10, 30, 50	0.10, 30, 50	0.10, 30, 50	0.10, 30, 50	0.10, 30, 50	0.10, 30, 50	0.10, 30, 50	0.10, 30, 50	0.10, 30, 50	0.10, 30, 50	0.10, 30, 50	0.10, 30, 50	0.10, 30, 50	0.10, 30, 50
	11c	SC	2.10	2.10	2.10	2.10	2.10	2.10	2.10	2.10	2.10	2.10	2.10	2.10	2.10	2.10
14	SC															
B12a	NEL	10	10	10	10	10	10	10	10	10	10	10	10	10	10	10
B12b	DTMB	P-1	0.3 at 35	0.3 at 35	0.3 at 35	0.3 at 35	0.3 at 35	0.3 at 35	0.3 at 35	0.3 at 35	0.3 at 35	0.3 at 35	0.3 at 35	0.3 at 35	0.3 at 35	0.3 at 35

Fig. B.1 — (Continued).



SHOT NO	LINE	STATION		GAGE ELEVATION IN FEET														
		DISTANCE FROM GZ (FT)	PROJAGENCY MEASUREMENT	3-280	3-281	3-282	3-283	3-284	3-285	3-286	3-287	3-288	3-289	3-290	3-291	3-292	3-293	3-294
I	MAIN	11c	SC	700	900	1050	1150	1250	1450	1600	1900	2100	2600	3100	3800	5000	6000	7800
		AIR P-1		0,10	0	0	0,10	0,10	0,10	0,10	0	0,10	0,10	0,10	0,10	0	0	0
		AIR Q-1					10	10					2 at 10					
		AIR TEMP																
		SWASSI																
		WIND											10					
		AIR P-1																
		EARTH COMP																

SHOT NO	LINE	STATION		GAGE ELEVATION IN FEET															
		DISTANCE FROM I.G.Z. (FT)	PROJAGENCY MEASUREMENT	7-200	7-280	7-281	7-282	7-283	7-284	7-285	7-286	7-287	7-288						
3.30	MAIN	11b	SC	0	1000	1500	2000	2500	3000	3500	4000	4500	5000	6000	7000	8000	9500	11,000	13,000
		AIR P-1		0,10	0,10	0,10	0,10	0,10	0,10	0,10	0,10	0,10	0,10	0,10	0,10	0,10	0,10	0,10	0,10
		AIR Q-1																	
		MECH GAGE P																	
		PEAK PRESSURE																	

SHOT NO	LINE	STATION		GAGE ELEVATION IN FEET															
		DISTANCE FROM GZ (FT)	PROJAGENCY MEASUREMENT	1-269	1-270	1-271	1-272	1-273	1-274	1-275	1-276	1-277	1-278	1-279					
7	MAIN	11	SC	14,040	14,530	15,610	16,405	16,780	16,960	17,090	17,200	17,300	17,340	17,410	17,520	17,640	18,090	19,060	19,710
		AIR P-1		0	0	0	0	0	0	0	0	0	0	0	0	0	0	0	0

Fig. B.2—Instrumentation Chart—Shots 1, 3, 4, 7 and 11.

209

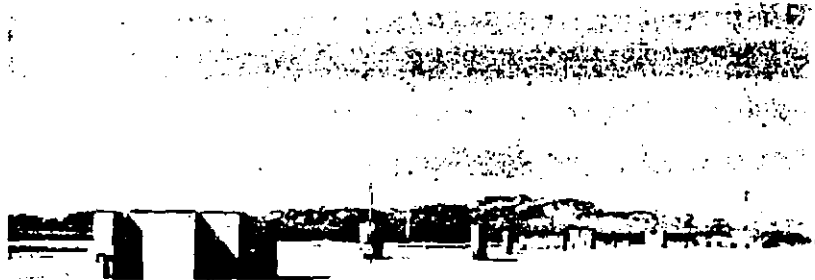


Fig. B.3—Cubicles on Arc at 4900-ft Radius.



Fig. B.4—A Typical Steel Cylinder (Project 3.3d).



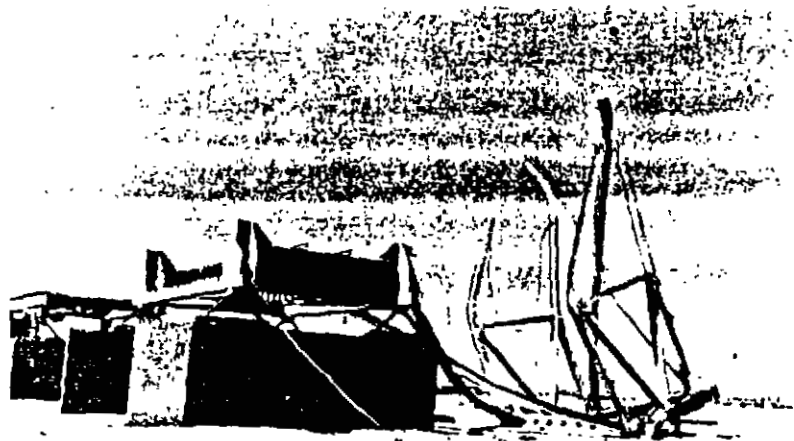


Fig. B.5—Plate Girder Section (Project 3.4f).

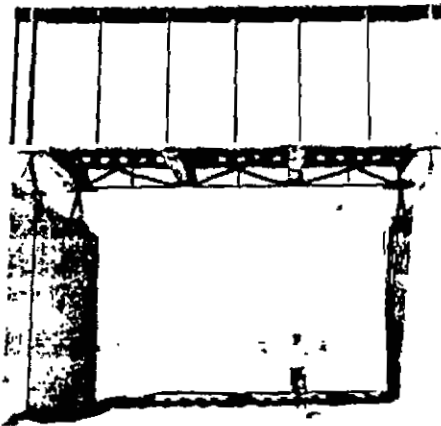


Fig. B.6 — Postshot Failure of Truss Section, Structure 3.4a.

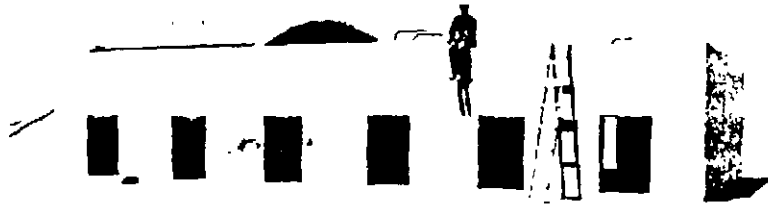


Fig. B.7—Typical Roof Panels in Reinforced Concrete Cell Structure.

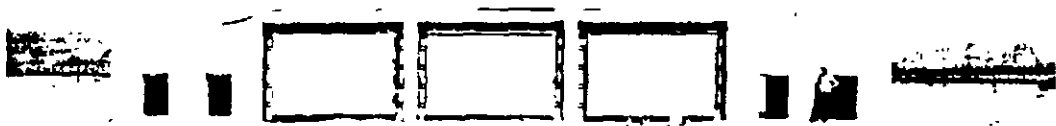


Fig. B.8—Structure 3.5c Wall Panels in Place Prior to Shot 9.

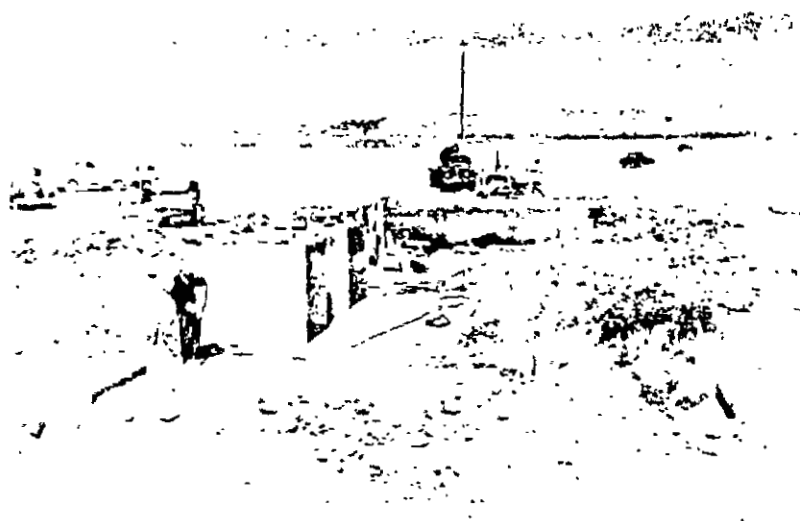


Fig. B.9—Structure 3.7 in the Process of Construction.

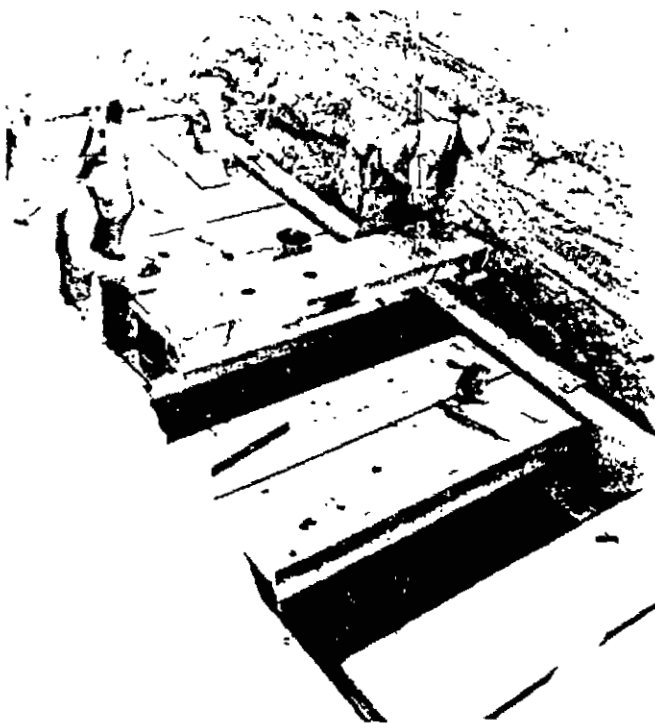


Fig. B.10—Placing Beam Strips on Structure 3.8.

215
215

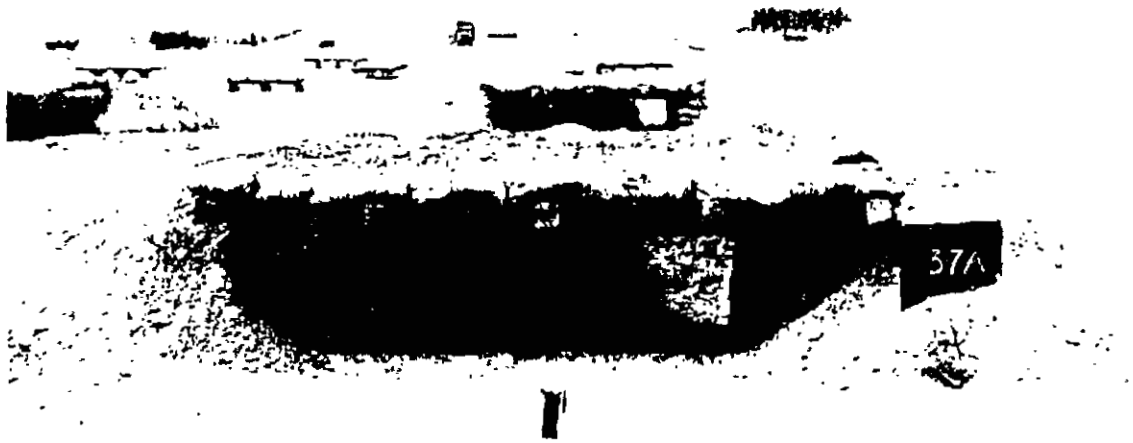


Fig. B.11 — View of Some Typical Emplacements Prior to Shot 9.

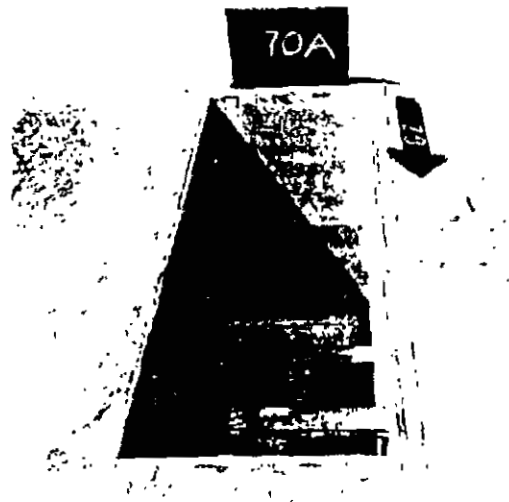


Fig. B.12 — Foxhole Lined with Aluminum Sheetting Prior to Shot 9.

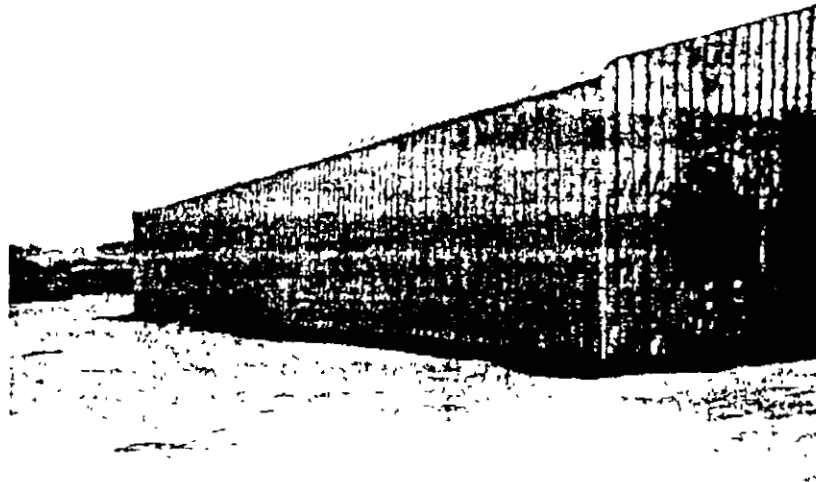


Fig. B.13 — Structure 3.11b After Shot 9.



Fig. B.14 — Structure 3.12 with Door Removed Prior to Shot 9.

2715



Fig. B.15 — Structure 3.13b Prior to Shot 9.

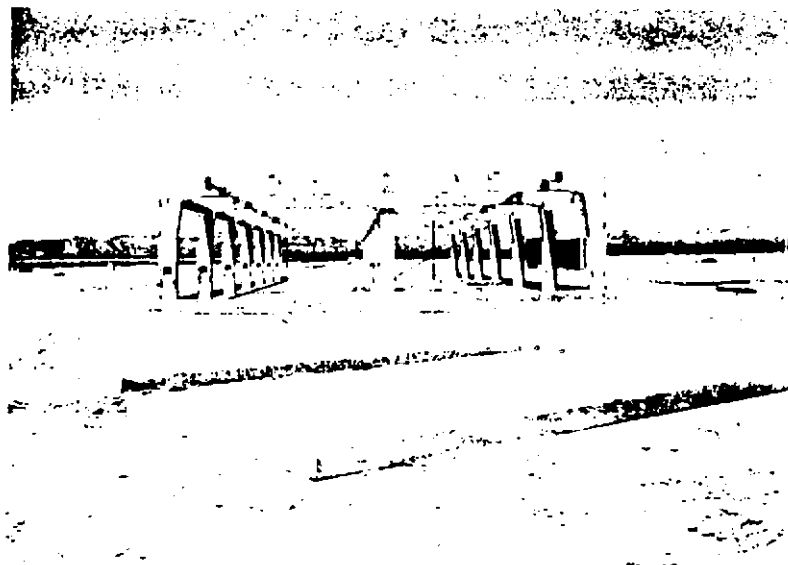


Fig. B.16 — Structure 3.14 Frame Without Siding.

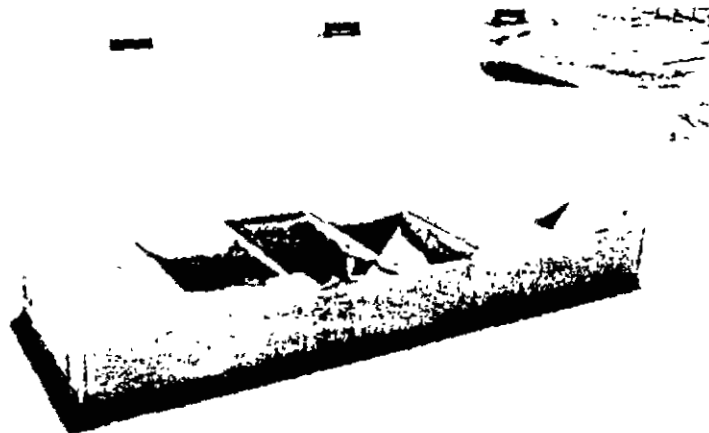


Fig. B.17 — Aerial View of Structure 3.14 After Shot 10.



Fig. B.18 — Corrugated Steel Shelter Before Placement of Earth Cover.

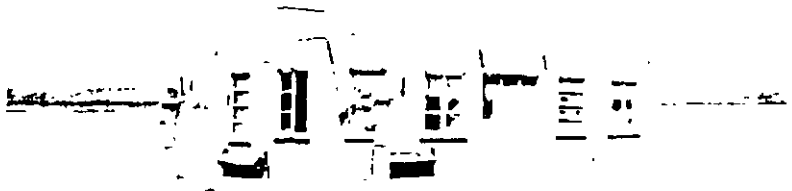


Fig. B.19 — Structure 3.16a After Shot 10.

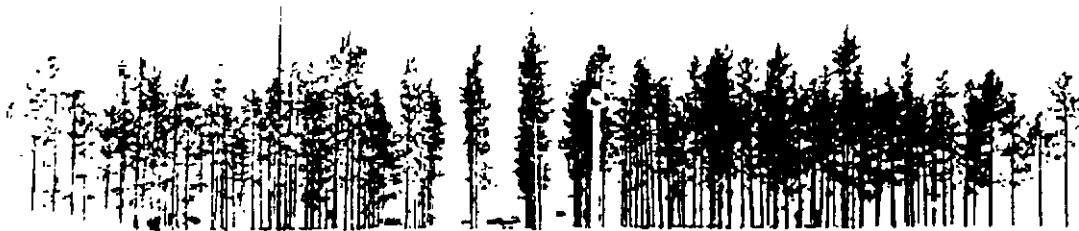


Fig. B.20 — Tree Stand Prior to Shot 9.

218



Fig. B.21 — Tree Stand After Shot 9.

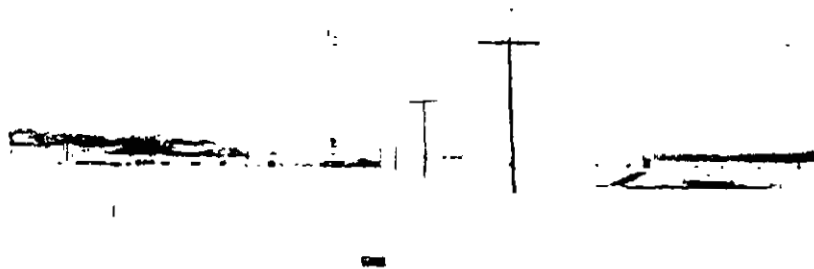


Fig. B.22 — Radial Pole Line with Aluminum Towers in the Distance.

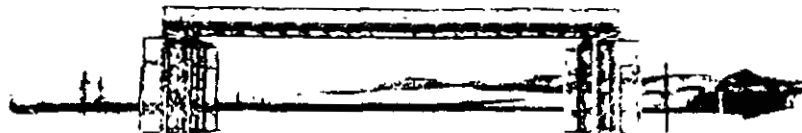


Fig. B.23 — Bailey Bridge at 4100 Ft Prior to Shot 9.

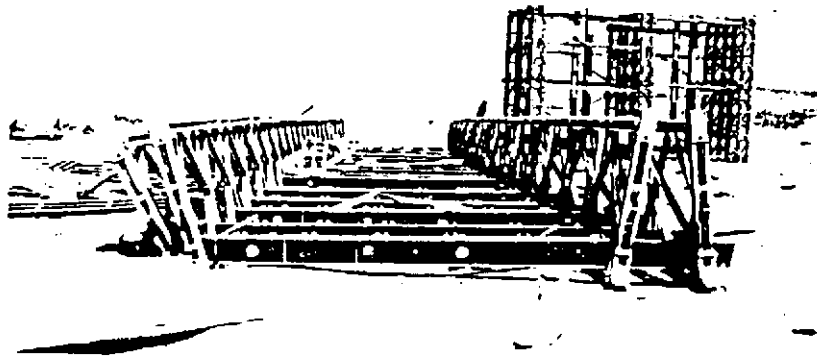


Fig. B.24—Bailey Bridge at 2100 Ft After Shot 10.

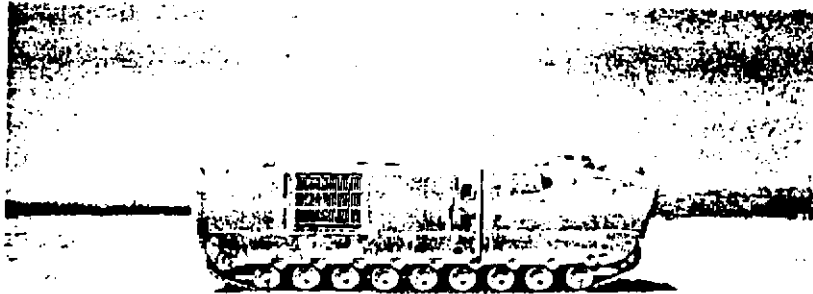


Fig. B.25—LVT in Position Prior to Shot 10.

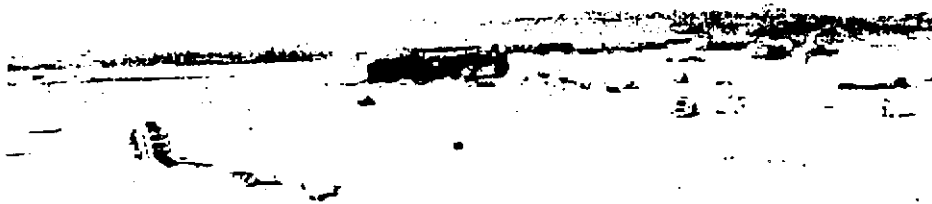


Fig. B.26—LVT at 1030 Ft After Shot 10.

12.20



Fig. B.27— Typical Quartermaster Corps POL Station Prior to Shot 9.

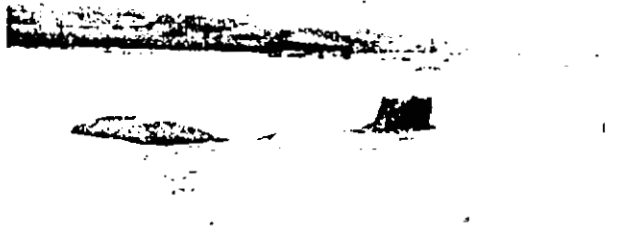


Fig. B.28— Typical Marine Corps Assault Type POL System Prior to Shot 9.

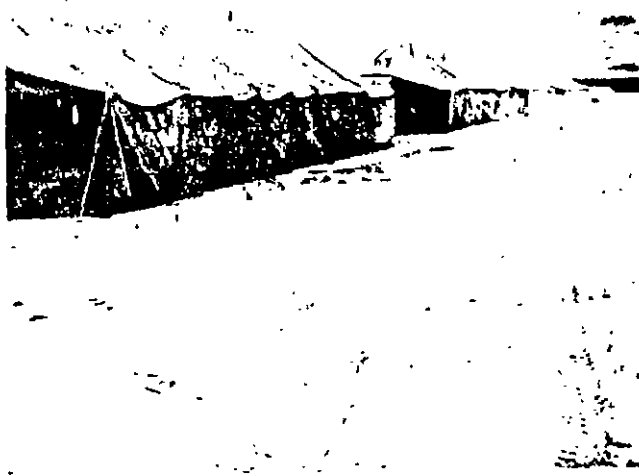


Fig. B.29 — Medical Installation Before Shot 9.

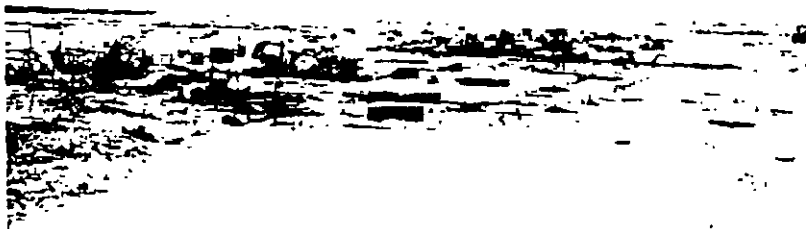


Fig. B.30 — Medical Installation at 4163 Ft After Shot 9.

727



Fig. B.31 — Structure 3.29c Showing Solid Curtain Walls. Three Air Force panels at extreme right.

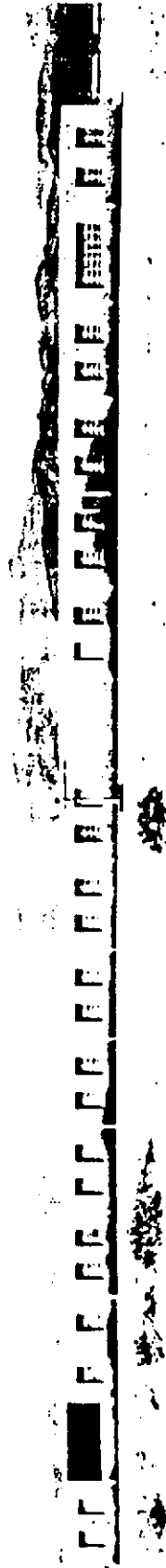


Fig. B.32—Structure 3.29d Showing Curtain Walls with Window Openings.



Fig. B.33—Nylon Thread and Carbon Paper Initiator on a Spring-wound Pressure-time Self-recording Gage.